THE

LONDON, EDINBURGH, AND DUBLIN

PHILOSOPHICAL MAGAZINE

AND

JOURNAL OF SCIENCE.

[SEVENTH SERIES.]

JANUARY 1936.

I. *On the Determination of the Dielectric Constants of Organic Liquids at Radio Frequencies.*—Part I. *Carbon Tetrachloride and Chloroform.* *By* R. M. DAVIES, *M.Sc., F.Inst.P., Lecturer in Physics, University College of Wales, Aberystwyth* *.

CONTENTS.

I. *Introduction.*

THE accurate measurement of dielectric constant (d.c.) has, of late, become a matter of great importance, more especially on account of the use of the quantity in the calculation of dipole moments. A survey of the numerical results obtained by different workers shows that considerable discrepancies exist even in the case of pure organic liquids of low electric conductivity (*v.*

* Communicated by Vice-Principal Gwilym Owen, M.A., D.Sc.

Tables IV. and V.). The work described in this paper was undertaken in order to attempt to obtain reliable values for the d.c. of some pure organic liquids, which could then be used in addition to benzene for calibration purposes. The liquids chosen were carbon tetrachloride and chloroform, and their d.c.s were determined at 20° C. and at 25° C. These two liquids were chosen since they can be obtained in a pure state and, in addition, are chemically stable.

D.c. measurements may either be absolute or comparative, and accurate measurements of this quantity are usually carried out by one of the following methods :—

(i.) Bridge methods at audio frequencies.
(ii.) Bridge methods at radio frequencies.
(iii.) Resonant circuit methods at radio frequencies.

When absolute values are required the first method has undoubted advantages, and, as developed by Hartshorn and Oliver [1], this method is capable of giving very accurate absolute results. The second method, although very attractive in theory, requires great care in practice [2]. As far as convenience and flexibility are concerned the third method is best, but it suffers from two main defects :—

(i.) It is difficult to apply the method to obtain *absolute* values, except by using condensers of special design and by elaborate calculation of certain corrections [3].
(ii.) Special precautions are necessary when dealing with liquids of appreciable electric conductivity [4] [5], [6], [7], [8].

In view of the fact that the d.c. of benzene has been determined with an accuracy of 2 in 10,000 by Hartshorn and Oliver [1], it is clear that ample accuracy for other non-conducting liquids can best be obtained by a reliable comparison method, adopting benzene as a standard liquid. This was the method adopted in the present work, and after a consideration of the relative merits of the three methods enumerated above it was decided that for comparative measurements an accuracy better than 1 in 1,000 in the electrical measurments could be obtained with the resonant circuit method provided suitable precautions were taken. On account of its greater simplicity, this method was therefore adopted.

II. *Description and Discussion of the Method.*

The principle underlying the comparison of d.c.s by the resonant circuit method is well-known. A resonant circuit is fitted up consisting of an inductance, a calibrated variable air condenser, and some form of resonance indicator; the appropriate terminal of the air condenser is earthed, and the circuit is adequately screened. A lead is taken from the insulated terminal of the air condenser, and this lead terminates in a switch used with the condenser used for the measurement of d.c.; one set of the plates of the d.c. condenser is permanently earthed whilst the other set is insulated, and by means of the switch this insulated set of plates can either be earthed or connected to the insulated terminal of the air condenser. The resonant circuit is coupled by a suitable coupling coil to a radio-frequency source of fixed frequency, and, using the resonance indicator, the circuit is tuned to resonance with the source by variation of the capacitance in the circuit. Resonance is obtained under the following conditions :—

I. D.c. condenser filled with air :

(*a*) Insulated plate of this condenser earthed.
(*b*) Insulated plate of this condenser connected to the insulated plate of the air condenser.

II. D.c. condenser filled with standardizing liquid of d.c. ϵ_s :

(*a*) Insulated plate of this condenser earthed.
(*b*) Insulated plate of this condenser connected to the insulated plate of the air condenser.

From the four readings of the calibrated variable air condenser obtained under these conditions, and from similar readings obtained with the d.c. condenser filled with liquid of unknown d.c. ϵ, the value of ϵ can be determined in terms of ϵ_s as shown below.

In order to investigate the conditions essential for accurate work it is necessary to consider matters in greater detail. The resonant circuit is shown in fig. 1 and may be considered as consisting of two parts. The first part will be taken to consist of those components which are permanently in circuit, namely, the main inductance, the coupling coil, the variable air condenser, the resonance

indicator, and the various leads, including the lead from the insulated terminal of the air condenser to the switch. In the figure the *total* inductance and resistance of this portion of the circuit is considered to be equivalent to a single coil of inductance L and resistance R, whilst the *total* capacitance in this part of the circuit is taken to be equivalent to a single condenser of capacitance C, devoid of losses. It is convenient to regard C as the sum of (i.) the capacitance of the variable air condenser, and (ii.) the remaining capacitances, such as those of the leads etc.; the latter will remain constant provided that the circuit does not change its geometrical form, and for this reason will be termed the constant capacitance C_c in the main circuit. In the figure the insulated terminal of the variable air condenser is represented by the point A, the switch

Fig. 1.

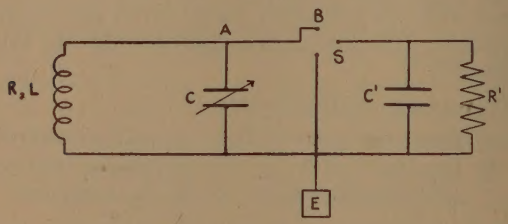

The resonant circuit.

by S, and the lead from A to S by AB; as we have already stipulated, the electrical constants of AB are included in R, L, and C.

The second part of the circuit will be taken to consist of those components which are switched into the resonant circuit when required; it therefore consists of the d.c. condenser together with the lead from S to the insulated terminal of this condenser. This portion may be represented by a capacitance C′ shunted by a resistance R′; C′ will consist of the capacitance of the d.c. condenser together with the lead from S to this condenser, whilst R′ represents the equivalent shunt resistance of the condenser. Strictly speaking the effect of the inductance of the leads from S to the d.c. condenser should be taken into account, but experiment and calculation show that the well-known correction for lead inductance amounts to

less than 1 in 10,000 in the present experiments, and it is therefore neglected.

The capacitance C′ of fig. 1 is the sum of three capacitances :—

(i.) The capacitance of the leads from S to that point on the leads where they enter the liquid when the d.c. condenser is filled with liquid.

(ii.) The capacitance between the earthed and insulated plates due to that portion of the electrostatic (e.s.) field which passes through the solid dielectric used to separate and support the insulated plates.

(iii.) The capacity between the earthed and insulated plates due to that portion of the e.s. field which does not pass through the solid dielectric.

The first remains unchanged whether the d.c. condenser is filled with air or liquid. The same is true of the second if the distribution of the lines of e.s. force through the solid remains unchanged when air is replaced by liquid ; this point is examined in greater detail later (*v* Section VIII.), and for the moment it will be assumed that this second part of C′ does remain unchanged.

Let the joint capacitance of (i.) and (ii.) be denoted by C'_n ; this constitutes the " non-replaceable " capacitance of the d.c. condenser.

Let the capacitance of (iii.) when the d.c. vessel is filled with air be C'_{ra} ; this may be termed the " replaceable air capacitance " of the d.c. condenser. When the d.c. condenser is filled with the standardizing liquid of d.c. ϵ_s let the capacitance of (iii.) be C'_{rs} ; clearly $C'_{rs}=\epsilon_s C'_{ra}$.

Let the value of C′ when the d.c. condenser is filled with air and with the standardizing liquid be C'_{a1} and C'_s respectively.

Then

$$C'_{a1}=C'_n+C'_{ra},$$

$$C'_s =C'_n+C'_{rs}=C'_n+\epsilon_s C'_{ra} ;$$

whence

$$C'_{ra}=\frac{C'_s-C'_{a1}}{\epsilon_s-1} \quad . \quad . \quad . \quad . \quad . \quad . \quad . \quad . \quad (2.1)$$

Thus the determination of $(C'_s-C'_{a1})$ yields the value of C'_{ra}, since the value of ϵ_s is known. It should be noted that this result does not involve C'_n, but it does assume

that C'_a remains unchanged; in practice this implies that the positions of the switch S and the d.c. condenser and its leads must remain the same in the measurements with the air-filled and with the liquid-filled condenser, *i. e.*, the leads and switch must be of rigid construction, the d.c. condenser must be fixed in position and must be filled with liquid in this position.

In a second experiment, with the standardizing liquid replaced by the liquid of unknown d.c. ϵ, let the value of C′ when the d.c. condenser is filled with air and with liquid be C'_{a2} and C'_u respectively. Then

$$\epsilon - 1 = \frac{C'_u - C'_{a2}}{C'_{ra}}. \quad . \quad . \quad . \quad . \quad . \quad . \quad (2.2)$$

If the replaceable air capacitance be the same as in the standardizing experiment, *i. e.*, if the d.c. condenser be rigidly constructed, the determination of $(C'_u - C'_{a2})$ yields the value of ϵ. It should be noticed that the assumption as to the constancy of the non-replaceable capacitance in the experiments with air-filled and with liquid-filled condenser applies here also. Another point worthy of notice is that no assumption has been made as to the non-replaceable capacitance being the same in the standardizing experiment and in the experiment with the liquid of unknown d.c. This means that between the two experiments it is permissible to remove the d.c. condenser from its fixed position and wash and dry it as necessary.

We have next to consider the evaluation of the differences $(C'_s - C'_{a1})$ and $(C'_u - C'_{a2})$ from the air condenser readings obtained under conditions I. *a*, I. *b*, II. *a*, II. *b* enumerated above.

In the present experiments the resonance detector consisted of a low resistance vacuo-thermojunction with its associated galvanometer; calibration showed that the galvanometer deflexion was proportional to the square of the current in the "heater" circuit of the junction. If in an experiment the galvanometer deflexions are plotted against the capacitance of the variable air condenser we obtain a resonance curve. When the galvanometer deflexion is a maximum δ_m, *i. e.*, when the current in the circuit is a maximum, the *total* capacity in the circuit is the resonance capacity; let its value be C_m.

For a given value of the pulsatance ω of the radio-frequency current the value of C_m depends on the circuit constants, and the expression for C_m for a resonant circuit containing a resistance in parallel with the capacitance has been given by Jezewski [9]. In the circuit of fig. 1, with C′ and R′ in circuit, let

$$C_0 = 1/\omega^2 L = C + C'. \quad . \quad . \quad . \quad . \quad . \quad (2.3)$$

C_0 is the resonant capacitance of the circuit in the case where R′ is infinite, and may be called the Kelvin resonant capacitance.

In the general case, when R′ is finite, the capacitance C_m which gives maximum current is given by

$$C_m = \frac{1}{2} C_0 \left[1 + \frac{2R}{R'}\right] \left[1 + \sqrt{1 + \frac{4\omega^2 L^2}{(2R + R')^2}}\right]. \quad (2.4)$$

Let R_1' and R_2' be the shunt resistances of the d.c. condenser when filled with air and with standardizing liquid respectively.

Let the capacitance of the variable air condenser when resonance is obtained in the conditions I. *a*, I. *b*, II. *a*, II. *b* enumerated above be C_{1a}, C_{1b}, C_{2a}, and C_{2b} respectively.

The readings involved in I. *a* and I. *b* are taken within a short time, and provided that the frequency of the generator is independent of the load it is permissible to assume that for these readings the pulsatance is constant and equal to ω_1 say. Between the first set of readings I. *a*, I. *b*, and the second set II. *a*, II. *b*, considerable time must elapse, since the d.c. condenser has to be filled with liquid and must be allowed to attain the temperature of the thermostat in which it is placed. It is therefore not permissible to assume that the pulsatance for readings II. *a* and II. *b* will be equal to ω_1. As before, it is permissible to assume that the pulsatance for readings II. *a* and II. *b* will be constant ; let it be equal to ω_2.

For the reading I. *a* we have (in the above notation)

$$C_m = C_c + C_{1a} = 1/\omega_1^2 L. \quad . \quad . \quad . \quad . \quad (2.5)$$

For the reading I. *b* we have

$$C_m = C_c + C_{1b} + C_{d1}'$$

$$= \frac{1}{2\omega_1^2 L} \left[1 + \frac{2R}{R_1'}\right] \left[1 + \sqrt{1 + \frac{4\omega_1^2 L^2}{(2R + R_1')^2}}\right]. \quad (2.6)$$

For the reading II. *a* we have

$$C_m = C_c + C_{2a} = 1/\omega_2^2 L. \quad . \quad . \quad . \quad . \quad . \quad (2.7)$$

Finally, for the reading II. *b* we have

$$C_m = C_c + C_{2b} + C_s'$$

$$= \frac{1}{2\omega_2^2 L}\left[1+\frac{2R}{R_2'}\right]\left[1+\sqrt{1+\frac{4\omega_2^2 L^2}{(2R+R_2')^2}}\right]. \quad (2.8)$$

Before discussing these equations in greater detail it is advisable to find the order of magnitude of the terms in square brackets in equations (2.6) and (2.8), and to do this we must first find the order of magnitude of R_1' and R_2'. This can be done using a well-known result [9], [10] for the r.m.s. value of the resonant current, I_m, in the circuit. If E_m be the r.m.s. value of the radio-frequency e.m.f. in the circuit, then

$$I_m = E_m \Big/ \left(R + \frac{L}{R' C_m}\right). \quad . \quad . \quad . \quad . \quad (2\,9)$$

In reading I. *a* let I_{ma} be the value of the current at resonance and δ_{ma} the corresponding galvanometer reading. From (2.9), since R′ is infinite,

$$I_{ma} = E_m/R.$$

In reading I. *b* let I_{mb} and δ_{mb} be the current and the galvanometer reading at resonance. Then

$$I_{mb} = E_m \Big/ \left(R + \frac{L}{R_1' C_m}\right),$$

whence

$$\frac{1}{R_1'} = \frac{RC_m}{L}\left[\frac{I_{ma}}{I_{mb}} - 1\right] = \frac{RC_m}{L}\left[\sqrt{\frac{\delta_{ma}}{\delta_{mb}}} - 1\right]. \quad (2.10)$$

In the present experiments the wave-length of the radio-frequency current used was about 800 m., whence $\omega = 2{\cdot}356 \times 10^6$; L was of the order of 0·225 mH., R of the order of 5 ohm, and C_m of the order of 800 $\mu\mu$F, whence $RC_m/L = 1{\cdot}77_8 \times 10^{-5}$. In a typical experiment δ_{ma} and δ_{mb} were found to be 10·12 cm. and 9·58 cm. respectively, whence

$$\therefore \left[\sqrt{\frac{\delta_{ma}}{\delta_{mb}}} - 1\right] = 0.028 \text{ and } R_1' = 2{\cdot}01 \times 10^6 \text{ ohm.}$$

Similar experiments with the d.c. condenser filled with benzene, chloroform, and carbon tetrachloride gave values for R′ which are practically the same as that found above for air, showing incidentally that the radio-frequency resistance of the condenser in the present experiments is due mainly to the solid insulation.

Using this value of R_1', we find that $2R/R_1'$ is of the order of 5×10^{-6}, and is therefore negligible in comparison with unity; $4\omega_1^2L^2/(2R+R_1')^2$ is of the order of 3×10^{-8}, which is also negligible in comparison with unity.

We are therefore justified in assuming that the right-hand sides of equations (2.6) and (2.8) are equal to $1/\omega_1^2L$ and $1/\omega_2^2L$ respectively, and a similar remark will apply to the corresponding equations for the cases where d.c. condenser is used with carbon tetrachloride and chloroform, *i. e.*, the resonant capacitances throughout are given by the simple Kelvin formula.

With this simplification we obtain from (2.5) and (2.6)

$$C_{1a}-C_{1b}=C'_{a1}, \quad . \quad . \quad . \quad . \quad . \quad (2.5\,a)$$

and from (2.7) and (2.8)

$$C_{2a}-C_{2b}=C'_{s}. \quad . \quad . \quad . \quad . \quad . \quad (2.6\,a)$$

These two equations, together with equation (2.1), give the replaceable air capacitance C'_{ra} in terms of the readings of the variable condenser and ϵ.

Carrying out a similar series of experiments with the liquid of unknown d.c. ϵ substituted for the standardizing liquid, we obtain similar equations for C'_u and C'_{a2}, which, in conjunction with equation (2.2), yield ϵ.

The above method involves the determination of the reading of the variable condenser which gives maximum galvanometer deflexion; if this is done directly the accuracy with which the reading can be determined is necessarily small, since at maximum galvanometer deflexion the slope of the resonance curve is zero. To avoid this difficulty we may proceed as follows. Suppose that on the resonance curve we draw chords parallel to the capacitance axis; the chord corresponding to a deflexion δ or a current I will intersect the resonance curve at two points corresponding to *total* capacitances C_1 and C_2 say; the capacitance corresponding to the mid-point of the chord will be $C_i=\frac{1}{2}(C_1+C_2)$. By choosing a value of δ which is about 2 to 5 per cent.

less than the maximum deflexion δ_m the points of intersection of the chord and curve will fall on a portion of the curve where the slope is great, and consequently C_1, C_2, and C_i can be located with much greater accuracy than C_m, the *total* capacitance at resonance. Jezewski has shown [9] that C_i is given by the equation

$$C_i = L \Big/ \left(\omega^2 L^2 + R^2 - \frac{E_m^2}{I^2}\right). \quad . \quad . \quad . \quad (2.11)$$

From equation (2.9)

$$E_m^2 = I_m^2 \left(R + \frac{L}{R'C_m}\right)^2,$$

whence

$$C_i = \frac{L}{\omega^2 L^2 + R^2 - \dfrac{\delta_m}{\delta}\left(R + \dfrac{L}{R'C_m}\right)^2}. \quad . \quad . \quad (2.12)$$

In the resonant circuit used in these experiments, $\omega^2 L^2$ is of the order of $2{\cdot}8 \times 10^5$, R of the order of 5 ohm, δ_m/δ of the order of 1·04, and $\left[R^2 - \frac{\delta_m}{\delta}\left(R + \frac{L}{R'C_m}\right)^2\right]$ of the order of unity; we may therefore assume the denominator to be $\omega^2 L$ without committing an error greater than 1 in $2{\cdot}8 \times 10^5$. C_i then becomes equal to C_m, and because of its greater accuracy this mid-chord method has been used throughout the present work for locating resonance capacitancies.

As it stands this method implies finding two values of the capacitance of the variable air condenser, one on either side of C_m, which give equal galvanometer readings. The lag of the vacuo-thermojunction makes the direct application of this principle inconvenient in practice, and the following practical method has been adopted. The reading of the variable air condenser for maximum deflexion is first found approximately, and then, by suitable choice of condenser settings, four points on the steep portions of the deflexion-condenser reading curve are obtained; two points are chosen so as to lie on the upper side of the resonance setting and the other two on the lower side. In practice the two points on the same side of the resonance setting differ in capacitance by $\frac{1}{2}°$

on the variable condenser scale, and this corresponds to about 0·73 $\mu\mu$F.; the points are chosen so as to lie approximately symmetrically with respect to the resonance point. The two points on either side of the resonance setting are then joined together by a straight line, giving two straight lines on either side of the resonance setting. In the immediate neighbourhood of the resonance point the sides of the deflexion-condenser reading curve are very steep, and the curve is practically symmetrical with respect to the ordinate through the resonance point : on this account the mid-point of a chord (parallel to the capacitance axis) of the actual resonance curve can be taken to coincide with the mid-point of a similar chord between the two straight lines mentioned above. Thus to find the resonance setting we read off from our straight line graph the two values of the variable condenser readings which correspond to a certain deflexion, and the mean of these readings is taken as the resonance setting. In order to obtain a good average the process is carried out for three values of the deflexion, and in practice the extreme values obtained never differ by more than 0·04° on the condenser scale ; since this corresponds to about 0·06 $\mu\mu$F. and the total capacitance in the circuit is of the order of 800 $\mu\mu$F., the accuracy of setting to a resonance point by this method is better than 1 in 10,000.

III. *The Valve Oscillator.*

As shown above, the frequency of the source of radio-frequency current used in these experiments need not remain constant for long lengths of time ; it is sufficient that it should remain constant for periods of the order of five minutes or so. Nevertheless frequency constancy is desirable, since it reduces errors in condenser calibration by making quantities such as C_{1a} and C_{2a} of equations (2.5) and (2.7) equal. On account of its good frequency stability it was decided to use a dynatron form of valve oscillator as the master oscillator in the source.

The main requirement as regards the source is that its frequency should be independent of the load imposed on it by the resonant circuit to which it is coupled. This is best achieved by coupling the master oscillator to the grid circuit of a second valve and using this second valve as an amplifier, taking care that the load imposed

on the master oscillator by the amplifier is as small as possible. It was decided to use a tuned-anode amplifier, and details of the complete source are shown in fig. 2.

The dynatron oscillator valve V_1 is a Mazda 2 v. 0·15 amp. screen-grid valve with the oscillatory circuit L_1C_1 in series with the anode. The inductance L_1 is an Igranic 75-turn coil of the type formerly used in wireless receivers, whilst the condenser C_1 is a wireless receiver type of variable air condenser fitted with a slow-motion

Fig. 2.

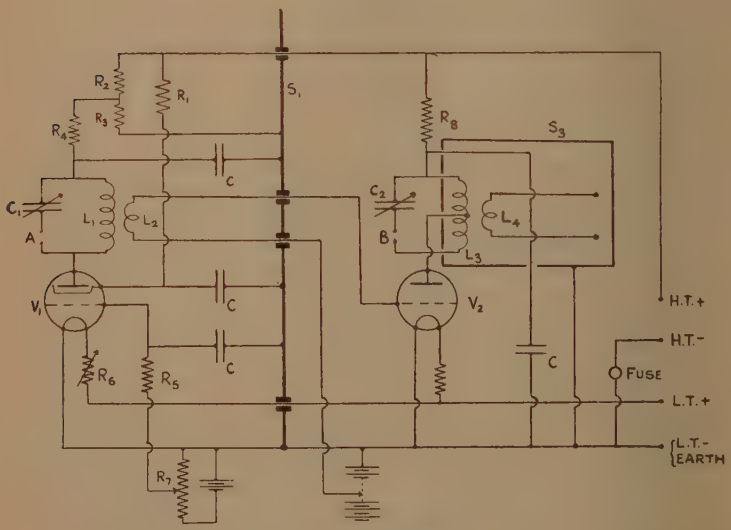

The valve oscillator.

dial; the maximum value of C_1 is 0·0005 μF. The gap A in the condenser branch of the oscillatory circuit L_1C_1 is connected to a "jack-socket" whose "jack" is connected to a vacuo-thermojunction with its associated galvanometer. When the "jack" is inserted in the socket the heater circuit of the vacuo-thermojunction is connected in the gap, and thus serves to detect and measure radio-frequency currents in the oscillatory circuit; when the "jack" is withdrawn the gap is short-circuited.

Preliminary experiments showed that variation of the voltages applied to the various electrodes of V_1 produced frequency variations; it was found possible, however, to find optimum values for these voltages, and when working at these values small changes in operating voltages produced but little effect on the frequency. The optimum values found were:—Filament voltage $=1{\cdot}9$ v.; grid voltage $=-2{\cdot}5$ v.; anode voltage $=40$ v.; screen-grid voltage $=120$ v. The high tension voltages were supplied by a 150 v. battery of accumulators, and in order to decouple the various circuits and to apply the appropriate voltages to the screen-grid and anode the resistances R_1 (4000 ohm), R_2 (20,000 ohm), R_3 (10,000 ohm), and R_4 (5,000 ohm), together with the condensers C (each 2 μF.), were used. The appropriate grid bias was obtained by tapping from a 10,000 ohm potentiometer R fed by a dry battery, the resistance R_5 (600 ohm) and the condenser C (2 μF.) serving to decouple this circuit. The low tension supply is from a 6 v. accumulator battery, and the rheostat R_6 serves to reduce this voltage to the working voltage of $1{\cdot}9$ v.

The amplifying valve V_2 is a Marconi-Osram L.S. 5 valve, and its grid terminal is connected to one end of the 40-turn Igranic coil L_2, which is magnetically coupled to L_1; the coupling between L_1 and L_2 is arranged to be as weak as is consistent with adequate output from the source. The remaining end of L_2 is connected to the grid-bias battery, which applies a negative bias of $10\frac{1}{2}$ v. to the grid of V_2. The tuned anode circuit of V_2 consists of a condenser C_2 similar to C_1 and a Lewcos 100 C.T. coil L_3, the anode of the valve being connected to the centre tap of the coil. The resistance R_8 (2,000 ohm) and the condenser C (2 μF.) serve to decouple this circuit. A vacuo-thermojunction (with its associated galvanometer) is permanently connected in the gap B in the condenser branch of the oscillatory circuit L_3C_2; this vacuo-thermojunction is used as an indicator to enable the L_3C_2 circuit to be tuned to the master oscillator frequency. The radio-frequency current in this circuit was usually of the order of 40 mA. The coil L_4 consists of about 20 turns of no. 22 S.W.G. copper-wire wound in a single layer on an ebonite former of about 1 cm. diameter; this coil functions as an inducing coil to the resonant circuit used in the d.c. measurement.

Three earthed aluminium boxes serve to screen the source. The first box contains the components to the left of S_1, whilst the second box contains the components to the right of S_1 with the exception of L_3 and L_4, which are contained in the third box S_3. The stability of V_2 and its associated circuits can be tested by applying all voltages except the filament voltage of V_1; in such a test no radio-frequency current was generated in the anode circuit of V_2, showing that V_2 and its associated circuits were stable and did not oscillate of their own accord.

To test whether the frequency of the source varied with the load the oscillator was coupled to a sensitive absorption wave-meter of the resonant circuit type, and to another resonant circuit which could be tuned to the source; the frequency of the source, as found by the wave-meter, was the same to within 1 in 5,000 whether the second circuit was tuned or untuned to the source.

The frequency range used in the present series of experiments was 350 to 390 kc. (wave-length range 860 to 770 m.).

IV. *The Dielectric Constant Condenser and the Screened Switches.*

The following conditions must be satisfied by a d.c. condenser used for comparative measurements :—

(1) It should be rigidly constructed, and the separation of the insulated and earthed plate systems should not be too small to diminish the effects of unavoidable changes in this separation.

(2) The insulated plate system and its leads should be perfectly screened.

(3) The solid material used for insulation should be arranged so that the electrostatic flux through the solid is the same whatever be the d.c. of the surrounding medium.

(4) The condenser must be constructed of a material which does not contaminate the liquid used.

(5) It should be capable of being fixed rigidly in a thermostat and of being filled *in situ* with liquid.

(6) It should be constructed so that a stream of pure dry air can be passed through it before, during, and after the introduction of the liquid.

(7) It should be capable of being raised to a temperature of about 30° C. for drying purposes.

(8) It should be constructed so that every portion of the contained liquid acquires the thermostat temperature.

These conditions (with the exception perhaps of (3)) are satisfied by the condenser which is shown to scale in plan in fig. 3 and in section in fig. 4 ; the details of the lid are shown in fig. 5, whilst the screened switching arrangements are shown in figs. 6 and 7. With the exception of the solid insulators the whole apparatus

Fig. 3.

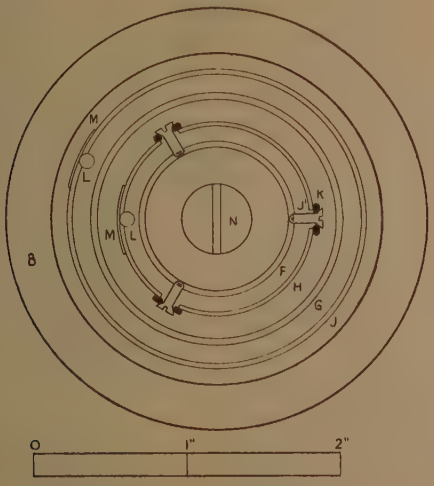

The dielectric constant condenser in plan.

is constructed of brass, all of which is chromium plated ; the use of a metal enables us to satisfy conditions (1), (2), (5), (7), and (8), whilst the liquids used were not contaminated by the chromium plating. In a series of experiments carried out in the summer of 1933 a condenser was used which was similar in construction but which was silver-plated ; when this condenser was dismantled at the end of the experiments the plating was found to have been badly attacked either by the liquids used in the experiments or by the alcohol and ether used for washing before drying. In the present

series the use of alcohol and ether was discontinued, and the drying carried out after washing with the liquid

Fig. 4.

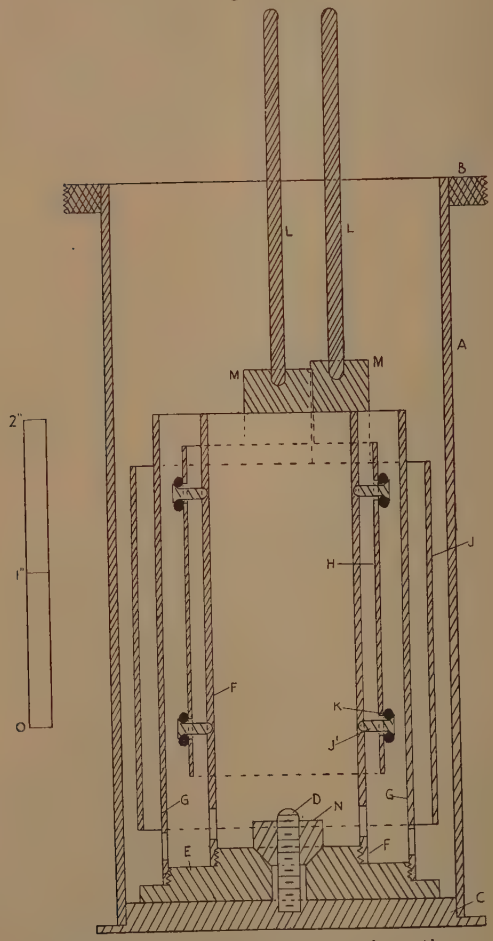

The dielectric constant condenser in section.

to be used in the experiment; when the condenser was dismantled at the end of the series no trace of contamination of the chromium plating was visible.

Referring to figs. 3 and 4, the condenser proper is seen to consist of two separate units—the container and the plate system. The container consists of a brass cylinder A closed at the lower end by a disk C, at whose centre a no. O B.A. vertical screw D is fixed; a screwed flange B is soldered to the upper end of the cylinder. The base of the plate system consists of a brass disk E, stepped and screwed as shown in fig. 4; this base can be firmly fixed to C by means of a conical nut N working on the screw D and bedding into a corresponding conical hole in E. Two coaxal cylinders F and G form the earthed plates of the condenser; these are screwed to the base E at their lower ends, and, to allow free circulation of liquid, a number of 3/16 in. diameter holes are drilled around their circumference just above the base. The two coaxal cylinders H and J form the insulated plates, and these are fixed to and insulated from the earthed plates F and G respectively; for the sake of clearness the method used for supporting and insulating the cylinders is shown for the inner pair only. In each of the earthed cylinders six no. 6 B.A. holes are tapped; three of these are at a distance of about $\frac{1}{2}$ in. from the upper end of the cylinder, and they are equally spaced along the circumference of the cylinder; the remaining three are similarly placed with respect to the lower end of the cylinder. Correspondingly placed clearing holes of 1/16 in. diameter are drilled in the appropriate insulated cylinder; glass washers K of about 1/32 in. internal diameter, about 3/32 in. external diameter, and about 1/16 in. thickness are then placed on the stems of the no. 6 B.A. taper-head screws J′, which are then screwed tightly home; care is taken that the various screws are adjusted so that the cylinders are approximately coaxal. This method of supporting and insulating the plates has proved entirely satisfactory in practice, since the replaceable air capacitance of the condenser has remained constant throughout the series of experiments.

To provide leads to the insulated cylinders short cylindrical sectors M of the appropriate radii are soldered to the cylinders, and to these are soldered 3/32 in. diameter brass rods L.

The details of the condenser lid are shown in fig. 5; it consists of a brass disk A stepped as shown, the dimensions being arranged so that it forms a good fit

on the mouth of the condenser container. The lid is fixed in position by a screwed cap (not shown) which works on the screwed flange B of fig. 4. Four holes, B, C, D, and E, are drilled through A; the holes B and C are tapped to fit the lower screwed ends of the brass cap F and the brass tube G respectively. The liquid under experiment is introduced into the condenser through B,

Fig. 5.

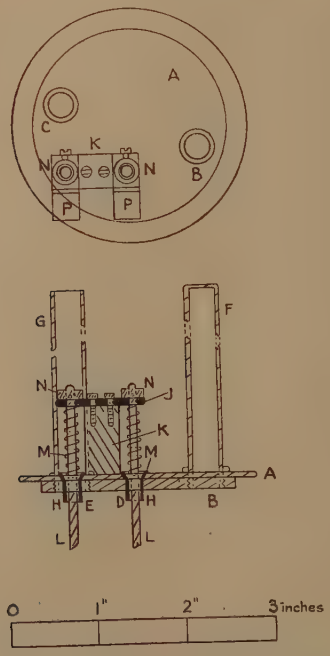

The lid of the dielectric constant condenser.

whilst pure dry air can be forced into the vessel through the tube G. The upper portions of the holes D and E are countersunk to a conical shape; pieces of glass tube H of the appropriate form fit into these holes, whilst the leads L from the insulated plates of the condenser pass through the tubes H. To prevent any possible sideplay in the leads they pass through tightly fitting holes in a piece of ebonite J which is fixed by two screws

on the upper surface of a brass block K, the lower surface of K being soldered to the upper surface of the lid A. The glass tubes H are kept in position by two springs M which are in compression between the glass tubes and the lower face of J. Two brass disks N are drilled and fitted with brass collars which fit on the upper ends of the leads L; these collars are provided with set-screws, so as to fix the disks in position on the leads. To each of the disks N is soldered a small rectangular piece of thin springy brass shim P; these pieces are used in conjunction with the switches to connect the leads either to earth or to the resonant circuit.

The switches are enclosed in a screening box which is also designed to support the d.c. condenser and to keep it fixed in position; the arrangement used is shown in plan and in section in fig. 6. The base consists of an annular brass ring A, to which is soldered a brass tube B. Two substantial bent wrought iron arms (not shown in fig.) are soldered to A; these are rigidly fixed to two tables on either side of the thermostat used, and they are adjusted so that A is a little above the water surface in the thermostat. The inner face of A is turned in the form of a step, as shown in the diagram, and its dimensions are adjusted so that the flange of the d.c. condenser can rest in the step. Two short screwed columns D are fixed to diametrically opposite points on A, and a brass strap C is drilled so that it fits on the screws cut on the upper portion of these columns. A strip of rubber is attached to the under surface of C, and when the condenser has been placed in position it is kept rigidly fixed by placing the strap C in position and securing it by the nuts E working on the screwed portion of D.

The lead F to the resonant circuit is brought into the screening box through a brass tube G which is soldered into the upper end of the tube B. An ebonite plug H serves to insulate the lead F, and the plug is prevented from rotating in the tube by three short brass screws. A piece of angle brass J is firmly fixed to the surface of H by means of two no. 4 B.A. brass screws, and contact is made between F and J by continuing F through a clearing hole in J and then bolting it down by the nut K.

The switch which connects F and J to the leads from the condenser is carried on the long brass pillars K′; at their lower ends these are fixed to the base plate A

and at their upper end a screw is cut. A brass strap L is drilled at its ends so that it can be fitted on the pillars

Fig. 6.

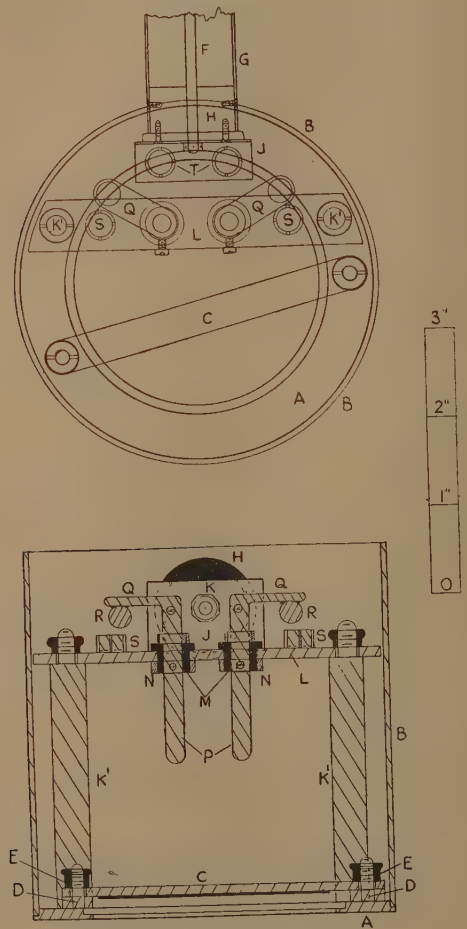

The switches and screening box.

K′ and can be bolted down by nuts working on the screwed portion of the pillars. Two ebonite bushes M are fitted into the strap L ; these also pass through brass collars N

which are soldered to L and which are provided with set-screws to prevent motion of the bushes. Two brass rods P pass through these bushes; at the upper ends of these rods brass arms Q are soldered, and, in turn, $\frac{1}{4}$ in. diameter steel balls R are soldered to the arms. Four saw-cuts are made in short pieces of brass tube S, $\frac{1}{4}$ in. internal diameter, and these are then soldered on L; they are placed and adjusted so that the balls R can be pushed home into them when the arms Q are properly placed. Two similar pieces of tube T are soldered on the angle plate J, and they also are adjusted and placed so that the balls R can be pushed home into them when the arm Q is properly placed. The height of the pillars K′ and the position of the springy brass rectangles P of fig. 5 are adjusted so that when the balls R are placed in the tubes S or T, contact is made between the springy brass rectangles connected to the insulated plates of the condenser and the lower ends of the switch rods P; thus either of the insulated plates of the condenser can be earthed or connected to the resonant circuit at will. It is true that this type of switch possesses considerable capacitance; this, however, is unimportant, since the switch capacitance is eliminated by the experimental method used. The important point is that the switch capacitance should remain constant during the experiment with any particular sample of liquid, and the above design does fulfil this condition.

When the d.c. condenser has to be placed in position the straps C and L are removed and the condenser lowered; the straps are then placed in their appropriate positions, and the condenser is manipulated by means of the long tube and cap of fig. 5, so that the springy brass strips of fig. 5 are correctly placed with respect to the switch rods P of fig. 6. When this has been done the straps are screwed down tightly.

It is clear that the above arrangement of insulated plates and switches gives three possible arrangements for use in d.c. measurement, viz. :—

(i.) Outer and inner insulated plates connected in parallel and both used for d.c. measurement.

(ii.) Inner insulated plate permanently earthed, outer insulated plate alone used for d.c. measurement.

(iii.) Outer insulated plate permanently earthed, inner insulated plate alone used for d.c. measurement.

In the experiments the third arrangement was not used, since the capacitance was too small; the other two arrangements were used, and they yield two independent values of the d.c. with any particular sample of liquid. In the second arrangement the gross capacitance of the condenser filled with air, together with leads and switches, was about 69 $\mu\mu$F., the replaceable air capacitance being about 60 $\mu\mu$F.; in the first arrangement the gross capacitance was about 122 $\mu\mu$F., the replaceable air capacitance being about 104 $\mu\mu$F.

The volume of liquid used for a measurement was sufficient to reach well above the tops of the cylindrical plates of the condenser, and the quantity required for this purpose was about 200 c.c.

V. *The Resonant Circuit.*

The main inductance coil of the resonant circuit was a stranded wire coil whose inductance was about 0·17 mH. and whose direct current resistance was 0·8 ohm. The vacuo-thermojunction used was one of 1·25 ohm heater resistance and 4·29 ohm couple resistance; it was used in conjunction with a Tinsley portable galvanometer of 7 ohm resistance whose sensitivity was 3·5 mm./μA.; although greater sensitivity could have been obtained with a more sensitive galvanometer the sensitivity of the galvanometer used was adequate, and its use enabled readings to be taken in rapid succession. The radio-frequency current in the resonant circuit at resonance was of the order of 5 mA.

The variable condenser system consisted of two Sullivan variable air condensers permanently connected in parallel; in the case of both condensers the capacitance was a linear function of scale-reading. The useful range of the larger condenser was from 100 to 1200 $\mu\mu$F., and the change in capacitance per degree rotation was about 7 $\mu\mu$F./degree; the smaller condenser was used between the 30° and 150° readings, corresponding to a capacitance range of 80 to 260 $\mu\mu$F. with a capacitance change of 1·4$_5$ $\mu\mu$F. per degree rotation. In order to lighten the labour of calibration the larger condenser was used as a semi-variable condenser, and changes in its capacitance were only

made between four definite selected scale-readings, these being chosen so that the capacitance difference between consecutive selected scale-readings was about 140 $\mu\mu$F. or 95° on the scale of the smaller condenser.

It will be noted that the expression obtained in the second section for the d.c. in terms of the experimentally observed quantities involves only the ratio of capacitancies, and hence the precise unit in which capacitance is expressed is immaterial. For convenience the unit chosen was one degree of the scale of the smaller condenser, and the three selected intervals on the larger condenser were expressed and found in terms of this unit. The smaller condenser was calibrated by dividing its scale into equal increments of capacitance, these equal increments being determined by the well-known method of finding the variable condenser readings for resonance with and without a small fixed capacitance which is equivalent to about 5° of the condenser scale. In these experiments, to allow for any correction due to lead inductance [11], the small calibrating condenser was mounted in the screening box used with the d.c. condenser, and was arranged so that it could be switched in and out of circuit by means of the switch used with the d.c. condenser. Several calibration curves were found in the course of the experiments, and all agreed within the limits of experimental error.

The main requirement of the resonant circuit is that its electrical characteristics should remain constant, and this can only be secured by careful screening, rigid construction, and avoidance of ferromagnetic substances in all parts of the circuit. The main inductance and the vacuo-thermojunction were enclosed in a stout earthed copper box; the coupling coil was enclosed in one of the screening boxes of the source; the variable condensers were screened by earthing the appropriate terminal and the d.c. condenser was screened by the method described above. To secure mechanical rigidity all components were screwed down wherever possible and all connexions in the resonant circuit were made with copper or brass rod whose diameter exceeded 3/16 in. Whenever a lead was to be taken from one screening box to another the method adopted was that shown in part in fig. 5; the lead, in the form of a brass rod, passed through ebonite plugs in the ends of a wider brass tube;

a screw thread is cut on the projecting ends of the rod, which is then firmly clamped by nuts screwed on the rod.

VI. *Purification of Materials.*

(i.) *Benzene.*

Commercially pure benzene, together with concentrated sulphuric acid, were shaken on a mechanical shaker for two or three days in order to free the benzene from thiophene ; to check the efficacy of the process the benzene was tested for thiophene by the indophenene reaction. The benzene was then washed with 2N alkali until free from acid, and finally with water until free from alkali. It was then dried overnight over calcium chloride, and finally fractionally frozen five times with the addition of a trace of phosphorus pentoxide. The product thus obtained was stored in the dark until required, when it was distilled over phosphorus pentoxide in a current of dry air. With the benzene used in the present experiments the preliminary purification up to and including the freezing was carried out in the Christmas vacation of 1933–34, the benzene being used in the summer vacation of 1934.

(ii.) *Carbon Tetrachloride.*

The commercially pure product was washed twice with 2N alkali (sodium hydroxide), then twice with dilute hydrochloric acid, and finally with water until free from acid. It was then dried overnight over calcium chloride, filtered, and the product obtained stored in the dark until required. Five samples were used ; samples no. 1, 2 and 4 (*v.* Tables of Results) were purified in this way in the Easter vacation of 1933 and used in the summer vacation of 1934 ; samples no. 3 and 5 were purified a few days before use, the calcium chloride being replaced by sodium sulphate (anhydrous) as a drying agent. The final stage in the purification consisted in distillation over phosphorus pentoxide in a current of dry air.

(iii.) *Chloroform.*

Seven samples were used. The first four samples were washed with dilute alkali (sodium hydroxide), dilute hydrochloric acid, and water. Samples no. 1 and 2

were dried over sodium sulphate, whilst samples no. 3 and 4 were dried over calcium chloride. The remaining samples were washed with dilute sodium hydroxide, dilute sulphuric acid, and water; sample no. 5 was not given a preliminary drying, whilst sample no. 6 was dried over anhydrous sodium sulphate, and sample no. 7 over calcium chloride. All samples were purified a few days before use, and were stored in the dark until required; the final stage in the purification consisted in distillation over phosphorus pentoxide in a current of dry air. It may be added that some samples of chloroform which had been purified a month or so before they were to be used showed decided signs of chemical decomposition, chlorine gas having been liberated in the vessel in which the liquid was kept; it was for this reason that the samples used in the present work were not purified until a few days before they were required.

From the chemical standpoint the main difficulty in the determination of d.c. arises from the presence of water in the substances used; with liquids of comparatively low d.c., such as those used in the present work, the effect of traces of water is likely to be pronounced, since its d.c. is in the neighbourhood of 80. As regards the solubility of the substances used in the present work in water, according to Heilborn [12], carbon tetrachloride is practically insoluble in water, 100 volumes of benzene dissolve 0·082 volumes of water at 22° C., whilst chloroform is soluble to 1 per cent. in water at 15° C. The magnitude of the effect of absorption of water on the d.c. can be judged from measurements of the d.c. of dry benzene and benzene-water solutions which have been carried out by Williams [13] and by Müller [14]. According to Williams the d.c. at 25° C. increased from 2·282 for dry benzene to 2·294 for benzene saturated with water (0·073 gm. water to 99·927 gm. benzene). According to Müller at 20° C. a solution of about 10 mg. water in 200 gm. benzene has a d.c. which is about 1 in 1000 greater than that of dry benzene, whilst a solution of about 17 mg. water in 200 gm. benzene has a d.c. which is about 3·5 in 1000 greater than that of dry benzene.

The magnitude of the effect will naturally be greater in the case of chloroform, and it is clear that, in the case of benzene and chloroform especially, the liquids must

be obtained in the dry state and must be prevented from coming into contact with anything which might cause the absorption of moisture. For this reason the final stage of purification of the liquids by distillation over phosphorus pentoxide in a current of dry air was not carried out until half an hour or so before the liquid was introduced into the test condenser.

For the same reason the use of water was avoided in washing the d.c. condenser; the procedure adopted was to empty the condenser as soon as the experiment with a particular liquid was completed and then allow it to drain overnight; the liquid used in a particular experiment was not used a second time but was kept for future washing of the condenser. In the morning the d.c. condenser was first carefully washed with a previously used sample of the liquid under test; it was then allowed to drain, and finally dried by being placed in an electrically heated oven at about 30° C., a current of pure dry air being passed through it. After an hour or so the oven was allowed to cool, and when the d.c. condenser had reached room-temperature it was placed in position in the thermostat, the current of pure dry air still passing through it.

In these experiments it is clearly essential that the volume of liquid used in the d.c. condenser should be the same in every case, and to ensure this the liquid is run into the condenser from a graduated pipette fitted with a stopcock; in order to avoid contamination the stopcock is lubricated with phosphorus pentoxide grease. The liquid (contained in the collecting vessel used in the distillation) is forced into the pipette by a current of dry air, the upper end of the pipette also being connected to a drying train; the arrangement used is very similar to that described in Sudborough and James, 'Practical Organic Chemistry,' fig. 60, except that in the present instance the apparatus was constructed entirely of glass to avoid contamination of the liquid.

The current of dry air through the d.c. condenser is maintained whilst the liquid is being introduced and is kept on until the experiment is over; by this means the liquid comes into contact with dry vessels and dry air only, and its chance of absorbing water is thus very small.

In order to obtain a measure of the purity of the samples used it was decided to determine the refractive index (R.I.) of the various samples ; the R.I. was chosen in preference to other physical properties partly on account of the intimate connexion between d.c. and R.I. and partly on account of the ease and accuracy with which it can be measured. The measurement of R.I. was carried out by means of a Zeiss Pulfrich refractometer using the radiation from a sodium-vapour lamp. The R.I. was determined at a temperature in the neighbourhood of 19·7° C., and in the tables given below the values have been reduced to 20° C., using the temperature coefficients given in the International Critical Tables (I.C.T.). No special precautions were taken to prevent absorption of water by the organic liquid in these experiments, the liquid cell being always cut off from communication with the air by a cork washer placed on top of the cell under the water circulating tube.

VII. *Experimental Results.*

As mentioned in Section I. d.c.s were measured at two temperatures in the neighbourhood of 20° and 25° C. ; these temperatures were determined accurately by a thermometer calibrated at the N.P.L., and were found to be 20·00±0·03° C. and 24·88±0·03° C. respectively.

The quantities given directly by experiment are, in the notation of Section II., $C'_{ra}(\epsilon_s-1)$ for the calibrating liquid and $C'_{ra}(\epsilon-1)$ for the other liquids, these quantities being determined from equations (2.1), (2.2), (2.5 *a*), (2.6 *a*), and similar equations. As previously stated all capacitances are expressed in terms of the mean capacitance per degree rotation of the smaller variable air condenser as the unit ; this corresponds approximately to 1·45 $\mu\mu$F.

(a) *Calibration.*

The value of C'_{ra} was found on three occasions in the course of the work, using three different samples of pure benzene and assuming Hartshorn and Oliver's values for its d.c. ; these values are

(i.) at 20·00° C. $\epsilon_s=2{\cdot}282_5$;

(ii.) at 24·88° C. $\epsilon_s=2{\cdot}272_8$.

The results obtained are summarized in Tables I. (i.) and I. (ii.), the former relating to arrangement (i.) of Section IV.—both sets of plates used in parallel—and the latter to arrangement (ii.) of the same Section—outer plate only used. The second column in the Table gives n_{20}, the R.I. at 20° C. for sodium light, the reduction to 20° C. being carried out using the coefficient (-64×10^{-5}) given in the I.C.T.

TABLE I. (i.).

Sample no.	n_{20}.	Temp. (° C.).	$(\epsilon_s-1)C'_{ra}$.	C'_{ra}.
1.....	$1{\cdot}5012_2$	20·00	$90{\cdot}83_9$	$70{\cdot}82_3$
		24·88	$89{\cdot}94_8$	$70{\cdot}66_3$
2.....	$1{\cdot}5011_9$	20·00	$90{\cdot}70_2$	$70{\cdot}71_8$
		24·88	$90{\cdot}00_5$	$70{\cdot}70_8$
3.....	$1{\cdot}5010_5$	20·00	$90{\cdot}96_7$	$70{\cdot}92_5$
		24·88	$90{\cdot}27_8$	$70{\cdot}92_2$

The mean values of $(\epsilon-1)\,C'_{ra}$ and C'_{ra}, together with their probable errors calculated according to the method of least squares, are

(*a*) at 20° C. $(\epsilon_s-1)\,C'_{ra}=90\ 83_6\pm0{\cdot}05_1$; $C'_{ra}=70{\cdot}82_2\pm0{\cdot}04_0$;

(*b*) at 24·88° C. $=90{\cdot}07_7\pm0{\cdot}06_8$; $=70{\cdot}76_4\pm0{\cdot}05_3$.

TABLE I. (ii.).

Sample no.	n_{20}.	Temp. (° C.).	$(\epsilon_s-1)C'_{ra}$.	C'_{ra}.
1.....	$1{\cdot}5012_2$	20·00	$52{\cdot}76_0$	$41{\cdot}13_5$
		24·88	$52{\cdot}24_3$	$41{\cdot}04_1$
2.....	$1{\cdot}5011_9$	20·00	$52{\cdot}68_5$	$41{\cdot}07_7$
		24·88	$52{\cdot}27_3$	$41{\cdot}06_5$
3.....	$1{\cdot}5010_5$	20·00	$52{\cdot}85_6$	$41{\cdot}21_0$
		24·88	$52{\cdot}38_6$	$41{\cdot}15_5$

The mean value of n_{20} is $1{\cdot}5011_5$; the value given in the I.C.T. is 1·501, and in Landolt and Börnstein 1·50144. The value of the R.I. of the samples of benzene used for calibration are thus seen to be in satisfactory agreement with the accepted values.

Whence mean values and probable errors are

(*a*) at 20·00°C. $(\epsilon_s-1)C'_{ra}=52{\cdot}76_7\pm0{\cdot}03_3$; $C'_{ra}=41{\cdot}14_1\pm0{\cdot}02_5$;

(*b*) at 24·88°C. $=52{\cdot}30_1\pm0{\cdot}02_9$; $=41{\cdot}08_7\pm0{\cdot}02_3$.

It is clear from the above results that the probable error nowhere exceeds 1 in 1000, its average value in fact being nearer 1 in 2000.

(b) *Carbon Tetrachloride.*

The results obtained with the five samples purified as described in the preceding Section are given in Tables II. (i.) and II. (ii.), the former relating to arrangement (i.) and the latter to arrangement (ii.).

TABLE II. (i.).

Sample no.	n_{20}.	Temp. (° C.).	$(\epsilon-1)C'_{ra}$.	ϵ.
1.....	$1{\cdot}4603_4$	20·00	$87{\cdot}69_1$	$2{\cdot}238_2$
		24·88	$86{\cdot}89_4$	$2{\cdot}227_9$
2.....	$1{\cdot}4603_6$	20·00	$87{\cdot}54_7$	$2{\cdot}236_2$
		24·88	$86{\cdot}89_9$	$2{\cdot}228_0$
3.....	$1{\cdot}4602_2$	20·00	$87{\cdot}61_6$	$2{\cdot}237_1$
		24·88	$86{\cdot}93_6$	$2{\cdot}228_6$
4.....	$1{\cdot}4603_0$	20·00	$87{\cdot}51_7$	$2{\cdot}235_7$
		24·88	$86{\cdot}75_2$	$2{\cdot}226_0$
5.....	$1{\cdot}4603_0$	20·00	$87{\cdot}46_0$	$2{\cdot}234_9$
		24·88	$86{\cdot}76_6$	$2{\cdot}226_2$

These figures given mean values and probable errors as follows :—

(*a*) at 20·00° C. $\epsilon=2{\cdot}236_4\pm0{\cdot}000_4$;

(*b*) at 24·48° C. $\epsilon=2{\cdot}227_3\pm0{\cdot}000_3$.

TABLE II. (ii.).

Sample no.	n_{20}.	Temp. (° C.).	$(\epsilon-1)C'_{ra}$.	ϵ.
1.....	$1{\cdot}4603_4$	20·00	$50{\cdot}88_1$	$2{\cdot}236_8$
		24·88	$50{\cdot}39_9$	$2{\cdot}226_6$
2.....	$1{\cdot}4603_6$	20·00	$50{\cdot}79_7$	$2{\cdot}234_7$
		24·88	$50{\cdot}39_4$	$2{\cdot}226_6$
3.....	$1{\cdot}4602_2$	20·00	$50{\cdot}84_7$	$2{\cdot}236_0$
		24·88	$50{\cdot}44_6$	$2{\cdot}227_8$
4.....	$1{\cdot}4603_0$	20·00	$50{\cdot}76_3$	$2{\cdot}234_9$
		24·88	$50{\cdot}32_2$	$2{\cdot}224_8$
5.....	$1{\cdot}4603_0$	20·00	$50{\cdot}82_1$	$2{\cdot}235_3$
		24·88	$50{\cdot}37_9$	$2{\cdot}226_2$

The mean values and probable errors are as follows :—

(*a*) at 20·00° C. $\epsilon = 2{\cdot}235_5 \pm 0{\cdot}000_3$;

(*b*) at 24·88° C. $\epsilon = 2{\cdot}226_4 \pm 0{\cdot}000_3$.

We may note that the discrepancy between the values obtained by arrangements (i.) and (ii.) amounts to less than 1 in 2,000, and since the values so obtained are independent results it shows that the systematic error in the method is small. It is also clear that the results given by samples 3 and 5 are in agreement with those given by samples 1, 2, and 4, which were purified on different occasions and by different methods (*v.* Section VI.).

Taking the mean of the results obtained by arrangements (i.) and (ii.) we obtain :—

(*a*) at 20·00° C. $\epsilon = 2{\cdot}236_0$;

(*b*) at 24·88° C. $\epsilon = 2{\cdot}226_9$.

Denoting the temperature coefficient of d.c. by $(d\epsilon/d\theta)$, we obtain from the above

$$\frac{d\epsilon}{d\theta} = -0{\cdot}00186_5,$$

giving for the final values of the d.c. at the two standard temperatures of 20° C. and 25° C.

(*a*) at 20° C. $\epsilon_{25} = 2{\cdot}236_0$;

(*b*) at 25° C. $\epsilon_{20} = 2{\cdot}226_7$.

The mean value of n_{20} is $1{\cdot}4603_0$, in excellent agreement with the value of 1·460 given in the I.C.T. and the value of $1{\cdot}4607_2$ given in Landolt and Börnstein.

(c) *Chloroform.*

The results obtained with the seven samples purified as described in the preceeding Section are given in Tables III. (i.) and III. (ii.), the former relating to arrangement (i.) and the latter to arrangement (ii.).

These figures give mean values and probable errors as follows :—

(*a*) at 20·00° C. $\epsilon = 4{\cdot}797_5 \pm 0{\cdot}001_1$;

(*b*) at 24·88° C. $\epsilon = 4{\cdot}711_3 \pm 0{\cdot}001_3$.

TABLE III. (i.).

Sample no.	n.	Temp. (° C.).	$(\epsilon-1)C'_{ra}$.	ϵ.
1.....	$1{\cdot}4460_3$	20·00	$268{\cdot}94_9$	$4{\cdot}796_1$
		24·88	$262{\cdot}38_5$	$4{\cdot}707_3$
2.....	$1{\cdot}4460_2$	20·00	$268{\cdot}76_1$	$4{\cdot}794_9$
		24·88	$262{\cdot}44_7$	$4{\cdot}709_0$
3.....	$1{\cdot}4460_3$	20·00	$269{\cdot}30_5$	$4{\cdot}802_6$
		24·88	$262{\cdot}92_3$	$4{\cdot}715_4$
4.....	$1{\cdot}4459_5$	20·00	$269{\cdot}33_8$	$4{\cdot}803_0$
		24·88	$263{\cdot}13_0$	$4{\cdot}718_4$
5.....	$1{\cdot}4460_2$	20·00	$269{\cdot}03_3$	$4{\cdot}798_7$
		24·88	$262{\cdot}76_5$	$4{\cdot}713_4$
6.....	$1{\cdot}4459_8$	20·00	$268{\cdot}44_5$	$4{\cdot}790_3$
		24·88	$262{\cdot}09_3$	$4{\cdot}703_7$
7.....	$1{\cdot}4461_5$	20·00	$268{\cdot}83_4$	$4{\cdot}795_8$
		24·88	$262{\cdot}62_5$	$4{\cdot}711_3$

TABLE III. (ii.).

Sample no.	n.	Temp. (° C.).	$(\epsilon-1)C'_{ra}$.	ϵ.
1.....	$1{\cdot}4460_3$	20·00	$156{\cdot}03_9$	$4{\cdot}792_8$
		24·88	$152{\cdot}26_4$	$4{\cdot}705_7$
2.....	$1{\cdot}4460_2$	20·00	$155{\cdot}88_6$	$4{\cdot}789_3$
		24·88	$152{\cdot}20_8$	$4{\cdot}704_5$
3.....	$1{\cdot}4460_3$	20·00	$156{\cdot}35_3$	$4{\cdot}800_7$
		24·88	$152{\cdot}59_6$	$4{\cdot}714_0$
4.....	$1{\cdot}4459_5$	20·00	$156{\cdot}47_5$	$4{\cdot}803_5$
		24·88	$152{\cdot}83_3$	$4{\cdot}719_6$
5.....	$1{\cdot}4460_2$	20·00	$156{\cdot}20_8$	$4{\cdot}796_8$
		24·88	$152{\cdot}57_8$	$4{\cdot}712_5$
6.....	$1{\cdot}4459_8$	20·00	$155{\cdot}87_5$	$4{\cdot}789_0$
		24·88	$152{\cdot}17_5$	$4{\cdot}703_6$
7.....	$1{\cdot}4461_5$	20·00	$156{\cdot}13_6$	$4{\cdot}795_3$
		24·88	$152{\cdot}47_6$	$4{\cdot}711_0$

From these results the following mean values and probable errors are obtained :—

(*a*) at 20·00° C. $\epsilon=4{\cdot}795_3\pm0{\cdot}001_4$;

(*b*) at 24·88° C. $\epsilon=4{\cdot}710_1\pm0{\cdot}001_5$.

We may note that the values given by the different samples are in good agreement ; this shows that the different methods used for purification (*v.* Section VI.) give consistent results. In addition the results given by the two independent arrangements (i.) and (ii.) differ

by less than 1 in 2,000, showing the absence of any large systematic error in the experiments.

Taking the mean of the results obtained by the two arrangements we obtain :—

(*a*) at 20·00° C. $\epsilon = 4{\cdot}796_4$;

(*b*) at 24·88° C. $\epsilon = 4{\cdot}710_7$.

From these results the value of the temperature coefficient is given by

$$\frac{d\epsilon}{d\theta} = -0{\cdot}0175_0,$$

giving for the final values of the d.c. at the two standard temperatures :—

(*a*) at 20° C. $\epsilon_{20} = 4{\cdot}796_4$; (*b*) at 25° C. $\epsilon_{25} = 4{\cdot}708_6$.

The mean value of n_{20} is $1{\cdot}4460_3$; the value given in the I.C.T. is 1·446, whilst that given in Landolt and Börnstein is $1{\cdot}4467_1$; the values found are thus in excellent agreement with the accepted values.

VIII. *Discussion of the Results.*

The excellent agreement between the two independent sets of results obtained both with carbon tetrachloride and with chloroform indicates that the main sources of error in the experiment have been eliminated. One possible source of error, however, remains to be discussed—the error due to the fact that the solid insulating material may not have been arranged so that the e.s. flux through the solid is the same whatever be the d.c. of the surrounding medium (*cf.* Section II. and Section IV., condition 3).

It is convenient to discuss this error from the standpoint of an expression given by Russell (' Alternating Currents,' vol. i. p. 12, equation *a*) for the capacitance of a condenser. Let the dielectric (of d.c. ϵ) between the two plates of the condenser be subdivided into a number of tubes of force ; at any point on one such tube let S be the normal cross-sectional area and ds an element of length of the tube. Let $\int_0^l \frac{ds}{S}$ represent the integral of $\frac{ds}{S}$ taken from the negative conductor ($s=0$) to the positive conductor

($s=l$). Then the capacitance C of the condenser is given by

$$C=\frac{\epsilon}{4\pi}\Sigma 1\Big/\left(\int_0^l \frac{ds}{S}\right), \quad . \quad . \quad . \quad . \quad . \quad (8.1)$$

the summation being taken over all the tubes in the field. It is clear from this equation that, quite apart from a change in capacitance due to a change in the d.c., a change in capacitance can be brought about by a change in $\Sigma 1\Big/\int_0^l\left(\frac{ds}{S}\right)$, *i. e.*, speaking generally, by a change in the length and cross-sectional area of unit tubes of force. Such a change is usually brought about by refraction of tubes of force when passing from one medium to another.

The bearing of this point on the present problem may be illustrated by reference to the particular case of a parallel plate condenser. Suppose that such a condenser consists of two parallel metal plates kept at a fixed distance apart by a single block of solid dielectric which is in the uniform region of the electric field. The total capacitance C_a of such a condenser when in air may be written

$$C_a=C_1+C_s, \quad . \quad . \quad . \quad . \quad . \quad . \quad (8.2)$$

where C_s represents the capacitance due to the solid spacing block and C_1 the capacitance due to the air in the remainder of the condenser.

If the condenser be now immersed in a dielectric of d.c. ϵ, and if the distribution of the tubes of force remains unchanged, *i. e.*, if refraction of the tubes of force is absent, then C_s will still represent the capacitance due to the solid block, and the capacitance due to the surrounding medium will be C_1. The total capacitance C_d under these conditions will therefore be

$$C_d=\epsilon C_1+C_s, \quad . \quad . \quad . \quad . \quad . \quad (8.3)$$

whence

$$(\epsilon-1)\,C_1=C_d-C_a, \quad . \quad . \quad . \quad . \quad . \quad (8.4)$$

which should be compared with equations (2.1) and (2.2), which form the basis of the method used in the present experiments. It is clear that under these conditions

the capacitance of the solid spacing block is eliminated by the process used in these experiments.

If, however, refraction of the tubes of force occurs when the condenser is immersed in the medium of d.c. ϵ, then the capacitance due to the solid spacing block will no longer be C_s, and, moreover, the distribution of tubes of force in the dielectric medium will differ from their distribution in air, and hence the capacitance due to this dielectric can no longer be written ϵC_1. The magnitude of the differences between the present and the former values of C_s and the medium capacitance will depend, amongst other factors, on the ratio of the d.c.s of the solid and the surrounding medium. It is thus clear that when refraction of lines of force occurs when the condenser is immersed in different media then equations (2.1), (2.2), and (8.4) are no longer correct, and the method adopted in the present experiments is no longer valid.

Two methods are available for overcoming this difficulty. The first method is to limit the amount of solid dielectric used to such an extent that, although the refraction effect may be present, the capacitance due to the solid spacing block is negligibly small in comparison with that due to the remainder of the condenser. The second method is to dispose the solid dielectric spacing blocks in such a way that refraction of the tubes of force is entirely absent.

With a cylindrical condenser the second method is difficult to apply, and hence the first method has been used in the present instance. With a parallel plate condenser it is, however, possible to apply the second method by using solid spacing blocks shaped in such a way that the faces exposed to the surrounding dielectric are perpendicular to the plates of the condenser, and by placing these blocks in the uniform region of the field ; the spacing blocks may, for example, be rectangular blocks with their edges parallel and perpendicular to the condenser plates, or, alternatively, cylinders with their generators perpendicular to the parallel plates.

Apart from the solid spacing blocks there is another effect which can bring about a somewhat similar change in the distribution of the tubes of force when the dielectric medium is changed. This effect can occur near the boundaries of the field, *e. g.*, near the outer edges of a parallel plate or a cylindrical condenser. In the neigh-

bourhood of such edges some of the tubes of force passing between the two condenser plates are situated in the space outside the plates owing to the inevitable fringing effect which always occurs at such edges. In order that the distribution of the tubes of force at such edges be independent of the d.c. of the medium in which they are immersed it is clearly necessary that this medium extends at least to the boundary of the field. If this is not the case then some of the outermost tubes will be partly in air and partly in the medium, and this will be accompanied by a change in the distribution of the tubes with the d.c. of this medium. This will bring about an effect similar to that discussed above in connexion with the solid spacing blocks, and therefore, in order that the theory on which the present work is based be valid, it is essential to ensure that the amount of liquid which is put into the condenser is sufficient to fill all the space which is occupied by tubes of force when the condenser is in air. This condition is amply fulfilled in the present experiments.

If the refraction effects discussed above are appreciable in the present work they would inevitably show themselves by a discrepancy between the results given by arrangements (i.) and (ii.), since the magnitudes of the effects would be different for the inner and outer cylinders on account of their different geometrical proportions. The agreement obtained thus shows that the design of the condenser is such that these effects are inappreciable, at least when dealing with d.c.s of the order of magnitude of carbon tetrachloride and chloroform.

In order to obtain further confirmation of this it was decided to carry out a supplementary experiment with the aid of a parallel plate condenser designed so that the two refraction effects should be negligible. The condenser consisted of three circular brass disks separated by rectangular glass blocks, with their faces perpendicular to the plates and situated in the uniform region of the field; this ensured that the first refraction effect was absent. The central plate was used as the insulated plate, whilst the two outer plates were earthed, and in order to avoid the second refraction effect the diameter of the central plate was considerably smaller than that of the outer plates. The plate system was rigidly constructed and was placed in an outer brass containing vessel.

The experiment consisted in finding the value of the product $(\epsilon-1)\,C'_{ra}$ (in the previous notation) for samples of carbon tetrachloride and chloroform with (*a*) the cylindrical condenser using arrangent (i.), (*b*) the cylindrical condenser using arrangement (ii.), and (*c*) the parallel plate condenser. If refraction effects are present in the two arrangements of the cylindrical condenser then the ratio of their replaceable air capacitances C'_{ra} to that of the parallel plate condenser should be different for carbon tetrachloride and chloroform because of the different dielectric constants of these liquids. Using identical samples of the two liquids in all cases will allow the ratio of the replaceable air capacitances to be identified with the ratio of the products $(\epsilon-1)\,C'_{ra}$.

Using two separate samples of each liquid in each condenser the ratio of the replaceable air capacitance of arrangement (i.) of the cylindrical condenser to that of the parallel plate condenser was found to be $1{\cdot}416_x$ with carbon tetrachloride and $1{\cdot}416_0$ with chloroform. The ratio of the replaceable air capacitance of arrangement (ii.) of the cylindrical condenser to that of the parallel plate condenser was found to be 0·8242 with carbon tetrachloride and 0·8236 with chloroform. These figures are in better agreement than 1 in 1000, and this satisfactory agreement confirms the fact that the refraction effects are negligible in the present instance.

IX. *Results of Previous Determinations.*

The results of previous determinations of the d.c. of carbon tetrachloride and chloroform are summarized in Tables IV. and V. The second and third columns of these Tables give the temperature at which the d.c.s were actually determined by the various experimenters, together with the results obtained at these temperatures; the fifth column gives the temperature coefficient $(d\epsilon/d\theta)$ where this quantity has been determined. The sixth column gives ϵ_{25}, the d.c. at 25° C., the reduction to this temperature having been made using the temperature coefficients found in the present work in cases where no temperature coefficient is given in the original work. The seventh column states whether the method used was absolute (A) or comparative (C), whilst the last column gives the value obtained or assumed for the d.c. of benzene;

Table IV.

Carbon Tetrachloride.

Author.	Date.	Temp. (°C.).	D.C.	$-\frac{d\epsilon}{d\theta}\times 10^3$.	ϵ_{25}.	A or C.	Method.	Freq.	D.C. of benzene.
I.C.T.	1925	20	2·24	1·4	$2\cdot23_3$	—	—	10^3-10^8	2·283
Harris [15]	1925	25	2·219	—	2·219	A	Br.	Audio	2·248
Francke [16]	1925	18	2·227	—	2·214	C	Res.	5×10^5	2·279
Williams & Krchma [17]	1926	25	2·230	—	2·230	A	Res.	10^6	2·282
Rolinsky [18]	1928	18	2·222	1·8	2·209	C	Res.	Radio	2·28
Stranathan [19]	1928	20	2·221	2·1	2·211	A	Heterodyne	$4\cdot76\times10^5$	2·279
Matsuike [20]	1929	25	2·197	1·5	2·197	A	—	Radio	2·267
Morgan & Lowry [21]	1930	20	2·241	2·0	2·231	A	Br.	10^3-10^5	2·284
Fairbrother [22]	1932	25	2·225	—	2·225	C	Res.	10^6	2·273
Müller [23]	1933	20	2·236	—	2·227	A	Res.	10^6	2·2820
Jenkins [24]	1934	25	$2\cdot227_7$	—	$2\cdot227_7$	C	Res.	6×10^5	2·2727
Author	1935	20	$2\cdot236_0$	1·87	$2\cdot226_7$	C	Res.	$3\cdot75\times10^5$	2·2825
		25	$2\cdot226_7$	—	—	—	—	—	2·2726

Table V.

Chloroform.

Author.	Date.	Temp. (° C.).	D.C.	$-\frac{d\epsilon}{d\theta}\times 10^2$.	ϵ_{25}.	A or C.	Method.	Freq.	D.C. of benzene.
I.C.T.	1925	20	5·05	1·85	$4{\cdot}95_7$	—	—	Audio	2·283
I.C.T.	1925	20	4·95	—	$4{\cdot}85_7$	—	—	10^6	2·283
I.C.T.	1925	20	4·93	—	$4{\cdot}83_7$	—	—	$6{\cdot}7\times 10^7$	2·283
Harris [15]	1925	25	4·642	—	4·642	A	Br.	Audio	2·248
Williams & Krchma [17]	1926	25	4·770	—	4·770	A	Res.	10^6	2·282
Matsuike [20]	1929	25	4·899	1·95	4·899	A	—	Radio	2·267
Ball [25]	1930	25	4·724	1·77	4·724	A	Br.	Audio	2·274
Morgan & Lowry [21]	1930	20	4·84	1·9	4·745	A	Br.	10^3-10^5	2·284
Jenkins [24]	1934	25	4·722	—	4·722	C	Res.	6×10^5	2·2727
Author	1935	20	4·796	1·75	4·709	C	Res.	$3{\cdot}75\times 10^5$	2·2825
		25	4·709	—	—	—	—	—	2·2726

this column is of some value in judging the accuracy of any particular determination, since the value given here can be compared with that given by Hartshorn and Oliver. The rows " I.C.T." give the values in the International Critical Tables, and are given here as a summary of determinations previous to the date of compilation (1925).

Referring to Table IV., and judging results by the care taken in the purification of materials and in the physical measurement, and by the value obtained for the d.c. of benzene, the work of Williams and Krchma [17], Morgan and Lowry [21], Fairbrother [22], Müller [23], and Jenkins [24] may be regarded as being of a high order of accuracy. Reducing the result given by Morgan and Lowry [21] to the value 2·2726 for the d.c. of benzene at 25° C., and taking the results just quoted, we obtain $2{\cdot}227_9$ as the mean value of these results for the d.c. of carbon tetrachloride at 25° C. This figure differs by about 1 in 2000 from the value obtained in the present work, and since the experimental error is of the same order of magnitude the agreement is satisfactory. This satisfactory agreement between the results of six independent investigators suggests the possibility of using carbon tetrachloride as a *secondary* standard of known d.c. (2·227 at 25° C.) for the purpose of calibration of d.c. condensers in cases where the accuracy required does not exceed 1 in 2000. Benzene will, of course, remain as the primary standard for use in cases where a greater accuracy is required, but the labour and trouble involved in the purification of benzene and its solubility in water place it at a disadvantage compared with carbon tetrachloride in cases where an accuracy of 1 in 2000 will suffice.

Referring to Table V., the agreement between the results obtained by different investigators is seen to be far from satisfactory. Taking the results of Williams and Krchma [17], Ball [25], Morgan and Lowry [21], and Jenkins [24] as typical results of good accuracy, we obtain a mean value of 4·739 for the d.c. of chloroform at 25° C., which is about 0·6 per cent. higher than that found in the present work. This discrepancy is certainly higher than the experimental error in the physical measurement, and suggests that it is probably due to difficulty in purification of the chloroform. The solubility

of chloroform in water and the fact that previous values are appreciably higher than that found by the author seem to suggest that the discrepancy may be due to absorption of water by chloroform.

To test the possible magnitude of this effect it was decided to determine the d.c. of A.R. chloroform as supplied by Messrs. Hopkin & Williams, Ltd., London; in this grade of chloroform most of the ordinary chemical impurities are absent, and the main impurity is water. The mean of four results for the d.c. of A.R. grade chloroform at 20° C. was 5·017, which is about 4·5 per cent. higher than the value of 4·796 found for the samples used in the present work. The value of the R.I. of A.R. grade chloroform at 20° C. was found to be $1{\cdot}4442_9$, which should be compared with the value $1{\cdot}4460_3$ found for the purified samples used.

In the present work it is unlikely that absorption of water has occurred in view of the excellent agreement obtained with samples purified by different methods and the agreement between the experimental and accepted values of the refractive index. Before chloroform can safely be used as a secondary standard for the calibration of d.c. condensers it is desirable that further determinations of its d.c. be carried out.

In conclusion, the author desires to express his sincere thanks to Vice-Principal Gwilym Owen for his constant interest and encouragement, to Messrs. L. E. Sulston and D. Owen for their help in the construction of the apparatus, to Prof. T. C. James for advice and the loan of the refractometer, and to his colleagues of the Chemistry Department, especially Dr. Matthew Williams, for their help in connexion with the chemical aspect of the work.

References.

(1) L. Hartshorn and D. A. Oliver, Proc. Roy. Soc. cxxiii. p. 664 (1929).
(2) D. W. Dye and T. I. Jones, J. I. E. E. lxxii. p. 169 (1933).
(3) S. Sugden, J. Chem. Soc. p. 768 (1933).
(4) M. Jezewski, *Zeit. f. Phys.* xlviii. p. 123 (1928).
(5) R. T. Lattey and O. Gatty, Phil. Mag. vii. p. 985 (1929).
(6) E. V. Appleton and W. H. J. Childs, Phil. Mag. vii. p. 969 (1930).
(7) M. Jezewski, *Phys. Zeit.* xxiv. pp. 88 & 561 (1933).
(8) R. T. Lattey and W. G. Davies, Phil. Mag. xii. p. 1111 (1931).
(9) M. Jezewski, *Zeit. f. Phys.* xliii. p. 442 (1927).
(10) R. T. Lattey, *Zeit. f. Phys. Chem.* cxix. p. 104 (1926).
(11) R. M. Davies, Phil. Mag. xx. p. 75 (1935).

(12) Heilbron, 'Dict. of Organic Compounds' (Eyre & Spottiswoode, London, 1934).
(13) J. W. Williams, *Phys. Zeit.* xxix. p. 204 (1928).
(14) F. H. Müller, *Phys. Zeit.* xxxv. p. 1009 (1934).
(15) H. Harris, J. Chem. Soc. p. 1049 (1925).
(16) Francke, *Ann. der Phys.* lxxvii. p. 159 (1925).
(17) Williams and Krehma, J. A. C. S. xlviii. p. 1888 (1926); *ibid.* xlix. p. 1676 (1927).
(18) Rolinsky, *Phys Zeit.* xxix. p. 658 (1928).
(19) Stranathan, Phys. Rev. xxxi. p. 653 (1928).
(20) Matsuike, Proc. Imp. Acad. Tokyo, v. p. 29 (1929).
(21) Morgan and Lowry, J. Phys. Chem. xxxiv. p. 2385 (1930).
(22) Fairbrother, J. Chem. Soc. p. 43 (1932).
(23) Müller, *Phys. Zeit.* xxxiv. p. 689 (1933).
(24) Jenkins, J. Chem. Soc. p. 480 (1934).
(25) Ball, J. Chem. Soc. p. 570 (1930).

April 1935.

II. *On the Dissociation of some Molecules with Free Valencies.* *By* H. Lessheim *and* R. Samuel, *Muslim University, Aligarh* *.

BAND spectra of certain molecules show a considerable increase of the energy of dissociation in some of the excited electronic levels, and it is frequently assumed that this phenomenon is due to the transfer of electrons from a premoted group to an unpremoted one. Recently, however, it has been shown [1] that such an increase of energy is closely connected with the presence of so-called odd electrons, and occurs therefore only in molecules which possess free valencies. Two types of molecules show this effect. A molecule, *e. g.*, NO, may possess a single odd electron which does not take part in the linkage. It has a disturbing influence on the linkage which is more or less eliminated by excitation. The other type consists of molecules like BeO, with two free valencies in the ground-state, which may form an additional bond on excitation.

That different theoretical explanations of the increased stability of the linkage are at all possible depends on the circumstance that there are two interpretations [2] of the method of molecular orbitals as long as we confine ourselves to the description of the completed molecule.

* Communicated by the Authors.

In one of the interpretations already the single electron possesses bonding power [3] and the phenomenon of linkage is attributed to its non-premotion. The other way of interpreting the orbital method conceives linkage as a phenomenon due to the inter-action of pairs of electrons, each from a different atom [2] [3]. The manner in which these two interpretations conceive an increase of dissociation energy on excitation is quite characteristic. If the odd electron takes part in the linkage, increased stability means a transfer of this electron to an orbital which is more strongly bonding than the previous one. If, however, the linkage rests only on pairs of electrons, the odd electron has a disturbing effect. Its excitation, which is a step in the direction to its complete removal, will lessen the disturbance as in the case of NO or CaF, and thus increase the stability, or it will have the opportunity of bringing about a second linkage as in the case of BeO, which then accounts for the additional bonding energy [2]. The principal difference of the two interpretations of the method of molecular orbitals becomes clear in the process of dissociation, and therefore in the present problem when the correlation to atomic terms of those molecular levels which exhibit increased energy of dissociation is accomplished. Theoretical and experimental consideration favour the interpretation of the orbital method as a pair bond theory of valency. One of the arguments is that it could be shown that in a case like NO the more stable molecular level arises from a configuration of the nitrogen atom in which the odd electron is already transferred to the M-shell, while in such cases like BeO or CaF, where an excitation of the metal atom is necessary before a linkage becomes possible, the more stable molecular level originates in a term of the metal atom in which both its *s* electrons are excited, *i. e.*, in an anomalous term. The following examples give some more illustrations of this behaviour. They are empirical facts, taken from band spectra, which by themselves do not depend on any theoretical view. But they appear again to emphasize the necessity of interpreting the orbital method as an electron-pair bond theory.

The values given below for the energies of dissociation are obtained by linear extrapolation of the vibrational levels.

Oxides of the Second Group.

The atoms of the second group are chemically inert in their ground-state ^1S on account of the closed helium-like configuration, s^2, and a linkage is possible only in an excited term, the s^2 group having undergone previous fission. Subsequently the ground-term of oxides like BeO arises from the term $sp\ ^3P$ of the metal; it is linked by one bond only, and the molecule shows an increased energy of dissociation in an excited electronic level which is correlated to the anomalous term $p^2\ ^3P$. In this term the molecule is doubly linked and the increase in energy is due to the second linkage.

The visible bands of beryllium oxide, due to the transition from the excited term $C\ ^1\Sigma$ to the ground-level

TABLE I.

Term.	Energies of dissociation.	$\nu_e + D' - D(^1\Sigma)$.
$A\ ^1\Sigma$.....	5·8	..
$B\ ^1\Pi$	4·4	..
$C\ ^1\Sigma$	7·5	4·3
D	3·3	2·5
E	3·1	2·5

$A\ ^1\Sigma$, have already been discussed from this point of view in preceding publications. Recently, however, L. Herzberg [4] has found a new band-system of this molecule in the near infra-red whose upper level is identical with the lower level $B\ ^1\Pi$ of the ultra-violet bands. This confirms that the state $A\ ^1\Sigma$ is the ground-level of the molecule and also that the extrapolated value of its energy of dissociation is correct. Furthermore, Harvey and Bell [5] have shown that the ultra-violet bands of BeO, found by Jevons and partly analysed by Bengtsson, in reality form two different systems, both having the same final level $B\ ^1\Pi$ and involving two excited levels D and E. Thus we have now in BeO five electronic levels, the nature of three of these levels, namely A, B, and C being definitely known, while that of D and E is still uncertain. Table I. gives the heat of dissociation and the energies of the products of dissociation, which are also exhibited in fig. 1.

A correlation of the ground-level of the molecule to $Be(2s^2\ ^1S)+O(^3P)$ is not possible, not only for the repulsion of the s^2 group, but also because the next excited terms of the atom, viz. :—$2s\ 2p\ ^3P$, $2s\ 2p\ ^1P$, and $2s\ 3s\ ^3S$, lie 2·71, 5·25, and 6·43 volts respectively above ^1S, no term in the neighbourhood of 4·3 volts being available. The

Fig. 1.

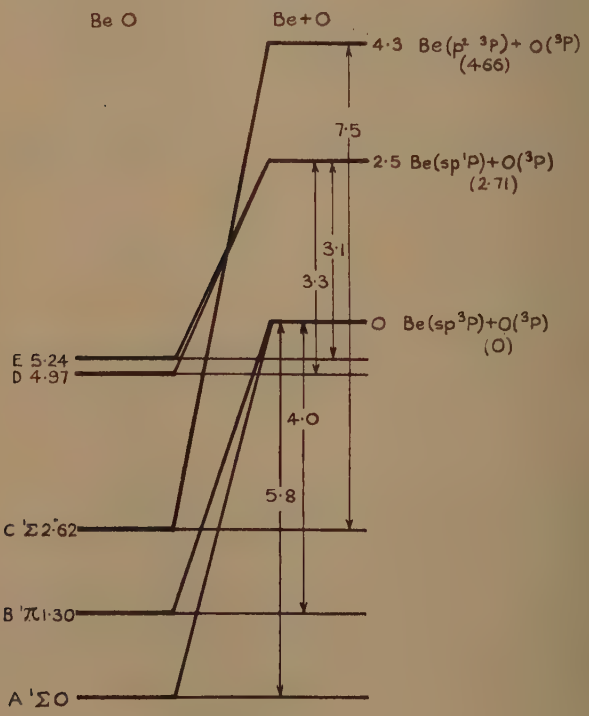

anomalous term $2p^2\ ^3P$ lies, however, 7·37 volts above the ground-level ; the energetic difference $2p^2\ ^3P-2s\ 2p\ ^3P$ is 4·66 volts in good agreement with the value 4·3 of the vibrational extrapolation. This correlates definitely the terms $A^1\Sigma$ and $B\ ^1\Pi$ to $Be(2s\ 2p\ ^3P)+O(^3P)$ and C to $Be(2p^2\ ^3P)+O(^3P)$.

The combination of oxygen in its ground-state $(2s^2\ 2p^4\ ^3P)$ with beryllium in its lowest state in which it is not

chemically inert, *i. e.*, $2s\,2p\,{}^3\mathrm{P}$, gives rise to several configurations of the molecule. Taking the order of the molecular groups for small internuclear distances as prevailing in BeO, the two lowest ones which have to be considered for the ${}^1\Sigma$ state are

$$\mathrm{K_1K_2}\,\sigma^2(2s)\quad \pi^4(2p)\quad \sigma^*(2s)\quad \sigma(2p),$$

and $$\mathrm{K_1K_2}\,\sigma^2(2s)\quad \pi^3(2p)\quad \sigma^*(2s)\quad \sigma^2(2p).$$

Either of them involves separated atoms with three s and five p electrons in all. The first configuration appears to be the ground-state of the singly linked molecule, but is incapable of forming the crystal, which is probably formed by the molecule in the second of the above configurations from which possibly also B ${}^1\Pi$ arises.

Several electronic configurations are possible for the C ${}^1\Sigma$ on account of the above correlation, but the considerable increase of the energy of dissociation indicates that

$$\mathrm{K_1K_2}\,\sigma(2s)\quad \pi^4(2p) - \sigma^2(2p)$$

corresponds to C ${}^1\Sigma$. Here the σ^* electron is transferred to the group $\sigma(2p)$ and possesses now the character of a p-electron in the separated atoms. A double bond results; in addition to the bond in $\pi^4(2p)$ a new link is produced in $\sigma^2(2p)$, since now electrons of either atom join in it.

There remain the two terms D and E, which both originate in the same energy level of the separated system, which lies 2·5 volts above the $2s\,2p\,{}^3\mathrm{P}$ term of Be, which is involved in the A and B terms of the molecule. The only atomic term giving this difference is the $2s\,2p\,{}^1\mathrm{P}$ of Be, which lies 2·54 volts above $2s\,2p\,{}^3\mathrm{P}$. The agreement is remarkably good. From this configuration of the separated atoms, however, no singlet terms of the molecule can possibly arise. Experimentally there is no evidence as to the nature of multiplicity of the levels, because it has not been possible to resolve bands involving these terms and to obtain their rotational analysis. In literature they are simply designated as probable ${}^1\Pi$ levels. The combination of these terms with B ${}^1\Pi$ gives rise to bands which show no strong Q heads. This proves at the most that the terms D and E are Π-terms, but throws no light on the multiplicity of the

levels. In the first instance, we have to remember that these bands are very weak, which probably indicates that a difference in multiplicity is involved in these transitions. Secondly, that these bands are not sufficiently resolved under high dispersion, *e. g.*, the second order of a 21 ft. grating, indicates that they have a complicated structure which one would not expect, if the transition involved were $^1\Pi \rightarrow {}^1\Pi$. This also is in favour of the assumption of a triplet nature of these

Fig. 2 *a*.

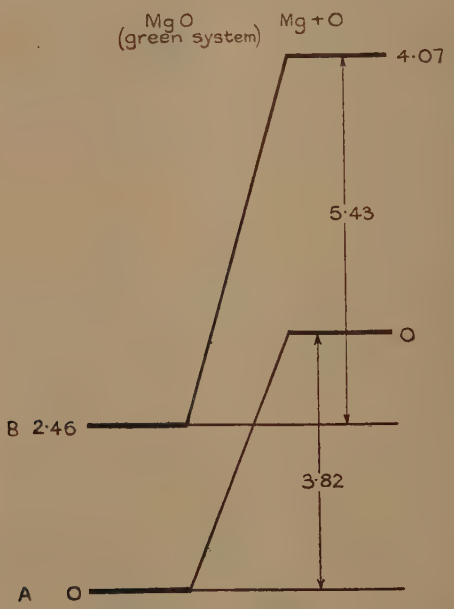

terms. The satisfactory correlation given above on considerations of the energies of dissociation and the term-values of the Be atom, also points in this direction, and there is no reason not to accept this evidence.

Similar results obtain in MgO. Mahanti [6] describes two band systems in the red and green regions, and in either of them the upper level shows an increased energy of dissociation (see figs. 2 *a* and 2 *b*). The excitation of the level of the separated atoms is the same for both systems, *i. e.*, 4·07 and 4·08 volts respectively. It is

Fig. 2 *b*.

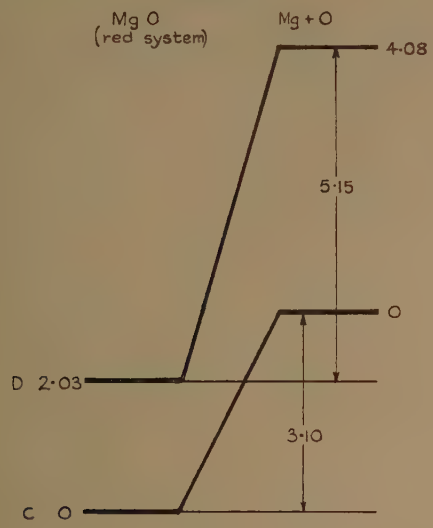
Mg O
(red system)
Mg + O
4·08
5·15
O
D 2·03
3·10
C O

Fig. 2 *c*.

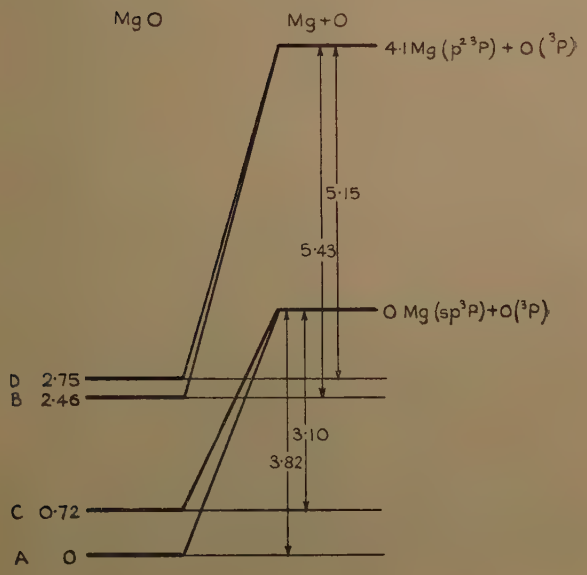
Mg O
Mg + O
4·1 Mg (p² ³P) + O (³P)
5·15
5·43
O Mg (sp³P)+O(³P)
D 2·75
B 2·46
3·10
3·82
C 0·72
A O

certain that we have to combine the molecular levels in analogy to BeO as shown in fig. 2*c*, and the term A with 3·82 volts of energy of dissociation will be the ground-level $^1\Sigma$ of the molecule. This is, however, immaterial for the present consideration; in any case we have an extrapolated difference of 4·1 volts of the atomic terms.

Among the normal terms of Mg there is none of the required energy from which the excited level of the molecule could possibly originate. In the series $3s\,ms$ ^{1}S and ^{3}S the seventh member reaches the neighbourhood of 4·1 volt above sp ^{3}P, in the series $3s\,mp$ ^{1}P the sixth or seventh member; in the series $3s\,md$ ^{1}D and ^{3}D the fifth or sixth member. It is not conceivable why just these higher terms should be involved and the first members should be passed over in that combination leading to the initial term of the most intense band-system of the molecule. The lowest anomalous term $3p^2$ ^{3}P lies, however, just 4·4 volts above the term $3s\,3p$ ^{3}P. This indicates clearly that the upper term of the molecule arises again from this anomalous term, and confirms our view that the strong increase of the energy of dissociation from 3·8 to 5·4 volts in the green, or from 3·1 to 5·2 volts in the red system respectively, is due to a second bond on the grounds of the second valency electron of Mg having also been transferred to the p-group. The configuration of the ground-level will correspond to that of BeO, the high melting-point of MgO indicating again free valencies in the crystalline state.

Among the oxides of the heavier atoms of the second group whose bands are analysed, *e. g.*, CaO, SrO, and BaO, similar conditions seem to prevail. On account of the decrease of energy of excitation in the term-system of the atoms, and on account of the low d-terms the number of available terms becomes so large that the molecular levels cannot be correlated to the atomic terms with certainty, unless the rotational analysis of the bands has been accomplished.

Halides of the Second Group.

The chemical inactivity of the s^2 group is manifested in a slightly different way among the halides of the second group. The ground term $^2\Sigma$ arises again by com-

bination of an unexcited halogen atom with a metal atom in the term $sp\ ^3P$, and these molecules possess again an excited term whose energy of dissociation is increased. The monovalency of the partner excludes a double bond,

Fig. 3 *a*.

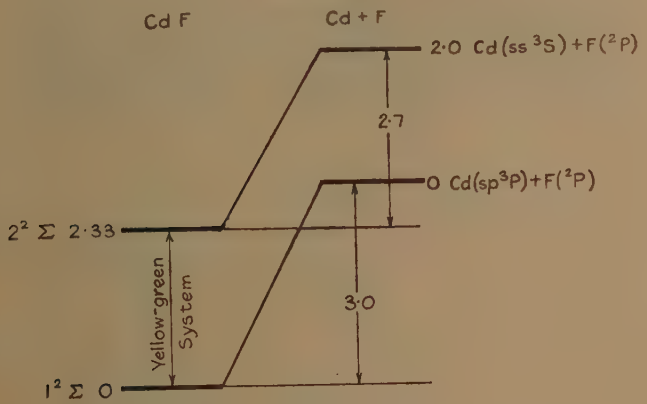

Fig. 3 *b*.

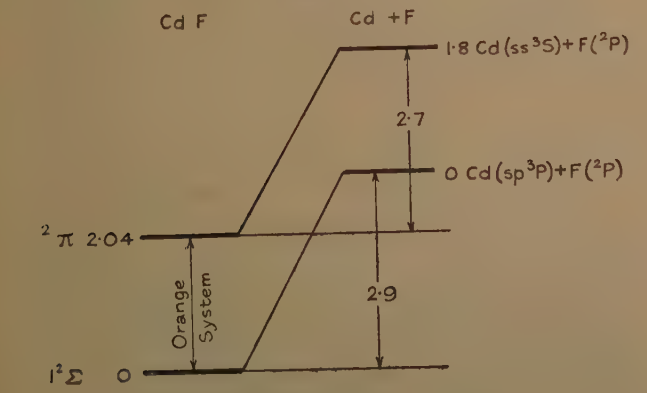

and the increase of dissociation energy is due to the removal of the odd electron of the metal atom which does not take part in the linkage and disturbs it. Therefore the extrapolation of the vibrational levels of this term leads to a state of the metal atom in which both its electrons are excited, *i. e.*, again to an anomalous

term, in general, $p^2\,{}^3P$, whereas terms with decreased energy of excitation have to be correlated to normal excited levels of the metal atom. In the preceding paper [1] the molecules BeF, MgF, CaF, and SrF have been discussed from this point of view. The linear extrapolation of the vibrational levels of the bands of these molecules is not very satisfactory on account of the large and varying distance between the heads and the (O, O) band, and the best agreement was obtained in CaF, where the data of the Q heads could be used.

Fig. 4.

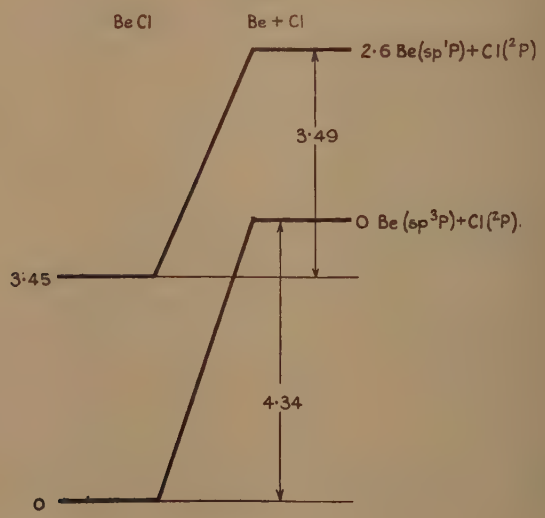

Recently the bands of several molecules of this type have been investigated, *i. e.*, cadmium fluoride and the chlorides of Be, Mg, Ca, Sr, and Ba. The bands of CdF show again [7] that the ground-level of the molecule is not formed by a combination of Cd $(5s^2\,{}^1S)+F(2p^5\,{}^3P)$, but by Cd $(5s\,5p\,{}^3P)+F({}^3P)$. From the orange system, where Q heads are available, the following figures are obtained :—Excitation of the molecule 2·04 volts, dissociation energy of the $^2\Sigma$ ground-state 2·9 volts, that of the excited $^2\Pi$ level 2·7 volts. The difference between the energies of the dissociation products is 1·8 volts

in the orange system or 2·0 volts in the yellow-green one. Fluorine does not possess any terms at all in this region, and the difference $5s\,5p\,{}^3\mathrm{P} - 5s^2\,{}^1\mathrm{S}$ of Cd is 3·7 volts and too large to allow a correlation of the ground-level of the molecule to that of the unexcited atoms. The figures clearly indicate the correlation of the unexcited $^2\Sigma$ term of CdF to Cd $(5s\,5p\,{}^3\mathrm{P}) + \mathrm{F}({}^3\mathrm{P})$ and of both the excited levels $^2\Sigma$ and $^2\Pi$ to Cd $(5s\,6s\,{}^3\mathrm{S}) + \mathrm{F}({}^3\mathrm{P})$, confirming again that the s^2 group is chemically inert.

In BeCl the excited term [8] lies 3·45 volts above the ground-level, and shows an energy of excitation of

Fig. 5.

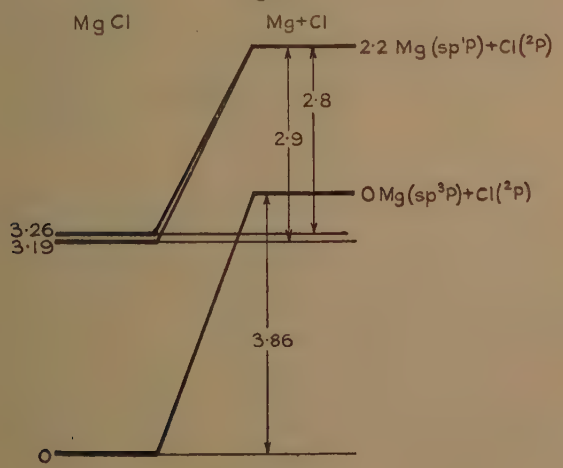

3·49 volts, while that of the ground-state is 4·34 volts. The energy of excitation of the dissociation products is accordingly 2·60 volts, in agreement with the term difference $2s\,2p\,{}^1\mathrm{P} - 2s\,2p\,{}^3\mathrm{P} = 2{\cdot}54$ volts of Be.

MgCl possesses [9] two excited terms, which arise from the same excited level of the separated system, the extrapolation yielding an energy of excitation of the dissociation products of 2·25 and 2·18 volts respectively. This value agrees with the term difference $3s\,4s\,{}^3\mathrm{S} - 3s\,3p\,{}^3\mathrm{P} = 2{\cdot}38$ volts. The dissociation energy decreases on excitation of the molecule, being 2·78 and 2·92 volts respectively in the two excited levels and 3·86 volts in the ground-state.

In CaCl five terms are known [10] including the ground-level $^2\Sigma$, involving in all three different levels of the separated system (fig. 6). The red system is due to a transition from a $^2\Pi$ level to the ground-state :—The energy of dissociation of the latter one is 3·5 volts and that of the $^2\Pi$ term is increased to 4·6 volts. The energy of excitation of $^2\Pi$ is 1·99 volts ; hence it originates from an atomic level 3·1 volts above that which is involved in the ground-level $^2\Sigma$. This agrees fairly well with the anomalous term $4p^2\ ^3$P of Ca, which lies 2·9 volts above

Fig. 6.

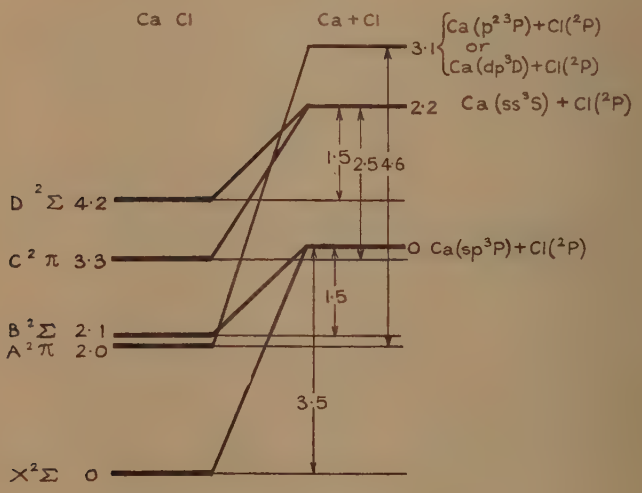

$4s\ 4p\ ^3$P. The upper level of the orange system is a $^2\Sigma$ term whose energy of dissociation is decreased to 1·5 volts. It arises, therefore, from a normal excited term of Ca. The extrapolation of the bands gives an energy of excitation of 2·2 volts in the separated atoms ; the excited normal term $4s\ 5s\ ^3$S of Ca lies 2·02 volts above ^{3}P.

For the ground-level $^2\Sigma$ of such a molecule the combination of the terms $sp\ ^3$P of the metal and $s^2\ p^5\ ^3$P of the halogen atom gives for small internuclear distances the configuration

$$\sigma^2(s)\ \pi^4(p)\ \sigma^*(s)\ \sigma^2(p).$$

The linkage is produced in that group which contains the p-electron of the metal, either $\pi(p)$ or $\sigma(p)$. The single $\sigma^*(s)$ electron is the odd s-electron of the metal; its excitation, transferring it to the next group $\pi^*(p)$, removes part of its disturbing influence, and the configuration of that $^2\Pi$ level, which possesses an enlarged dissociation energy, is given by

$$\sigma^2(s)\ \pi^4(p) - \sigma^2(p)\ \pi^*(p).$$

By the excitation of the molecule an s-electron of the separated atoms has become a p-electron; hence this term is formed by an unexcited halogen atom and a metal atom in the anomalous term $p^2\ ^3\mathrm{P}$. If, on the other hand, an electron of the bonding group is excited, the bond is weakened. Since both the groups $\pi^4(p)$ and $\sigma^2(p)$ have to be considered, various configurations are possible for those observed $^2\Sigma$ and $^2\Pi$ levels as show a decreased energy of dissociation.

The Non-Bonding Character of the s^2 Group.

The non-bonding character of the s^2 group is also of some interest for the theory of valency, because the s^2 group constitutes, in the majority of cases, the so-called lone pair [11] of chemistry, to which the coordinate linkage is attributed. Theoretically the non-bonding character of a complete s-shell is established [12], and nothing is to be added any more to it. In current literature on the band spectra of oxides and halides of the alkaline earth metals, however, the correlation of the ground-level of these molecules to the $^1\mathrm{S}$ term of the metals is sometimes mentioned as an alternative suggestion. The energies of dissociation decrease rapidly from the compounds of beryllium to those of magnesium, and slightly from them towards those of the heavier atoms. The change in the energies of excitation of the metal atoms, however, is quite different. The term difference *e. g.*, $^3\mathrm{P}-{}^1\mathrm{S}$, corresponding to the resonance line, which decreases from magnesium towards the heavier atoms of the main group of the periodic system, is considerably enlarged in the subgroup; in beryllium, however, this energy is not increased but of the same order as in Mg. Since the extrapolation of the vibrational levels is not completely accurate, the energy of the

$^3P-{}^1S$ transition comes sometimes sufficiently close to the lowest energy of excitation of the dissociation products to allow of a correlation of the molecular ground-level to the ^1S term of the metal. It can be seen, however, that such a coincidence is fortuitous. For this purpose we consider the different possible correlations from an entirely empirical point of view.

In Table II. we have collected all the available data of the oxides and halides of the metals of the second group, leaving aside only Ba and Sr, where the excited terms are all of them so close to the ground-level that no correlation can be given, the differences between the terms being already of the same order of magnitude as the error of the linear extrapolation. Column 1 contains the terms of the molecules; the excited terms with an increased energy of dissociation are marked with an asterisk. Columns 2 and 3 contain their energies of excitation and dissociation (in volts), 4 the excitation energies of the products of dissociation. Column 5 contains the corresponding energies of excitation of the metal atom as given above, *i. e.*, assuming that the ground-level of the molecule involves the term $sp\ ^3P$. The anomalous term is given as $^3P'$; it is mostly the term $p^2\ ^3P$, only in Sr the anomalous term $dp\ ^3P$ lies lower, and is therefore included. In column 6 those term differences are given which are nearest to those of column 4, under the assumption that the ground-level of the molecule arises from the ground-level of the metal atom. There are certainly a number of molecules in which also this correlation would be possible from an empirical point of view; but it is of greater importance that there exist also a number of cases in which this correlation, which assumes a bonding force of the s^2 group, is not possible at all.

The simplest case is that of CdF. In Cd the term difference $^3P-{}^1S$ possesses the highest value, and therefore the excitation energy of the products of dissociation is simply insufficient. Since the term $5s\ 5p\ ^3P$ is the lowest excited term, a correlation according column 4 would imply that the energies of dissociation are incorrect by 85 per cent. On the other hand, the energy of excitation and the bond energy of BeF are high, but the energy of excitation of Be comparatively low. Thus the value obtained from the vibrational extrapolation is 30 per cent

Table II.

1 Molecular term.	2. ν_e.	3. D.	4. $\nu_e+D'-D''$.	5. Correlation from ^3P.	6. Correlation from ^1S.
			Beryllium Fluoride.		
$^2\Sigma$	0	5·42	0	....	....
$^2\Pi$	4·10	4·83	3·51	$^3S-^3P=3·72$	$^3P-^1S=2·71$
			Magnesium Fluoride.		
$^2\Sigma$	0	3·7	0	....	....
$^2\Pi^*$	3·4	4·0	3·7	$^3P'-^3P=4·4$	$^3P-^1S=2·70$
			Calcium Fluoride.		
$1\,^2\Sigma$	0	3·2	0	....	....
$^2\Pi^*$	2·0	4·5	2·7	$^3P'-^3P=2·87$	$^3D-^1S=2·51$
$2\,^2\Sigma$	2·3	2·9	2·0	$^3S-^3P=2·02$	$^3P-^1S=1·87$
			Strontium Fluoride.		
$1\,^2\Sigma$	0	3·10	0	....	....
$^2\Pi^*$	1·89	4·15	2·9	$^3P'-^3P=2·88$	$^3S-^1S=3·62$
$2\,^2\Sigma$	2·14	2·97	2·0	$^3S-^3P=1·85$	$^3D-^1S=2·24$
			Cadmium Fluoride.		
$1\,^2\Sigma$	0	3·0 2·9	0	....	....
$^2\Pi$	2·04	2·7	1·8	$^3S-^3P=2·64$	$^3P-^1S=3·71$
$2\,^2\Pi$	2·3	2·7	2·0		
			Beryllium Chloride.		
$X(^2\Sigma)$	0	4·34	0	....	....
$A(^2\Pi)$	3·45	3·49	2·60	$^1P-^3P=2·54$	$^3P-^1S=2·71$
			Magnesium Chloride.		
$X(^2\Sigma)$	0	3·86	0	....	....
$B(^2\Pi)$	3·26	2·92	2·25	$^3S-^3P=2·38$	$^3P-^1S=2·70$
			Calcium Chloride.		
$X\,^2\Sigma$	0	3·5	0	....	....
$A\,^2\Pi^*$	1·99	4·6	3·1	$^3P'-^3P=2·87$ or $3d4p\,^3P'-^3P=2·98$	$^1P-^1S=2·92$
$B\,^2\Sigma$	2·1	1·5	0	....	....
$C\,^2\Pi$	3·3	2·5	2·2	$^3S-^3P=2·02$	$^3P-^1S=1·87$
$D\,^2\Sigma$	4·2	1·5			
			Beryllium Oxide.		
$A\,^1\Sigma$	0	5·8	0	....	....
$B\,^1\Pi$	1·30	4·4	0	....	....
$C\,^1\Sigma^*$	2·62	7·5	4·3	$^3P'-^3P=4·66$	$^1P-^1S=5·25$
$D\,(^3\Pi)$	4·97	3·3	2·5	$^1P-^3P=2·54$	$^3P-^1S=2·71$
$E\,(^3\Pi)$	5·24	3·1	2·5		
			Magnesium Oxide.		
$A\,(^1\Sigma)$	0	3·82	0	....	....
B^*	2·46	5·43	4·1	$^3P'-^3P=4·44$	$^1P-^1S=4·33$

higher than that of the term difference $^3P-{}^1S$ of Be; the next excited term, $2s\ 2p\ {}^1P$, lies 5·25 volts above the ground-term, and is therefore also out of question. The conditions of MgF are still similar to those of BeF and the value of column 4 is 37 per cent. higher than that of column 6. Only when we proceed to heavier molecules, or to chlorides, in which the energies of dissociation and excitation are decreased, correlations of the ground-level of the molecule to the ^1S state of the metal are possible. Even then the correlation of other excited terms of the molecule is often open to objection. Thus in SrF the correlation of $1\ {}^2\Sigma$ to the ground-term and of $2\ {}^2\Sigma$ to the ^3D term of Sr is empirically correct inside of 10 per cent.; the same is true if we correlate $2\ {}^2\Sigma$ to ^3P and $^2\Pi$ to ^3S, only that the linear extrapolation of the bands yields then 10 and 20 per cent. energy too much instead of too little when compared with that of the atomic levels.

On the other hand, the correlation according to column 5 is consistent, especially the excited molecular terms, which exhibit an increased energy of dissociation and are always correlated to an anomalous term of the metal; in the majority of cases, *i. e.*, in BeF, CaF, SrF, BeCl, MgCl, CaCl, BeO, and MgO, the agreement of the figures of columns 4 and 5 is correct for all terms to about 1 to 2 per cent. Since already one clear example like CdF would be enough to decide the question, we may take it that the non-bonding character of the s^2 group is also established from a purely experimental standpoint.

The remarkably good agreement prevailing in the majority of cases throws also light on the question of hybridization. That part of the bonding wave-function in the ground-state of the molecule which arises from the sp configuration of the metal atom is, of course, a hybrid of an s and a p electron function, and thus forms a stronger bond than an ordinary p function would. When, however, on excitation, as in BeO etc., a double bond results, it consists of two p bonds superposed; this is apparently the reason why the energy of dissociation, though increased, is not doubled. Furthermore, it has sometimes been suggested that the ground-state of the molecule, instead of being actually formed by the metal atom in $sp\ {}^3P$, is formed from the $s^2\ {}^1S$ term, but perturbed by a neighbouring p term in such a way as to render a linkage possible. In this case the actual wave-function of the metal atom would be a hybrid of the s^2 and sp

functions. It is, however, clear that the complete absence of experimental evidence of such a perturbation, the validity of an ordinary quadratic formula for the vibrational levels, and the satisfactory correlation of the dissociation products to the atomic terms using such a formula eliminate every possibility of a hybridization of this type, and we can safely say that all the neighbouring terms are too far distant to be of any importance. At higher vibrational levels the attractive curve originating from $sp\ ^3P$ intersects the repulsive one from $s^2\ ^1S$; thus by means of a moderate activation energy, which brings the system to the point of intersection, the molecule may well be formed by combining a metal atom in $s^2\ ^1S$ with its partner. This, however, is immaterial for the present view, because we notice nothing of that point of intersection when we extrapolate the potential curve from the lowest unperturbed vibrational levels.

As already discussed, the above considerations are corroborated by the crystal structure of the oxides of the metals of the second group. If the metal atom would participate in the linkage—not with the $sp\ ^3P$ term only, but with a hybrid of terms—a double link would result already in the ground-state of the molecule, and a crystal formed by such saturated molecules would possess a low melting-point. Wave-mechanical considerations have shown [13] that the extremely high melting-point of these substances directly indicates true chemical linkages between the molecules in the lattice, or, in other words, free valencies of the single molecule. It is interesting to note that the high melting-point still prevails in those crystals which, like CaO, possess the structure of the NaCl type. This shows again that the only indication as to the type of linkage prevailing in the crystal lattice is given by the melting-point and not by the lattice structure itself. A crystal is always formed in that structure which under the particular conditions has the minimum of energy irrespective of the physical nature of the bonding forces, which can therefore not be inferred from the lattice type, and molecules like CaO are covalently linked in the crystalline state, even though they may possess an NaCl lattice *. The fact that it is

* The conclusions drawn by Sen Gupta [14] on the ionic nature of the linkage of CaO in order to explain the absorption spectrum are obviously not valid. The actual explanation is the same as in the case ZnO discussed elsewhere. (*Cf.* R. Samuel, "Absorption Spectra and Chemical Linkage," Ind. Ac. Sci., Symposium, 1935.)

possible to describe certain properties on the assumption of the presence of polarized ions shows only that this is already a reasonable approximation.

Oxides of the Fifth Group.

The terms of the molecule NO have been correlated to those of the separated atom in a preceding paper [1] as follows :—

$N(2s^2\ 2p^3\ {}^4S)+O(2s^2\ 2p^4\ {}^3P)=NO(X\ {}^2\Pi)$
(ground-level, D = 6·70 volts) ;
$N(2s^2\ 2p^2\ 3s\ {}^4P)+O(2s^2\ 2p^4\ {}^3P)=NO(A\ {}^2\Sigma)$
(D = 10·67 volts) ;
$N(2s^2\ 2p^3\ {}^2P)+O(2s^2\ 2p^4\ {}^3P)=NO(B\ {}^2\Pi)$
(D = 4·46 volts) ;

and for the homologous molecule PO in the same manner * :—

$P(3s^2\ 3p^3\ {}^4S)+O(2s^2\ 2p^4\ {}^3P)=PO(X\ {}^2\Pi)$
(ground-level, D = 6·47 volts) ;
$P(3s^2\ 3p^2\ 4s\ {}^4P)+O(2s^2\ 2p^4\ {}^3P)=PO(A\ {}^2\Sigma)$
(D = 7·90 volts).

The energy differences of the products of dissociation, as obtained from band-spectra, agree very well with the known term differences of the atoms. The combination of an unexcited nitrogen and an unexcited oxygen atom gives the ground-level of the molecule ; a molecular term of decreased energy of dissociation results, if the unexcited oxygen atom combines with an excited nitrogen atom which possesses still the same electronic configuration, but is in a term belonging to a different multiplet system. If, however, the linkage takes place between an unexcited oxygen atom and a nitrogen atom in a state in which the odd electron, which does not take part in the linkage, is removed to the next shell, a molecular term is obtained whose energy of dissociation is considerably increased. This is a typical case which proves the disturbing influence exercised by an odd electron not contributing to the linkage, but representing a free valency. Because N^+ (like C) possesses just that number of p-electrons which—

* These figures have been taken from the measurements of Petrikaln [15], whose results are also those given in the tables of Jevons [16]. Ghosh and Ball [17] give nearly the same values.

from the view-point of a pair bond theory of linkage—are required by the divalent oxygen atom, and would match best its electronic configuration to produce a stable saturated molecule, the molecule ion $(NO)^+$ will be linked stronger than the molecule (NO) and the

Fig. 7.

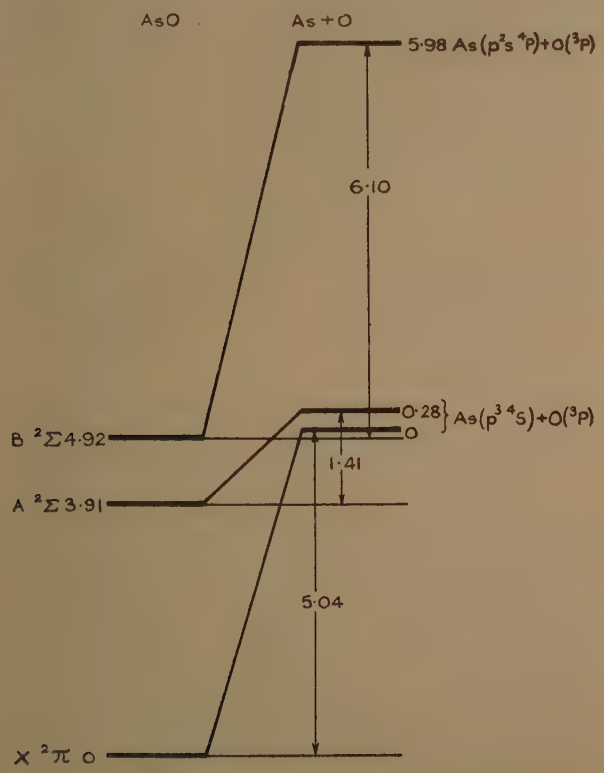

gradual excitation of the series electron of NO up to the point of ionization brings about a series of molecular terms with gradually increasing energy of dissociation.

The spectrum of AsO has been recently analysed by various investigators [18], who found two band-systems in the ultra-violet region. They are produced by the combination of either of two excited $^2\Sigma$ terms A and B

with the ground-level $X\,^2\Pi$. The excitation energy of the transition $A\,^2\Sigma - X\,^2\Pi$ is 3·91 volts, that of $B\,^2\Sigma - X\,^2\Pi$ is 4·92 volts. The energies of dissociation of $X\,^2\Pi$, $A\,^2\Sigma$, and $B\,^2\Sigma$ are 5·07, 1·41, and 6·10 volts respectively *. Hence $A\,^2\Sigma$ originates from the same level of the separated atoms as the ground-level, whereas the products of dissociation of $B\,^2\Sigma$ involve an atomic level excited by 5·98 volts. The term $4s^2\,4p^2\,5s\,^4P$ of As lies 6·26 volts above the ground-term; the agreement is very good, the error being 0·28 volts only. Obviously the same correlation holds good in AsO as in NO and PO :—

$As(4s^2\,4p^3\,^4S) + O(^3P) = AsO(X\,^2\Pi)$ and $AsO(A\,^2\Sigma)$;

$As(4s^2\,4p^2\,5s\,^4P) + O(^3P) = AsO(B\,^2\Sigma)$;

Fig. 8 *a*.

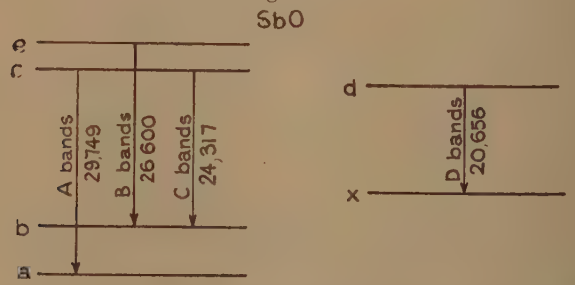

and the excited molecular term with increased energy of dissociation is again formed by an As atom in that configuration in which the odd electron is removed to the next shell.

Four band-systems of SbO have been found by Mukherjee [19], who terms them the systems A, B, C, and D. A and C come from the same initial level, B and C possess a common final level; a transition between the terms of the D-system and those of any other one has not been found. For the sake of convenience we shall call the lower level of the A-system (*a*), and its upper level (*c*), it being also the upper level of the C-system. The lower level of the B- and C-systems we shall call (*b*) and the upper level of the B-bands (*e*). Finally, we call the initial level of the D-system (*d*), and its final level (*x*) (see fig. 8 *a*). If the term value

* Mean values derived from Connelly's data for the Q heads. As to the reason for this selection *cf.* F. Morgan and E. N. Shawhan, Phys. Rev. xlvii. p. 192 (1935).

of (*a*) is taken as 0, the energies of excitation of (*b*), (*c*), and (*e*) are 0·67, 3·67, and 3·95 volts respectively, and (*d*) lies 2·55 volts above (*x*). The energies of dissociation of these terms are in volts : $D_a=3{\cdot}55$, $D_b=6{\cdot}18$, $D_c=1{\cdot}63$, $D_e=2{\cdot}25$, $D_x=5{\cdot}30$, and $D_d=2{\cdot}81$. Since

Fig. 8 *b*.

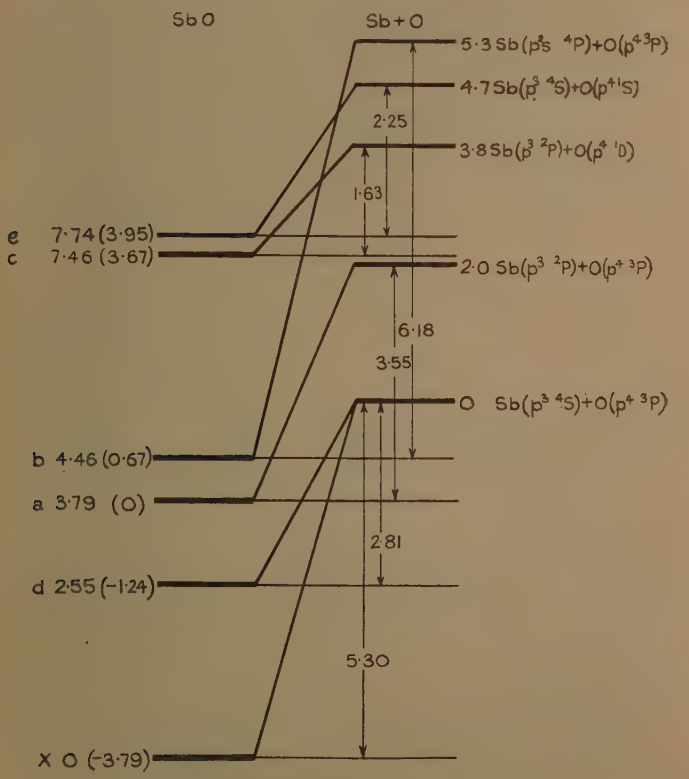

no transition is known between the one group of four terms and the other group of two terms, no complete term system of the molecule is yet established ; but as the view-point of the present paper has been confirmed for the molecules NO, PO, and AsO, the same theory may be applied to SbO with some confidence,

and allows, indeed, to find out the ground-level of the molecule and the relative position of the excited terms.

The term b is certainly not the ground-level of the molecule, lying above a, but possesses the highest energy of dissociation, *i. e.*, it is similar to the term ($A\ ^2\Sigma$) of NO and PO. The terms (d) and (x) originate in the same level of the separated atoms as the two lowest terms of AsO, and the energy of dissociation of (x) is larger than that of any one other than (b), as in NO, PO, and AsO. We have, therefore, to assume that (x) is the ground-level of the molecule. In other words, we assume that (x) and (d) are produced by combination of unexcited atoms, and that the difference of energy between the products of dissociation of (a) and (x) is about 2 volts, *i. e.*, the term value of the first excited term of Sb. This choice

TABLE III.

		Energy level of the separated system.	Energy difference of corresponding atomic terms.
SbO (x) SbO (d)	$= Sb(5s^2\ 5p^3\ ^4S) + O(p^4\ ^3P)$.	0	....
SbO (a)	$= Sb(5s^2\ 5p^3\ ^2P) + O(p^4\ ^3P)$ . .	2·0	2·02
SbO (b)	$= Sb(5s^2\ 5p^2\ 6s\ ^4P) + O(p^4\ ^3P)$	5·3	5·34
SbO (c)	$= Sb(5s^2\ 5p^3\ ^2P) + O(p^4\ ^1D)$ . .	3·8	3·98
SbO (e)	$= Sb(5s^2\ 5p^3\ ^4S) + O(p^4\ ^1S)$ . .	4·7	4·17

brings the level (x) by 3·79 volts below (a), and it is confirmed at once, because now the other levels of the separated atoms agree perfectly well with the lowest terms of Sb and O, and, furthermore, the excited term (b) with increasing energy of dissociation is correlated to the only atomic term in which the odd electron is transferred to the next shell (*vid.* Table III.).

Some of these correlations may have to be modified, when the energies of dissociation and the character of the terms are better determined. The choice of (x) as the ground-level and of (b) as that involving the term $5p^2\ 6s\ ^4P$ of Sb appear to be established by the ratio of their energies of dissociation and by the energy difference of the products of dissociation of (a) and (b), equalling exactly the term difference $5p^2\ 6s\ ^4P - 5p^3\ ^2P$ of Sb.

The electronic configuration of the molecules of this type is in the ground-state

$$\sigma^2(s)\ \sigma^{*2}(s)\ \pi^4(p)\ \sigma^2(p)\ \pi^*(p).$$

The excitation of the upper $^2\Sigma$ term with increased energy of dissociation transfers the π^* electron to the next group according to its correlation to the p^2s ^{4}P term of the atom :—

$$\sigma^2(s)\ \sigma^{*2}(s)\ \pi^1(p)\ \sigma^2(p) - \sigma(s).$$

Other possible configurations are

$$^2\Pi : \sigma^2(s)\ \sigma^{*2}(s)\ \pi^3(p)\ \sigma^2(p)\ \pi^{*2}(p)\ ;$$

and $$^2\Sigma : \sigma^2(s)\ \sigma^{*2}(s)\ \pi^4(p)\ \sigma(p)\ \pi^{*2}(p).$$

The former one, correlated to the (p^3 ^{2}P) level, occurs, *e. g.*, in the spectrum of NO ; the latter one, correlated to the ground-levels of the atoms, occurs in AsO.

Summary.

(i.) Among the oxides and halides of the metals of the second group a good agreement between the energy of excitation of the products of dissociation and the terms of the metal atom obtains always, if the ground-level of the molecule is correlated to the excited term sp ^{3}P of the metal. Besides the molecules BeF, MgF, CaF, SrF, already examined before, the following have been considered : BeO, MgO ; CdF, BeCl, MgCl, CaCl.

(ii.) In some of the molecules of these types also a correlation of the ground-level to the repulsive term s^2 ^{1}S would seem to be possible, but others strictly contradict such a correlation. This is particularly evident in a case like CdF. Here the term difference $5s\ 5p\ ^3\mathrm{P} - 5s^2\ ^1\mathrm{S}$ is enlarged, the metal belonging to the subgroup of the periodic table, while the energies of excitation and dissociation of the molecule are not very different from others of this type. Consequently, one would have to assume that the linear extrapolation of the vibrational levels is incorrect by 85 per cent. in order to obtain a correlation of the lowest state of the molecule to the ^{1}S term of Cd.

This not only establishes the repulsive character of the s^2 group, but also, since no perturbation is observed in the bands, the absence of that type of hybridization which involves more than one term of the metal atom (q-linkage). This is also borne out by the crystal structure

of the oxides, which cannot be explained unless the single molecule exhibits still free valencies.

(iii.) In all the above molecules terms whose energy of excitation is larger than that of the ground-level are automatically correlated to an anomalous term of the metal atom.

(iv.) In the molecules NO, PO, and AsO the term with an increased energy of dissociation involves a configuration of the corresponding atom of the fifth group, in which one electron is excited to the next shell. A reasonable correlation can be obtained in SbO on the assumption that it behaves similarly.

This shows again that the increase of stability on excitation in these molecules is always due to the excitation of that electron which does not take part in the linkage, but represents a free valency.

References.

(1) H. Lessheim and R. Samuel, *Zeits f. Phys.* lxxxiv. p. 637 (1933); lxxxviii. p. 276 (1934).
(2) H. Lessheim and R. Samuel, Proc. Ind. Ac. Sci. (Bangalore) (A) i. p. 623 (1935).
(3) F. Hund, *Zeits. f. Phys.* lxxiii. p. 1 (1931); lxxiv. p. 429 (1932).
(4) L. Herzberg, *Zeits. f. Phys.* lxxxiv. p. 571 (1933).
(5) A. Harvey and H. Bell, Proc. Phys. Soc. (Lond.) xlvii. p. 415 (1935).
(6) P. C. Mahanti, Phys. Rev. xlii. p. 609 (1932).
(7) R. K. Asundi, R. Samuel, and M. Zaki-Uddin, Proc. Phys. Soc. (Lond.), xlvii. p. 235 (1935).
(8) W. R. Frederickson and M. E. Hogan, jun., Phys. Rev. xlvi. p. 454 (1934).
(9) A. E. Parker, Phys. Rev. xlvii. p. 349 (1935).
(10) A. E. Parker, Phys. Rev. xlvii. p. 349 (1935); R. K. Asundi, Curr. Sci. iii. p. 153 (1934); Proc. Acad. Sci. Bangalore, i. p. 830 (1935).
(11) N. V. Sidgwick, 'The Electronic Theory of Valency' (Oxford, 1927).
(12) G. Gentile, *Zeits. f. Phys.* lxiii. p. 795 (1930); J. C. Slater, Phys. Rev. xxxii. p. 349 (1928); J. C. Slater and J. G. Kirkwood, Phys. Rev. xxxvii. p. 682 (1931); H. Margenau, Phys. Rev. xxxviii. p. 747 (1931); W. G. Penney, Phys. Rev. xlii. p. 585 (1932).
(13) F. Hund, *Zeits. f. Phys.* lxxiv. p. 1 (1932).
(14) P. K. Sen Gupta, Bull. Ac. Sci. (Allahabad), iii. p. 203 (1934).
(15) A. Petrikaln, *Zeits. f. Phys.* li. p. 395 (1928).
(16) W. Jevons. 'Report on Band Spectra,' London, Physical Society, 1932.
(17) P. N. Ghosh and G. N. Ball, *Zeits. f. Phys.* lxxi. p. 362 (1931); *cf.* also A. K. Sen Gupta, Proc. Phys. Soc. (Lond.) xlvii. p. 247 (1935).
(18) F. C. Connelly, Proc. Phys. Soc. (Lond.) xlvi. p. 790 (1934); E. N. Shawhan and F. Morgan, Phys. Rev. xlvii. p. 199 (1935); F. A. Jenkins and L. A. Strait, Phys. Rev. xlvii. p. 436 (1935).
(19) B. C. Mukherjee, *Zeits. f. Phys.* lxx. p. 552 (1931).

III. *Modulus of Elasticity of Materials for Small Stresses.*

By R. H. Evans, *M.Sc., Ph.D., and* R. H. Wood, *B.Sc.* *

Introduction.

IT was suggested by Rayleigh [1] that it was probable that the value of Young's Modulus for a metal, as found by a static method, would be different from that which corresponded to a dynamical condition such as prevails in the propagation of sound. The variation would depend on the difference between the isothermal and adiabatic elasticities of the metal. In solids the calculated difference is inappreciable, Kelvin [2] having found the ratio of the dynamic to the static modulus of elasticity to be 1·0026 for iron. Experiments, however, have often shown that the value of Young's modulus derived from the velocity of weak longitudinal vibrations in rods was appreciably higher than that obtained by the ordinary static methods, the experimental difference in the values being greater than that expected in the adiabatic and isothermal moduli [3]. It is therefore probable that the modulus of elasticity of materials at very low stresses, as measured by static methods, will exhibit very marked variations with the magnitude of the applied stress.

In the case of rocks and artificial stone a more complex phenomenon arises, in that the deformation generally increases after the stress has been applied. In a perfectly elastic solid the applied stress will produce an instantaneous deformation, which would then remain constant so long as the stress was kept constant. But with rocks and artificial stones the deformation may increase for considerable intervals of time resulting in a permanent set after the stress is removed. This is usually known as plasticity. Very often a large proportion of the apparent set is ultimately recovered, the phenomenon being referred to as elastic afterworking. Several terms have been adopted in connexion with the elastic imperfection of materials. Clerk Maxwell, for instance, originated the term "time of relaxation," this meaning the time taken by a material to come to a steady condition corresponding to a given stress. The elastic yielding

* Communicated by Prof. W. T. David, Sc.D., M.Inst.C.E.

of rocks under continued stress is important in dynamical geology, as it naturally illustrates the possibility of the folding of rocks and of the phenomena concerning the change of slope brought about by the continuous action of creep. D. W. Phillips [4] has also shown the significance of yielding in the formation of certain types of rock fractures and in the fall of roofs in mines. The elasticity of rocks under low stresses is directly connected with the deformation of the earth's crust, and a knowledge of the magnitude of the elastic constants is necessary to calculate the velocity of propagation of seismic waves [5]. The actual velocity of propagation has been determined by seismologists with reasonable accuracy, and dynamics has been applied by physicists to the study of geological phenomena.

The magnitude and importance of creep, which is so marked in many building materials, is now recognized in the design of structures, and attention is being devoted to it by numerous investigators. Little, however, is known of the actual mechanism of creep, and in view of this and of the above considerations it is thought that an investigation concerning the elasticity of metals and building materials for small stresses would help in elucidating the complex phenomena involved in the elastic and plastic behaviour of materials. These experiments have, as a matter of fact, made it possible to give a rational explanation for the rapid changes in the values of the modulus near zero stress in both tension and compression. In addition, the tests [8] have shown that as the range of the applied stress is decreased the modulus increases, which seems to indicate that the strain is approaching that due to the elastic distortion of the crystals, the limit to the range of applied stress depending on the sensitiveness of the extensometers.

Apparatus and Experimental Procedure.

The instruments used in this investigation were two mirror extensometers supplied by Messrs. Coates Machine Tool Co. In principle each consisted of two knife edges, about 1/100 in. apart, carrying the rotating spindle mechanism. A very high degree of magnification is obtained by the rotation of the spindle, the movement of which is observed optically by means of mirrors,

illuminated scales, and Davon microscopes. At the same time a reference mirror was used to correct for any tilting of the column. In this way it was found comparatively easy to detect strains as small as one-millionth of an inch. The mirror instruments are carried by extensometer frames of the Ewing pattern except that the screws in the Ewing extensometer are replaced by collars having knife-edges, these being firmly clamped to the column under test. The lower extensometer head is clamped to the lower collar, and is consequently unable to undergo any angular rotation due to the change in length of the column. The upper extensometer head rests on the upper collar by means of two hardened steel points, and the two heads are connected together at the back by means of a 5/8 in. diameter invar steel rod with piano wire, of 1/16 in. diameter, at the ends to effect resilient hinges. At the front, another invar steel rod hangs from the upper head, as in Ewing's extensometer, only a piece of piano wire again effects a resilient joint. This hanging frame at the front is guided and carries the mirror instrument, the plunger of the mirror instrument being in mechanical contact with a differential micrometer reading to 1/50,000 in. and fixed to the lower head. The multiplication factor of the strain is 3 in this extensometer, instead of 2 as in Ewing's, and the gauge length 30 in. The equivalent gauge length is therefore 90 in.

The columns tested in compression were usually 2 in. square in section and comprised of columns of steel, cast iron, glass, slate, marble, granite, sandstone, and concrete. It was considered desirable to include a variety of materials: steel on account of its supposed constant modulus; cast iron for its marked metallic crystalline structure; marble and granite as typical crystalline aggregates; slate and sandstone as being typical of other natural stones; glass and rubber as amorphous materials and, lastly, concrete as a very common example of artificial stone. For the small stresses, loads up to 100 lb. were applied directly to the top of the column to eliminate any inaccuracy of the loading. For higher loads a double lever dead-weight testing machine having a range of 20,000 lb. was used. With such high magnification of the strains, it was always necessary to have an identical column alongside

the column under test for making the necessary corrections due to any variations in laboratory temperature and humidity conditions, particularly when an appreciable time was taken in applying and removing the load as in making observations during a complete cycle of loading.

Experimental Results.

Many graphs have been obtained from each of the columns tested, and in this paper it is only possible to give typical results. Considering first the steel column fig. 1 shows some of the observations made for low and moderate steel stresses. The sudden drop in the value

Fig. 1.

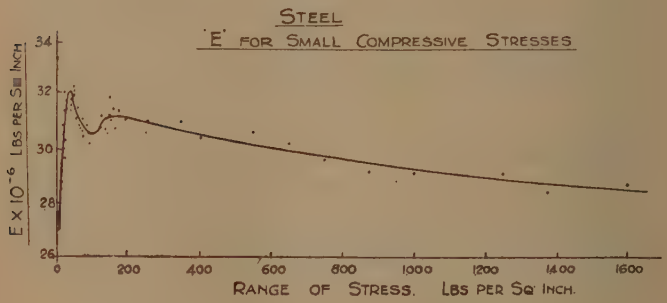

of the modulus near zero stress may at first sight be considered to be due to mechanical back-lash in the mirror instrument. It is clear, however, that the presence of back-lash would have the effect of increasing and not decreasing the modulus near zero stress. In addition, in all these experiments mechanical back-lash, if any, was reduced to a minimum by rotating the mirror mechanism, by means of the differential micrometer, in the required direction before every change of load, and each point on the graphs is the mean of six repetitions. The modulus reaches a maximum value at a stress of 40 lb. per sq. in. and afterwards decreases almost exponentially to the normal value of $28{\cdot}5 \times 10^6$ lb. per sq. in. Fig. 2 (*a*) and (*c*) shows the observations made for cast iron under small and high repeated ranges of compressive stress respectively. Again, there is a very

marked drop in the value of Young's modulus near zero stress, while the general form of the graph in fig. 2 (*c*) is very similar to that in fig. 1.

Fig. 2.

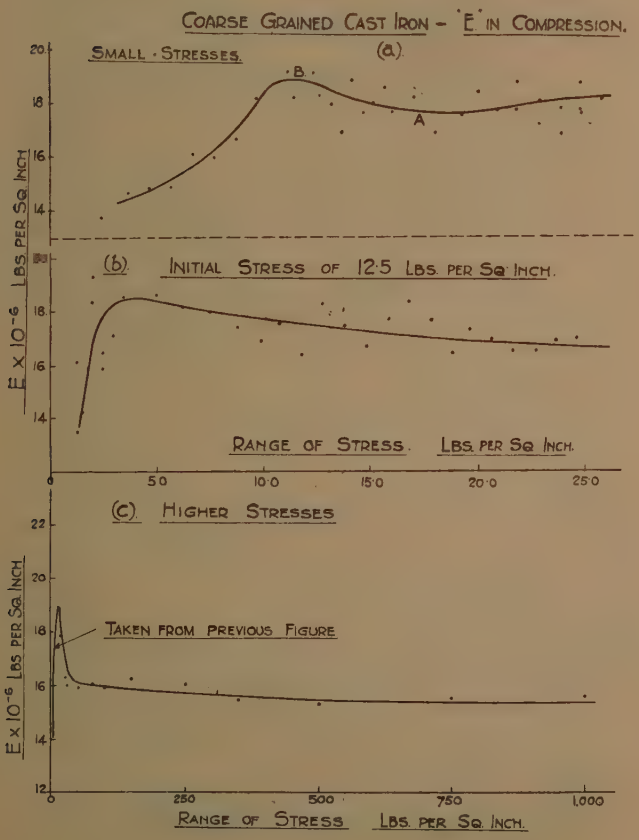

The glass column tested in compression had a section of $3 \times 1\frac{1}{2}$ in., and great care was taken to apply the load centrally and to distribute the stress at the ends by means of thick steel caps. Fig. 3 shows the values of the modulus for small ranges of stress. The general character of this graph agrees closely with that of

steel and cast iron. As before, the modulus increases very rapidly as the stress is increased from zero, reaches a maximum, and then decreases to its ordinary value. Figs. 4 (*a*, *b*), 5 (*a*, *c*), 6 (*a*, *b*) illustrate some of the results obtained for slate, marble, granite, Horsforth grit, concrete,

Fig. 3.

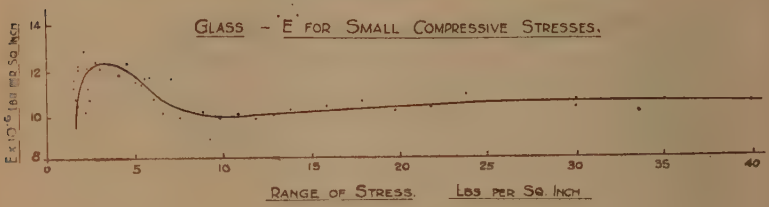

Fig. 4.

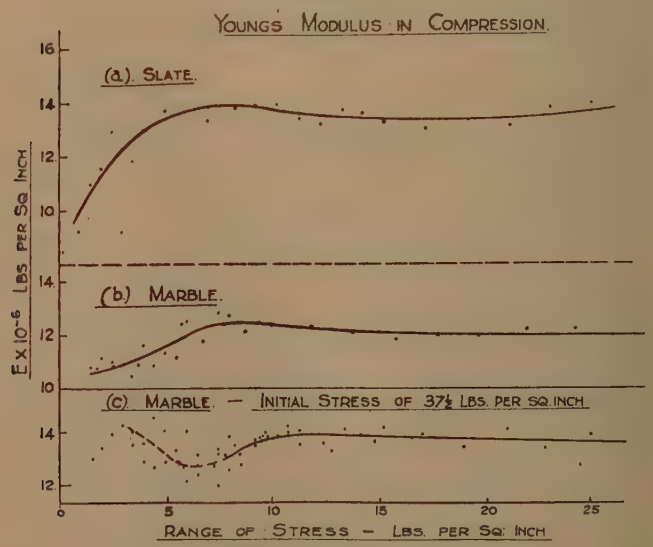

and sandstone. Generally speaking these curves show characteristics similar to those of steel and cast iron. It is of interest to note the constancy of the modulus for slate at all stresses above about 10 lb. per sq. in. In no other material tested in connexion with this investigation has the value of the modulus been so sensibly constant.

When first loading such materials as concrete and sandstone an appreciable set is generally observed after the

Fig. 5.

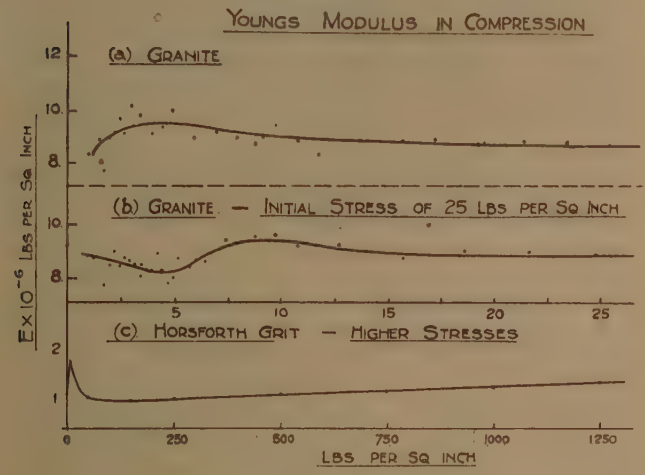

Fig. 6.

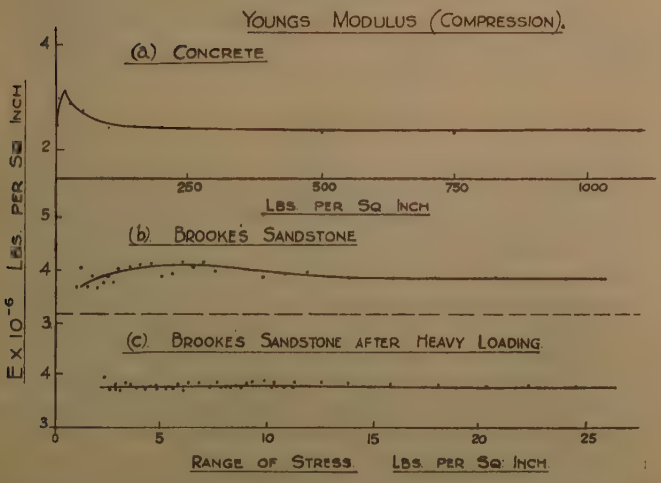

removal of all the load, and the value of the modulus obtained will naturally vary with the rate of loading and

with repetition of load. For tests at the higher stresses the columns were usually brought into a "state of ease," either by repeating the load a number of times or by allowing the column to stand under the maximum load of the cycle for some appreciable length of time before taking any observations [6]. For the lower stresses the column had not been previously loaded, and the creep at these values of stress was quite negligible during the time taken in repeating the load as compared with the immediate strain.

The most significant characteristic of all the curves referred to above is the sharp rise in the value of the modulus as the range of the applied stress is increased from zero. This phenomenon, therefore, appears to be connected only with very small ranges of stress from zero. A question that naturally arises now is the extent to which an externally applied initial stress will modify the shape of the curve for the values of the moduli when these are calculated from the increments of strain above this external initial stress. Many such curves were obtained for varying values of initial stress, a typical curve being shown in fig. 2 (*b*) for cast iron with an initial stress of 12·5 lb. per sq. in. The shape of the graph will naturally vary with the magnitude of the applied initial stress, and figs. 4 (*c*) and 5 (*b*) show the results obtained ultimately after several increments of the applied initial stress.

Discussion of Results.

The outstanding characteristic of the above curves for the moduli of materials that requires some theoretical explanation is the very rapid rise in the value of the modulus with increase of stress from zero when no additional initial stress is applied. It is desirable to formulate a theory which is applicable to an aggregate of crystals, or to the stones as they are obtained from the quarry.

As it does not seem possible to explain this phenomenon by considering the materials to be composed of a mixture of elastic and viscous elements, or by means of the theory of elasticoviscosity [7], it remains to find some condition that is present in both metals and crystalline and non-crystalline aggregates, and which may particularly affect the results at the smaller stresses. Tests by Prof. Coker

and others on model specimens using polarized light have emphasized the presence and importance of initial stresses in most castings after cooling, while glass has to be specially annealed in the process of manufacture to relieve it of these internal stresses. Materials like concrete, sandstone, marble, slate, and granite will be subjected to initial stresses due to shrinkage, quarrying, sawing, and other causes.

Considering then the effect of initial stresses it is clear that the internal forces must balance, and that some elements must be in tension and others in compression.

Fig. 7.

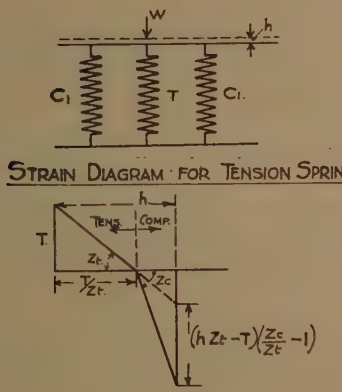

Again, for many materials the modulus of elasticity in tension is generally less than that in compression, and valuable information concerning the above phenomenon may be derived by examining the effect of this on the observed modulus when a column having initial internal stresses is loaded in compression.

The state of affairs in the column is equivalent to a system of springs joined in parallel, each spring having a different stiffness. It is sufficient for this purpose to consider three springs, as shown in fig. 7, one having an initial tension T and the others initial compressions C_1 and C_2 respectively. Let Z_t be the stiffness of the tension spring and Z_c that of the compression springs, Z_t being less than Z_c.

Let an external load W be applied to the system of springs and suppose the change of length is h. The modulus of the whole system will be proportional to $\frac{W}{h}$, and so long as the tension spring remains in tension

$$E \propto \frac{W}{h} \propto 2Z_c + Z \quad . \quad . \quad . \quad . \quad . \quad . \quad (1)$$

But if the load W is sufficient to cast the tension spring into compression we have, from a consideration of the work done on the three springs,

$$\tfrac{1}{2}Wh = C_1h + \tfrac{1}{2}h^2Z + C_2h + \tfrac{1}{2}h^2Z - \left\{ Th - \tfrac{1}{2}h^2Z_t - \tfrac{1}{2}\left(h - \frac{T}{Z_t}\right)^2 (Z_c - Z_t) \right\},$$

and since $T = C_1 + C_2$,

$$E \propto \frac{W}{h} \propto 2Z_c + Z_t + \left(1 - \frac{T}{hZ_t}\right)^2 (Z_c - Z_t). \quad . \quad . \quad (2)$$

When $h = \infty$, $E \propto 3Z_c$ or the system of springs behaves as if there were no initial tension.

When

$$h = \frac{T}{Z_t}, \quad E \propto 2Z_c + Z_t.$$

Equation (2) is $>$ (1) and approaches the limiting value of $3Z_c$. This result shows that a material composed of elastic elements having different stiffnesses, some being in tension and others in compression, would show a rise in the value of the modulus in direct compression at small stresses as the tension elements were converted into compression elements with increase of stress. If, in addition, the modulus in compression decreased gradually with increase of the range of stress, this being a common property of rocks and natural and artificial stones as shown by Gilchrist and Evans [8], the net result would be a rapid rise in the value of the modulus near zero followed by a gradual fall as the range of stress continued to increase, in much the same way as illustrated in the above graphs. On the other hand, if Z_t were greater than Z_c the material would show a fall in the value of the modulus in direct compression at small stresses.

In order to demonstrate this result a model was constructed which will be referred to as the "cast iron composite column." Cast iron is probably one of the most common materials in which the difference between the tension and compression moduli is most marked. A composite column was made by arranging nine one-inch square columns, 36 in. long, in a square pattern, the columns being clamped together and the ends milled to equal lengths. Large steel heads were fastened to the columns with $\frac{1}{2}$-in. screws and securely tightened, after having first inserted 1/1000 in. packings under five of the columns. Thus five of the columns were put

Fig. 8.

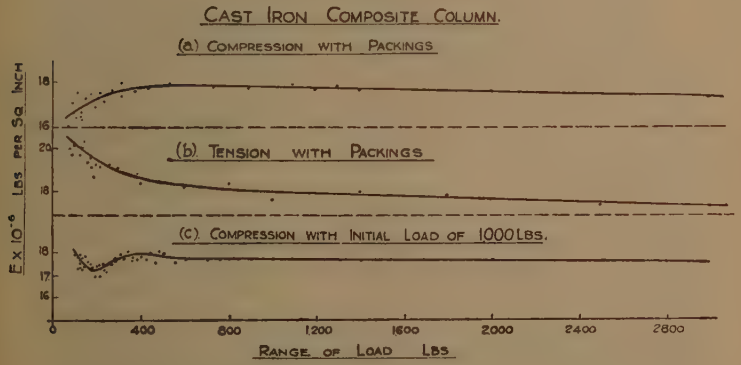

into initial compression and four into initial tension. In this way a new or composite column was constructed, itself in a state of internal stress, to represent the state of affairs which must have existed in the specimens tested. The extensometers were mounted in the usual way and the column loaded at stresses much higher than previously, as the phenomenon witnessed at low stresses with other materials should now occur at higher stresses with this composite column in consequence of the increased internal stress. The results obtained are plotted in fig. 8 (*a*), while fig. 8 (*c*) shows the results when using an initial load of 1000 lb. as base. These latter results in fig. 8 (*c*) compare very favourably with those in figs. 4 (*c*) and 5 (*b*), and have been obtained at much higher stresses than before. With low initial loads it

will be observed that an initial load causes the modulus to vary more rapidly near zero stress. This is due to the difference in slope between the stress-strain diagram when some elements in a column are initially in tension and others in compression, and the diagram when all the tension elements have been converted into compression. With an initial load the reference stress is nearer to this point where the slope increases abruptly. Consequently, the secant modulus, for increasing ranges of stress above some initial stress, is proportional to the slopes of the lines joining this reference stress to corresponding points on the original stress strain diagram. It will thus increase more rapidly as the reference stress approaches the point where the slope increases suddenly. After several increments of the external initial stress there is no further marked change in the value of the modulus. The somewhat irregular variations in figs. 4 (*c*), 5 (*b*), and 8 (*c*) near zero stress are probably due to a variation in the value of the ratio of the modulus in tension to the modulus in compression of the elements or crystals subjected to initial stresses. The magnitude of these initial stresses will not only vary from one element to another but also from one specimen to another.

Thus it will be seen that the internal stress theory is also in agreement with experimental results when it is applied to such materials as marble, sandstone, and concrete. When these, however, have been subjected to heavy loading it must be remembered that such heavy loading produces a plastic as well as an elastic distortion. Before the first loading the columns have internal stresses due to the varying causes already indicated. Consequently, this plastic distortion will be more pronounced in the case of those elements with initial compression if the applied load is compressive, and these elements will exhibit a greater permanent set on removal of the load. The material as a whole would therefore tend to be deprived of its initial stress by heavy loading, and it would be expected that the variations in the modulus of elasticity near zero range of stress would be removed to some appreciable extent. Fig. 6 (*c*) shows that this applies to a column of sandstone after three weeks of heavy loading to about two-thirds of the breaking stress.

In the case of steel or cast iron it may be possible to remove the internal stresses by annealing. This,

therefore, should materially reduce the peculiarity in the behaviour of the modulus near zero stress. D. K. Froman [9], for example, states that annealing of metals may be connected with the divergence from Hooke's law at small stresses. Also L. C. Tyte [10], in his experiments on the elastic extension of metal wires under longitudinal stress, found that all metals tested showed deviations from Hooke's law and that for annealed metals the deviation increased with increase of crystal size. The cast iron column, which had been previously tested for the results given in figs. 2 (*a*), 2 (*b*), 2 (*c*), was consequently annealed and loaded again to very small stresses. In this

Fig. 9.

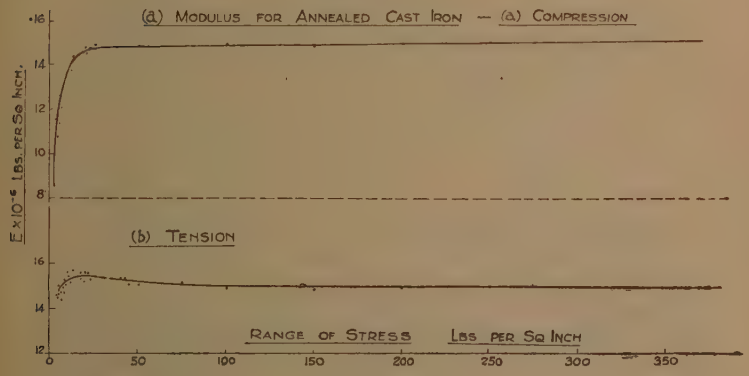

case the behaviour of the modulus, illustrated in fig. 9 (*a*), has been slightly affected in the required direction, but it is obvious from the continued drop near zero range of stress that the internal stresses have not been entirely removed. With metals there may be always some slight internal stresses due to a continual variation of temperature in the laboratory. The magnitude of the internal stress in, say, a steel column may be roughly estimated from a knowledge of the stress necessary to reach the peak value of the modulus, the stress necessary to reach the peak modulus being some measure of the average internal tension.

The above theoretical investigation concerning the cause of these changes in the values of the modulus

of elasticity may be readily extended to the case of a specimen tested in tension instead of compression when initial stresses are present. Using the same notation as before for the equivalent three-spring system and considering the whole system, we have for the case when the springs initially in compression remain in compression,

$$E \propto \frac{W}{h} \propto 2Z_c + Z_t \quad . \quad . \quad . \quad . \quad . \quad . \quad (3)$$

If, however, the springs initially in compression are thrown into tension

$$E \propto \frac{W}{h} \propto 2Z_c + Z_t - \left\{ 2Z_c - \frac{2(C_1+C_2)}{h} - Z_t\left(1-\frac{C_1}{hZ_c}\right)^2 - Z_t\left(1-\frac{C_2}{hZ_c}\right)^2 + \frac{1}{h^2Z_c}(C_1^2+C_2^2) \right\}$$

or

$$E \propto 2Z_c + Z_t - (Z_c - Z_t)\left\{ \left(1-\frac{C_1+C_2}{hZ_c}\right)^2 + \left(1-\frac{2C_1C_2}{h^2Z_c^2}\right) \right\} \quad . \quad . \quad . \quad (4)$$

And since by hypothesis $h > \frac{C_1}{Z_c}$ or $\frac{C_2}{Z_c}$ it follows that (4)<(3).

Evidently, then, the value of the modulus will fall when the compression elements are thrown into tension, and the limiting value of the modulus then becomes (when $h=\infty$) $\propto 3Z_t$, this being the same result as that for a column having no initial stress. Fig. 10 shows the results of testing the original cast iron column in tension under very small stresses. The graph is definitely different in form from all those obtained in compression. Again, fig. 8 (*b*) gives the results obtained with the " cast iron composite column " when tested in tension. These results, when compared with those observed in compression and shown in fig. 7 (*a*), also show the effect of the internal stresses on the modulus, and the general characteristics are in agreement with those deduced in the above theoretical reasoning for tensile tests.

Tensile tests on steel, brass, nickel, copper, and aluminium rods, $\frac{3}{8}$ in. diameter, have been also carried out by D. K. Froman [9] in connexion with the value

of the modulus at small stresses. His results show that Young's modulus increases very rapidly as the stress is increased from zero, reaches a maximum at a comparatively small stress, and then decreases exponentially to the ordinary value. It will be noticed that these results of Froman on metals in tension agree with the authors' results on metals in compression. Steel has been used in both investigations, and, from the above theory concerning the effect of the internal stresses on the modulus, it is clear that the modulus at low stresses will rise or fall rapidly according as to whether the modulus of the steel in tension is greater or less than the modulus in compression. In the case of steel the modulus in compression is often slightly below that

Fig. 10.

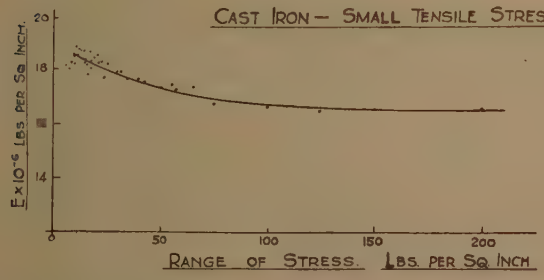

in tension [11], and it appears that this must have been the case in Froman's experiments. In the authors' experiments, however, the modulus of the steel column in compression is somewhat greater than that in tension, and it is probable that the ratio between them varies from one specimen to another. Froman also annealed one set of steel rods and found that there was little change in the value of the modulus and that the shape of the graphs remained precisely the same. This is in agreement with the authors' observations on an annealed cast iron column. It appears, therefore, that internal stresses of very low magnitude are sufficient to produce these phenomena in the values of the modulus near zero stress.

It is also of interest to investigate the effect of annealing the cast iron column, already referred to, by examining the results obtained in tension before and after annealing.

These are given in figs. 10 and 9 (*b*). As in compression the difference in the shape of the graph is slight, and it must be again concluded that annealing has not entirely removed the initial stresses.

These experiments are being extended at the present moment to examine the behaviour of rocks and natural and artificial stones in tension. Attention is also being devoted to the value of Poisson's ratio for elastic and plastic strains.

The authors wish to thank the Department of Scientific and Industrial Research for a maintenance grant for one of them (R. H. W.), and also Prof. W. T. David for his constant encouragement in carrying out these experiments.

References.

(1) Rayleigh, ' Theory of Sound, i.
(2) Kelvin, ' Encyclopedia Britannica,' New Werner ed. vii.
(3) G. F. C. Searle, ' Experimental Elasticity.'
(4) D. W. Phillips, Inst. of Mining Engineers, lxxx. (1931); lxxxii. (1932).
(5) H. Nagaoka, Phil. Mag. l. (1900).
(6) Adams and Coker, Carnegie Institution, Washington, 1906.
(7) H. Jeffreys, Proc. Roy. Soc. A, cxxxviii. (1932).
(8) Gilchrist and Evans, British Association, 1932.
(9) D. K. Froman, Phys. Rev. xxxv. (1930).
(10) L. C. Tyte, Phil. Mag. xiii. (1932).
(11) Univ. of Illinois, Bulletin, No. 115.

IV. *Turbulent Flow in a Circular Pipe.* *By* A. Fage, *A.R.C.Sc., of the Aerodynamics Department, The National Physical Laboratory* †.

1. Abstract.

EXPERIMENTS on turbulent flow in a square pipe made with the aid of an ultramicroscope are described in an earlier paper (1). These experiments gave valuable information on the nature of turbulent flow, especially near a wall, but they suffered from the disadvantage that the turbulent velocities measured cannot be related to the frictional stresses on the wall, because the flow is asymmetrical about the axis. This disadvantage does

† Communicated by E. F. Relf, A.R.C.Sc.

not arise for a circular pipe because, at a sufficient distance from the entry, the flow is symmetrical about the axis. An examination of turbulent flow in a circular pipe is capable, therefore, of yielding information which cannot be obtained from a square pipe, and for this reason the present work † was undertaken.

Apart from the introduction of measures to improve accuracy, the method of measurement was the same as that described in earlier papers [1], [5]. To minimize astigmatic distortion of view, illumination and observation of the flow were made through a parallel-sided glass cell surrounding the pipe. Distributions of the mean velocity (U), of the maximum longitudinal velocity fluctuation (u_1), and of the maximum angular deviations from the axial direction of the paths of particles moving in axial and tangential planes were measured. Maximum values of the radial component of disturbed velocity (v_1) and of the tangential component (w_1) were deduced from the observations by a more satisfactory method than that used in the earlier experiments.

The measurements of the mean velocity (U) taken with the ultramicroscope were found to be in very close agreement, except near the wall, with Pitot measurements made by Stanton; and the ultramicroscope measurements linked up satisfactorily with those taken, very near the wall, by Stanton with small surface tubes.

Observation on an axial plane revealed the fact that the maximum deviation of particles moving away from the wall is greater than that of those moving towards the wall. The distributions of the turbulent components u_1/U, v_1/U, and w_1/U in a circular pipe bear a general resemblance to those in a square pipe; but the ratios u_1/v_1 and u_1/w_1 on the axis are greater. The ratios u_1/U_* and w_1/U_* (where the frictional velocity U_* is $\sqrt{f/\rho}$, and f is the intensity of surface friction) have their maximum values at a distance from the wall given by $y_1=\dfrac{22{\cdot}4\nu}{U_*}$, and it is shown that it is at this distance that the curve of mean velocity, plotted in the form U/U_* against $\log\dfrac{U_*y_1}{\nu}$, experiences a notable change in shape.

† Permission to communicate the results was kindly given by the Aeronautical Research Committee.

2. List of Symbols.

ρ = Density.
μ = Coefficient of viscosity.
ν = Kinematic coefficient of viscosity.
D = Diameter of pipe.
R = Radius of pipe.
OX, OY, and OZ = Rectangular system of axes (OX coincident with the axis of pipe and OY radial).
y_1 = Distance from wall.
f = Intensity of surface friction.
$U_* = \sqrt{f/\rho}$.
U_0 = Mean rate of flow through pipe.
U = Mean velocity at any point.
U_c = Mean velocity on the axis.
Θ_{xy1} = Maximum angular deviation, from OX direction, of particles passing through a point in the plane XOY, and moving in this plane towards the wall.
Θ_{xy2} = Maximum angular deviation, from OX direction, of particles passing through a point in the plane XOY, and moving in this plane away from the wall.
Θ_{xz} = Maximum angular deviation, from OX direction, of particles passing through a point in a plane parallel to XOZ.
u_1, v_1 and w_1 = Maximum values of the three components of disturbed velocity.

3. Water System.

A diagrammatic sketch of the water system is given in fig. 1. The frictional measurements were made for a circular brass pipe having an internal diameter 1·064 in. and an overall length 130 in. The inlet end was faired. A uniform flow through the pipe was maintained by a constant difference between the water levels in the inlet and exhaust tanks. Water was supplied direct to the inlet tank ($4 \times 2 \times 2$ ft.) from the mains. The intensity of surface friction was determined from the drop of pressure between two holes 12 in. apart, the upstream

hole being 102 in. (96 diameters) from the entry. The pressure measurements were made with a 13-in. Chattock gauge, in which water in contact with carbon tetrachloride (specific gravity 1·5890 at 25° C.) was used.

Fig. 1.

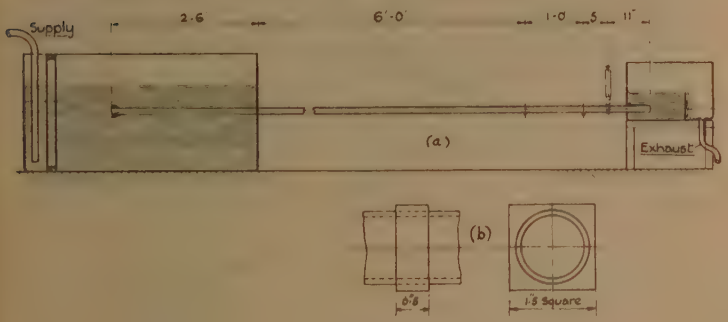

Fig. 2.

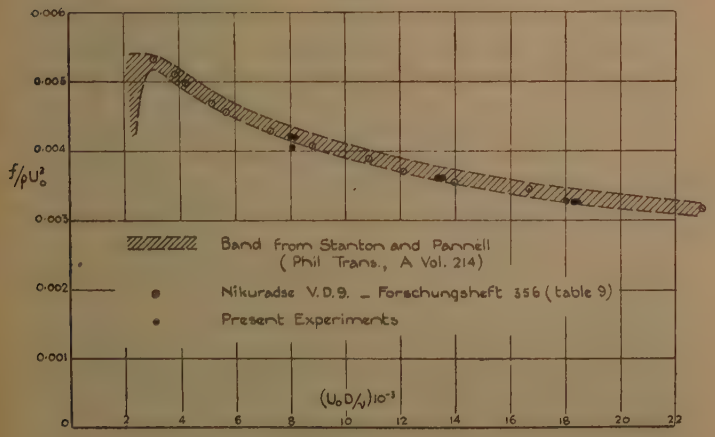

The mean rate of flow (U_0) was determined from the measured rate of discharge.

Values of the frictional coefficient $f/\rho U_0^2$ are plotted (black dots) against U_0D/ν in fig. 2. These values are in close agreement with those obtained by Nikuradse (ref. 4. table ix.), and both sets fall within the region

(shaded band) covered by the observations of Stanton and Pannell [3].

The flow was observed through a 6 in. length of glass tube inserted in the brass pipe. The central part of this tube, where observation was made, was surrounded by a parallel-sided glass cell (see fig. 1 (*b*)), to lessen astigmatic distortion. The inner diameter of the glass tube was slightly greater than that of the brass pipe (1·076 in. against 1·064 in.), and continuity of surface at the brass-glass junctions (especially at the upstream one) was obtained by careful fairing with "Durofix." The observation section was 119 in. (about 110 diameters) from the entry. The friction on the wall of the glass was deduced from the curve for the brass pipe, the Reynolds number taken being that for the glass tube †.

(4) Mean Velocity.

Ultramicroscope.

The method of velocity measurement ‡ depends on the fact that small particles moving through a light beam appear as bright points of light when they are viewed through a microscope travelling at the speed at which they move. Instead of moving the whole microscope, the eyepiece and microscope tube are held fixed, and the objective is rotated in the direction of motion of the fluid. When the flow is turbulent, the velocity component in the mean direction of flow fluctuates continually between the limits $(U \pm u_1)$, and particles can only appear as points of light provided the objective is rotated within the corresponding speed-range. In practice the value of $(U-u_1)$ is obtained by increasing the speed of the objective (in short steps) until "stationary" particles (or streaks normal to the flow) first appear, and the value of $(U+u_1)$ by increasing the speed further until they just cease to appear. If N_2 and N_1 are the two limits of rotational speed, the mean velocity U is given by $\frac{C}{2}[N_1+N_2]$, where C is a factor obtained by direct calibration. The value of $\frac{u_1}{U}$ is given by

$$\frac{(N_1-N_2)}{(N_1+N_2)}.$$

† (U_0D/ν) glass $= 0{\cdot}989$ (U_0D/ν) brass for the same volume-discharge.
‡ See ref. (1) for a more complete description.

The magnification was too high to allow the flow in the horizontal axial plane of the pipe to be viewed directly, and an image of this field was viewed through the microscope. This image (magnification 1 to 1) was obtained outside the pipe by an anastigmat lens ($f=2$ in.) carried on the microscope tube (fig. 3).

A circular beam of light of diameter 0·275 in., obtained from a 5 amp. carbon arc and a suitable lens system, was passed through the water (fig. 3). This beam was slightly distorted during its passage through the system, and at the centre of the pipe the section was elliptical (depth 0·320 in. and width 0·275 in. approx.). The

Fig. 3.

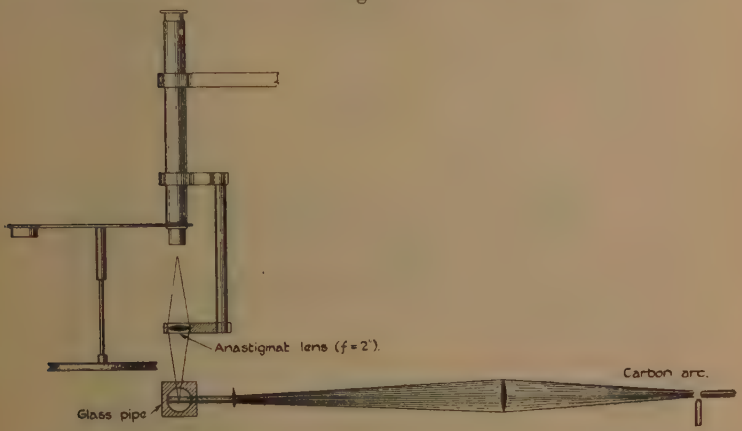

image given by the anastigmat lens had a depth of 0·180 in. and a width of 0·275 in. (approx.). This image was viewed through the microscope under a magnification of about 40 to 1. The length of the magnified path of a particle passing through the widest part of the light beam was about 11·0 in. With this length of path the error arising from an uncertainty whether particles appear as points does not exceed $\pm 0{\cdot}27$ per cent., provided that streaks of length greater than 0·03 in. are not mistaken for points [5].

The position of a point in the pipe is specified with reference to rectangular axes OX, OY, OZ, where OX is taken coincident with the pipe axis, OY is radial, and OZ is at right angles to OX and OY.

The radial position of a point was measured with the device shown in fig. 4. This device consists of a rod carrying a slider free to move radially, under the action of a spring, in a groove at one end. The upper surface of the slider is graduated, and in an axial plane of the rod. The rod has a close fit in the pipe and, when located in position, the free end of the slider is pressed by the spring against the wall of the pipe. Longitudinal grooves cut in the rod allow a calibration to be made with water flowing through the pipe. When in position, the rod projects beyond the exit end of the pipe, and a spirit level, attached to this end, indicates when the plane of the slider is horizontal.

The microscope was traversed radially by a micrometer-screw. To calibrate, the microscope was focussed on

Fig. 4.

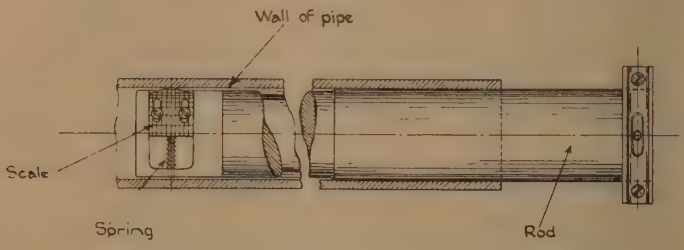

the scale of the slider, and the readings of the micrometer recorded against the known distances of the graduations from the wall. Experience showed that with this method of measurement the distance of a point of observation from the wall could be determined to within $\pm 0{\cdot}001$ in. Before the rod was withdrawn, the light beam was aligned so that its axis was horizontal and in the plane of the upper surface of the slider on which the microscope was focussed. It was possible, therefore, to ensure that only those particles which passed through the widest part of the light beam were under observation; and, as a further precaution, attention was confined to those particles which were sharply in focus. Particles from finely powdered pumice were added to those particles always present in tap-water, to facilitate observation.

Distributions of mean velocity were measured at $U_0D/\nu = 8090$, 13440 and 18340. The observations taken are given in Table I., and they are plotted in fig. 5.

Fig. 5.

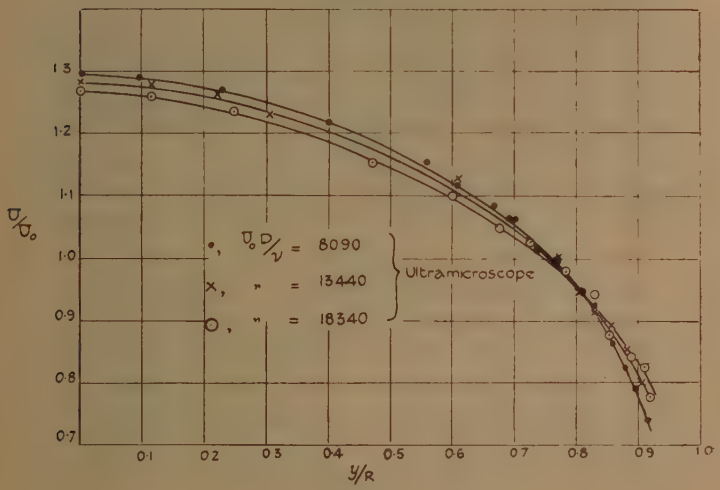

TABLE I.

$U_0D/\nu = 8090$.			$U_0D/\nu = 13440$.			$U_0D/\nu = 18340$.		
y/R.	U/U_0.	u_1/U.	y/R.	U/U_0.	u_1/U.	y/R.	U/U_0.	u_1/U.
0	1·295	0·150	0	1·281	0·175	0	1·268	0·160
0·097	1·289	0·145	0·116	1·276	0·175	0·117	1·258	0·160
0·231	1·269	0·160	0·222	1·262	0·175	0·249	1·234	0·170
0·401	1·212	0·185	0·305	1·227	0·195	0·471	1·150	0·220
0·558	1·153	..	0·608	1·125	0·255	0·601	1·096	0·245
0·588	..	0·255	0·767	0·995	0·330	0·677	1·045	0·275
0·607	1·112	0·230	0·811	0·941	0·340	0·725	1·020	0·280
0·670	1·080	0·270	0·837	0·914	0·390	0·786	0·975	0·325
0·693	1·062	..	0·862	0·894	0·415	0·835	0·942	0·350
0·700	1·058	0·285	0·889	0·854	0·460	0·861	0·878	0·380
0·770	0·992	0·340	0·913	0·802	0·510	0·894	0·841	0·425
0·814	0·941	0·410				0·916	0·822	0·490
0·831	0·919	0·410				0·928	0·772	0·475
0·866	0·864	0·460						
0·887	0·820	0·505						
0·905	0·784	0·545						
0·926	0·734	0·585						

Pitot Tube.

Total-head distributions for air at $U_0D/\nu=18950$ were also measured. For these experiments a 6 in. length of brass pipe of internal diameter 1·064 in. was substituted for the glass tube of the water system, and an airtight box for the water exhaust tank. Air was drawn through the pipe by a centrifugal fan connected by a long rubber pipe to the exhaust box.

The exploring tube was made from fine hypodermic steel tubing compressed at the mouth into a rectangular shape. The dimensions of the opening were 0·009 in. (width) and 0·044 in. (depth); the external dimensions of the mouth were 0·020 in. (width) and 0·060 in. (depth).

TABLE II.

$U_cD/\nu=24000$; $U_0D/\nu=18950$ (predicted value).

y/R.	U/U_c.	y/R.	U/U_c.	y/R.	U/U_c.	y/R.	U/U_c.
0	1·000	0·419	0·930	0·780	0·790	0·921	0·687
0·137	0·992	0·452	0·921	0·814	0·772	0·936	0·669
0·170	0·988	0·513	0·905	0·827	0·759	0·945	0·653
0·232	0·977	0·546	0·888	0·842	0·754	0·964	0·589
0·263	0·971	0·607	0·870	0·871	0·736	0·968	0·577
0·325	0·956	0·639	0·854	0·874	0·730		
0·357	0·947	0·686	0·836	0·897	0·710		
		0·733	0·814				
		0·758	0·803				

The pressure at the mouth was measured against the static pressure at a hole in the side of the pipe, and the velocity was calculated directly from these total-head readings. The exploration was made at a distance 112D from the mouth of the pipe. The frictional resistance was determined, for the range $3000<U_cD/\nu<19000$, from the pressure drop between the holes used in the water experiments.

The Pitot tube was traversed across the pipe by a micrometer screw. A calibration for the tube position was obtained with a cylindrical gauge having concentric circles of known radii engraved on one end. This gauge just fitted the pipe, and was mounted with its engraved end in the same plane as the mouth of the tube. The micrometer reading was taken as the centre of the mouth (viewed under a microscope) traversed across each circle.

These readings plotted against radius gave a linear calibration within one or two-thousandths of an inch. The distance of the centre of the mouth from the pipe wall, deduced from this calibration, when the tube just made electrical contact with the wall, was 0·011 in. This value agrees within 0·001 in. with that obtained from the width of the tube (0·020 in.), on the assumption that contact was made at the mouth.

The velocity results, deduced from the total-head readings against the static pressure at the wall, are given in Table II.

Figs. 6 (*a*) & (*b*).

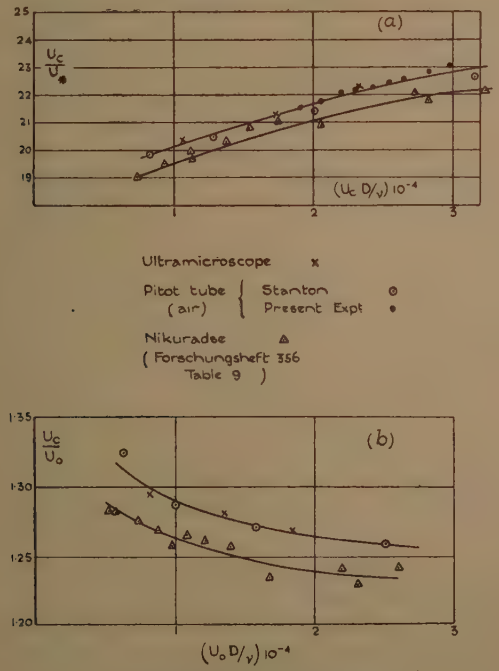

5. Discussion of Results.

Mean Velocity.

Comparisons of the velocity results with those obtained by Stanton and Pannell [3] and Nikuradse [4] are made in figs. 6 and 7. In fig. 6 (*a*) values of U_c/U_* are plotted

against $U_c D/\nu$. The ultramicroscope results for water are in close agreement with the Pitot results for air flowing through the same pipe, and with the Pitot results of Stanton and Pannell. Nikuradse's results (deduced from table ix., ref. 4) are about 3 per cent. lower.

Good agreement between the ultramicroscope results and the Pitot results of Stanton and Pannell is also shown in fig. 6 (*b*) †—where values of U_c/U_0 are plotted against

Fig. 7.

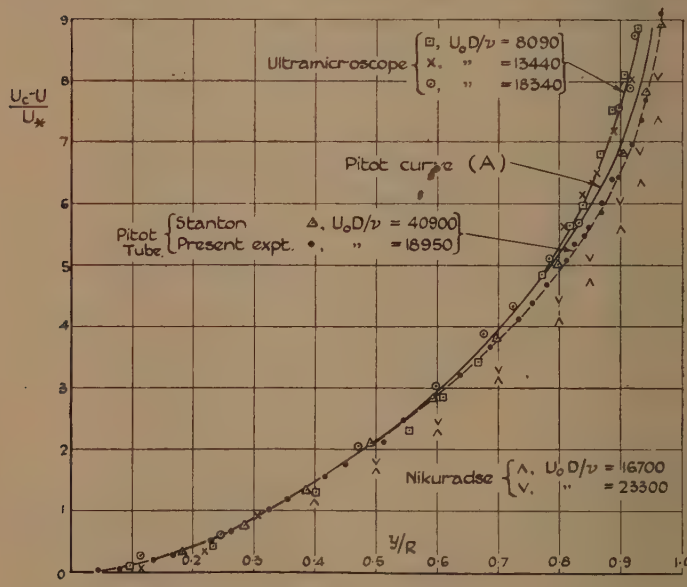

$U_0 D/\nu$—but Nikuradse's results (table ix., ref. 4) are low (about 2·2 per cent.).

Theoretical considerations lead to the conclusion that the curve $\left(\frac{U_c - U}{U_*}\right)$ against y/R is independent of the Reynolds number, except near the wall. The results for $U_0 D/\nu = 8090$, 13440, and 18340 are plotted in this form in fig. 7, and it is seen that a curve can be drawn

† Values of U_c/U_0 for the present air experiments cannot be included because measurements of the mean rate of flow, U_0, were not made.

to pass fairly closely through them. The Pitot results obtained by Stanton † (ref. 6) and by the author are also plotted; they are in close agreement, but the curve (dotted) on which they lie departs progressively, as the wall is approached, from that passing through the ultra-microscope results.

The reading of a Pitot tube in a disturbed stream depends not only on the local mean velocity, U, and the local mean static pressure, p, but also on the turbulence in the stream. It is generally believed that the total pressure at the mouth is more likely to be $(p+\frac{1}{2}\rho U^2+\frac{1}{2}\rho\overline{q^2})$ than $(p+\frac{1}{2}\rho U^2)$, where q is the resultant turbulent velocity; and if the value of the mean static pressure at the wall is p, the velocity (U_P) deduced from the Pitot reading is $U\sqrt{\left(1+\frac{\overline{q^2}}{U^2}\right)}$, which may be written

$$U\left(1+\frac{\overline{q^2}}{2U^2}\right),$$

since $\frac{\overline{q^2}}{U^2}$ is small. Further, the root mean sqaure of each of the components (u, v, w) of the turbulent velocity can be taken as one-third of the maximum values ‡ (u_1, v_1, and w_1), and writing $\overline{q^2}=\overline{u^2}+\overline{v^2}+\overline{w^2}$, the velocity deduced from the Pitot reading becomes,

$$U_P=U\left(1+\frac{1}{18}\left[\frac{\overline{u_1^2}}{U^2}+\frac{\overline{v_1^2}}{U^2}+\frac{\overline{w_1^2}}{U^2}\right]\right). \quad . \quad . \quad (1)$$

On the above assumptions the velocity (U_P) overestimates the true mean velocity (U) by

$$\frac{U}{18}\left[\left(\frac{u_1}{U}\right)^2+\left(\frac{v_1}{U}\right)^2+\left(\frac{w_1}{U}\right)^2\right].$$

There is, however, no evidence that the mean static pressure at the wall is p; on the contrary, it may be,

† Stanton's paper does not give the value of ν, or the mean velocity of flow U_0. The value of U_* is given, and the value of U_0 has been obtained from the (U_0/U_C, U_0D/ν curve given in a later paper by Stanton and Pannell (ref. (3)), the value of ν assumed being that for a temperature 16·5° C. The value of U_*/U was calculated from the value of $f/\rho U_0^2$ taken from the ($f/\rho U_0^2$, U_0D/ν) curve in the same paper.

‡ Townend has shown that this relation holds in a square pipe [ref. 7].

as suggested by Taylor's Vorticity Transport Theory, that $(p+\frac{1}{2}\rho\overline{q^2})$ is constant across a section, and then U_P would be equal to U. Further research † is needed before it can be decided whether any correction should be made for turbulence, and, in view of this uncertainty, values of U_P/U have been calculated from the above relation and the values of u_1/U, v_1/U and w_1/U given later in the paper. It is seen in Table III. that the difference between U_P and U is small on the axis, but rises to about 3·5 per cent. at 0·05R from the wall. The corresponding overestimation in the rate of discharge is about 1·3 per cent. The Pitot curve (A) of fig. 7 was obtained from values of U determined from relation (1) above. This curve lies about midway between

TABLE III.

Values of U_p/U.

y/R.	$U_0D/\nu=18400$.	$U_0D/\nu=13500$.
0	1·002	1·002
0·3	1·003	1·003
0·6	1·0065	1·0065
0·75	1·0125	1·0125
0·80	1·0165	1·0160
0·90	1·0285	1·0285
0·95	1·0355	1·0355

the ultramicroscope curve and the Pitot curve obtained when the velocity is calculated directly (in the usual way) from the total-head reading against static pressure at the wall. It should be added that it has been assumed that the Pitot reading gives the pressure at the geometrical centre of the mouth, and that no correction for any wall interference has been applied.

Values of $\frac{U_c-U}{U_*}$ obtained at $U_0D/\nu=16700$ and 23300 by Nikuradse (table vii., ref. 4) are plotted in fig. 7. These values lie below the ultra-microscope and the Pitot values; but it should be added that values obtained by Nikuradse at higher Reynolds numbers are in much closer agreement.

† This Research is now in hand.

Recently [11] the distribution of velocity across a section of a circular pipe has been calculated by Dr. Goldstein on the Vorticity Transport Theory, and also by Prof. Taylor on a modified form of this theory. Each solution contains only one arbitrary constant, and its value is determined by making the value calculated at $y=0{\cdot}7R$ agree with that observed. The suppositions of Dr. Goldstein differ from those of

Fig. 8.

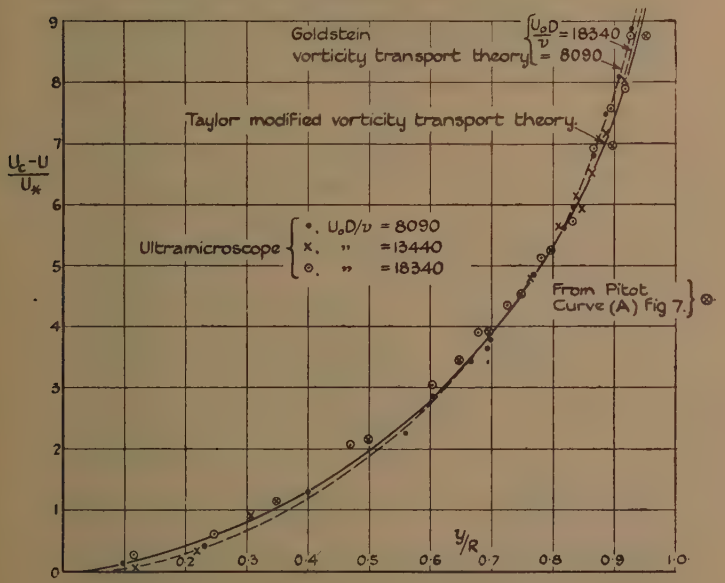

Prof. Taylor, but the distributions obtained are of the same character, and both are in close agreement with that measured by Stanton, except near the wall. Taylor's distribution is given in fig. 8 by the full line, and Goldstein's distribution (calculated for $U_0D/\nu=8090$ and 18340, and including the effect of viscosity) by the dotted lines. The ultramicroscope values of $\frac{U_c-U}{U_*}$ are included, and they fall close to the theoretical curves. In addition, a few values taken from the Pitot curve (A)

of fig. 7 are plotted (crosses in circles) : they also lie near the theoretical curves.

The distribution of velocity near the wall can be illustrated by plotting values of U/U_* against $\log \frac{U_* y_1}{\nu}$, where y_1 is the distance from the wall. The results of the present experiments, and those of Stanton [8], taken with surface tubes (at somewhat lower Reynolds numbers), are plotted in this form in fig. 9. A curve can be drawn to pass fairly closely through all these results. This curve is straight over the greater part of its length, but a somewhat sharp bend occurs at about

Fig. 9.

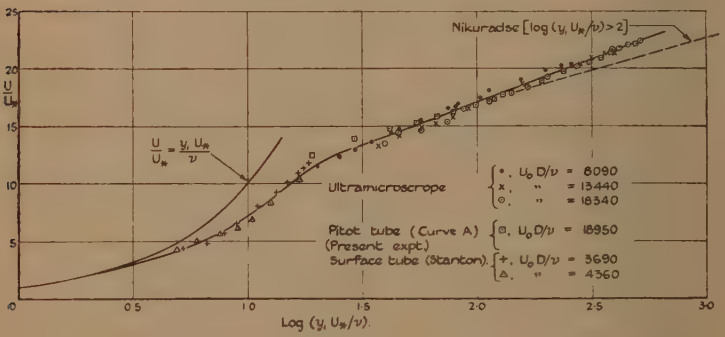

$\log \frac{U_* y_1}{\nu} = 1{\cdot}35$, that is, at $y_1 = \frac{22{\cdot}4\nu}{U_*}$. It will be shown later that at this distance from the wall the flow is most disturbed. The diagram also shows that the curve drawn through Stanton's observations taken with surface tubes merges into the curve for linear velocity distribution $\frac{U}{U_*} = \frac{y_1 U_*}{\nu}$ at about $\log \frac{U_* y_1}{\nu} = 0{\cdot}4$, *i. e.*, $\frac{U_* y_1}{\nu} = 2{\cdot}5$. The thickness of the thin viscous layer within which the velocity increases linearly with the distance from the surface appears, therefore, to be about $\frac{2{\cdot}5\nu}{U_*}$. It is here relevant to mention that experiments on rough pipes made by Nikuradse [9] show that roughness does not affect the

resistance to flow until the average height of the excrescences exceeds $3\nu/U_*$; and it appears—as suggested by Prandtl and Schlichting [10]— that excrescences only affect the resistance when they project beyond the thin viscous layer at the surface. The results here given show that this layer can be defined as the region within which the velocity increases linearly with the distance from the surface.

Nikuradse [4] found that values of U/U_* for smooth pipes fell closely on a straight line when they were plotted against $\log \frac{y_1 U_*}{\nu}$. This line, shown dotted in fig. 9, lies somewhat below that passing through the present results.

Fig. 10.

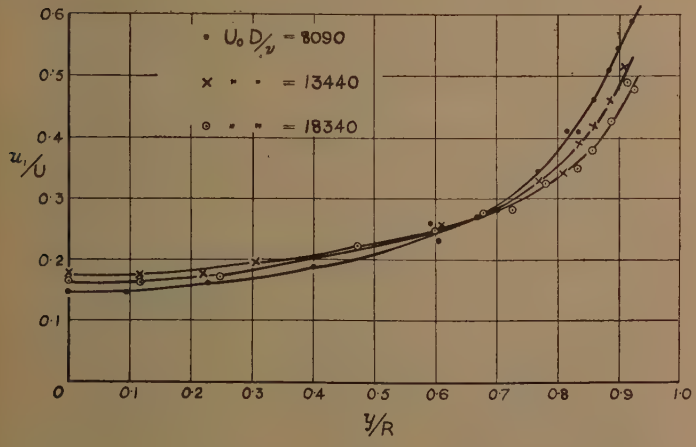

(6) Turbulence Measurements.

(*Ultramicroscope.*)

Distributions of the maximum longitudinal component of disturbed velocity, u_1, were measured in the manner described earlier in the paper. The observations of u_1/U obtained are given in Table I., and they are plotted against y/R in fig. 10.

Distributions of the maximum lateral component of disturbed velocity (v_1) normal to the wall (direction OY)

TABLE IV.

Values of Θ°_{xy1}.

$U_0D/\nu=8090$.		$U_0D/\nu=13440$.		$U_0D/\nu=18340$.	
y/R.	Θ°_{xy1}.	y/R.	Θ°_{xy1}.	y/R.	Θ°_{xy1}.
0·070	4·0	0·256	5·3	0·256	4·5
0·257	4·8	0·443	5·3	0·269	5·1
0·350	5·1	0·628	7·1	0·730	7·9
0·372	4·9	0·721	9·1	0·785	10·5
0·693	7·7	0·814	11·3	0·814	9·8
0·768	9·1	0·861	13·3	0·861	10·8
0·830	10·3	0·907	12·1	0·907	10·8
0·861	13·1				
0·907	13·1				
0·930	10·5				

Values of $-\Theta^{\circ}_{xy2}$.

$U_0D/\nu=8090$.		$U_0D/\nu=13440$.		$U_0D/\nu=18340$.	
y/R.	$-\Theta^{\circ}_{xy2}$.	y/R.	$-\Theta^{\circ}_{xy2}$.	y/R.	$-\Theta^{\circ}_{xy2}$.
0·070	4·0	0·256	5·2	0·256	3·8
0·350	5·3	0·443	9·4	0·442	7·7
0·372	5·2	0·535	10·7	0·535	10·6
0·700	12·0	0·628	14·7	0·674	14·7
0·722	12·6	0·686	16·5	0·707	15·5
0·768	14·4	0·814	19·0	0·814	19·5
0·830	19·7	0·861	20·0	0·907	20·5
0·861	20·2	0·907	18·0		
0·907	17·4				
0·930	16·9				

On axis ($y=0$): $\Theta^{\circ}_{xy1}=\Theta^{\circ}_{xy2}=\Theta^{\circ}_{xz}=\Theta^{\circ}$.

$U_0D/\nu=8090$.	$U_0D/\nu=13440$.	$U_0D/\nu=18340$.	Earlier work (ref. (1)).	
			U_0D/ν.	Θ°.
4·0, 3·8 } 3·9	6·1, 4·5, 4·0 } 4·25	4·2, 4·2, 4·5 } 4·3	5400	5·75
			6260	6·25
			7500	6·25

were deduced from the maximum angular deviation (from the direction OX) of the paths of particles observed with the microscope focussed on the axial plane XOY. These deviations were measured, as in earlier work [1], by a fine platinum wire mounted in the focal plane of the eyepiece and capable of rotation about the axis of the microscope.

As the wall is approached, the maximum angular deviations, Θ_{xy2}, of the particles moving away from the wall are greater than the maximum deviations,

Fig. 11.

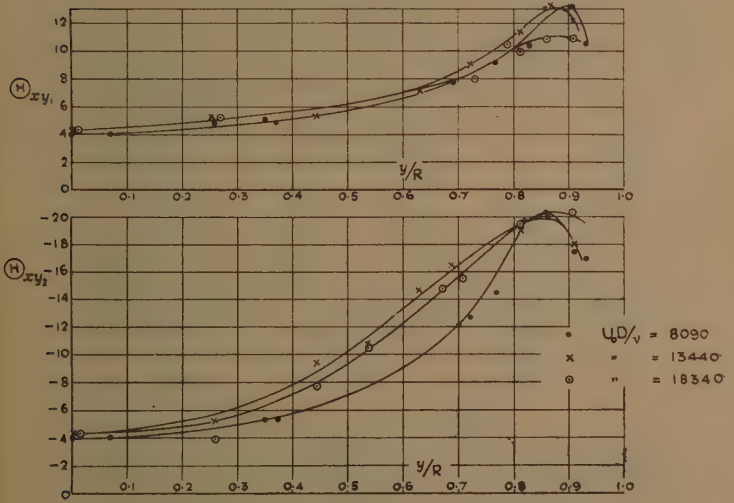

Θ_{xy1}, of the particles moving towards the wall. The observations of Θ_{xy1} and Θ_{xy2} taken are given in Table IV., and they are plotted against y/R in fig. 11. The values for the central region of the pipe are small, and they could not be measured with great accuracy. An idea of this accuracy can be gathered from the repeat values given at the bottom of the table. These values are smaller than those which would be expected from a few observations taken, at a lower Reynolds number, in an earlier experiment [1]. For this reason observation was made for a long time before the values given in Table IV. were accepted.

Both Θ_{xy1} and Θ_{xy2} have maximum values (about 13° and −20° respectively) at about 0·12R from the wall.

In previous work [1] the value of v_1 was predicted from the relation † $v_1 = U \tan\left[\frac{\Theta_{xy1} - \Theta_{xy2}}{2}\right]$. This relation is not altogether satisfactory, and the one given later in § 8 is now preferred. The distribution of v_1/U, deduced from faired experimental data in the manner described in § 8, are given in fig. 13.

TABLE V.

Values of Θ°_{xz}.

(Values on axis given in Table IV.)

$U_0D/\nu = 8090$.		$U_0D/\nu = 13440$.		$U_0D/\nu = 18340$.	
y/R.	Θ°_{xz}.	y/R.	Θ°_{xz}.	y/R.	Θ°_{xz}.
0·270	4·6	0·315	5·0	0·265	5·5
0·390	5·8	0·400	6·4	0·315	5·5
0·530	7·7	0·442	7·0	0·463	6·8
0·625	9·9	0·550	8·6	0·525	8·3
0·696	13·4	0·648	10·3	0·608	10·8
0·742	16·3	0·746	14·7	0·700	15·2
0·804	19·8	0·859	23·5	0·775	19·1
0·860	24·5	0·926	31·1	0·824	22·1
0·913	27·5			0·913	29·0
0·922	29·5			0·930	34·0
0·940	32·8				

Distributions of the maximum lateral component of disturbed velocity (w_1) (tangential direction) were deduced from observations of the maximum angular deviations (from the OX direction) of the paths of particles observed with the microscope focussed on planes parallel to XOZ ‡. The microscope was focussed with a micrometer screw, and the position of a plane of focus was determined from a calibration obtained by focussing on the uppermost generators of brass cylinders of known diameter resting on the bottom of the glass pipe. To ensure that observation was confined to a thin lamina, the highest magnification possible was used, and attention was confined to particles which were sharply in focus.

† Θ_{xy2} is negative.

‡ The axis OY is now taken in the vertical direction.

The observations of Θ_{xz} are given in Table V. and they are plotted in fig. 12. Values of w_1/U were obtained by the relation in § 9. The distributions of w_1/U obtained when faired values of u_1/U and Θ_{xz} are substituted in this relation are given in fig. 13.

(7) Discussion of Turbulence Results.

The curves of fig. 13 bear a general resemblance to those obtained for a square pipe (fig. 7 (*b*), ref. (1)).

Fig. 12.

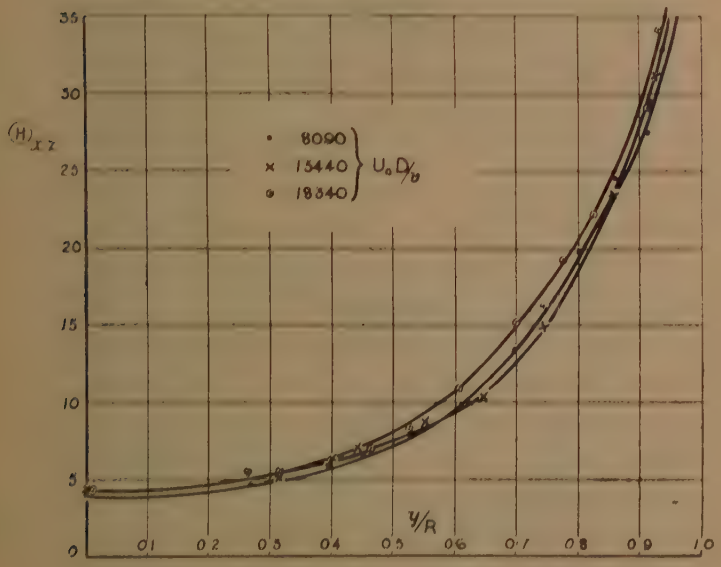

The value of u_1/U increases from the centre to the wall and has a tendency to become constant (but not so definitely as for a square pipe) near the wall; the value of v_1/U increases slowly with the distance from the axis, reaches a maximum (at $y = 0{\cdot}86R$), and then falls to zero at the wall; and the value of w_1/U increases with y, and rises rapidly as the wall is approached. On the axis the longitudinal component u_1/U is about double (actually 2·2 to 1) the lateral components v_1/U and w_1/U, whereas the ratio obtained for a square pipe, at about the same

value of the Reynolds number † $U_0 m/\nu$, was appreciably smaller (about 1·17 to 1).

The turbulence results are presented on a $\log \frac{U_* y_1}{\nu}$ base in fig. 14, where curves of u_1/U_* are drawn through actual observations, and those of v_1/U_* and w_1/U_* through

Fig. 13.

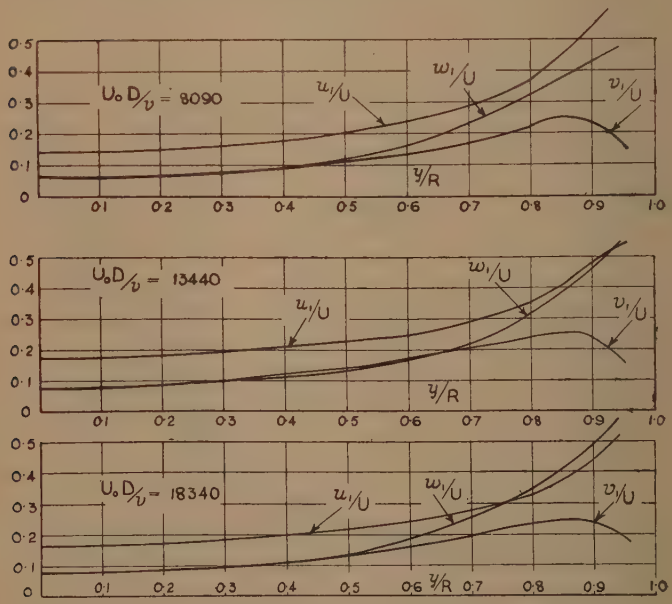

faired values. The three curves of u_1/U_* rise, as the wall is approached, to about the same maximum at

$$\log \frac{U_* y_1}{\nu} = 1{\cdot}35, \quad i.\,e. \quad \frac{U_* y_1}{\nu} = 22{\cdot}4.$$

This is a significant result, for it is at this value of $\frac{U_* y_1}{\nu}$ that the curve of U/U_* has a notable bend (see fig. 9). The curves of w_1/U_* also rise to maximum values at about

† m is the hydraulic mean depth.

$\log \frac{U_* y_1}{\nu} = 1{\cdot}35$, but the values are different, and decrease as $U_0 D/\nu$ increases.

The turbulence components u_1/U_*, v_1/U_*, and w_1/U_* are functions of $\frac{U_* y_1}{\nu}$ and y_1/R. The curves (*a*) and (*b*)

Fig. 14 (*a*), (*b*), (*c*).

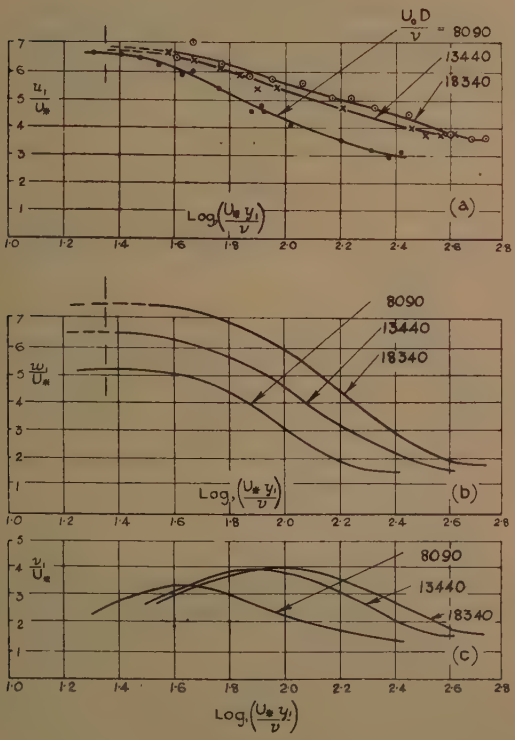

of fig. 14 indicate that near the wall the components u_1/U_* and w_1/U_* depend principally on the parameter $\frac{U_* y_1}{\nu}$. On the other hand, diagram (*c*) shows that the relation between v_1/U_* and $\frac{U_* y_1}{\nu}$ depends particularly

on the Reynolds number. This conclusion is to be expected. for the curves of fig. 13 show that v_1/U depends almost entirely on y/R, and not on the Reynolds number, and at each value of $U_0 D/\nu$ the maximum value of v_1/U is 0·25, and occurs at about 0·14R from the wall.

8. Prediction of the value of v_1/U from the Observations of u_1/U, Θ_{xy1}, and Θ_{xy2}.

The method is based on the assumption that particles moving in the plane XOY fall within an ellipse a fixed time interval after they have passed through a point in this plane when the time interval is sufficiently small.

Fig. 15.

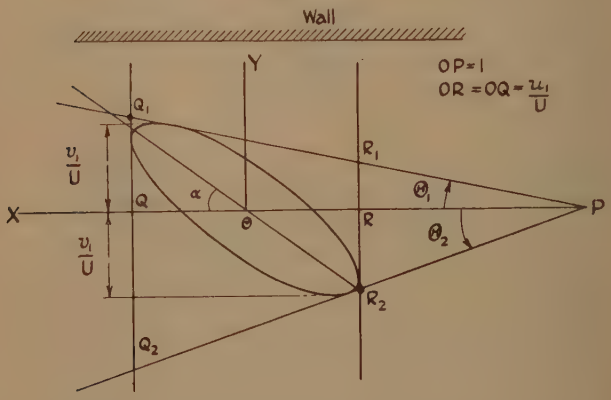

The equation of this ellipse is determined from the observations of the maximum obliquities Θ_{xy1} and Θ_{xy2}, the maximum velocity $(U+u_1)$, and the minimum velocity $(U-u_1)$ made at the point.

If P be a point in the XOY plane, then a particle must fall, at a time $\triangle t$ after passing through P, within the area $R_1R_2Q_2Q_1$ shown in fig. 15, where the lines R_1R_2 and Q_1Q_2 are normal to OX, and at distances $(U-u_1)\triangle t$ and $(U+u_1)\triangle t$ respectively from P, and the lines PR_1Q_1 and PR_2Q_2 make angles Θ_{xy1} and Θ_{xy2} respectively with OX. It is assumed that the particle also falls within an ellipse inscribed in this space with its centre on OX.

Let the scale of fig. 15 be fixed by making PO=1. Then, with the axes chosen, the equation of the lines

R_1R_2 and Q_1Q_2 are $x=-u_1/U$ and $x=u_1/U$ respectively, and the equations of the lines PR_1Q_1 and PR_2Q_2 are $x\tan\Theta_{xy1}+\tan\Theta_{xy1}=y$ and $x\tan\Theta_{xy2}+\tan\Theta_{xy2}=y$ respectively. The equation of the inscribed ellipse is given by $Ax^2+2Hxy+By^2=1$, where

$$B=\frac{4\left(\frac{U}{u_1}\right)^2}{\left[\left(\frac{U}{u_1}\right)^2-1\right]\left[(\tan\Theta_{xy1}-\tan\Theta_{xy2})^2-\left(\frac{U}{u_1}\right)^2(\tan\Theta_{xy1}+\tan\Theta_{xy2})^2\right]}$$

$$A=-B\tan\Theta_{xy1}.\tan\Theta_{xy2}\left[\left(\frac{U}{u_1}\right)^2-1\right],$$

and

$$2H=B\left[\tan\Theta_{xy2}+\tan\Theta_{xy1}\right]\left[\left(\frac{U}{u_1}\right)^2-1\right].$$

The value of v_1/U is given by $\left[\frac{A}{AB-H^2}\right]^{\frac{1}{2}}$.

The angle α which the major axis of the ellipse makes with OX is given by $\tan 2\alpha=\left(\frac{2H}{A-B}\right)$. The major and minor semi-axes of the ellipse are given by

$$a=(A\cos^2\alpha+2H\sin\alpha\cos\alpha+B\sin^2\alpha)^{-\frac{1}{2}}$$

and

$$b=(A\sin^2\alpha-2H\sin\alpha\cos+B\cos^2\alpha)^{-\frac{1}{2}}.$$

A measure of the correlation between the longitudinal and lateral velocity fluctuations can be obtained from the ellipse.

Results calculated from the above relations and faired values of u_1/U, Θ_{xy1}, and Θ_{xy2} are given in Table VI. In previous work it was assumed that the value of v_1/U was given by $\tan\left[\frac{\Theta_{xy1}-\Theta_{xy2}}{2}\right]$. Values of v_1/U (calculated by the present method) divided by $\tan\left[\frac{\Theta_{xy1}-\Theta_{xy2}}{2}\right]$ are given in the last column. It is seen that the values given by the new method differ from those of the old by about 1·5 per cent. at $y=0$ to about 15 per cent. at $y=0{\cdot}9R$.

The present method can only be used provided that $\left(\frac{U+u_1}{U-u_1}\right)$ is greater than $-\left(\frac{\tan \Theta_{xy2}}{\tan \Theta_{xy1}}\right)$. When $\left(\frac{U+u_1}{U-u_1}\right)=-\left(\frac{\tan \Theta_{xy2}}{\tan \Theta_{xy1}}\right)$ the ellipse shrinks to the

TABLE VI.

U_0D/ν.	y/R.	$\alpha°$.	b/a.	v_1/U.	$U \tan\left[\frac{\Theta_{xy1}-\Theta_{xy2}}{2}\right]^{v_1}$.
8090 ..	0	0	0·475	0·068	0·990
	0·2	0	0·490	0·076	0·990
	0·4	11·0	0·475	0·095	0·985
	0·6	23·1	0·360	0·132	0·960
	0·7	25·7	0·335	0·166	0·940
	0·8	25·3	0·345	0·219	0·895
	0·85	21·0	0·425	0·251	0·870
	0·90	8·8	0·410	0·238	0·825
13440 ..	0	0	0·425	0·074	0·985
	0·35	20·6	0·370	0·105	0·975
	0·65*	37·2	$-0·350\,i$	..	(0·940)‡
	0·80	31·1	0·350	0·242	0·905
	0·85	24·4	0·475	0·261	0·890
	0·90	13·0	0·435	0·242	0·855
18340 ..	0	0	0·465	0·074	0·985
	0·35	12·0	0·475	0·097	0·965
	0·65†	35·1	$-0·275\,i$	..	(0·935)‡
	0·80	34·7	0·155	0·233	0·900
	0·85	30·9	0·295	0·246	0·890
	0·90	22·8	0·355	0·240	0·855

* Range of imaginary b is about $0·46<y/R<0·75$.
† Range about $0·53<y/R<0·78$.
‡ Assumed values.

straight line Q_1R_2 (see fig. 15),and when $\left(\frac{U+u_1}{U-u_1}\right)<-\left(\frac{\tan \Theta_{xy2}}{\tan \Theta_{xy1}}\right)$ the curve has two distinct branches extending to infinity and touching the lines R_1R_2, Q_1Q_2, PR_1Q_1, and PR_2Q_2 externally. For this reason, values of v_1/U could not be calculated from observations

taken at $\frac{U_0 D}{\nu} = 13440$ and 18340 over the limited range $0{\cdot}50 < y/R < 0{\cdot}75$ (approx.); and the values there were taken from curves drawn through values of

$$\frac{v_1}{U \tan\left[\frac{\Theta_{xy1} - \Theta_{xy2}}{2}\right]}$$

above and below this range. There is little doubt that in practice a closed oval curve † is obtained, but the assumption that this curve is an ellipse with its axis on OX (fig. 15) may not be strictly true. It is to be expected that oval curves closely resembling ellipses can be obtained from the observations in the region where the method fails, for ellipses would be obtained at $y = 0{\cdot}65R$ if the values of $\frac{-\Theta_{xy2}}{\Theta_{xy1}}$ measured at $\frac{U_0 D}{\nu} = 13440$ and 18340 had been smaller by 14 per cent. and 9 per cent. respectively.

9. Prediction of w_1/U.

The relation for w_1/U (obtained directly from that for v_1/U by substituting w_1/U for v_1/U, and Θ_{zz} for Θ_{xy1} and $-\Theta_{xy2}$,) is

$$\frac{w_1}{U} = \left[1 - \left(\frac{u_1}{U}\right)^2\right]^{\frac{1}{2}} . \tan \Theta_{zz}.$$

In conclusion, the writer wishes to acknowledge his great indebtedness to Mr. W. S. Walker for assistance in the experimental work described in the paper.

References.

(1) Fage and Townend, Proc. Roy. Soc. A, cxxxv. pp. 656–684 (1932).
(2) Fage and Townend, Aero. Res. Cttee. R. & M. 1474, (1932–33).
(3) Stanton and Pannell, Phil. Trans. Roy. Soc. A, ccxiv. pp. 199–224 (1914).
(4) Nikuradse, *V. D. I.* Forschungsheft 356 (1932).
(5) N. P. L. Aero. Staff, Aero. Res. Cttee. R. & M. no. 1651.
(6) Stanton, Proc. Roy. Soc. A, lxxxv. pp. 366–376 (1911).
(7) Townend, Proc. Roy. Soc. A, cxlv. pp. 180–211 (1934).
(8) Stanton, Marshall, and Bryant, Proc. Roy. Soc. A, xcvii. pp. 413–434 (1920).
(9) Nikuradse, *V. D. I.* Forschungsheft 361 (1933).
(10) Prandtl and Schlichting, *Werft Reederei Hafen*, xv. p. 1 (1934).
(11) Not yet published.

† Such curves have been obtained by Townend.

V. *The Stresses in a Disk Wheel under Loads applied to the Rim.* *By* L. CHITTY *and* A. J. S. PIPPARD, *City and Guilds College, Imperial College, South Kensington* *.

1. THIS paper forms one of a series dealing with the stresses in wheels of different types †, and treats the case in which a continuous disk replaces the spoke system. The hub is considered to be rigid and firmly held, and the loads are applied in the plane of the wheel to any point on the rim. The wheel may be a simple disk or it may have a rim, as shown in fig. 1 ; both cases are considered.

Fig. 1.

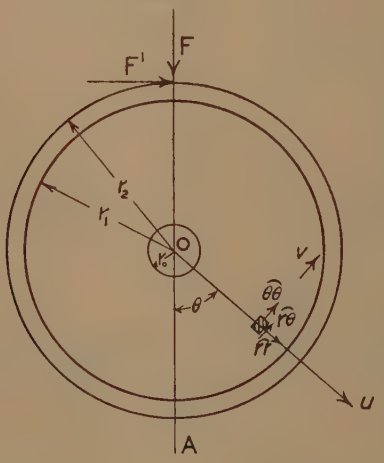

* Communicated by the Author.

† "On the Stresses in a Spoked Wheel under Loads applied to the Rim," A. J. S. Pippard & J. F. Baker, Phil. Mag. ii. pp. 1234–1253 (Dec. 1926).

"On a Theoretical and Experimental Investigation of the Stresses in a Radially Spoked Wire Wheel under Loads applied to the Rim," A. J. S. Pippard & W. E. Francis, Phil. Mag. xi. pp. 233–285 (Feb. 1931).

"The Stresses in a Wire Wheel with non-Radial Spokes under Loads applied to the Rim," A. J. S. Pippard & M. J. White, Phil. Mag. sec. 7, xiv. pp. 209–233 (Aug. 1932).

"The Stresses in a Wire Wheel under Side Loads on the Rim," A. J. S. Pippard & W. E. Francis, Phil. Mag. sec. 7, xiv. pp. 436–445 (Sept. 1932).

2. Let r_0 be the radius of the hub,
r_1 the outer radius of the disk,
r_2 the outer radius of the rim,
t_d the constant thickness of the disk,
t_r the constant thickness of the rim.
E Young's modulus for the material of both disk and rim,
η Poisson's ratio,

and let
$$\frac{r_0}{r_1}=p, \quad \frac{r_1}{r_2}=q, \quad \frac{t_r}{t_d}=k,$$

and
$$\sigma=\frac{\eta}{1+\eta}.$$

Under any system of loading applied in the plane of the wheel to the outside of the rim the radial and tangential strains in the disk where it is attached to the rigid hub must be zero. The strains at the outer boundary of the disk must be compatible with those at the inner boundary of the rim.

3. The external loading of the rim is expressed in terms of infinite series, and in the first instance the solution of the problem is obtained for the most general case of loading, attention being directed later to the particular case of a single load, either radial or tangential.

The origin of polar coordinates will be taken at the centre of the wheel and the datum line as OA in fig. 1. Then at any point (r_2, θ) the radial and tangential mean surface tractions are respectively taken to be

$$\left.\begin{aligned} \mathrm{R}_2&=a_0+\sum_{n=1}^{\infty}(a_n\cos n\theta+a_n'\sin n\theta),\\ \mathrm{T}_2&=c_0+\sum_{n=1}^{\infty}(c_n\cos n\theta+c_n'\sin n\theta),\end{aligned}\right\} \quad . \quad . \quad (1a)$$

and at the inner surface of the rim, *i. e.*, at (r_1, θ), they are respectively $-\mathrm{R}_1$ and $-\mathrm{T}_1$ where

$$\left.\begin{aligned} \mathrm{R}_1&=b_0+\sum_{1}^{\infty}(b_n\cos n\theta+b_n'\sin n\theta),\\ \mathrm{T}_1&=d_0+\sum_{1}^{\infty}(d_n\cos n\theta+d_n'\sin n\theta).\end{aligned}\right\} \quad . \quad . \quad (1b)$$

The total forces are transmitted from the inner edge of the rim to the outer edge of the disk, and it will be assumed

that their intensities are inversely proportional to the thickness of material. The radial and tangential mean surface tractions applied to the outer edge of the disk are therefore kR_1 and kT_1 respectively.

The constants a_n, a_n', c_n and c_n' are determined by the actual external load system, but b_n, b_n', d_n and d_n' are unknown and have to be found. From the general conditions of equilibrium for the rim, however, we obtain the following relationships :—

$$\left.\begin{aligned} r_2(a_1-c_1')&=r_1(b_1-d_1'),\\ r_2(a_1'+c_1)&=r_1(b_1'+d_1),\\ r_2^2c_0&=r_1^2d_0. \end{aligned}\right\} \quad . \quad . \quad . \quad . \quad (2)$$

4. In an investigation of the stresses in a ring * Filon has shown that, treating the problem as one of generalized plane stress, the most complete solution for the stress function χ which leads to single valued displacements is of the form

$$\begin{aligned} \chi=&A_0\log r+B_0\theta+C_0r^2\\ &+B_1r^3\cos\theta+C_1\frac{\cos\theta}{r}\\ &\qquad+D_1\{(1-2\sigma)r\log r\cos\theta-2(1-\sigma)r\theta\sin\theta\}\\ &+B_1'r^3\sin\theta+C_1'\frac{\sin\theta}{r}\\ &\qquad+D_1'\{(1-2\sigma)r\log r\sin\theta+2(1-\sigma)r\theta\cos\theta\}\\ &+\sum_{n=2}^{\infty}[A_nr^n+B_nr^{n+2}+C_nr^{-n}+D_nr^{-n+2}]\cos n\theta\\ &+\sum_{n=2}^{\infty}[A_n'r^n+B_n'r^{n+2}+C_n'r^{-n}+D_n'r^{-n+2}]\sin n\theta, \quad . \quad (3) \end{aligned}$$

where $A_n, B_n \ldots$ etc. are constants to be determined. The stresses on an element at the point (r, θ) are then

$$\left.\begin{aligned} \widehat{rr}&=\frac{1}{r^2}\frac{\partial^2\chi}{\partial\theta^2}+\frac{1}{r}\frac{\partial\chi}{\partial r},\\ \widehat{r\theta}&=-\frac{1}{r}\frac{\partial^2\chi}{\partial r\,\partial\theta}+\frac{1}{r^2}\frac{\partial\chi}{\partial\theta},\\ \widehat{\theta\theta}&=\frac{\partial^2\chi}{\partial r^2}, \end{aligned}\right\}$$

* "The Stresses in a Circular Ring," L. N. G. Filon, Inst. of Civil Engineers, Selected Engineering Papers, no. 12.

which give

$$\widehat{rr} = \frac{A_0}{r^2} + 2C_0$$
$$+\left[2B_1 r - 2\frac{C_1}{r^3} - (3-2\sigma)\frac{D_1}{r}\right]\cos\theta$$
$$+\left[2B_1' r - 2\frac{C_1'}{r^3} - (3-2\sigma)\frac{D_1'}{r}\right]\sin\theta$$
$$-\sum_{2}^{\infty}[n(n-1)A_n r^{n-2} + (n+1)(n-2)B_n r^n$$
$$+n(n+1)C_n r^{-n-2} + (n-1)(n+2)D_n r^{-n}]\cos n\theta$$
$$-\sum_{2}^{\infty}[n(n-1)A_n' r^{n-2} + (n+1)(n-2)B_n' r^n$$
$$+n(n+1)C_n' r^{-n-2} + (n-1)(n+2)D_n' r^{-n}]\sin n\theta, \quad \ldots \quad (4\,a)$$

$$\widehat{r\theta} = \frac{B_0}{r^2}$$
$$+\left[2B_1 r - 2\frac{C_1}{r^3} + (1-2\sigma)\frac{D_1}{r}\right]\sin\theta$$
$$-\left[2B_1' r - 2\frac{C_1'}{r^3} + (1-2\sigma)\frac{D_1'}{r}\right]\cos\theta$$
$$+\sum_{2}^{\infty}[n(n-1)A_n r^{n-2} + n(n+1)B_n r^n$$
$$-n(n+1)C_n r^{-n-2} - n(n-1)D_n r^{-n}]\sin n\theta$$
$$-\sum_{2}^{\infty}[n(n-1)A_n' r^{n-2} + n(n+1)B_n' r^n$$
$$-n(n+1)C_n' r^{-n-2} - n(n-1)D_n' r^{-n}]\cos n\theta, \quad (4\,b)$$

$$\widehat{\theta\theta} = -\frac{A_0}{r^2} + 2C_0$$
$$+\left[6B_1 r + 2\frac{C_1}{r^3} + (1-2\sigma)\frac{D_1}{r}\right]\cos\theta$$
$$+\left[6B_1' r + 2\frac{C_1'}{r^3} + (1-2\sigma)\frac{D_1'}{r}\right]\sin\theta$$
$$+\sum_{2}^{\infty}[n(n-1)A_n r^{n-2} + (n+1)(n+2)B_n r^n$$
$$+n(n+1)C_n r^{-n-2} + (n-1)(n-2)D_n r^{-n}]\cos n\theta$$

$$+\sum_{2}^{\infty}[n(n-1)A_n'r^{n-2}+(n+1)(n+2)B_n'r^n$$
$$+n(n+1)C_n'r^{-n-2}+(n-1)(n-2)D_n'r^{-n}]\sin n\theta.$$
$$\ldots \quad (4\,c)$$

5. If u and v are the radial and tangential displacements of an element at the point (r, θ) we have *

$$\left.\begin{aligned} E(1-\sigma)u &= -\frac{\partial\chi}{\partial r}+(1-\sigma)r\frac{\partial\psi}{\partial\theta} \\ \text{and} \\ E(1-\sigma)v &= -\frac{\partial\chi}{r\partial\theta}+(1-\sigma)r^2\frac{\partial\psi}{\partial r}, \end{aligned}\right\}$$

where ψ is a displacement function such that

$$\frac{\partial}{\partial r}\left(r\frac{\partial\psi}{\partial\theta}\right)=\nabla^2\chi$$

and

$$\nabla^2\psi=\left[\frac{\partial^2}{\partial r^2}+\frac{1}{r}\frac{\partial}{\partial r}+\frac{1}{r^2}\frac{\partial^2}{\partial\theta^2}\right]\psi=0.$$

Hence the expressions for u and v developed in terms of the same constants as before, A_n, B_n, etc. are

$$E(1-\sigma)u=-\frac{A_0}{r}+2(1-2\sigma)C_0r$$
$$+\left[(1-4\sigma)B_1r^2+\frac{C_1}{r^2}+D_1\{1-(3-4\sigma)\log r\}\right.$$
$$\left.+(1-\sigma)F_1\right]\cos\theta$$
$$+\left[(1-4\sigma)B_1'r^2+\frac{C_1'}{r^2}+D_1'\{1-(3-4\sigma)\log r\}\right.$$
$$\left.+(1-\sigma)F_1'\right]\sin\theta$$
$$-\sum_{2}^{\infty}[nA_nr^{n-1}+\{n+1-(3-4\sigma)\}B_nr^{n+1}$$
$$-nC_nr^{-n-1}-\{n-1+(3-4\sigma)\}D_nr^{-n+1}]\cos n\theta$$
$$-\sum_{2}^{\infty}[nA_n'r^{n-1}+\{n+1-(3-4\sigma)\}B_n'r^{n+1}$$
$$-nC_n'r^{-n-1}-\{n-1+(3-4\sigma)\}D_n'r^{-n+1}]\sin n\theta,$$
$$\ldots \quad (5\,a)$$

* See 'A Treatise on Photo-Elasticity,' Coker and Filon, p. 168 (1931).

$$E(1-\sigma)v = -\frac{B_0}{r} + (1-\sigma)F_0 r$$
$$+\left[(5-4\sigma)B_1 r^2 + \frac{C_1}{r^2} + D_1(3-4\sigma)\log r - (1-\sigma)F_1\right]\sin\theta$$
$$-\left[(5-4\sigma)B_1' r^2 + \frac{C_1'}{r^2} + D_1'(3-4\sigma)\log r - (1-\sigma)F'_1\right]\cos\theta$$
$$+\sum_2^\infty [nA_n r^{n-1} + \{n+1+(3-4\sigma)\}B_n r^{n+1} + nC_n r^{-n-1} + \{n-1-(3-4\sigma)\}D_n r^{-n+1}]\sin n\theta$$
$$-\sum_2^\infty [nA_n' r^{n-1} + \{n+1+(3-4\sigma)\}B_n' r^{n+1} + nC_n' r^{-n-1} + \{n-1-(3-4\sigma)\}D_n' r^{-n+1}]\cos n\theta, \quad . \quad . \quad . \quad (5\,b)$$

where F_0, F_1 and F_1' are three further constants which define rigid body displacements and do not therefore appear in χ.

6. To obtain a solution for the case of a disk with a rim the radial and shearing stresses $\widehat{rr}$ and $\widehat{r\theta}$ obtained from equations (4 *a*) and (4 *b*) when $r=r_1$ are equated to kR_1 and kT_1 respectively. Also u and v are made zero when $r=r_0$. The resulting equations are just sufficient to determine the disk constants, A_n, B_n, ... etc. in terms of k and the unknown coefficients b_n, b_n', d_n and d_n'.

The stress and displacement equations for the rim are similar to those for the disk with the constants A_n, B_n, etc. replaced by new values A_n, B_n, etc. The equation of $\widehat{rr}$ and $\widehat{r\theta}$ when $r=r_2$ to R_2 and T_2 respectively, and of $\widehat{rr}$ and $\widehat{r\theta}$ when $r=r_1$ to R_1 and T_1 respectively, yields a sufficient number of equations to determine the rim constants in terms of the known quantities a_n, a_n', c_n and c_n', and the unknowns b_n, b_n', d_n and d_n'.

The relation of b_n, b_n', d_n and d_n' to a_n, a_n', c_n and c_n' is obtained from the condition for compatibility of strains at $r=r_1$ where the disk and rim are joined, and the disk and rim constants are thus completely determined.

7. The disk is held rigidly at the inner boundary $r=r_0$ and loaded at the outer boundary $r=r_1$, so that the unknown radial and tangential mean surface tractions are

$$\left.\begin{aligned} k\mathrm{R}_1 &= kb_0+\sum_1^\infty (kb_n\cos n\theta+kb_n'\sin n\theta),\\ k\mathrm{T}_1 &= kd_0+\sum_1^\infty (kd_n\cos n\theta+kd_n'\sin n\theta). \end{aligned}\right\} \quad . \quad (6)$$

If we put $r_0/r_1=p$, then the expressions for the unaccented constants take the form

$$\left.\begin{aligned} \mathrm{A}_0/r_0^2 &= kb_0(1-2\sigma)/\{1+(1-2\sigma)p^2\},\\ \mathrm{B}_0/r_1^2 &= kd_0,\\ 2\mathrm{C}_0 &= kb_0/\{1+(1-2\sigma)p^2\},\\ (1-\sigma)\mathrm{F}_0 &= kd_0/p^2,\\ \mathrm{B}_1r_1 &= k\{(b_1+d_1')2(1-\sigma)-(b_1-d_1')(1-p^2)\}/\\ &\qquad 8(1-\sigma)\{1+(3-4\sigma)p^4\},\\ \mathrm{D}_1/r_1 &= -k(b_1-d_1')/4(1-\sigma),\\ 2\mathrm{C}_1/r_0^3 &= -\{2(3-4\sigma)\mathrm{B}_1r_0+\mathrm{D}_1/r_0\},\\ 2(1-\sigma)\mathrm{F}_1 &= 4\mathrm{B}_1r_0^2-\mathrm{D}_1\{1-2(3-4\sigma)\log r_0\}, \end{aligned}\right\} \quad . \quad . \quad . \quad (6a)$$

and for $n>1$

$$\left.\begin{aligned} 2n(n-1)\mathrm{A}_nr_1^{n-2} &= -k\{(n-1)(b_n+d_n')+(b_n-d_n')\}\\ &\qquad +p^{2n-2}\mathrm{N}_\mathrm{A}/\mathrm{P}_n,\\ 2(n+1)\mathrm{B}_nr_1^n &= k(b_n+d_n')-p^{2n-2}\mathrm{N}_\mathrm{B}/\mathrm{P}_n,\\ 2n(n+1)\mathrm{C}_nr_0^{-n-2} &= -p^{n-4}\mathrm{N}_\mathrm{C}/\mathrm{P}_n,\\ 2(n-1)\mathrm{D}_nr_0^{-n} &= -p^{n-2}\mathrm{N}_\mathrm{D}/\mathrm{P}_n, \end{aligned}\right\} \quad . \quad . \quad . \quad (6b)$$

where P_n, N_A, N_B, N_C and N_D are functions of n of the form

$$\left.\begin{aligned} \mathrm{P}_n &= \{(3-4\sigma)+p^{2n-2}\}\{1+(3-4\sigma)p^{2n+2}\}\\ &\qquad +(n^2-1)p^{2n-2}(1-p^2)^2,\\ \mathrm{N}_\mathrm{B} &= k(b_n+d_n')\{\mathrm{P}_n-(3-4\sigma+p^{2n-2})\}/p^{2n-2}\\ &\qquad +k(b_n-d_n')(n+1)(1-p^2),\\ \mathrm{N}_\mathrm{D} &= k(b_n+d_n')(n-1)(1-p^2)\\ &\qquad +k(b_n-d_n')\{1+(3-4\sigma)p^{2n+2}\},\\ \mathrm{N}_\mathrm{A} &= (n-1)\mathrm{N}_\mathrm{B}+\mathrm{N}_\mathrm{D},\\ \mathrm{N}_\mathrm{C} &= \mathrm{N}_\mathrm{B}-(n+1)\mathrm{N}_\mathrm{D}. \end{aligned}\right\} \quad . \quad (6c)$$

The corresponding expressions for the accented constants for all values of n, including $n=1$, are obtained from the above by writing b_n' for b_n and $-d_n$ for d_n'.

Inspection shows that in the case of a disk in which p is a fairly small fraction (so that terms in p^{2n-2} soon become negligible) it is only necessary to calculate a few of the constants accurately. The first few values of C_n and D_n will influence the stresses and displacements, particularly in the neighbourhood of the hub, but as soon as n becomes large we have appreciably

$$\left.\begin{aligned} 2n(n-1)A_n r_1^{n-2} &= -k\{(n-1)(b_n+d_n')+(b_n-d_n')\}, \\ 2(n+1)B_n r_1^{n} &= \quad k(b_n+d_n'), \end{aligned}\right\}. \quad (6\,d)$$

while terms in C_n and D_n can be neglected.

The terms in (6 *d*) give rise to what may be called the slowly converging terms.

8. The loading conditions for the rim are given by (1 *a*) and (1 *b*). The constants for the rim are given in Filon's paper *, but are repeated here in rather different form. Writing $r_1/r_2=q$, they are

$$\left.\begin{aligned} \bar{A}_0/r_1^2 &= -(a_0-b_0)/(1-q^2), \\ \bar{B}_0/r_1^2 &= d_0=c_0/q^2, \\ 2\bar{C}_0 &= (a_0-b_0q^2)/(1-q^2), \\ \bar{B}_1 r_2 &= [2(1-\sigma)\{(a_1+c_1')-(b_1+d_1')q^3\} \\ &\qquad -(a_1-c_1')(1-q^2)]/8(1-\sigma)(1-q^4), \\ \bar{D}_1/r_1 &= -(b_1-d_1')/4(1-\sigma) = -(a_1-c_1')/4(1-\sigma)q, \end{aligned}\right\}. \quad (7\,a)$$

$$2C_1/r_1^3 = -(b_1+d_1')/2+2B_1r_1-D_1/r_1,$$

and for $n>1$

$$\left.\begin{aligned} 2n(n-1)\bar{A}_n r_2^{n-2} &= -(a_n-c_n')-(n-1)x_n-\bar{N}_A/Q_n, \\ 2(n+1)\bar{B}_n r_2^{n} &= \quad x_n+\bar{N}_B/Q_n, \\ 2n(n+1)\bar{C}_n r_1^{-n-2} &= -(b_n+d_n')-(n+1)y_n+\bar{N}_C/Q_n, \\ 2(n-1)\bar{D}_n r_1^{-n} &= y_n+\bar{N}_D/Q_n, \end{aligned}\right\}. \quad (7\,b)$$

where

$$\left.\begin{aligned} x_n &= (a_n+c_n')-(b_n+d_n')q^{n+2}, \\ y_n &= (a_n-c_n')q^{n-2}-(b_n-d_n'), \\ Q_n &= (1-q^{2n-2})(1-q^{2n+2})-(n^2-1)q^{2n-2}(1-q^2)^2, \end{aligned}\right\}. \quad (7\,c)$$

* *Loc. cit.* p. 8.

and
$$\left.\begin{aligned} N_B &= x_n(1-q^{2n-2}-Q_n)+y_n(n+1)q^n(1-q^2),\\ N_D &= x_n(n-1)q^{n-2}(1-q^2)+y_n(1-q^{2n+2}-Q_n),\\ N_A &= (n-1)N_B+q^n(N_D+y_nQ_n),\\ N_C &= q^n(N_B+x_nQ_n)-(n+1)N_D. \end{aligned}\right\} \quad (7d)$$

The accented constants can be obtained from the above by writing a_n', $-c_n$, b_n' and $-d_n$ for a_n, c_n', b_n and d_n' respectively.

The three further constants for the rim, $\bar{F}_0$, $\bar{F}_1$ and $\bar{F}_1'$ are determined by the condition of compatibility of strains at the juncture of the disk and rim.

9. When the radial and tangential strains in the rim and disk at their common radius r_1 are equated the following relations are obtained :

$$b_0\left[1+(1-2\sigma)p^2q^2+(k-1)\frac{(1-2\sigma)}{2(1-\sigma)}(1-p^2)(1-q^2)\right] = a_0[1+(1-2\sigma)p^2],$$

$$d_0=c_0/q^2 \quad \text{(from equation (2))},$$

$$(1-\sigma)\bar{F}_0=(1-\sigma)F_0-(k-1)d_0,$$

$$(b_1+d_1')\left[1+(3-4\sigma)p^4q^4+(k-1)\frac{(3-4\sigma)}{4(1-\sigma)}(1-p^4)(1-q^4)\right] = (a_1+c_1')\{1+(3-4\sigma)p^4\}q - \frac{(a_1-c_1')}{2(1-\sigma)}\left[\{1+(3-4\sigma)p^4\}q(1-q^2)-\frac{k}{q}(1-p^2)(1-q^4)\right],$$

$$(b_1-d_1')=(a_1-c_1')/q \quad \text{(from equation (2))},$$

$$8(1-\sigma)^2\bar{F}_1/r_1=8(1-\sigma)^2F_1/r_1-(k-1)(b_1+d_1') -(k-1)(b_1-d_1')\{1-2(3-4\sigma)\log r_1\}, \quad \ldots \quad (8a)$$

and for $n>1$

$$\left.\begin{aligned} (k-1)(b_n+d_n') &= 8(1-\sigma)(n+1)(B_n-\bar{B}_n)r_1^n,\\ -(k-1)(b_n-d_n') &= 8(1-\sigma)(n-1)(D_n-\bar{D}_n)r_1^{-n}, \end{aligned}\right\}$$

whence

$$(b_n+d_n') = \frac{4(1-\sigma)q^n[(a_n+c_n')(f_1k+f_2)+(n+1)(a_n-c_n')(1-q^2)(f_3k+f_4)]}{G_1k^2+k(G_2-G_1-G_3)+G_3},$$

$$(b_n-d_n') = \frac{4(1-\sigma)q^{n-2}[(n-1)(a_n+c_n')(1-q^2)(f_5k+f_6)+(a_n-c_n')(f_7k+f_8)]}{G_1k^2+k(G_2-G_1-G_3)+G_3}, \quad \ldots \quad (8b)$$

where

$$f_1=(3-4\sigma)(1-p^{2n-2})(1-q^{2n-2})\{1+(3-4\sigma)p^{2n+2}\}$$
$$+(n^2-1)p^{2n-2}(1-p^2)\{(1-p^2)(1-q^{2n-2})$$
$$+4(1-\sigma)(1-q^2)/q^2\},$$

$$f_2=\{(3-4\sigma)+q^{2n-2}\}\mathrm{P}_n,$$

$$f_3=(3-4\sigma)q^{2n-2}(1-p^{2n-2})\{1+(3-4\sigma)p^{2n+2}\}$$
$$+p^{2n-2}(1-p^2)\left\{(n^2-1)q^{2n-2}(1-p^2)\right.$$
$$\left.+\frac{4(1-\sigma)(1-q^{2n+2})}{q^2(1-q^2)}\right\},$$

$$f_4=-q^{\ -2}\mathrm{P}_n,$$

$$f_5=(3-4\sigma)(1-p^{2n+2})\{(3-4\sigma)+p^{2n-2}\}-p^{2n-2}(1-p^2)$$
$$\times\left\{(n^2-1)(1-p^2)-\frac{4(1-\sigma)q^2(1-q^{2n-2})}{(1-q^2)}\right\},$$

$$f_6=\mathrm{P}_n,$$

$$f_7=(3-4\sigma)(1-p^{2n+2})(1-q^{2n+2})\{(3-4\sigma)+p^{2n-2}\}$$
$$-(n^2-1)p^{2n-2}(1-p^2)\{(1-p^2)(1-q^{2n-2})$$
$$-4(1-\sigma)q^{2n}(1-q^2)\},$$

$$f_8=\{1+(3-4\sigma)q^{2n+2}\}\mathrm{P}_n,$$

. . . (8 *c*)

and

$$\mathrm{G}_1=[(3-4\sigma)^2(1-p^{2n-2})(1-p^{2n+2})$$
$$-(n^2-1)p^{2n-2}(1-p^2)^2]\mathrm{Q}_n,$$

$$\mathrm{G}_2=\{4(1-\sigma)\}^2[\{(3-4\sigma)+(pq)^{2n-2}\}\{1+(3-4\sigma)(pq)^{2n+2}\}$$
$$+(n^2-1)(pq)^{\ n-2}(1-p^2q^2)^2],$$

$$\mathrm{G}_3=\mathrm{P}_n[\{(3-4\sigma)+q^{2n-2}\}\{1+(3-4\sigma)q^{2n+2}\}$$
$$+(n^2-1)q^{2n-2}(1-q^2)^2],$$

. . . (8 *d*)

where P_n and Q_n are the values given in (6 *c*) and (7 *c*).

As soon as terms in p^{2n-2} can be neglected we have approximately

$$\left.\begin{aligned}
&f_1k+f_2=(3-4\sigma)[k+(3-4\sigma)-(k-1)q^{2n-2}],\\
&f_3k+f_4=(3-4\sigma)(k-1)q^{2n-2},\\
&f_5k+f_6=(3-4\sigma)\{(3-4\sigma)k+1\},\\
&f_7k+f_8=(3-4\sigma)[(3-4\sigma)k+1-(3-4\sigma)(k-1)q^{2n+2}],\\
&G_1k^2+k(G_2-G_1-G_3)+G_3\\
&\quad=(3-4\sigma)\{(3-4\sigma)k+1\}\{k+(3-4\sigma)\}\\
&\qquad-(3-4\sigma)(k-1)q^{2n-2}[\{(3-4\sigma)k+1\}\\
&\qquad\times\{1+(n^2-1)(1-q^2)^2\}+(3-4\sigma)\{k+(3-4\sigma)\}q^4\\
&\qquad-(3-4\sigma)(k-1)q^{2n+2}].
\end{aligned}\right\} \quad . \quad (9)$$

Ultimately, when terms in q^{2n-2} can be neglected,

$$(b_n+d_n')=\frac{4(1-\sigma)q^n(a_n+c_n')}{(3-4\sigma)k+1},$$

$$(b_n-d_n')=\frac{4(1-\sigma)q^{n-2}\{(a_n+c_n')+(n-1)(a_n-c_n')(1-q^2)\}}{k+(3-4\sigma)}$$

. . . (10)

10. *The Case of a Single Radial Load* F *at* $\theta=\pi$.—The coefficients in (1 *a*) are obtained in the usual manner by integration, and we have

$$\left.\begin{aligned}
-F&=\int_0^{2\pi} R_2t_rr_2\,d\theta=a_0 2\pi t_rr_2,\\
-F\cos n\pi&=\int_0^{2\pi} R_2t_rr_2\cos n\theta\,d\theta=a_n\pi t_rr_2,\\
-F\sin n\pi&=\int_0^{2\pi} R_2t_rr_2\sin n\theta\,d\theta=a_n'\pi t_rr_2,
\end{aligned}\right\}$$

whence

$$a_0=-\frac{F}{2\pi t_rr_2},\quad a_n=-\frac{F(-)^n}{\pi t_rr_2},\quad a_n'=0. \quad . \quad (11)$$

The coefficients c_0, c_n and c_n' are zero.

To avoid mathematically infinite stresses the load may be uniformly distributed over the arc $\pi-\phi<\theta<\pi+\phi$; the coefficients in (11) are then

$$a_0=-\frac{F}{2\pi t_rr_2},\quad a_n=-\frac{F(-)^n}{\pi t_rr_2}\frac{\sin n\phi}{n\phi},\quad a_n'=0. \quad (11\,a)$$

The Case of a Single Tangential Load F′ *at* $\theta=\pi$.—In this case

$$c_0=-\frac{F'}{2\pi t_r r_2},\quad c_n=-\frac{F'(-)^n}{\pi t_r r_2},\quad c_n'=0,\quad .\quad (12)$$

while $a_0=a_n=a'_n=0$.

Infinite stresses may be avoided in this case by assuming a triangular law of distribution for the load over the arc $\pi-\phi<\theta<\pi+\phi$; the coefficients in (12) are then

$$c_0=-\frac{F'}{2\pi t r_2},\quad c_n=-\frac{F'(-)^n}{\pi t_r r_2}\frac{(1-\cos n\phi)}{n^2\phi^2},\quad c_n'=0.\quad (12a)$$

11. *Calculation for a Disk without Rim.*—As an example of the method, the stresses in a rimless disk were calculated for a particular case. The disk was assumed to be held rigidly at the inner boundary, and two cases of loading were taken—those of a single radial and a single tangential load respectively. The disk was assumed to be made of nitro-cellulose, since it is hoped at a later date to make a photo-elastic analysis of the same case for comparison with the present calculation.

The outer radius, r_1, was 5 inches and the inner, r_0, was 0·5 inch, so that $p=r_0/r_1=0{\cdot}1$. E was taken as 3×10^5 lbs. per square inch and η as 0·4.

The resulting displacements and stresses are shown in figs. 2–13.

Radial Load.—Here $k=1$, and by comparison with (11) we have

$$\left.\begin{aligned} b_0&=-\frac{F}{2\pi t_d r_1},\quad b_n=-\frac{F(-)^n}{\pi t_d r_1},\quad b_n'=0,\\ d_n&=d_n'=0. \end{aligned}\right\}\quad .\quad (13)$$

Only the unaccented constants in (6*a*) have values, and these are readily calculated, as also are the values P_n, N_A, N_B, N_C and N_D in (6*c*) for the first few values of n. The slowly converging terms which have been separated out in (6*b*) and are shown in (6*d*) can be dealt with separately.

The slowly converging terms can be split up into known trigonometrical series * and summed for all values of n.

* See Appendix.

Fig. 2.

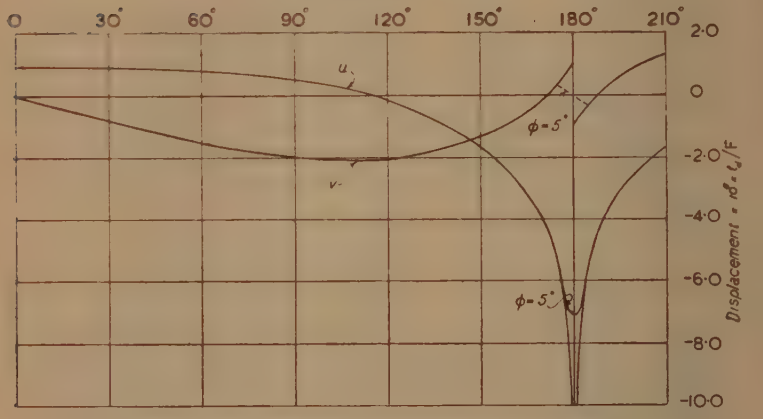

Radial and tangential displacements on outer edge under radial load F at $\theta=\pi$.

Fig. 3.

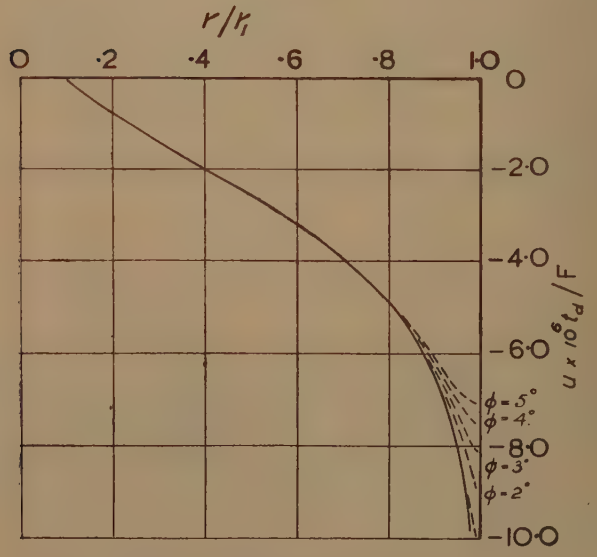

Radial displacement at $\theta=\pi$ under radial load F at $\theta=\pi$.

Fig. 4.

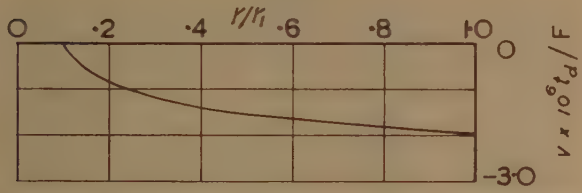

Tangential displacement at $\theta = \pi/2$ under radial load F at $\theta = \pi$.

Fig. 5.

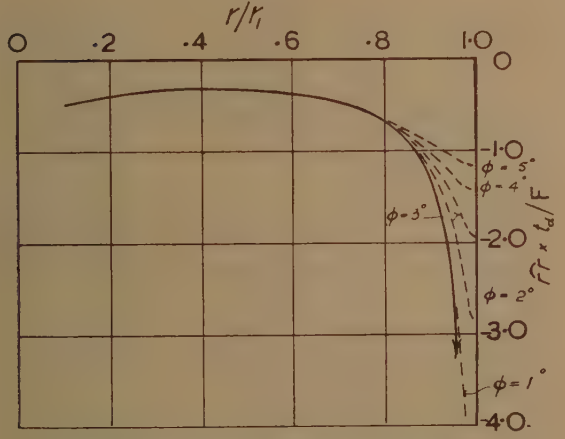

Radial stress at $\theta = \pi$ under radial load at $\theta = \pi$.

Fig. 6.

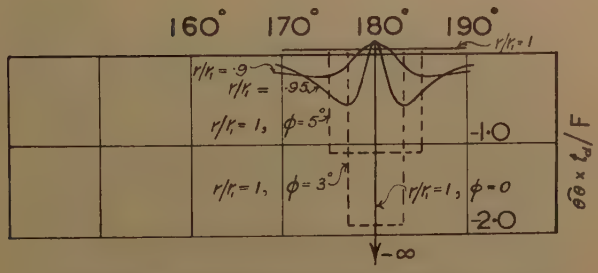

Hoop stress in neighbourhood of applied radial load.

Fig. 7.

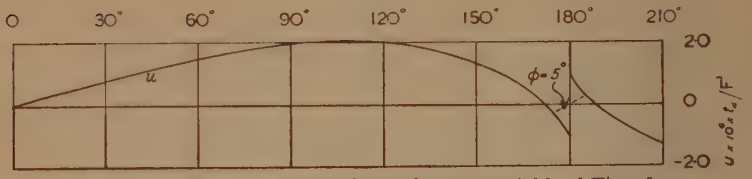

Radial displacement on outer edge under tangential load F′ at $\theta=\pi$.

Fig. 8.

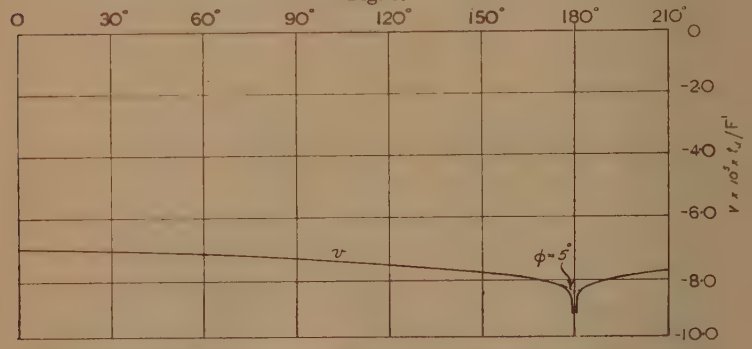

Tangential displacement on outer edge under tangential load F′ at $\theta=\pi$.

Fig. 9.

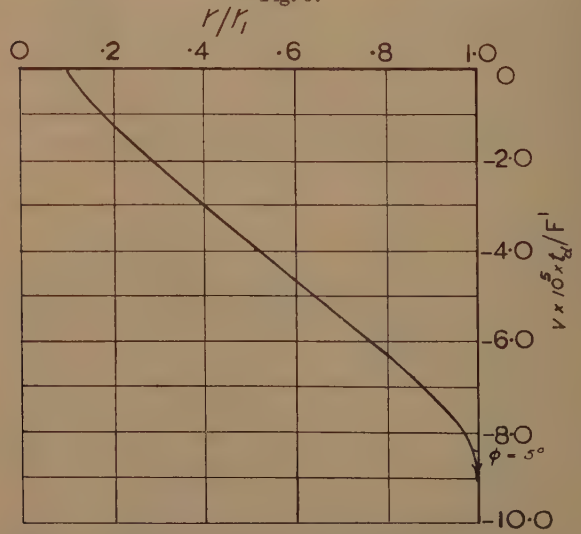

Tangential displacement at $\theta=\pi$ under tangential load F′ at $\theta=\pi$.

Fig. 10.

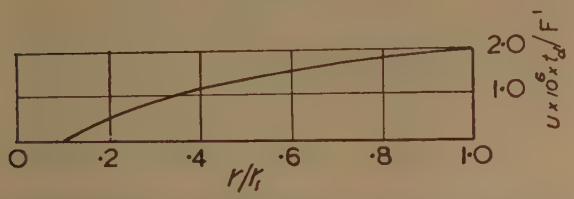

Radial displacement at $\theta = \pi/2$ under tangential load F′ at $\theta = \pi$.

Fig. 11.

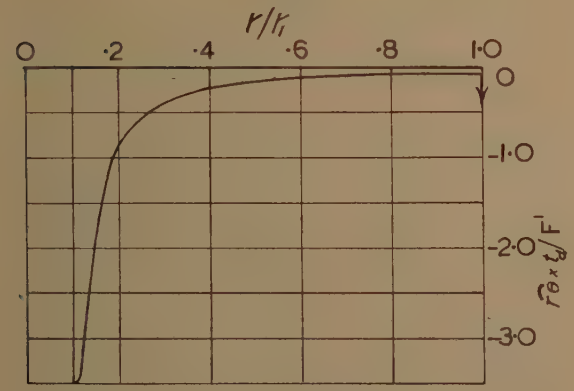

Shear stress at $\theta = \pi$ under tangential load F′ at $\theta = \pi$.

Fig. 12.

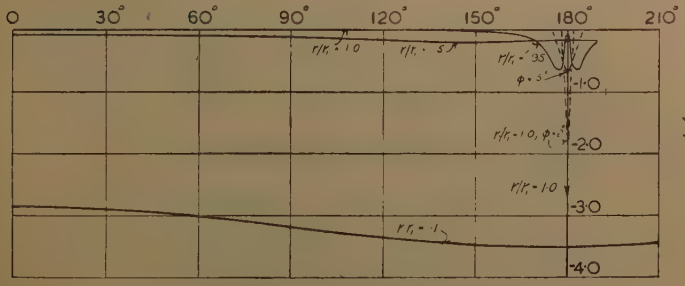

Shear stress under tangential load at $\theta = \pi$.

Thus the slow terms in $E(1-\sigma)u$ are

$$-\sum_2^\infty \frac{b_n}{2}\left[-\frac{n}{n-1}\cdot\frac{r^{n-1}}{r_1^{n-2}}+\frac{\{n+1-(3-4\sigma)\}}{n+1}\frac{r^{n+1}}{r_1^{n}}\right]\cos n\theta$$

$$=\sum_2^\infty \frac{b_n}{2}\left[\left(\frac{r_1^2-r^2}{r}\right)\frac{r^n}{r_1^n}+\frac{r_1}{n-1}\frac{r^{n-1}}{r_1^{n-1}}\right.$$

$$\left.+\frac{(3-4\sigma)r_1}{n+1}\frac{r^{n+1}}{r_1^{n+1}}\right]\cos n\theta.$$

If we write

$$z=1+2\frac{r}{r_1}\cos\theta+\frac{r^2}{r_1^2}, \quad . \quad . \quad . \quad . \quad (14)$$

Fig. 13.

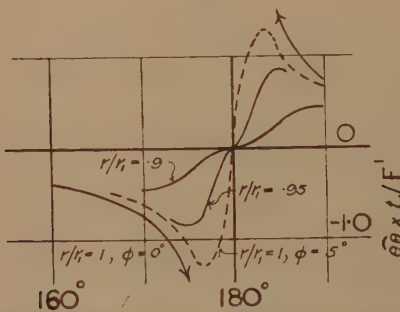

Hoop stress in neighbourhood of applied tangential load.

then the slow terms in $E(1-\sigma)u$ are

$$\frac{F}{\pi t_d}\left[\frac{1}{2}\left(1-\frac{r^2}{r_1^2}\right)\left\{\frac{\cos\theta+r/r_1}{z}-\cos\theta\right\}\right.$$

$$+\frac{(3-4\sigma)}{2}\frac{r}{r_1}\left(1-\frac{r}{2r_1}\cos\theta\right)-(1-\sigma)\cos\theta\log z$$

$$\left.-(1-2\sigma)\sin\theta\tan^{-1}\left\{\frac{r/r_1.\sin\theta}{1+r/r_1.\cos\theta}\right\}\right]. \quad . \quad (15)$$

Similarly, the slow terms in $E(1-\sigma)v$ are

$$\frac{F}{\pi t_d}\left[\frac{1}{2}\left(1-\frac{r^2}{r_1^2}\right)\sin\theta\left(1-\frac{1}{z}\right)\right.$$

$$-\frac{(3-4\sigma)}{4}\frac{r^2}{r_1^2}\sin\theta+(1-\sigma)\sin\theta\log z$$

$$\left.-(1-2\sigma)\cos\theta\tan^{-1}\left\{\frac{r/r_1.\sin\theta}{1+r/r_1.\cos\theta}\right\}\right]. \quad . \quad (16)$$

The slow terms in $\widehat{rr}$ are

$$-\frac{F}{2\pi t_d r_1}\left[\left(1-\frac{r^2}{r_1^2}\right)\frac{(\cos 2\theta-1+z)}{z^2}+\left(1+\frac{r^2}{r_1^2}\right)\frac{(\cos 2\theta+r/r_1.\cos\theta)}{z}\right], \quad . \quad (17)$$

the slow terms in $\widehat{r\theta}$ are

$$\frac{F}{2\pi t_d r_1}\left(1-\frac{r^2}{r_1^2}\right)\frac{r_1}{r}\sin\theta\left\{1-\frac{1-r^2/r_1^2}{z^2}\right\} \quad . \quad (18)$$

and the slow terms in $\widehat{\theta\theta}$ are

$$\frac{F}{2\pi t_d r_1}\left[\left(1-\frac{r^2}{r_1^2}\right)\frac{r_1}{r}\left\{\cos\theta-\frac{2r/r_1+(1+r^2/r_1^2)\cos\theta}{z^2}\right\}-2\frac{r^2}{r_1^2}\frac{(\cos 2\theta+r/r_1.\cos\theta)}{z}\right]. \quad . \quad (19)$$

The above expressions lead to infinite values for u, $\widehat{rr}$, and $\widehat{\theta\theta}$ and a finite discontinuity in v directly under the load. This may be avoided by considering the load as uniformly distributed over a small arc $\pi-\phi<\theta<\pi+\phi$. The coefficients (13) will then be modified as indicated in (11 *a*). The summations for the general point (r, θ), though straight forward, are then somewhat lengthy, and since the manner in which the load is applied only affects the stresses in its immediate neighbourhood, it is sufficient to indicate the modified values in this region.

Thus, if $r=r_1$, then in the region

$$\left.\begin{aligned}\pi<\theta+\phi<3\pi,\\ -\pi<\theta-\phi<\pi,\end{aligned}\right\} \quad . \quad . \quad . \quad . \quad . \quad (20)$$

the slow terms in $E(1-\sigma)\,u$ are

$$-\frac{F}{2\pi t_d\phi}\left[\frac{(1-4\sigma)}{2}\cos\theta\sin\phi+(1-\sigma)\{\sin(\theta+\phi)\log 2[1+\cos(\theta+\phi)]-\sin(\theta-\phi)\log 2[1+\cos(\theta-\phi)]\}+(1-2\sigma)\{(\pi-\phi)(1+\cos\theta\cos\phi)-(\pi-\theta)\sin\theta\sin\phi\}\right], \quad . \quad . \quad . \quad . \quad (21)$$

the slow terms in $\mathrm{E}(1-\sigma)v$ are

$$-\frac{\mathrm{F}}{2\pi t_d\phi}\Big[\frac{(5-4\sigma)}{2}\sin\theta\sin\phi$$
$$+(1-\sigma)\{[1+\cos(\theta+\phi)]\log 2\,[1+\cos(\theta+\phi)]$$
$$-[1+\cos(\theta-\phi)]\log 2[1+\cos(\theta-\phi)]\}$$
$$-(1-2\sigma)\{(\pi-\phi)\sin\theta\cos\phi+(\pi-\theta)\cos\theta\sin\phi\}\Big]. \quad (22)$$

and the slow terms in $\widehat{rr}$ are

$$-\frac{\mathrm{F}}{2\pi t_d r_1\phi}[2\cos\theta\sin\phi+\pi-\phi]. \quad . \quad . \quad . \quad (23)$$

The slow terms in $\widehat{\theta\theta}$ are also given by (23). There will still be a finite discontinuity in $\widehat{\theta\theta}$* at $\theta=\pi-\phi$ and $\theta=\pi+\phi$.

It may also be noted that for $r<r_1$ the slow terms in $\widehat{rr}$ when $\theta=\pi$ are

$$-\frac{\mathrm{F}}{2\pi t_d r_1\phi}\Big[\Big(1-\frac{r^2}{r_1^2}\Big)\frac{r_1/r.\sin\phi}{1-2r/r_1.\cos\phi+r^2/r_1^2}$$
$$-\Big(1+\frac{r^2}{r_1^2}\Big)\frac{r_1}{r}\sin\phi+2\tan^{-1}\Big\{\frac{r/r_1.\sin\phi}{1-r/r_1.\cos\phi}\Big\}\Big]. \quad (23a)$$

Tangential Load.—The procedure is exactly similar to that for the radial load. Again $k=1$, and by comparison with (12) we have

$$d_0=-\frac{\mathrm{F}'}{2\pi t_d r_1}, \quad d_n=-\frac{\mathrm{F}'(-)^n}{\pi t_d r_1}, \quad d_n'=0, \quad b_n=b_n'=0. \quad (13')$$

Only the constants with suffix 0 and the accented constants will have values. The slowly converging terms can again be summed separately for all values of n.

The slow terms in $\mathrm{E}(1-\sigma)u$ are

$$\frac{\mathrm{F}'}{\pi t_d}\Big[\frac{1}{2}\Big(1-\frac{r^2}{r_1^2}\Big)\sin\theta\Big(1-\frac{1}{z}\Big)$$
$$+\frac{(3-4\sigma)}{4}\frac{r^2}{r_1^2}\sin\theta-(1-\sigma)\sin\theta\log z$$
$$+(1-2\sigma)\cos\theta\tan^{-1}\Big\{\frac{r/r_1.\sin\theta}{1+r/r_1.\cos\theta}\Big\}\Big], \quad (15')$$

* *Cf.* "The Stresses produced in a Semi-Infinite Solid by Pressure on part of the Boundary," Love, Phil. Trans. A, vol. ccxxviii. (1929).

and the slow terms in $E(1-\sigma)v$ are

$$\frac{F'}{\pi t_d}\left[-\frac{1}{2}\left(1-\frac{r^2}{r_1^2}\right)\left\{\frac{\cos\theta+r/r_1}{z}-\cos\theta\right\}\right.$$
$$+\frac{(3-4\sigma)}{2}\frac{r}{r_1}\left(1-\frac{r}{2r_1}\cos\theta\right)-(1-\sigma)\cos\theta\log z$$
$$\left.-(1-2\sigma)\sin\theta\tan^{-1}\left\{\frac{r/r_1.\sin\theta}{1+r/r_1.\cos\theta}\right\}\right]. \quad . \quad (16')$$

The slow terms in $\widehat{rr}$ are

$$-\frac{F'}{2\pi t_d r_1}\left(1-\frac{r^2}{r_1^2}\right)\frac{r}{r_1}\frac{(\sin 3\theta+2r/r_1.\sin 2\theta+r^2/r_1^2\sin\theta)}{z^2}, \quad . \quad . \quad . \quad (17')$$

the slow terms in $\widehat{r\theta}$ are

$$\frac{F'}{2\pi t_d r_1}\frac{r}{r_1}\left[\frac{4\sin^2\theta(\cos\theta+r/r_1)}{z^2}-\cos\theta\right], \quad . \quad (18')$$

and the slow terms in $\widehat{\theta\theta}$ are

$$\frac{F'}{2\pi t_d r_1}\frac{r_1}{r}\sin\theta\left[\left(1-\frac{r^2}{r_1^2}\right)\left(\frac{1-r^2/r_1^2}{z^2}-1\right)\right.$$
$$\left.+2\left(1+\frac{r^2}{r_1^2}\right)\left(1-\frac{1}{z}\right)\right]. \quad . \quad . \quad . \quad (19')$$

The above expressions lead to infinite values for v and $\widehat{r\theta}$ and an infinite discontinuity in $\widehat{\theta\theta}$ just under the load. This may be avoided by considering the load as distributed according to a triangular law over a small arc $\pi-\phi<\theta<\pi+\phi$. The coefficients in (13′) are then modified as indicated in (12 *a*).

12. *Calculation for a Disk with a Rim.*—The influence of a rim upon the stresses in a disk held rigidly at the hub has been investigated for the particular case of a single radial load applied to the rim at $\theta=\pi$.

The disk was of the same dimensions and material as that described in para. 11, and the rim was of the same material, so that $q=r_1/r_2=\cdot 9091$. Three relative thicknesses of disk and rim were considered, viz., $t_r/t_d=2$, 3 and 4. In each case the radial stress in the disk was calculated at the point of juncture with the rim in the direct line of the load. The values of this stress are shown

in fig. 14 for a point load on the rim and for the same load spread over 4° and 10° of arc.

To evaluate the constants A_n, B_n . . . . for the disk the coefficients a_n, c_n', b_n, d_n' had first to be determined. The coefficients a_0, a_n and c'_n are given in para. 10, and the coefficients b_0, d_0, b_n+d_n', b_n-d_n' were evaluated from (8 *a*) and (8 *b*). Although the approximations for the component functions given in (9) were very soon sufficiently accurate, the values in (8 *b*) only slowly approached the ultimate approximate values given by (10). It was therefore found convenient to tabulate the values (8 *b*) and the difference between these values and those given

Fig. 14.

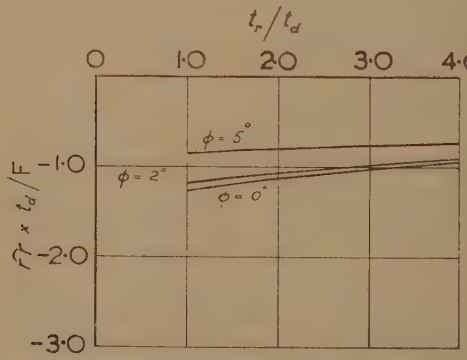

Radial stress in disk at $\theta=\pi$ at juncture of disk and rim under radial load on rim at $\theta=\pi$.

by (10). The contribution made by (10) to the slowly converging terms (6 *d*) could then be summed directly to infinity, as explained in para. 11, but that due to the difference between (8 *b*) and (10) had to be dealt with by tabulation.

Appendix.

If $\quad a<1, \quad -\pi<x<\pi,$

$$-a\sin(m+x)+a^2\sin(m+2x)-a^3\sin(m+3x)+\ldots$$

$$=-\frac{\{a^2\sin m+a\sin(m+x)\}}{1+2a\cos x+a^2} \quad . \quad . \quad . \quad (1)$$

$$-a\cos(m+x)+a^2\cos(m+2x)-a^3\cos(m+3x)+\ldots$$

$$=-\frac{\{a^2\cos m+a\cos(m+x)\}}{1+2a\cos x+a^2} \quad . \quad . \quad . \quad (2)$$

$$-a\sin(m+x)+\frac{a^2}{2}\sin(m+2x)-\frac{a^3}{3}\sin(m+3x)+\ldots$$

$$=-\tfrac{1}{2}\sin m\log(1+2a\cos x+a^2)$$

$$-\cos m\tan^{-1}\left\{\frac{a\sin x}{1+a\cos x}\right\} \quad . \quad . \quad . \quad . \quad (3)$$

$$-a\cos(m+x)+\frac{a^2}{2}\cos(m+2x)-\frac{a^3}{3}\cos(m+3x)+\ldots$$

$$=-\tfrac{1}{2}\cos m\log(1+2a\cos x+a^2)$$

$$+\sin m\tan^{-1}\left\{\frac{a\sin x}{1+a\cos x}\right\} \quad . \quad . \quad . \quad . \quad (4)$$

$$-a\sin(m+x)+2a^2\sin(m+2x)-3a^3\sin(m+3x)+\ldots$$

$$=-\frac{a\{\sin(m+x)+2a\sin m+a^2\sin(m-x)\}}{(1+2a\cos x+a^2)^2} \quad . \quad . \quad (5)$$

$$-a\cos(m+x)+2a^2\cos(m+2x)-3a^3\cos(m+3x)+\ldots$$

$$=-\frac{a\{\cos(m+x)+2a\cos m+a^2\cos(m-x)\}}{(1+2a\cos x+a^2)^2} \quad . \quad (6)$$

$$-\sin x+\tfrac{1}{2}\sin 2x-\tfrac{1}{3}\sin 3x+\ldots.=-\frac{x}{2}, \quad \text{if } -\pi<x<\pi,$$

$$=\frac{2\pi-x}{2}, \quad \text{if } \pi<x<3\pi. \quad . \quad . \quad . \quad . \quad (7)$$

$$-\cos x+\tfrac{1}{2}\cos 2x-\tfrac{1}{3}\cos 3x+\ldots.=-\tfrac{1}{2}\log 2(1+\cos x),$$

$$\text{unless } x=\pi. \quad . \quad . \quad (8)$$

VI. *On the Electrical and Acoustic Conductivities of Cylindrical Tubes bounded by Infinite Flanges.* By Louis V. King, *F.R.S., Macdonald Professor of Physics, McGill University, Montreal* *.

§ 1. *Introduction.*

UNDER the title "Correction for Open End" Lord Rayleigh, in his 'Theory of Sound'†, has considered the electrical problem of a semi-infinite cylindrical conductor of radius a continuous with an unlimited

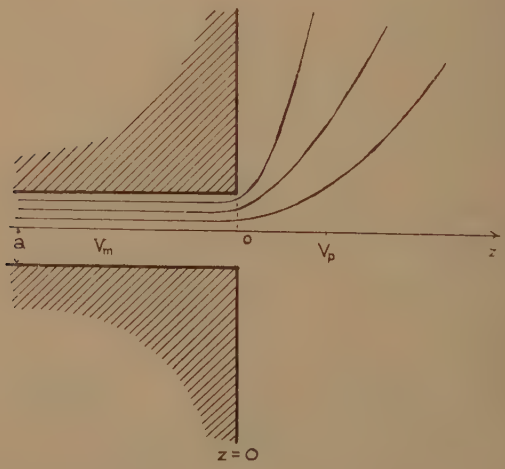

medium of the same conductivity bounded by an infinite plane, as shown in the figure. The resistance R_m of a length l of the cylindrical conductor and that of the entire medium to the right of the flange, R_p, is usually written in the form

$$R = R_m + R_p = \frac{\tau}{\pi a^2}(l + \alpha), \quad . \quad . \quad . \quad . \quad (1)$$

where τ is the specific resistance of the conducting material and $R_m = l\tau/(\pi a^2)$ is the resistance of a length l

* Communicated by the Author.

† Rayleigh, 'Theory of Sound' (Second Edition, 1896), ii. Appendix A, p. 487.

of the cylinder undisturbed by the divergence of current at the end.

It is readily shown by elementary methods that α, the "correction to the end," is greater than $\frac{1}{4}\pi a$ and less than $8a/(3\pi)$, or

$$\cdot 78540 < \alpha/a < \cdot 84883. \quad . \quad . \quad . \quad . \quad . \quad (2)$$

Rayleigh's method of calculating α/a is equivalent to assuming a potential gradient of the form

$$(\partial V/\partial z)_{z=0} = 1 + \mu(\rho/a)^2 + \mu'(\rho/a)^4 \quad . \quad . \quad . \quad (3)$$

over the section of the conductor in the plane $z=0$ of the infinite flange. The total rate of generation of heat throughout all space is given by

$$W = \frac{1}{\tau}\int\left\{\left(\frac{\partial V}{\partial x}\right)^2 + \left(\frac{\partial V}{\partial y}\right)^2 + \left(\frac{\partial V}{\partial z}\right)^2\right\} dx\,dy\,dz, \quad (4)$$

calculated throughout the conductor. By Green's theorem the expression for W in the cylindrical portion of the conductor, as well as that in the conductor to the right of the flange, may be expressed as an integral over the circle $\rho=a$ in the plane of the flange. According to a well-known principle, W is a minimum, and the essential point of Rayleigh's procedure is to adjust μ and μ' in (3) to conform to this condition. In this way the value usually quoted,

$$\alpha/a = \cdot 82422, \quad . \quad . \quad . \quad . \quad . \quad . \quad . \quad (5)$$

is obtained, and is considered by Lord Rayleigh as "probably pretty close to the truth."

The problem was again considered by Daniell*, who replaces (3) by

$$(\partial V/\partial z)_{z=0} = A + B(1-\rho^2) + C(1-\rho^2)^{-\frac{1}{2}} \quad . \quad . \quad (6)$$

and adjusts A, B, and C to make W a minimum. In a second paper he assumes

$$(V)_{z=0} = A' + B'(1-\rho^2) + C'(1-\rho^2)^2 + D'(1-\rho^2)^3 \quad (7)$$

and adjusts A', B', C', and D' to make W a minimum. His final result is to show that with these assumptions

$$\cdot 82141 < \alpha/a < \cdot 82168. \quad . \quad . \quad . \quad . \quad (8)$$

* Daniell, P. J., "The Coefficient of End-Correction," Phil. Mag. xxx. July 1915, pp. 137–146; xxx. August 1915, pp. 248–256.

In discussing the acoustic impedance of cylindrical tubes bounded by infinite flanges Rayleigh* states that "under this form the problem does not seem capable of exact solution." It is evident that the analysis leading to (5) is approximate, inasmuch as no provision is made for the continuity of V or $\partial V/\partial\rho$ on both sides of the circular opening in the plane of the flange. While the approximation (5) is probably sufficient for practical purposes, it is difficult to estimate its limits of error and the possible influence of additional terms in equation (3).

The interest of the present paper is that an exact solution of this class of problems may be obtained by the use of well-known inversion theorems associated with Bessel functions. In particular it is shown that α/a is expressed as the ratio of two infinite determinants the elements of which are functions of the roots of $J_1(x)=0$.

In a first method we obtain an increasing sequence of values commencing with $\frac{1}{4}\pi$,

$$\alpha/a \mid \cdot 78540 \quad \cdot 80656 \quad \cdot 81270 \quad \cdot 81550 \quad \cdot 81706 \quad \cdot 81805 \quad \cdot 81873 \quad . \quad . \quad . \quad (9)$$

as more and more rows and columns of the determinants are included in the calculation.

A second method gives rise to a decreasing sequence, commencing with $8/(3\pi)$,

$$\alpha/a \mid \cdot 84883 \quad \cdot 83304 \quad \cdot 82843 \quad \cdot 82635 \quad \cdot 82517 \quad \cdot 82445 \quad \cdot 82391 \quad . \quad . \quad (10)$$

as more elements of the determinants are taken into account.

The convergence of the ascending and descending sequences to the same limit is seen to be somewhat slow. It would appear in general that the exact solution of electrical and wave-potential problems associated with circular cylinders of finite length leads to a type of analysis involving the solution of integral equations and the use of infinite determinants.

§ 2. *Statement of the Problem.*

We consider as a simple example of this type the electrical problem of determining the "correction to the

* Rayleigh, "On the Theory of Resonance," Phil. Trans. clxi. pp. 77–118 (1870); 'Scientific Papers,' i. p. 53.

end," α/a in the case of a semi-infinite cylinder of specific resistance τ continuous with an unlimited medium of the same material bounded by an infinite flange in the plane $z=0$. We denote by V_m the potential in the cylindrical portion of the conductor, on the negative or minus side of the plane $z=0$, and by V_p the corresponding potential on the positive side of the infinite flange. In cylindrical coordinates (ρ, z) the components of current are given by

$$u_\rho = -\frac{1}{\tau}\frac{\partial V}{\partial \rho} \quad \text{and} \quad u_z = -\frac{1}{\tau}\frac{\partial V}{\partial z}, \quad . \quad . \quad (11)$$

while the potentials V_m and V_p both satisfy the differential equation $\nabla^2 V = 0$, or, in cylindrical coordinates,

$$\frac{\partial^2 V}{\partial \rho^2} + \frac{1}{\rho}\frac{\partial V}{\partial \rho} + \frac{\partial^2 V}{\partial z^2} = 0. \quad . \quad . \quad . \quad (12)$$

Appropriate solutions for V_p and V_m are

$$V_p = \int_0^\infty e^{-\lambda z} J_0(\lambda\rho) f(\lambda)\, d\lambda, \quad . \quad . \quad . \quad (13)$$

and

$$V_m = Az + B + \sum_{s=1}^{\infty} e^{\lambda_s z} A_s J_0(\lambda_s \rho). \quad . \quad . \quad (14)$$

Since $u_\rho = 0$ at the boundary $\rho = a$ of the cylinder, we have

$$J_1(\lambda_s a) = 0, \quad . \quad . \quad . \quad . \quad . \quad (15)$$

so that $j_s = \lambda_s a$ are the roots of $J_1(x) = 0$.

The problem before us is to determine the "kernel" $f(\lambda)$ of the integral equation (13) and the coefficients A_s of (14) from the continuity of V and $\partial V/\partial z$ over the boundary $z=0$, within the circle $\rho = a$. Outside this circle, over the flange, $u_z = 0$, so that we have the further boundary condition

$$(\partial V_p/\partial z)_{z=0} = 0, \quad (a < \rho < \infty) \quad . \quad . \quad (16)$$

in addition to

$$(\partial V_p/\partial z)_{z=0} = (\partial V_m/\partial z)_{z=0}$$

$$\text{and} \quad (V_p)_{z=0} = (V_m)_{z=0}, \quad (0 < \rho < a). \quad . \quad (17)$$

If we denote by $(V_m)_{z=-l}$ the potential at a point on the axis of the cylinder at a distance l on the negative side from the plane $z=0$, and by $(V_p)_{z\to\infty}$ that on the

positive side at a very great distance from the flange, it follows from (13) and (14) that when l/a is sufficiently large

$$(V_p)_{z\to\infty} - (V_m)_{z=-l} = Al - B = -(R_p + R_m)I, \quad (18)$$

where I is the total current over the cross-section of the conductor flowing from left to right. On calculating I at $z=-l$, we have, when l/a is sufficiently large,

$$I = \pi a^2 (u_z)_{z=-l} = -\frac{\pi a^2}{\tau}\left(\frac{\partial V}{\partial z}\right)_{z=-l} = -\frac{\pi a^2}{\tau} A. \quad (19)$$

By definition of α according to (1) we have

$$R_p + R_m = \frac{\tau}{\pi a^2}(l+\alpha). \quad . \quad . \quad . \quad . \quad (20)$$

It follows immediately from (18), (19), and (20) that

$$\alpha = -B/A. \quad . \quad . \quad . \quad . \quad . \quad . \quad (21)$$

§ 3. *Determination of the Kernel* $f(\lambda)$.

In order to determine $f(\lambda)$ there are two inversion theorems available.

(i.) The solution of the integral equation

$$\int_0^\infty \lambda G_\nu(\lambda) J_\nu(\lambda\rho)\, d\lambda = F_\nu(\rho), \ (0 < \rho < a):$$

$$\int_0^\infty \lambda G_\nu(\lambda) J_\nu(\lambda\rho)\, d\lambda = 0, \ (a < \rho < \infty) \quad . \quad . \quad (22)$$

is

$$G_\nu(\lambda) = \int_0^a F_\nu(\rho) J_\nu(\lambda\rho)\rho\, d\rho. \quad . \quad . \quad . \quad (23)$$

This result is well known as a particular case of Hankel's inversion-theorem *.

(ii.) Not so well known is the solution of the integral equation having a discontinuous kernel †,

* Watson, 'Theory of Bessel Functions' (Cambridge University Press, 1922), § 14.4, p. 456.

† The explicit form of the theorem contained in equations (24)–(27) is easily derived from results due to H. M. Macdonald (Proc. Lond. Math. Soc. (1) xxvi. p. 257 (1895)), quoted in H. Bateman's 'Partial Differential Equations,' p. 474 (Cambridge University Press, 1932). Special cases of such theorems due to Beltrami are quoted in A. G. Webster's 'Partial Differential Equations of Mathematical Physics,' p. 372, equation (187) (Stechert and Co., New York, 1933).

$$\int_0^\infty g_\nu(\lambda)J_\nu(\lambda\rho)\,d\lambda = f_\nu(\rho),\ (0<\rho<a):$$

$$\int_0^\infty \lambda g_\nu(\lambda)J_\nu(\lambda\rho)\,d\lambda = 0,\ (a<\rho<\infty), \quad . \quad (24)$$

where

$$g_\nu(\lambda) = \lambda^{\frac{1}{2}}\int_0^a \phi(x)J_{\nu-\frac{1}{2}}(\lambda x)\,dx, \quad . \ . \ . \quad (25)$$

and

$$\phi(x)x^{\nu-\frac{1}{2}} = \frac{2}{\pi}f(0) + \frac{2x}{\pi}\int_0^{\frac{1}{2}\pi} f'(x\sin\theta)\,d\theta, \quad . \quad (26)$$

where

$$f(\rho) = \sqrt{(\tfrac{1}{2}\pi)}\rho^\nu f(\rho). \ . \ . \ . \ . \ . \quad (27)$$

(i.) The first boundary condition of (17), together with (16), gives for the determination of $f(\lambda)$ the integral equation

$$\int_0^\infty \lambda f(\lambda)J_0(\lambda\rho)\,d\lambda = \left\{ \begin{matrix} -A - \sum\limits_s A_s\lambda_s J_0(\lambda_s\rho), & (0<\rho<a) \\ 0 \qquad\qquad\qquad\quad , & (a<\rho<\infty) \end{matrix} \right\},$$

$$. \ . \ . \quad (28)$$

of which the solution is easily found to be according to (23)

$$f(\lambda) = -\frac{Aa}{\lambda}J_1(\lambda a) - a\lambda J_1(\lambda a)\sum_s \frac{A_s\lambda_s J_0(\lambda_s a)}{\lambda^2-\lambda_s^2}, \quad . \quad (29)$$

in the derivation of which use is made of the fact that $J_1(\lambda_s a)=0$. The summation $\sum\limits_s$ extends to all positive roots of $J_1(x)=0$.

(ii.) The second boundary condition (17), together with (16), gives rise to the integral equation

$$\int_0^\infty f(\lambda)J_0(\lambda\rho)d\lambda = B + \sum_s A\,J_0(\lambda_s\rho),\ (0<\rho<a):$$

$$\int_0^\infty \lambda f(\lambda)J_0(\lambda\rho)\,d\lambda = 0,\ (a<\rho<\infty). \quad . \quad (30)$$

The solution according to equations (25), (26), (37)

presents no difficulty. We easily find on making use of the well-known formula

$$\int_0^{\frac{1}{2}\pi} \mathrm{J}_1(\lambda_s a \sin\theta)\, d\theta = \frac{1-\cos(a\lambda_s)}{a\lambda_s}, \quad . \quad . \quad (31)^*$$

$$\phi(x) = \sqrt{(2/\pi)}x^{\frac{1}{2}} + \sqrt{(2/\pi)}x^{\frac{1}{2}} \sum_s \mathrm{A}_s \cos x\lambda_s, \quad . \quad . \quad (32)$$

and, finally,

$$f(\lambda) = \frac{2}{\pi}\mathrm{B}\frac{\sin\lambda a}{\lambda} + \frac{1}{\pi}\sum_s \mathrm{A}_s \left\{ \frac{\sin(\lambda-\lambda_s)a}{\lambda-\lambda_s} + \frac{\sin(\lambda+\lambda_s)a}{\lambda+\lambda_s} \right\}. \quad . \quad . \quad (33)$$

§ 4. *First Method for the Determination of* α/a.

It is evident from (28) that $f(\lambda)$ as determined by (29) ensures that over the plane $z=0$, $\partial \mathrm{V}_p/\partial z = \partial \mathrm{V}_m/\partial z$ for $0<\rho<a$, and $\partial \mathrm{V}_p/\partial z = 0$ for $a<\rho<\infty$, while $f(\lambda)$ as determined from (30) makes $\mathrm{V}_p = \mathrm{V}_m$ for $0<\rho<a$ and $\partial \mathrm{V}_p/\partial z = 0$ for $a<\rho<\infty$. Thus both the axial and radial components of current will be continuous within the circle $\rho=a$ over the plane $z=0$ if we determine the coefficients A, B, A_1, A_2, ... A_s ... so that the expressions (29) and (33) represent the same function for all values of the variable λ. On writing successively $\lambda=0$ and $\lambda=\lambda_\sigma$ with $\sigma=1, 2, 3, \ldots$ in each of these equations, we obtain an infinite set of linear equations for the determination of the coefficients in question. We write $j_\sigma = a\lambda_\sigma$ for the σ'th root of $\mathrm{J}_1(x)=0$, and denote

$$\left.\begin{aligned} \mathrm{S}_{0\sigma} = \frac{\sin j_\sigma}{j_\sigma}, \quad \mathrm{S}_{\sigma s} = \mathrm{S}_{s\sigma} = \tfrac{1}{2}\left\{ \frac{\sin(j_\sigma - j_s)}{j_\sigma - j_s} + \frac{\sin(j_\sigma + j_s)}{j_\sigma + j_s} \right\} \\ \mathrm{C}_\sigma = \frac{\pi}{4} j_\sigma \mathrm{J}_0{}^2(j_\sigma). \end{aligned}\right\}. \quad . \quad . \quad . \quad (34)$$

Corresponding to $\lambda=0$ and $\lambda=\lambda_\sigma$ we have, respectively,

$$\mathrm{B} + \sum_s \mathrm{A}_s \mathrm{S}_{0s} = -\frac{\pi}{4}\mathrm{A}a, \quad \mathrm{B}\mathrm{S}_{0\sigma} + \sum_s \mathrm{A}_s \mathrm{S}_{\sigma s} = -\mathrm{C}_\sigma \mathrm{A}_\sigma. \quad (35)$$

The coefficients B, A_1, A_2, A_3, ... are thus the solutions of the linear equations

* Gray and Mathews, 'Bessel Functions,' Second Edition, 1931 (Macmillan and Co., London), p. 39; or Watson, 'Theory of Bessel Functions,' § 12.11 (1), p. 373.

$$\left.\begin{aligned}
&B+A_1S_{01}+A_2S_{02}+A_3S_{03}+\ldots &&=-\frac{\pi}{4}Aa,\\
&BS_{01}+A_1(S_{11}+C_1)+A_2S_{12}+A_3S_{13}+\ldots &&=0,\\
&BS_{02}+A_1S_{12}+A_2(S_{22}+C_2)+A_3S_{23}+\ldots &&=0,\\
&BS_{03}+A_1S_{13}+A_2S_{23}+A_3(S_{33}+C_3)+\ldots &&=0.\\
&\ldots\quad\ldots\quad\ldots\quad\ldots\quad\ldots
\end{aligned}\right\}\quad(36)$$

In the usual notation of determinants we at once have from (21)

$$\frac{\alpha}{a}=-\frac{B}{Aa}=\frac{\pi}{4}\frac{\triangle_{11}}{\triangle},\qquad(37)$$

where $\triangle$ is the determinant whose elements are the coefficients of B, A_1, A_2, A_3,.... etc., and $\triangle_{11}$ is its first minor.

With

$$j_1=3{\cdot}8317\quad j_2=7{\cdot}0156\quad j_3=10{\cdot}1735\text{ etc.}$$
$$J_0(j_1)=-{\cdot}40276\quad J_0(j_2)={\cdot}30016\quad J_0(j_3)=-{\cdot}24970\text{ etc.},$$

we find on computing $S_{\sigma s}$ and C_σ from (34) that with numerical coefficients the determinant $\triangle$ corresponding to the equations (36) becomes, on making use of the first six roots of $J_1(x)=0$,

$$\triangle=\begin{vmatrix}
1-{\cdot}166145+{\cdot}095310-{\cdot}066907+{\cdot}051561-{\cdot}041944+{\cdot}035353\\
1{\cdot}052236-{\cdot}052228+{\cdot}040007-{\cdot}032461+{\cdot}027324-{\cdot}023596\\
1{\cdot}031721-{\cdot}031543+{\cdot}026477-{\cdot}022828+{\cdot}020077\\
1{\cdot}022718-{\cdot}022144+{\cdot}019842-{\cdot}017839\\
1{\cdot}017683-{\cdot}017612+{\cdot}016352\\
1{\cdot}014474-{\cdot}014421\\
1{\cdot}012250
\end{vmatrix}.\qquad(38)$$

The determinant is symmetrical, and only those elements to the right of the diagonal are entered.

When s is large we have for the s'th root of $J_1(x)=0$

$$j_s\sim s\pi+\tfrac{1}{4}\pi-\frac{3}{8j_s},\qquad(39)^*$$

and a useful check in computing the additional elements of the determinant (38) is obtained from the use of the approximate formulæ

$$S_{os}\sim\frac{(-1)^s}{2j_s}\left\{1-\frac{3}{8j_s}\right\},\quad S_{\sigma s}\sim\frac{(-1)^{s+\sigma}}{2(j_\sigma+j_s)},\quad S_{ss}+C_s\sim1+\frac{1}{4j_s}\qquad(40)$$

* Gray and Mathews, 'Bessel Functions,' Appendix III., p. 260; Watson, 'Theory of Bessel Functions,' § 15.53.

as long as $s>3$, $\sigma>3$ and four significant figures are employed.

The numerical computation of the determinant (38) and of its first minor is most easily carried out by a method due to Chiò, in which the determinant is successively reduced to one of lower rank *. The arithmetical work is not excessive in view of the fact that the original and each successive determinant is symmetrical, while at any stage more elements can be computed and used in the calculations if necessary.

On calculating α/a in this way from (38) to include successively 1, 2, 3, 4, 5, 6, and 7 rows and columns, we obtain the following increasing sequence of values,

α/a	·7853982	·8065570	·8127050	.8155030	·8170606	·8180540	·8187266.

. . . (41)

§ 5. *Second Method for the Determination of* α/a.

If we determine the coefficients B, A_1, A_2,... A_s,... in the first of the relations (30) according to the usual procedure of Fourier-Bessel expansions, we ensure that $V_p=V_m$ over the plane $z=0$ within the circle $\rho=a$. On multiplying each side by $\rho J_0(\lambda_s\rho)$, and integrating from 0 to a, we obtain the results

$$\left.\begin{aligned} \tfrac{1}{2}A_s a\, J_0(a\lambda_s) &= \int_0^\infty \frac{\lambda J_1(\lambda a)}{\lambda^2-\lambda_s^2} f(\lambda)\, d\lambda, \\ \tfrac{1}{2}Ba &= \int_0^\infty \frac{f(\lambda)}{\lambda} J_1(\lambda a)\, d\lambda. \end{aligned}\right\} \quad . \quad . \quad (42)$$

The boundary condition $\partial V_p/\partial z=\partial V_m/\partial z$ over the plane $z=0$ for $0<\rho<a$, and $\partial V_p/\partial z=0$ for $a<\rho<\infty$ is now satisfied if we substitute for $f(\lambda)$ in (42) the expression (29)†.

If we write

$$B_s=A_s\lambda_s J_0(\lambda_s a), \qquad \lambda_s a=j_s, \quad . \quad . \quad . \quad (43)$$

and σ for s in (29), we have

$$\frac{f(\lambda)}{a} = -\frac{A\, J_1(\lambda a)}{\lambda} - \sum_\sigma B_\sigma \frac{\lambda J_1(\lambda a)}{\lambda^2-\lambda_\sigma^2}. \quad . \quad . \quad (44)$$

* The method is described in Whittaker and Robinson's 'Calculus of Observations' (Blackie and Son, London, 1924), chapter v. p. 71.

† The substitution of the equivalent expression (33) is easily proved to lead to the identity $A_s=A_s$ in view of Gallop's discontinuous integral (Watson, 'Theory of Bessel Functions,' § 13.49 (1), p. 422).

We now denote

$$I_{s\sigma}=\frac{1}{a}\int_0^\infty \frac{\lambda^2 J_1^2(\lambda a)\,d\lambda}{(\lambda^2-\lambda_s^2)(\lambda^2-\lambda_\sigma^2)}, \qquad I_{0s}=\frac{1}{a}\int_0^\infty \frac{J_1^2(\lambda a)\,d\lambda}{\lambda^2-\lambda_s^2}, \quad (45)$$

we find from (42)

$$\left.\begin{aligned} AI_{0s}+\sum_\sigma B_\sigma I_{s\sigma}&=-\tfrac{1}{2}B_s/(a\lambda_s),\\ AI_{00}+\sum_\sigma B_\sigma I_{0\sigma}&=-\tfrac{1}{2}B/a. \end{aligned}\right\} \quad . \quad . \quad (46)$$

The coefficients A, B_1, B_2, ... B_s... are thus the solutions of the infinite set of linear equations

$$\left.\begin{aligned} &AI_{00}+B_1I_{01}+B_2I_{02}+B_3I_{03}+\ldots &&=-\tfrac{1}{2}B/a,\\ &AI_{01}+B_1\left(I_{11}+\frac{1}{2j_1}\right)+B_2I_{12}+B_3I_{13}+\ldots &&=0,\\ &AI_{02}+B_1I_{12}+B_2\left(I_{22}+\frac{1}{2j_2}\right)+B_3I_{23}+\ldots &&=0,\\ &AI_{03}+B_1I_{13}+B_2I_{23}+B_3\left(I_{33}+\frac{1}{2j_3}\right)+\ldots &&=0.\\ &\ldots \quad \ldots \quad \ldots \quad \ldots \quad \ldots \end{aligned}\right\} \quad . \quad (47)$$

In the usual notation of determinants we at once have from (21)

$$\frac{\alpha}{a}=-\frac{B}{Aa}=\frac{2\triangle}{\triangle_{11}}, \quad . \quad . \quad . \quad . \quad (48)$$

where $\triangle$ is the determinant whose elements are the coefficients of A, B_1, B_2, B_3 ... etc., and $\triangle_{11}$ is its first minor.

§ 6. *On the Numerical Calculation of the Integrals* I_{0s}, $I_{\sigma s}$, I_{ss}.

(i.) *Convergent Expansion for* I_{0s}.

According to a well-known formula we have for $\rho<a$

$$\int_0^\infty \frac{J_1(\lambda a)\,J_0(\lambda\rho)}{\lambda}\,d\lambda=F\left(\tfrac{1}{2},-\tfrac{1}{2}:1,\frac{\rho^2}{a^2}\right)=\frac{2}{\pi}E\left(\frac{\rho}{a}\right), \quad (49)^*$$

where $E(\rho/a)$ is the complete elliptic integral of the second kind to modulus ρ/a.

We also have, in view of the fact that $J_1(\lambda_s a)=0$,

$$\int_0^a \rho J_0(\lambda\rho)\,J_0(\lambda_s\rho)\,d\rho=\frac{a\lambda J_0(\lambda_s a)\,J_1(\lambda a)}{\lambda^2-\lambda_s^2}, \quad . \quad (50)$$

* Watson, 'Theory of Bessel Functions,' § 13.4 (2), p. 401.

so that on multiplying each side of (49) by $\rho J_0(\lambda_s\rho)$ and integrating from 0 to a we have, according to (45),

$$a^2 J_0(j_s) I_{0s} = \frac{2}{\pi}\int_0^a \rho J_0(\lambda_s\rho) E(\rho/a)\, d\rho. \quad . \quad . \quad (51)$$

It is now convenient to write $\rho\lambda_s = x$, $a\lambda_s = j$, the suffix s being temporarily omitted. According to the well-known expansion we have

$$\frac{2}{\pi} E\left(\frac{x}{j}\right) = \sum_{n=0}^{\infty} \frac{a_{2n}}{j^{2n}} x^{2n}, \quad . \quad . \quad . \quad . \quad (52)$$

where

$$\left.\begin{aligned} a_0 &= 1,\ a_2 = -\frac{1}{4},\ a_4 = -\frac{3}{64},\ \cdots \\ a_{2n} &= -\left(\frac{1}{2}\cdot\frac{3}{4}\cdot\ \cdots\ \frac{2n-1}{2n}\right)^2 \frac{1}{2n-1}. \end{aligned}\right\} \quad . \quad . \quad (53)$$

It follows from (51) that

$$I_{0s} J_0(j) = \frac{1}{j^2}\sum_{n=0}^{\infty} \frac{a_{2n}}{j^{2n}} \int_0^j x^{2n+1} J_0(x)\, dx. \quad . \quad . \quad (54)$$

On integration by parts we have, remembering that $J_1(j) = 0$,

$$\int_0^j x^{2n+1} J_0(x)\, dx = -2n\int_0^j x^{2n} J_1(x)\, dx. \quad . \quad . \quad (55)$$

The integral on the right may now be expressed in terms of Lommel's polynomials $S_{\mu,\nu}(j)$. We find

$$\int_0^j x^{2n} J_1(x)\, dx = 2nj\, J_1(j)\, S_{2n+1,0}(j) - j\, S_{2n,1}(j)\, J_0(j). \quad (56)^*$$

In view of the fact that $J_1(j) = 0$, only the second term of (56) survives.

We have, further,

$$S_{2n,1}(j) = (-1)^{n-1} j^{2n-1}\left(\frac{2}{j}\right)^{2n-2} \Gamma(n)\,\Gamma(n+1) \times \sum_{m=0}^{n-1} \frac{(-1)^m (\frac{1}{2}j)^{2m}}{\Gamma(m+1)\,\Gamma(m+2)}. \quad . \quad (57)^\dagger$$

We thus have, from (54),

$$I_{0s} = \frac{2}{j}\sum_{n=0}^{\infty} \frac{n a_{2n}}{j^{2n}} S_{2n,1}(j). \quad . \quad . \quad . \quad . \quad (58)$$

* Watson, ' Theory of Bessel Functions,' §10.74 (3), p. 350.
† Watson, ' Theory of Bessel Functions,' §10.71, p. 347.

A somewhat more convergent series is obtained from (58) by making use of the recurrence-formula

$$S_{2n+2,1}(j)=j^{2n+1}-2n(2n+2)\,S_{2n,1}(j). \quad . \quad . \quad (59)^*$$

We thus obtain

$$I_{0s}=\sum_0^\infty \frac{a_{2n}}{2n+2}-\sum_0^\infty \frac{a_{2n}}{2n+2}\frac{1}{j^{2n+1}}\,S_{2n+2,1}(j). \quad . \quad (60)$$

Since $S_{2,1}(j)=j$, the first terms in the summations cancel, and on writing $(n+1)$ for n in (57) we obtain the expansion

$$I_{0s}=\sum_{n=1}^\infty \frac{a_{2n}}{2n+2}+\frac{1}{2}\left(\frac{2}{j}\right)^2 \times \sum_{n=1}^\infty (-1)^{n-1}a_{2n}(n\,!)^2\left(\frac{2}{j}\right)^{2n-2}\sum_{m=0}^n \frac{(-1)^m(\frac{1}{2}j)^{2m}}{\Gamma(m+1)\Gamma(m+2)}. \quad . \quad . \quad . \quad (61)$$

The first series is easily summed, since, according to (50), we have

$$\int_0^\infty \frac{J_1(\lambda a)\,J_0(\lambda\rho)}{\lambda}\,d\lambda=\frac{2}{\pi}E\left(\frac{\rho}{a}\right)=a_0+\sum_1^\infty a_{2n}\frac{\rho^{2n}}{a^{2n}}.$$

On multiplying each side by ρ, and integrating from 0 to a, we have

$$I_{00}=\int_0^\infty \frac{J_1^2(x)\,dx}{x^2}=\frac{4}{3\pi}-\frac{1}{2}+\sum_1^\infty \frac{a_{2n}}{2n+2}. \quad . \quad (62)$$

We thus have for purposes of computation

$$\left.\begin{aligned} &I_{0s}=\frac{4}{3\pi}-\frac{1}{2}+\frac{1}{2}\left(\frac{2}{j}\right)^2\sum_{n=1}^\infty (-1)^{n-1}a_{2n}(n\,!)^2\left(\frac{2}{j}\right)^{2n-2}\sum_0^n,\\ &\text{where}\\ &\sum_0^n=1-\frac{(\frac{1}{2}j)^2}{1\,!\,2\,!}+\frac{(\frac{1}{2}j)^4}{2\,!\,3\,!}-\frac{(\frac{1}{2}j)^6}{3\,!\,4\,!}+\cdots\frac{+(-1)^n(\frac{1}{2}j)^{2n}}{n\,!\,(n+1)\,!}. \end{aligned}\right\} \quad (63)$$

It will be noticed that the second summation in (63) consists of the first n terms of the power-series for $(2/j)J_1(j)$. Since $J_1(j)=0$, $\sum_n$ tends rapidly to zero as $n\to\infty$ for all the roots $j=j_s$. As a result the above expansion for I_{0s} is highly convergent, and the computation

* Watson, 'Theory of Bessel Functions,' §10.72 (2), p. 348.

of numerical values for successive roots $j=j_s$ is a simple matter.

(ii.) *Convergent expansion for* I_{ss}.

By integration by parts we easily obtain the result

$$\int_0^\infty \frac{xJ_1(x)\,J_1'(x)}{x^2-j^2}\,dx=-\tfrac{1}{2}I_{0s}+I_{ss}. \quad . \quad . \quad (64)$$

If we write $xJ_1'(x)=-J_1(x)+xJ_0(x)$ in the above integral, we have

$$\int_0^\infty \frac{xJ_1(x)J_1'(x)}{x^2-j^2}\,dx=-I_{0s}+\int_0^\infty \frac{xJ_0(x)\,J_1(x)}{x^2-j^2}\,dx. \quad (65)$$

It thus follows from (64) and (65) that

$$I_{ss}=-\tfrac{1}{2}I_{0s}+\int_0^\infty \frac{xJ_0(x)\,J_1(x)}{x^2-j^2}\,dx. \quad . \quad . \quad . \quad (66)$$

We now make use of the well-known formula, valid for $\rho<a$,

$$\int_0^\infty J_0(\lambda a)\,J_0(\lambda\rho)\,d\lambda=\frac{1}{a}F\left(\tfrac{1}{2},\tfrac{1}{2}:1,\frac{\rho}{a}\right)=\frac{2}{\pi a}K\left(\frac{\rho}{a}\right), \quad (67)^*$$

where $K(\rho/a)$ is the complete elliptic integral of the first kind to modulus ρ/a. If we now multiply each side of (67) by $\rho J_0(\lambda_s\rho)$, and integrate from 0 to a, we obtain the result

$$\int_0^\infty \frac{xJ_0(x)\,J_1(x)}{x^2-j^2}\,dx=\frac{1}{J_0(j)}\,\frac{1}{j^2}\,\frac{2}{\pi}\int_0^j xJ_0(x)K\left(\frac{x}{j}\right)dx. \quad (68)$$

Since (51) is equivalent to

$$I_{0s}=\frac{1}{J_0(j)}\,\frac{1}{j^2}\,\frac{2}{\pi}\int_0^j xJ_0(x)\,E\left(\frac{x}{j}\right)dx, \quad . \quad . \quad (69)$$

we obtain from (66), (68), and (69)

$$I_{ss}=\tfrac{1}{2}I_{0s}+2I_{ss}', \quad . \quad . \quad . \quad . \quad . \quad . \quad (70)$$

where

$$I_{ss}'=\frac{1}{2}\,\frac{1}{J_0(j)}\cdot\frac{1}{j^2}\,\frac{2}{\pi}\int_0^j xJ_0(x)\left\{K\left(\frac{x}{j}\right)-E\left(\frac{x}{j}\right)\right\}dx. \quad (71)$$

We now make use of the expansion

$$\frac{1}{\pi}\left\{K\left(\frac{x}{j}\right)-E\left(\frac{x}{j}\right)\right\}=-\sum_{n=1}^{\infty}\frac{n\,a_{2n}}{j^{2n}}x^{2n}, \quad . \quad . \quad (72)$$

where a_{2n} are the coefficients given in (63).

* Watson, 'Theory of Bessel Functions,' §13.4 (2), p. 401.

We thus have

$$J_0(j)\, I_{ss}' = -\frac{1}{j^2}\sum_{n=1}^{\infty}\frac{n a_{2n}}{j^{2n}}\int_0^j x^{2n+1} J_0(x)\, dx. \quad . \quad (73)$$

On comparing with (54) the expansion required is (61) with a_{2n} replaced by $-n a_{2n}$. Thus

$$I_{ss}' = -\sum_{n=1}^{\infty}\frac{n a_{2n}}{2n+2} - \frac{1}{2}\left(\frac{2}{j}\right)^2 \sum_{n=1}^{\infty}(-1)^{n-1} n a_{2n} (n!)^2 \left(\frac{2}{j}\right)^{2n-2} \times \sum_{m=0}^{n}\frac{(-1)^m (\frac{1}{2}j)^{2m}}{\Gamma(m+1).\Gamma(m+2)}. \quad . \quad (74)$$

The first series is easily summed, since we have, according to (72), (67), and (50),

$$-\sum_{n=1}^{\infty} n a_{2n}\frac{\rho^{2n}}{a^{2n}} = \frac{1}{\pi}\left\{K\left(\frac{\rho}{a}\right) - E\left(\frac{\rho}{a}\right)\right\} = \frac{1}{2}\left\{a\int_0^{\infty} J^0(\lambda a) J_0(\lambda\rho)\, d\lambda - \int_0^{\infty} J_1(\lambda a) J_0(\lambda\rho)\frac{d\lambda}{\lambda}\right\}.$$

On multiplying each side by ρ, and integrating from 0 to a, we find

$$-\sum_{n=1}^{\infty}\frac{n a_{2n}}{2n+2} = \frac{1}{2}\left\{\int_0^{\infty} J_0(x) J_1(x)\frac{dx}{x} - \int_0^{\infty}\frac{J_1^2(x)\, dx}{x^2}\right\}$$

or

$$-\sum_{n=1}^{\infty}\frac{n a_{2n}}{2n+2} = \frac{1}{2}\left\{\frac{2}{\pi} - \frac{4}{\pi 3}\right\} = \frac{1}{3\pi}. \quad . \quad . \quad (75)$$

We thus have, from (74), a suitably convergent formula for I_{ss}',

$$I_{ss}' = \frac{1}{3\pi} - \frac{1}{2}\left(\frac{2}{j}\right)^2 \sum_{n=1}^{\infty}(-1)^{n-1} n a_{2n} (n!)^2 \left(\frac{2}{j}\right)^{2n-2} \sum_{0}^{n}, \quad (76)$$

in which $\sum_{0}^{n}$ has the same meaning as in (63). It is evident, on comparing (76) with (63), that once a schedule of computation has been set up for calculating I_{0s} it is only necessary to multiply each term by n before summation to obtain I_{ss}', and hence by adding $\frac{1}{2} I_{0s}$ according to (70) to obtain I_{ss}.

(iii.) *Computation of* $I_{\sigma s}$.

It is at once evident from (45) that on resolution into partial fractions we have

$$I_{s\sigma} = \frac{j_s^2 I_{0s} - j_\sigma^2 I_{0\sigma}}{j_s^2 - j_\sigma^2}, \quad . \quad . \quad . \quad . \quad . \quad (77)$$

so that the computation of these coefficients is a simple matter when the values of I_{0s} and $I_{0\sigma}$ are known.

(iv.) *Numerical Computation of α/a.*

On making use of the formulæ (63), (76), and (77) of this section, we find the following infinite determinant on which the computation of α/a depends:—

$$\Delta = \begin{vmatrix} \cdot4244132 - \cdot0445572 - \cdot0170126 - \cdot0092232 - \cdot0059006 - \cdot0041290 - \cdot0031015 \\ \cdot2514780 - \cdot0053030 - \cdot0033823 - \cdot0024152 - \cdot0018158 - \cdot0014573 \\ \cdot1401329 - \cdot0021603 - \cdot0016379 - \cdot0012735 - \cdot0010611 \\ \cdot0982167 - \cdot0012540 - \cdot0009863 - \cdot0008488 \\ \cdot0759405 - \cdot0007748 - \cdot0007047 \\ \cdot0628289 - \cdot0006456 \\ \cdot0527029 \end{vmatrix} . \quad (7$$

As the determinant is symmetrical, only those elements to the right of the diagonal are entered. Elements corresponding to the first six roots of $J_1(x)=0$ are calculated.

On calculating $\frac{\alpha}{a} = \frac{2\Delta}{\Delta_{11}}$ in this way from (78) by Chiò's method, to include 1, 2, 3, 4, 5, 6, and 7 rows and columns in succession, we obtain the following decreasing sequence of values for α/a, commencing with $I_{00}=8/(3\pi)$:

$$\alpha/a \mid \cdot8488264 \quad \cdot8330387 \quad \cdot8284340 \quad \cdot8263520$$
$$\cdot8251744 \quad \cdot8244460 \quad \cdot8239120 \ldots \quad (79)$$

§ 7. *Summary and Conclusions.*

(1) The well-known problem of calculating the end-resistance of a semi-infinite cylindrical conductor of radius a continuous with an unlimited medium of the same conductivity bounded by an infinite insulating flange is rigorously solved by making use of inversion-theorems related to the theory of Bessel functions.

(2) The potential within the cylinder is represented by the usual expansion

$$V_m = Az + B + \sum_{s=1}^{\infty} e^{\lambda_s z} A_s J_0(\lambda_s \rho), \text{ with } J_1(\lambda_s a)=0, (z<0), \text{ (i.)}$$

while that in the unlimited medium is represented by the infinite integral

$$V_p = \int_0^{\infty} e^{-\lambda z} f(\lambda) J_0(\lambda\rho)\, d\lambda, (z>0) \ldots \text{ (ii.)}$$

(3) To solve the problem it is necessary to "match" the two solutions over the plane of the flange within the circle $\rho=a$. We must have

$$(\partial V_p/\partial z)_{z=0}=(\partial V_m/\partial z)_{z=0} \text{ and } (V_p)_{z=0}=(V_m)_{z=0}, \ (0<\rho<a), \quad . \ . \ . \ \text{(iii.)}$$

to ensure continuity of axial and radial current components, while over the flange we have

$$(\partial V_p/\partial z)_{z=0}=0, \quad (a<\rho<\infty). \quad . \ . \ \text{(iv.)}$$

(4) The boundary conditions (iii.) and (iv.) lead to integral equations of the type

$$\int_0^\infty \lambda G_0(\lambda)J_0(\lambda\rho)\,d\lambda=F_0(\rho), \quad (0<\rho<a):$$

$$\int_0^\infty \lambda G_0(\lambda)J_0(\lambda\rho)\,d\lambda=0, \ (a<\rho<\infty), \quad . \ \text{(v.)}$$

and

$$\int_0^\infty g_0(\lambda)J_0(\lambda\rho)\,d\lambda=f_0(\rho), \quad (0<\rho<a):$$

$$\int_0^\infty \lambda g_0(\lambda)J_0(\lambda\rho)\,d\lambda=0, \quad (a<\rho<\infty), \ . \ \text{(iv.)}$$

for which solutions are known.

(5) By the use of these solutions two expressions for $f(\lambda)$ are obtained in terms of the coefficients A, B, A_1, A_2, . . . A_s . . . . If the latter are determined so that these two expressions represent the same function for all values of the variable λ, all the boundary conditions (iii.) and (iv.) are satisfied. As a result these coefficients are the solutions of an infinite set of linear equations, and the "correction to the length," α/a, is given as the ratio of two infinite determinants the elements of which are functions of the roots of $J_1(x)=0$. The numerical evaluation of the ratio gives for α/a the increasing sequence

$$\alpha/a \,|\, \frac{\pi}{4}=\cdot78540 \quad \cdot80656 \quad \cdot81270 \quad \cdot81550$$
$$\cdot81706 \quad \cdot81805 \quad \cdot81873, \ . \ \text{(vii.)}$$

as 1, 2, 3, 4, 5, 6, and 7 rows and columns are included.

(6) A second method of determining α/a depends on the evaluation of the coefficients A_s by the usual Fourier-Bessel procedure when the expressions (i.) and (ii.) are made equal within the circle $\rho=a$ over the plane

$z=0$ of the flange. On substituting for $f(\lambda)$ the expression obtained from the integral equation making $(\partial V_p/\partial z)_{z=0}=(\partial V_m/\partial z)_{z=0}$ we obtain for the coefficients another infinite set of linear equations, and α/a is the ratio of the corresponding infinite determinants. On including in succession 1, 2, 3, 4, 5, 6, and 7 rows and columns we obtain for α/a the decreasing sequence

$$\alpha/a \mid \frac{8}{3\pi} = \cdot 84883 \quad \cdot 83304 \quad \cdot 82843 \quad \cdot 82635$$
$$\cdot 82517 \quad \cdot 82445 \quad \cdot 82391. \quad . \quad \text{(viii.)}$$

(7) It will be noticed from (vii.) and (viii.) that the sequences for α/a converge somewhat slowly to the same theoretical limit. It would require the inclusion of twelve or more roots of $J_1(x)=0$ in the infinite determinants $\triangle$ to make the corresponding values of α/a agree to one part in a thousand. The arithmetic means of the sequences (vii.) and (viii.) ultimately converge to the required theoretical limit, and give the numbers

$$\cdot 81711 \quad \cdot 81980 \quad \cdot 82057 \quad \cdot 82093 \quad \cdot 82112$$
$$\cdot 82125 \quad \cdot 82132. \quad . \quad . \quad \text{(ix.)}$$

The above sequence of arithmetic means tends to give a value of α/a within the limits obtained by Daniell,

$$\cdot 82141 < \alpha/a < \cdot 82168,$$

and both computations as they stand indicate that Rayleigh's estimate ·82422 is a little in excess of the correct limit.

(8) The method of analysis presented in this paper is easily extended to the computation of the resistance of a cylindrical column continuous with an unlimited medium of the same (or different) conductivity bounded at each end by infinite flanges.

In the field of acoustics it is well known that α/a is also the first approximation to the correction to the theoretical length of a resonating column whose circumference is small compared to the wave-length; in fact, an exact solution of this problem is indicated, and will depend, as does the simple electrical one, on the solution of an infinite set of linear equations for the coefficients of the cylindrical wave-functions which replace the solutions of Laplace's equation (i.) and (ii.) in the simple potential theory.

July 5, 1935.

VII. *The Temperature Dependence of Free Electron Specific Heat.* *By* EDMUND C. STONER, *Ph.D.* (*Cambridge*), *Reader in Physics at the University of Leeds* *.

1. *Introduction.*

THE application of the Fermi-Dirac statistics gives an immediate explanation of the absence of any appreciable contribution to the specific heat from free or nearly free electrons in metals. For free electrons the specific heat in the lower temperature range is given by

$$(C_v)_e = \frac{3}{2}Nk\frac{\pi^2}{3}\left(\frac{kT}{\epsilon_0}\right), \quad . \quad . \quad . \quad . \quad (1.1)$$

where N is the number of electrons, ϵ_0 the maximum electronic energy in the completely degenerate state (at absolute zero). This expression may be applicable, with sufficient approximation, up to several thousand degrees. In the limit for the higher temperature range the classical result is obtained

$$(C_v)_e = \tfrac{3}{2}Nk. \quad . \quad . \quad . \quad . \quad . \quad . \quad (1.2)$$

For the low and high temperature range the expressions for C_v may be obtained in the form of series with ascending powers of T and 1/T respectively; of these series, (1.1) and (1.2) are the first terms. In this paper higher terms of the series will be obtained. There appears to be no convenient method of dealing precisely with the intermediate temperature range, and in the low temperature range there are difficulties due to the fact that the treatment involves the use of asymptotic series. It is nevertheless possible to determine how the specific heat varies with temperature over the whole range with an approximation which appears to be amply sufficient for all practical purposes.

The conclusion that the specific heat of free electrons is very small at ordinary temperatures has a considerable indirect importance, in that it removes at once a fundamental objection which could be raised to a free electron treatment of conductivity and related properties of

* Communicated by Prof. R. Whiddington, F.R.S.

metals on the basis of classical statistics. It cannot be claimed, however, that the results for the variation over the whole temperature range have a wide field of direct application. On the one hand, if the electrons can be treated as free the electronic specific heat will be small and will be given with sufficient exactness at ordinary temperatures by the limiting low temperature expression (1.1); on the other, it is only for a few metals, such as the alkali metals, that the energy distribution of electrons in unfilled bands approaches that for free electrons. The electronic specific heat will depend in general (in the ordinary temperature range) on the number of quantum states per unit energy range at the top of the Fermi distribution. If this number varies with the square root of the energy, as for free electrons, the results obtained here may indeed be readily applied. The value of the detailed discussion of free electrons lies mainly, however, in the fact that sufficiently exact results can be obtained for this limiting case to provide a basis for discussion of the effect on the electronic specific heat of energy distributions of other types, and to provide a check on any calculations made.

Applications will not be considered here, as it is hoped in a future paper to deal with the question of electronic specific heat in the more general case and also with the related problem of electronic paramagnetism, and to consider some of the thermal and magnetic properties of particular metals in the light of the discussion. After a statement of the formulæ required in the application of Fermi-Dirac statistics to the free electron problem (2), expressions are obtained for the energy and specific heat at high (3) and low temperatures (4), attention being directed to the range of validity of the formulæ. The main formulæ obtained are then expressed in a form convenient for calculations, and which enables their numerical significance to be readily appreciated (5).

2. *Preliminary Formulæ.*

A detailed account of the derivation of the basic formulæ required in the application of the Fermi-Dirac statistics is given in the number of articles, among which one by Nordheim * is particularly relevant to the

* L. Nordheim, Müller-Pouillet's *Lehrbuch der Physik*, IV. iv. p. 271 (Braunschweig, 1934); *Ann. der Phys.* ix. p. 607 (1931).

present treatment. Here only the essential outlines will be given, the symbols used corresponding to those in a previous paper on free electron susceptibility *.

Let N be the number of electrons in the volume V considered, E the total energy.

$$N=\sum_s 1/\{\exp(\epsilon_s/kT-\eta)+1\}, \quad . \quad . \quad . \quad (2.1)$$

$$E=\sum_s \epsilon_s/\{\exp(\epsilon_s/kT-\eta)+1\}. \quad . \quad . \quad . \quad (2.2)$$

The summation is taken over all the quantum states. Owing to the quasi-continuous distribution of quantum states with respect to energy or momentum the summation may be replaced by an integration. Let P (ϵ) be the number of quantum states corresponding to a range of energy from 0 to ϵ, $\nu(\epsilon)$ the number of states per unit energy range. The number of states per unit momentum range, representing momentum by p, is

$$\frac{dP}{dp}=4\pi p^2 V g/h^3, \quad . \quad . \quad . \quad . \quad . \quad (2.3)$$

where g is a statistical weight factor, giving the number of states corresponding to a single translational state. For electrons $g=2$, corresponding to the two directions of spin.

For electrons in a field free region

$$\epsilon=p^2/2m, \quad . \quad . \quad . \quad . \quad . \quad . \quad (2.4)$$

so that

$$\left.\begin{aligned}\nu(\epsilon)&=\frac{dP(\epsilon)}{d\epsilon}=\frac{dP(\epsilon)}{dp}\frac{dp}{d\epsilon}\\&=(8\pi V m^{3/2}2^{1/2}/h^3)\,\epsilon^{1/2}.\end{aligned}\right\} \quad . \quad . \quad . \quad (2.5)$$

The maximum electron energy in the completely degenerate state will be denoted by ϵ_0, which is given by

$$\epsilon_0=(h^2/2m)(3N/8\pi V)^{2/3}. \quad . \quad . \quad . \quad . \quad (2.6)$$

From (2.5) and (2.6)

$$\nu(\epsilon)=\frac{3}{2}\frac{N}{\epsilon_0}\left(\frac{\epsilon}{\epsilon_0}\right)^{1/2} \quad . \quad . \quad . \quad . \quad . \quad . \quad (2.7)$$

* E. C. Stoner, Proc. Roy. Soc. In course of publication.

The integral forms for (2.1) and (2.2) become

$$N=\int_0^\infty \frac{\nu(\epsilon)\,d\epsilon}{\exp(\epsilon/kT-\eta)+1}, \quad . \quad . \quad . \quad (2.8)$$

$$E=\int_0^\infty \frac{\epsilon\,\nu(\epsilon)\,d\epsilon}{\exp(\epsilon/kT-\eta)+1}. \quad . \quad . \quad . \quad (2.9)$$

The significance of η may be noted.

Let $$\eta=\zeta/kT. \quad . \quad . \quad . \quad . \quad . \quad . \quad (2.10)$$

Then ζ is the value of ϵ at which half the states are occupied; ζ is the energy corresponding to what is usually referred to as the top of the Fermi distribution. For $T\to 0$, $\zeta\to\epsilon_0$. (This form of expression of the significance of η is, of course, appropriate only for the lower temperature range.)

Inserting the value (2.7) for $\nu(\epsilon)$, the expressions for N and E become

$$N=\frac{3}{2}N\,\epsilon_0^{-3/2}\int_0^\infty \frac{\epsilon^{1/2}\,d\epsilon}{\exp(\epsilon/kT-\eta)+1}, \quad . \quad (2.11)$$

$$E=\frac{3}{2}N\,\epsilon_0^{-3/2}\int_0^\infty \frac{\epsilon^{3/2}\,d\epsilon}{\exp(\epsilon/kT-\eta)+1}. \quad . \quad (2.12)$$

These expressions are simplified by a change of variables.

Let $$x=\epsilon/kT. \quad . \quad . \quad . \quad . \quad . \quad (2.13)$$

Then $$N=\frac{3}{2}N\left(\frac{kT}{\epsilon_0}\right)^{3/2}\int_0^\infty \frac{x^{1/2}\,dx}{e^{x-\eta}+1}, \quad . \quad . \quad (2.14)$$

$$E=\frac{3}{2}NkT\left(\frac{kT}{\epsilon_0}\right)^{3/2}\int_0^\infty \frac{x^{3/2}\,dx}{e^{x-\eta}+1}. \quad . \quad . \quad (2.15)$$

It is convenient to use the abbreviation

$$F_k(\eta)=\int_0^\infty \frac{x^k\,dx}{e^{x-\eta}+1}. \quad . \quad . \quad . \quad . \quad (2.16)$$

(It may be noticed that E may be expressed by

$$E=NkT\{F_{3/2}(\eta)/F_{1/2}(\eta)\}, \quad . \quad . \quad . \quad (2.17)$$

which is the form given by Nordheim.)

To obtain the specific heat an expression for E is required as a function of T, and involving the constants N and ϵ_0. (The value of ϵ_0, given by 2.6, depends on V, but the partial differentiation is carried out to obtain the

specific heat at constant volume, C_v.) The equation (2.14) provides an implicit equation for the determination of η.

$$F_{1/2}(\eta)=\frac{2}{3}\left(\frac{\epsilon_0}{kT}\right)^{3/2} \quad . \quad . \quad . \quad . \quad . \quad (2.18)$$

It is the value of η obtained from (2.18) which is to be used in (2.15) in obtaining a suitable expression for the energy.

Expressions for $F_k(\eta)$ may be obtained in the form of series for $\eta<0$ and $\eta>>1$, corresponding roughly to $\epsilon_0<kT$ and $\epsilon_0>>kT$—that is, to high and low temperatures.

$\eta<0$ ($\epsilon_0<kT$)

$$F_k(\eta)=\{\Gamma(k+1)\}\left(e^{\eta}-\frac{e^{2\eta}}{2^{k+1}}+\frac{e^{3\eta}}{3^{k+1}}-\ldots\right). \quad (2.19)$$

For $k=\frac{1}{2}$,

$$\Gamma(k+1)=\tfrac{1}{2}\sqrt{\pi}\,; \quad \text{for } k=\tfrac{3}{2}, \quad \Gamma(k+1)=\tfrac{3}{4}\sqrt{\pi}.$$

Let

$$c_n=1-\frac{1}{2^n}+\frac{1}{3^n}-\frac{1}{4^n}\ldots \quad . \quad . \quad (2.20)$$

For $|\eta|<<1$, $F_k(\eta)$ may be expressed as a power series in η, the first terms being given by

$$F_k(\eta)=\{\Gamma(k+1)\}\,(c_{k+1}+\eta c_k\ldots). \quad . \quad . \quad (2.21)$$

Results based on the use of this series have been applied as a check on interpolations in the immediate neighbourhood of $\eta=0$; but the range of values of η for $\eta>0$ for which it may be conveniently applied is very limited, and for $\eta<0$ the series (2.19) may be used. The following approximate values of c_n have been obtained :—

$$c_{1/2}=\cdot 605, \quad c_{3/2}=\cdot 763, \quad c_{5/2}=\cdot 866 \quad . \quad . \quad (2.22)$$

$\eta>>1$ ($\epsilon_0>>kT$)

$$F_k(\eta)=\frac{1}{k+1}\eta^{k+1}+2\{c_2 k\eta^{k-1}+c_4 k(k-1)(k-2)\eta^{k-3}+\ldots\}.$$
$$\ldots \quad (2.23)$$

Of the coefficients, $c_2=\pi^2/12$; c_4 and c_6 have been approximately evaluated :

$$c_2=\pi^2/12=\cdot 822, \quad c_4=\cdot 947, \quad c_6=\cdot 985. \quad . \quad (2.24)$$

The form (2.23) is that given by Nordheim. The integral is represented by an asymptotic series which, for non-integral values of k, diverges after a certain term. A more detailed investigation has been made by Gilham *, who gives the following expression :—

$$F_k(\eta)=\frac{\eta^{k+1}}{k+1}\left[1+2\left\{c_2\frac{(k+1)k}{\eta^2}+\ldots\right.\right.$$
$$\left.\left.+c_{2n}\frac{(k+1)k\ldots(k-2n+2)}{\eta^{2n}}\right\}\right]+I_{2n}, \quad (2.25)$$

where

$$I_{2n}<\frac{2(2n+2)c_{2n+2}}{\eta^{2n+1-k}}\,k(k-1)\ldots(k-2n)|. \quad (2.26)$$

This enables the maximum error made in using a definite number of terms in the series to be estimated. Further reference will be made to this point below ; it may be noted here, however, that no useful purpose is served by using more than a small number of terms for η either large or small.

3. *High Temperatures.*

The condition $\eta<0$ for (2.19) corresponds to an approach to the conditions in which classical statistics is applicable. Roughly the condition corresponds to $kT>\epsilon_0$ or to high temperatures. An appropriate expression for the energy under these conditions will be obtained.

From (2.14) and (2.19)

$$N=\frac{3}{2}N\left(\frac{kT}{\epsilon_0}\right)^{3/2}\frac{\sqrt{\pi}}{2}\left(e^{\eta}-\frac{e^{2\eta}}{2^{3/2}}+\frac{e^{3\eta}}{3^{3/2}}-\ldots\right). \quad (3.1)$$

Let
$$\frac{4}{3\sqrt{\pi}}\left(\frac{\epsilon_0}{kT}\right)^{3/2}=y=e^{\eta}-\frac{e^{2\eta}}{2^{3/2}}+\frac{e^{3\eta}}{3^{3/2}}\ldots \quad (3.2)$$

$$e^{\eta}=ay+by^2+cy^3. \quad (3.3)$$

By substituting this expression for e^{η} in (3.2), and equating coefficients of powers of y, the coefficients a, b, c may be found ; with the result

$$e^{\eta}=y+\frac{1}{2\sqrt{2}}y^2+\left(\frac{1}{4}-\frac{1}{3\sqrt{3}}\right)y^3. \quad (3.4)$$

* C. W. Gilham, Proc. Leeds Phil. Soc. In course of publication.

From (2.15) and (2.19)

$$\mathrm{E}=\frac{3}{2}\mathrm{N}k\mathrm{T}\left(\frac{k\mathrm{T}}{\epsilon_0}\right)^{3/2}\frac{3\sqrt{\pi}}{4}\left(e^{\eta}-\frac{e^{2\eta}}{2^{5/2}}+\frac{e^{3\eta}}{3^{5/2}}\cdots\right). \quad (3.5)$$

Substituting the expression (3.4) for e^{η}, and evaluating coefficients,

$$\mathrm{E}=\frac{3}{2}\mathrm{N}k\mathrm{T}(1+\cdot177y-3\cdot30\times10^{-3}y^2\ldots)$$

$$=\frac{3}{2}\mathrm{N}k\mathrm{T}\left\{1+\cdot133\left(\frac{\epsilon_0}{k\mathrm{T}}\right)^{3/2}-1\cdot86\times10^{-3}\left(\frac{\epsilon_0}{k\mathrm{T}}\right)^{3}\ldots\right\}$$

$$\ldots \quad (3.6)$$

Finally, differentiating

$$\mathrm{C}_v=\left(\frac{\partial\mathrm{E}}{\partial\mathrm{T}}\right)_v=\frac{3}{2}\mathrm{N}k\left[1-6\cdot65\times10^{-2}\left(\frac{\epsilon_0}{k\mathrm{T}}\right)^{3/2}\right.$$

$$\left.+3\cdot72\times10^{-3}\left(\frac{\epsilon_0}{k\mathrm{T}}\right)^{3}\ldots\right]. \quad (3.7)$$

The series (3.1) and (3.5) are convergent for $e^{\eta}<1$ or $\eta<0$. The value of $(k\mathrm{T}/\epsilon_0)$ for $\eta=0$ may be found by the use of (2.14) and (2.21).

For $\eta=0$

$$\left.\begin{aligned}\frac{4}{3\sqrt{\pi}}\left(\frac{\epsilon_0}{k\mathrm{T}}\right)^{3/2}&=c_{3/2}=\cdot763,\\ (k\mathrm{T}/\epsilon_0)&=\cdot991.\end{aligned}\right\}\ldots \quad (3.8)$$

The value of E for $\eta=0$ may be found from (2.17) and (2.21).

For $\eta=0$, $(k\mathrm{T}/\epsilon_0)=\cdot991$,

$$\left.\begin{aligned}\mathrm{E}&=\left(\mathrm{N}k\mathrm{T}\,\frac{3\sqrt{\pi}}{4}c_{5/2}\right)\Big/\left(\tfrac{1}{2}\sqrt{\pi}c_{3/2}\right),\\ &=1\cdot702\mathrm{N}k\mathrm{T},\\ \mathrm{E}/\mathrm{N}\epsilon_0&=1\cdot702(k\mathrm{T}/\epsilon_0)=1\cdot687.\end{aligned}\right\}\ldots \quad (3.9)$$

The series (3.6) and (3.7) are appropriate over a range given sufficiently closely by $(k\mathrm{T}/\epsilon_0)>1$. Two terms are adequate to determine E and C_v to within 1 per cent. over this higher range. Owing to the alternating character of the series useful limits are defined over a range of values of $k\mathrm{T}$ for which $k\mathrm{T}<\epsilon_0$. A check is provided by

the following expression for E, derived by the use of (2.21). This expression is appropriate only for $|\eta| << 1$. (The range $-1 < \eta < +1$ corresponds approximately to $2{\cdot}8 > (kT/\epsilon_0) > {\cdot}7$.)

$$E = NkT\{1{\cdot}513 + {\cdot}187(\epsilon_0/kT)^{3/2}\}. \quad . \quad . \quad (3.10)$$

A detailed discussion of the errors arising from the use of a limited number of terms in the series (3.6) and (3.7) for the larger values of (kT/ϵ_0) is hardly necessary for the derivation of the results of physical interest, as will be apparent from the numerical treatment of the results in section 5. It does, however, appear to be difficult to determine narrow limits for E and C_v with mathematical rigour in the range in which η is positive and not large. The process of smooth interpolation which is used below in dealing with this range is justified on physical grounds and by the consideration that the character of the basic integrals is not such as to suggest special peculiarities in the variation of E and C_v with T over any part of the range.

4. *Low Temperatures.*

Appropriate expressions for E and C_v will now be obtained for the range $\eta >> 1$, corresponding roughly to $\epsilon_0 >> kT$ or to low temperatures.

From (2.10)

$$N = \frac{3}{2}N\left(\frac{kT}{\epsilon_0}\right)^{3/2} F_{1\cdot 2}(\eta). \quad . \quad . \quad . \quad . \quad . \quad (4.1)$$

From (2.25)

$$F_{1\cdot 2}(\eta) = \frac{2}{3}\eta^{3/2}\left[1 + 2\sum_{n=1}^{n} c_{2n}\frac{(3/2)(1/2)\ldots(5/2-2n)}{\eta^{2n}}\right] + I_{2n}.$$

$$. \quad . \quad . \quad (4.2)$$

$$I_{2n} < \frac{2(2n+2)c_{2n+2}}{\eta^{2n+1/2}}\,|\,(1/2)(-1/2)\ldots(1/2-2n)\,| = L_{2n}.$$

$$. \quad . \quad . \quad (4.3)$$

The question now arises as to how many terms in the series (4.2) should be used. It is sufficient to restrict the discussion to the use of one, two, or three terms in

the summation, with remainders I_2, I_4, and I_6, whose moduli are respectively less than L_2, L_4, and L_6.

$$\frac{L_6}{L_4} \doteqdot \frac{33}{\eta^2}, \quad \frac{L_4}{L_2} \doteqdot \frac{105}{8\eta^2}. \quad . \quad . \quad . \quad . \quad . \quad (4.4)$$

Thus for $\eta < \sqrt{33} = 5{\cdot}75$ the maximum error is increased by the use of more than two terms; for $\eta < \sqrt{105/8} = 3{\cdot}6$ by the use of more than one term in the summation. These limitations must be borne in mind in connexion with the final series which will be obtained for E and C_v. It is hardly necessary to deal separately with different ranges of values for η. A three-term series will be used, and rough criteria (based on the more exact criteria above) will be sufficient to decide on how many terms should be utilized in the final series obtained.

From the series

$$F_{1/2}(\eta) = \frac{2}{3}\eta^{3/2}\left(1 + \frac{3c_2}{2}\eta^{-2} + \frac{9c_4}{8}\eta^{-4} + \frac{315c_6}{32}\eta^{-6} \ldots\right). \quad (4.5)$$

An inverse series is obtained as before, giving

$$\eta = \frac{\epsilon_0}{kT}\left\{1 + \alpha\left(\frac{\epsilon_0}{kT}\right)^{-2} + \beta\left(\frac{\epsilon_0}{kT}\right)^{-4} + \gamma\left(\frac{\epsilon_0}{kT}\right)^{-6}\right\}, \quad (4.6)$$

with

$$\alpha = -c_2, \qquad \beta = -\tfrac{3}{4}c_2^2 - \tfrac{3}{4}c_4,$$

$$\gamma = -\frac{5}{3}c_2^3 - \frac{9}{8}c_2c_4 - \frac{105}{16}c_6.$$

The expression (4.6) for η is now substituted in the series for E, namely, from (2.15) and (2.25):

$$E = \frac{3}{2}NkT\left(\frac{kT}{\epsilon_0}\right)^{3/2}\left[\frac{2}{5}\eta^{5/2}\left\{1 + 2\left(\frac{15}{4}c_2\eta^{-2} - \frac{15}{16}c_4\eta^{-4} - \frac{225}{64}c_6\eta^{-6}\right)\right\}\right]. \quad (4.7)$$

For this series

$$\left.\begin{aligned} L_6 < L_4 \quad &\text{for} \quad \eta > 4{\cdot}5, \\ L_4 < L_2 \quad &\text{for} \quad \eta > 2{\cdot}3. \end{aligned}\right\} \quad . \quad . \quad . \quad (4.8)$$

The limitations on the number of terms to be taken

are not so stringent for the $F_{3/2}$ as for the $F_{1/2}$ series. Making the substitution (4.6) :

$$E=\frac{3}{5}N\epsilon_0\left[1+a\left(\frac{kT}{\epsilon_0}\right)^2+b\left(\frac{kT}{\epsilon_0}\right)^4+c\left(\frac{kT}{\epsilon_0}\right)^6\right], \qquad (4.9)$$

with $$a=5c_2=\frac{5\pi^2}{12}, \qquad b=-\frac{15}{4}c_2{}^2-\frac{15}{4}c_4,$$

$$c=-\frac{65}{12}c_2{}^3-\frac{45}{8}c_2c_4-\frac{375}{16}c_6.$$

Inserting numerical values from (2.24)

$$E=\frac{3}{5}N\epsilon_0\left[1+4{\cdot}11_1\left(\frac{kT}{\epsilon_0}\right)^2-6{\cdot}08_6\left(\frac{kT}{\epsilon_0}\right)^4-30{\cdot}7_0\left(\frac{kT}{\epsilon_0}\right)^6\right]. \qquad (4.10)$$

As a rough criterion based on (4.8) the best approximation is obtained by taking the series as far as the T^6 term for $\eta>4{\cdot}5$, and as far as the T^4 term for $4{\cdot}5>\eta>2{\cdot}3$. For $\eta<2{\cdot}3$ it is not possible to obtain a good approximation by means of the series. The intermediate range corresponds approximately from (4.1) and (4.5) to $\cdot21<(kT/\epsilon_0)<\cdot38$.

By differentiating (4.10) with respect to T a series expression is obtained for the specific heat at low temperature, with limitations similar to those just discussed.

$$C_v=\left(\frac{\partial E}{\partial T}\right)_v=Nk\left[4{\cdot}93_3\left(\frac{kT}{\epsilon_0}\right)-14{\cdot}6_0\left(\frac{kT}{\epsilon_0}\right)^3-110\left(\frac{kT}{\epsilon_0}\right)^5\right]. \qquad (4.11)$$

The formula is inappropriate for $kT/\epsilon_0>\cdot38$; in the range $\cdot21<(kT/\epsilon_0)<\cdot38$ the best approximation is obtained with the first two terms, below that range with the three terms.

5. *Free Electron Energy and Specific Heat : Collected Formulæ and Numerical Results.*

In order that the magnitudes involved may be more immediately appreciated the expressions obtained will be transformed so as to give the energy and specific heat in convenient units—calories and calories per degree, per gram atom. Further, the maximum zero point

electron energy, ϵ_0, will be expressed as V_0 electron volts (one electron volt $= 1{\cdot}591 \times 10^{-12}$ erg).

Let q = number of free electrons per atom,

n_v = number of atoms per unit volume.

From (2.6)

$$V_0 = 3{\cdot}618 \times 10^{-15}(qn_v)^{2/3}.$$

For strictly free electrons V_0 would range from about 1·5 to 7 volts for different metals. The results will also be directly applicable to electrons in unfilled energy bands in a metal, even when they are not free in the narrower sense, provided that the number of quantum states per unit energy range varies as the square root of the energy, as for free electrons (see eq. (2.5)). The energy width of the occupied portion of a band in the completely degenerate state, represented by V_0, may be considerably less than for the same number of free electrons. The results give an immediate indication of the dependence of specific heat, and its temperature variation, on band width, under these conditions. For the alkali metals, and copper, silver, and gold, the free electron type of energy distribution of states is closely approached. For metals generally there may be wide divergences, and in dealing with the general case the expression of the results in terms of V_0 (or ϵ_0) is not convenient.

Let E = energy of free electrons per gram atom in calories.

C_v = electronic specific heat per gram atom in calories per degree.

R = gas constant. (1·986 cal. deg.$^{-1}$ mole^{-1}).

The formulæ obtained for E and C_v at high ((3.6) and (3.7)) and low temperatures ((4.10) and (4.11)) may be readily transformed by making use of the appropriate conversion factors :

$$(T/V_0) = 1{\cdot}160 \times 10^4\,(kT/\epsilon_0).$$

The transformed formulæ are given below :

(*a*) $(kT/\epsilon_0) > 1 \quad (T/V_0) > 1{\cdot}160 \times 10^4$;

$$\frac{E}{RqV_0} = \left(\frac{T}{V_0}\right)\left[1{\cdot}500 + 2{\cdot}49_3 \times 10^5\left(\frac{V_0}{T}\right)^{3/2} - 4{\cdot}35_6 \times 10^9\left(\frac{V_0}{T}\right)^3\right], \quad \ldots \quad (5.1)$$

$$\frac{C_v}{Rq} = 1{\cdot}500 - 1{\cdot}24_6 \times 10^5 \left(\frac{V_0}{T}\right)^{3{\cdot}2} + 8{\cdot}71_2 \times 10^9 \left(\frac{V_0}{T}\right)^3 . \quad . \quad . \quad (5.2)$$

(*b*) $\quad kT/\epsilon_0 \ll 1 \qquad T/V_0 \ll 1{\cdot}160 \times 10^4 ;$

$$\left(\frac{E}{RqV_0}\right) \times 10^{-4} = {\cdot}696_0 + 2{\cdot}12_6 \times 10^{-8} \left(\frac{T}{V_0}\right)^2 - 2{\cdot}33_8 \times 10^{-16} \left(\frac{T}{V_0}\right)^4 - 8{\cdot}76_6 \times 10^{-24} \left(\frac{T}{V_0}\right)^6 , \quad . \quad . \quad . \quad (5.3)$$

$$\frac{C_v}{Rq} = 4{\cdot}25_2 \times 10^{-4} \left(\frac{T}{V_0}\right) - 9{\cdot}35_2 \times 10^{-12} \left(\frac{T}{V_0}\right)^3 - 5{\cdot}25_9 \times 10^{-19} \left(\frac{T}{V_0}\right)^5 . \quad . \quad . \quad . \quad (5.4)$$

These series (*b*) are suitable for $kT/\epsilon_0 < {\cdot}2$, corresponding to $(T/V_0) \times 10^{-4} < {\cdot}23$. In the range ${\cdot}2 < kT/\epsilon_0 < {\cdot}38$ corresponding to ${\cdot}23 < (T/V_0) \times 10^{-4} < {\cdot}44$, a better approximation is obtained by dropping the last term given above. For $(T/V_0) \times 10^{-4} > {\cdot}44$ this series representation is unsatisfactory.

The variation of E and of C_v with T, as given by the use of different numbers of terms in the above series representations, is shown graphically in figs. 1 and 2.

The expressions used for the high temperature range are rigorously justifiable for $kT/\epsilon_0 > 1$ ($T/V_0 \times 10^{-4} > 1{\cdot}160$). It has been shown that the low temperature expressions give a very close approximation for $kT/\epsilon_0 < {\cdot}2$ ($T/V_0 \times 10^{-4} < {\cdot}23$), and that a good approximation is obtained for $kT/\epsilon_0 < {\cdot}38$ or $T/V_0 \times 10^{-4} < {\cdot}44$ by dropping the last term. The numerical results show that in the range ${\cdot}3 < T/V_0 \times 10^{-4} < {\cdot}5$ the values for E given by the high temperature expression (5.1) agree to within 1 per cent with those given by the low temperature expression (5.3) without the last term. There is thus a satisfactory practical justification for the use of the high temperature expression (5.1) for interpolation over the range from $(T/V_0) \times 10^{-4} = {\cdot}3$ up to $(T/V_0) \times 10^{-4} = 1{\cdot}16$. Since the C_v curve gives the derivative of the E curve, the corresponding interpolation for C_v is readily carried out. An examination of the curves, or of the numerical results on which they are based, indicates that E and C_v

may be determined with the expressions used with an uncertainty of less than 1 per cent. over the whole temperature range.

Finally a table of numerical results is given. For $(T/V_0)\times 10^{-4} \leqq \cdot 3$ the values are found from (5.3) and (5.4); for $(T/V_0)\times 10^{-4} \geqq \cdot 5$ from (5.1) and (5.2). For $(T/V_0)\times 10^{-4} = \cdot 4$ the high and low temperature expressions

Fig. 1.

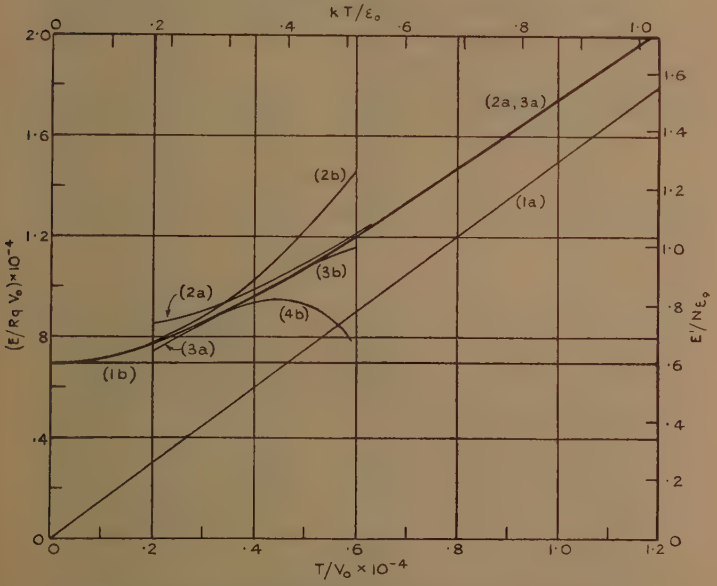

Variation with temperature of quasi-free electron energy.

E = electronic energy per gram atom.
q = number of quasi-free electrons per atom.
V_0 = maximum electron energy in completely degenerate state in electron volts.
1 *a*, 2 *a*, and 3 *a* are obtained with 1, 2, and 3 terms of the high temperature expression (5.1); 1 *b*, 2 *b*, 3 *b*, 4 *b* with 1, 2, 3, and 4 terms of the low temperature expression (5.3). The values of (kT/ϵ_0) are shown on the upper scale; the right-hand scale gives $(E'/N\epsilon_0)$, where E′ is the energy of N electrons.

give values agreeing to within 1 per cent. for E; a slight interpolation is necessary for C_v (see figs. 1 and 2). In the table are also given values of (kT/ϵ_0), the relation being

$(kT/\epsilon_0) = \cdot 862_1 (T/V_0) \times 10^{-4}$; and of $(E'/N\epsilon_0)$, the relation being $(E'/N\epsilon_0) = \cdot 862_1 (E/RqV_0) \times 10^{-4}$.

Fig. 2.

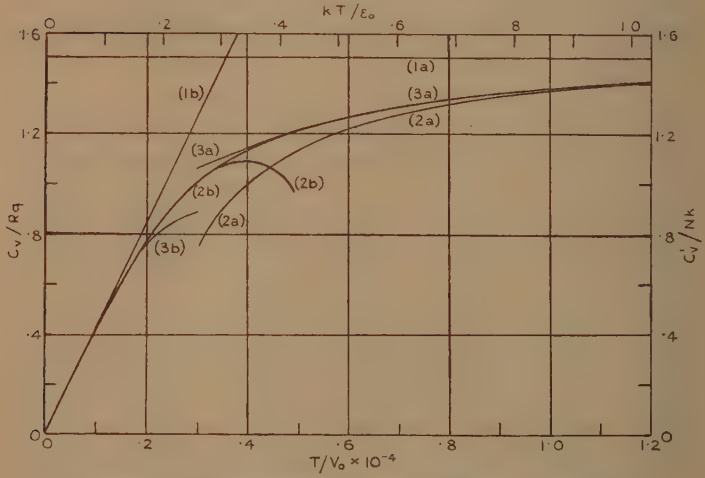

Variation with temperature of quasi-free electron specific heat.

C_v—specific heat in calories per degree per gram atom. See legend of fig 1 for other symbols.

1 *a*, 2 *a*, and 3 *a* are obtained with 1, 2, and 2 terms of the high temperature expression (5.2); 1 *b*, 2 *b*, and 3 *b* with 1, 2, and 3 terms of the low temperature expression (5.4).

Summary.

Previous results for free electrons show that at the low temperature limit the specific heat is proportional to the temperature, at the high temperature limit constant. Results are obtained in this paper for the variation of the energy, E, and the specific heat, C_v, over the whole temperature range.

Further terms are obtained in the series valid for $kT/\epsilon_1 > 1$ and $kT/\epsilon_0 << 1$, where ϵ_0 is the maximum electron energy in the completely degenerate state ; and estimates are made of the range of values of kT/ϵ_0 for which a limited number of terms in these series may be used to give good approximations. The following expressions are obtained for C_v.:—

$kT/\epsilon_0 > 1$:

$$C_v = \frac{3}{2}Nk\left[1 - 6{\cdot}65\times10^{-2}\left(\frac{\epsilon_0}{kT}\right)^{3/2} + 3{\cdot}72\times10^{-3}\left(\frac{\epsilon_0}{kT}\right)^{3}\right];$$

$kT/\epsilon_0 << 1$:

$$C_v = Nk\left[4{\cdot}93\left(\frac{kT}{\epsilon_0}\right) - 14{\cdot}6\left(\frac{kT}{\epsilon_0}\right)^{3}\right].$$

Numerical Values for the Variation of the Quasi-free Electron Energy and Specific Heat with Temperature.

$\left(\frac{T}{V_0}\right)\times10^{-4}$.	$\left(\frac{E}{RqV_0}\right)\times10^{-4}$.	$\frac{C_v}{Rq} = \frac{C_v'}{Nk}$	$\frac{kT}{\epsilon_0}$.	$\frac{E'}{N\epsilon_0}$.
0·0	·696	0·00	0·00	·600
·1	·717	·415		
·2	·777	·775	·172	·67
·3	·865	1·02		
·4	·97$_0$	1·13	·345	·84
·5	1·08$_5$	1·21		
·6	1·21$_0$	1·27	·517	1·04
·7	1·339	1·31		
·8	1·472	1·34$_3$	·690	1·26
·9	1·607	1·36$_6$		
1·0	1·745	1·38$_4$	·862	1·50
1·1	1·884	1·39$_8$		
1·2	2·025	1·41$_0$	1·034	1·74
1·3	2·166	1·42$_0$		
1·4	2·308	1·42$_8$	1·207	1·99
1·5	2·451	1·43$_5$		
Limit.	$1{\cdot}5\left(\frac{T}{V_0}\right)\times10^{-4}$	1·500	—	$1{\cdot}5\left(\frac{kT}{\epsilon_0}\right)$

E = electronic energy per gram atom.
C_v = electronic specific heat per gram atom.
q = number of quasi-free electrons per atom.
V_0 = maximum electron energy (or width of occupied portion of electronic energy band) in completely degenerate state in electron volts, corresponding to ϵ_0.
E′, C_v' = energy and specific heat for N electrons.
R, k = gas constants per mole and per molecule.

To obtain an accuracy within 1 per cent. the first of these expressions may be used in practice for $kT/\epsilon_0 > {\cdot}5$; the second for $kT/\epsilon_0 < {\cdot}3$. A slight interpolation enables the whole range to be covered.

The temperature variation of E and C_v is shown in diagrams and a table of numerical results is given. The conditions under which the results may be applied to electrons in metals are indicated.

I am indebted to Mr. C. W. Gilham for much helpful discussion and for allowing me to make use of some unpublished work.

Physics Department,
University of Leeds.
October 1935.

VIII. *Optical Relativity as tested by Rotational Quality.* *By Sir* Joseph Larmor, *F.R.S.**

THE sensitiveness of phase in rotational polarization early commended itself to Lord Rayleigh, and, following him, to D. B. Brace, in succession to less delicate experiments by Mascart, as a means of testing whether the direction of a ray relative to the earth's velocity v round the sun had influence on its velocity of travel. The experimental result came out as negligible up to *and including* the second order of v/c. In H. A. Lorentz's second memoir (1895) † on electron theory he had explored this question, which there belonged to his main subject of moving media, yet seemed to rest content with an answer that gave an effect of the first order of v/c, that is even of the same order as the astronomical aberration of light. In my book 'Æther and Matter' (1900)

* Communicated by the Author.

† The writer has recently noticed in a very successful popular exposition of these matters the date 1895 assigned to Prof. Lorentz's exact spatial transformation. It may be well to record for clearness, and for the sake of historical accuracy, that the transformation as holding up to the first order, which explains the astronomical aberration of light, that being of course a result quite on a grand scale, dates from 1892, when the idea of personal or local time was introduced, while the transformation holding up to the second order, which succeeds in explaining the various observed optical and electric relativities up to that order, was first given in 1900 in the book 'Æther and Matter' above referred to. The remark that this spatial transformation is exact came from Lorentz in 1905 by an independent investigation, including its statement in exact form for the electrodynamic fields of free space; also nearly simultaneously in reverse form from Einstein. But in optical applications, for instance within the electronic model of an atom, the size of the electrons must be relatively so great as to restrict the validity of the transformation to the quite adequate second order as already in 1900 worked out and applied.

the subject was taken up and examined (ch. xiii. pp. 211–220), doubtless, however, in too condensed a manner, for Lorentz seems later to have concluded that it claimed to assert error in his investigation; whereas (p. 215) it was my own different argument that led to a different result, one upholding relativity as against his apparent implicit denial of it under circumstances of rotational waves. I gave way at the time to Lorentz's great authority (I think in the Phil. Mag.) without any close scrutiny. But now that I have more leisure it has been proper, even urgent, to return to the question; and I have not been able to discover any flaw in my main analysis (pp. 212–214), which is of ordinary classical type. The discrepancy is therefore presumably an affair of mode of formulation of the theory or of the interpretation of the results. My result was formulated as for an observer and his apparatus at rest in the æther, as one was permitted to imagine in those early days*: it was that the convective effect of a structural rotational modulus (a, b, c giving component rotation along the ray as determined in footnote, p. 206) is simply (p. 214) to alter the dielectric modulus K (or optical index squared) by a factor $1-v/\mathrm{KV}'$, where V′ is the mean velocity of the ray relative to the transmitting medium, namely by Fresnel's formula $\mathrm{V}_0-v/\mathrm{K}$ where V_0 is its velocity without the convection—different be it noted from the Doppler effect, unless K is unity. Into this result the direction of v relative to the rotational quality does not enter; it is its magnitude alone that may affect phenomena —that is, relativity is proved to subsist (in this rather unusual crystalline manner) up to and including the second order of v/C.

(In the experiment one of the interfering optical paths traverses the crystal, the other is outside it; the principle is that the null effect of the translatory motion of the whole rigid system, regarded as free of the inscrutable rotational quality, would not be affected by turning it into a new orientation; there remains to include the much smaller effect of rotational quality, with its far more delicate mode of test. A positive result would fix the direction and amount of the earth's absolute motion, just as in the Michelson experiments.)

* Now each observer is related to his own personal æther with respect to which he is at rest.

The memoir of Lorentz is not here accessible; but I find that in my original investigation ('Æther and Matter,' p. 214) I appended this reconciliation with it which appears to be quite satisfactory—namely, that my result, which was amenable to first-order relativity, was made up of rotational change of velocity of the ray relative to the medium as given by Lorentz's formula and the part of the velocity of the medium that is transferable to the ray by Fresnel's convection formula, here applicable without modification, neither of these separately being relativist.

In like manner as regards magneto-optic rotation also (p. 217) the effect of convection of the medium proves to be obtained simply by substituting, in the formula for propagation in the body at rest, for the velocity of light in resting æther its velocity in the convected transmitting medium following Fresnel's formula; and here also relativity is satisfied.

But in the investigation the phrase "fixed in the æther" requires elucidation or, perhaps, enlargement. The fixture concerned is relative to the frame of the observer and his instruments, which constitute for each observer his own personal æther as ensured to him by relativity—a procedure now verified by abundant successful applications. This is, however, really the assumption of relativity in advance, and the argument now takes the converse but not decisive form that no result is to be discoverable from its use that is at variance with observation. Thus, as above noted, when a medium, whether rotational or not, is convected with velocity v, the observer can determine the magnitude of v if he can measure its effect on a train of waves, but cannot determine its direction, for in his apparatus he has no fixtures for direction, as he has own observing system for the datum mark of translatory velocity. And this result appears to hold for crystalline quality, however complex.

A fundamental remark is here relevant about relativity in general. In the early modes of Maxwell and Rayleigh the procedure was to frame a physical theory rational on the merits of the subject, and then to ascertain whether it conformed to the principle. This is illustrated by the present discussion of optical rotations. On the other hand Lorentz, who sat lightly to relativity, did not

pursue that principle at all in his early work on the subject that we have been discussing. Another interpretation of relativity may conceivably explain such lack of interest; this other procedure, also often useful, builds up no particular dynamical theory of the phenomena concerned, but starts from algebraic generalities, and makes the principle into a practical test for restricting this wide "formalism" into more definite shape. A relativity of this kind is thus made, sometimes even explicitly, the foundation of abstract physics; and the tendency to replace dynamical analogy by purely algebraic "parallelism" naturally expands. Such formalism must be used cautiously as a parallel to nature; for it can readily be extended into a world-scheme more general than the actual province of nature under review; for example, in the treatment of the differential equation of the recent wave mechanics of n particles with its $3n$ auxiliary spatial dimensions. Long ago Newcomb found relaxation from his astronomical calculations by proving that a closed hollow rubber ball may be turned inside out without tearing if a fourth dimension of space is provided for the operation; in the very significant Minkowskian relativist scheme a fourth dimension (*i. e.*, a formalism) is actually provided which only differs from the other three by having an imaginary modulus. Thus a question arises as to whether Newcomb's theorem is limited to real dimensions or whether, if some experimenter happens to claim success in finding a way of performing the feat, he ought to be assured that it is provided for by relativity. This example illustrates the limitations of a "formalism"; for security it would have to be closely explored in detail, as it may provide within its algebraic frame a world far too wide for our range of parallelism with actuality, while too limited to include its intimate extensions, a difficulty actually not unknown. And just here comes in the mathematical contrast between the correlation of fact, which is between a pair of discrete observational frames, and the Minkowskian expansion into a continuous algebra of frames, involving a fourfold continuum, yet with the distinguishing feature of the frames, namely their convection which represents our world of motion, entirely concealed.

Holywood, N. Ireland.
Sept. 18, 1935.

IX. *Photographic Measurements of the Magnetic Rotatory Dispersion of Water.* *By* I. T. Pierce, *M.Sc.*, *and* R. W. Roberts, *D.Sc.**

Introduction.

MEASUREMENTS on the magnetic rotatory dispersion of water in the violet and ultra-violet regions of the spectrum have been made by a number of investigators using photographic methods, and recently by Bruhat and Guinier †, who employed a new photo-electric method.

The precision attained by Bruhat and Guinier is effectively one part in a thousand for wave-lengths ·5893 μ to ·2483 μ, which, as they show, greatly exceeds the precision of the photographic determinations. The high precision of the photo-electric method has been achieved on the optical side, by using a beam of rather large extent which was rendered monochromatic by means of a double monochromator. Such conditions, however, cannot always be obtained in magneto-optical work. For example, in investigations concerning the rotation of absorbing substances and of crystals, one is obliged to employ beams of rather small extent and of such narrow spectral width that it would be difficult to isolate them by means of a double monochromator. Under these circumstances, where the light flux is relatively weak, it is advantageous to use photographic methods.

As the photographic measurements, even in the less exacting case of water, are rather divergent ‡ it seemed to us worth while to enquire whether more precise results could be obtained by photographic means. We have therefore taken up anew such measurements on water for eleven lines in the mercury spectrum from ·5780 μ to ·2483 μ.

Apparatus and Method.

Of the photographic methods which have been proposed for the determination of optical rotations in the ultra-violet, that of crossed nicols seems most likely to be free

* Communicated by Prof. L. R. Wilberforce, M.A.

† G. Bruhat and A. Guinier, *Journ. de Phys.* iv. p. 691 (1933).

‡ *Vide* figs. 1–4 and Table V.

from systematic error. This method has been investigated in detail by Bruhat and Pauthenier *, but, so far as we know, no results obtained by this method over a wide range of wave-lengths have as yet been published. We have on a previous occasion † used this method to determine the magnetic rotation of water and of a number of solutions for wave-lengths $\cdot 5780\,\mu$ to $\cdot 3130\,\mu$. The accuracy of the results then obtained was sufficient to encourage us to extend the method to shorter wave-lengths.

In the present measurements it was possible to obtain much larger rotations than those given previously, as owing to the transparency of water a much larger path in the field could be employed. A preliminary investigation showed that with the largest current (16 amps.) which we could safely pass through the electromagnet, the rotation obtained with a cell occupying as much as possible of the gap between the pole pieces increased with increasing length of the gap. We have used a cell 9 cm. in length.

The cell was made of brass, the inside and end faces of which were gold-plated to prevent chemical action. As a further precaution against possible contamination in the metallic cell the water was changed each day. Silica end-plates of thickness 1·5 mm. were held on to the end faces by means of screws, and a thin layer of paraffin wax served to make the cell watertight. Under these conditions the plates were reasonably free from strain. The cell was so constructed that its end faces were inclined at a small angle to each other in order to prevent multiply reflected light from reaching the spectrograph. Borings were constructed in the cell so that its temperature could be controlled by circulating a stream of water from a thermostatically regulated reservoir. The temperature of the water under investigation in the cell was measured by means of a thermo-couple in a potentiometer circuit. This temperature varied slightly with the room-temperature and that of the magnet, but was always $22 \pm 0{\cdot}3^\circ$ C. The cell was mounted geometrically, and was adjusted so that the end-plate facing the analyzer was perpendicular to the axis of rotation of the analyzer circle.

* G. Bruhat and M. Pauthenier, *Rev. d'Opt.* vi. p. 163 (1927).

† R. W. Roberts, L. A. Wallace, and I. T. Pierce, Phil. Mag. xvii. p. 934 (1934).

The optical system was the same as before, except that the lens L_1 * and the stop S_4^1 were removed and the mercury-vapour lamp was placed immediately behind S_2 (except for series IV., as explained later). Previously we used a different slit-width of the spectrograph for each spectral line examined, but in the present work we have kept the same slit-width for all the lines. The effective wave-lengths of the chosen lines were then deduced with the aid of Lowry's tables † from observations on the natural rotation of a quartz end plate of thickness 1·92 mm.

For the lines ·5780 μ and ·5461 μ, Ilford Hypersensitive Panchromatic plates were used. We preferred to obtain the rotations by photography rather than by visual observation, as this procedure required no modification of our apparatus, and consequently the same beam has been used for all the wave-lengths.

For the remaining wave-lengths we used Ilford Golden Isozenith plates. An attempt was made to increase the sensitiveness of these plates in the further ultra-violet by oiling them, but for the region of the spectrum in which we were interested we found that this process actually gave decreased sensitiveness. Exposures of one minute were given for all wave-lengths except for the lines ·2536 μ and ·2483 μ, for which exposures of two minutes were necessary.

All plates which gave unsymmetrical microphotometer curves were discarded. Plates giving irregular or unsymmetrical curves were obtained most often on the lines of shorter wave-length.

The Observations.

Four series of observations, denoted by I., II., III., and IV., were taken under different conditions. In series I., II., and IV. the diameter of the polarizer diaphragm S_3 was 6·27 mm., and for series III. it was 4·14 mm. After series I. had been taken one of the end-plates was removed and replaced by one showing less double refraction. In series IV. the light from the mercury-vapour lamp was sent through a monochromator before entering the system, the exit hole of the mono-

* The notation is the same as that of fig. 1 in our previous paper.

† T. M. Lowry and W. R. C. Coode-Adams, Phil. Trans, A, ccxxvi. p. 391 (1927).

chromator being at S_2. For both III. and IV. the pole pieces of the electromagnet were brought nearer to the end plates of the cell, so that larger rotations were obtained.

The plates were examined on a non-recording microphotometer of the Moll pattern, constructed in the labo-

TABLE I.

Observed Rotations.

	I.		II.		III.		IV.	
λ in Å.	*a.*	*b.*	*a.*	*b.*	*a.*	*b.*	*a.*	*b.*
5780	16·708		16·696		18·146		18·125	
	0·690	16·018	0·719	15·977	0·735	17·411	0·720	17·405
5461	18·884		18·851		20·518		20·499	
	0·787	18·097	0·803	18·048	0·829	19·689	0·804	19·695
4357	31·010		30·977		33·734		33·697	
	1·348	29·662	1·326	29·651	1·389	32·345	1·328	32·369
4046·5	36·766		36·752		39·936		39·972	
	1·565	35·201	1·580	35·172	1·632	38·304	1·582	38·390
3652	46·850		46·805		50·864		50·907	
	1.969	44·881	1·995	44·810	2·052	48·812	1·998	48·909
3341·5	58·170		58·142		63·356		63·240	
	2·475	55·695	2·439	55·703	2·535	60·821	2·443	60·797
3132	68·597		68·516		74·528		74·608	
	2·881	65·716	2·836	65·680	2·943	71·585	2·848	71·760
2803·5	92·302		92·147		100·251		100·546	
	3·818	88·48	3·806	88·34	3·895	96·36	3·813	96·73
2653	108·005		107·849		117·373		117·27	
	4·392	103·61	4·355	103·49	4·452	112·92	4·36	112·91
2536	123·562		123·533		134·517		134·76	
	4·921	118·64	4·911	118·62	4·981	129·54	4·94	129·82
2483	132·015		132·138		—		—	
	5·241	126·77	5·168	126·97	—	—	—	—

a. Rotation of cell containing water; rotation of end-plates.
b. Deduced rotation of water.

ratory and specially designed to facilitate the examination of our plates.

The observed rotations of the cell and its end-plates and the deduced rotations of the water are given in Table I. Only two observations are given for the wavelength ·2483 μ, owing to the difficulty of obtaining good plates for this line.

Table II. gives the ratio of the rotations for the different wave-lengths to that for the wave-length ·4357 μ for each of the four series. The mean value of the ratio for each wave-length is recorded in the last column.

Except for the wave-length ·5780 μ the deviations from the mean are in general less than two in a thousand. A variation of this amount can be accounted for by lack of precision of our current control. As might be expected, however, our calculations indicate that the errors in the mean values are distinctly less than this.

TABLE II.

λ in Å.	I.	II.	III.	IV.	Mean.
5780	0·5400	0·5388	0·5371	0·5377	0·5384
5461	0·6101	0·6087	0·6087	0·6085	0·6090
4357	1·0000	1·0000	1·0000	1·0000	1·0000
4046·5	1·1867	1·1862	1·1842	1·1860	1·1858
3652	1·5131	1·5112	1·5091	1·5110	1·5111
3341·5	1·8777	1·8786	1·8804	1·8783	1·8787
3132	2·2155	2·2151	2·2132	2·2169	2·2152
2803·5	2·9831	2·9794	2·9790	2·9884	2·9825
2653	3·4931	3·4904	3·4911	3·4882	3·4907
2536	3·9998	4·0006	4·0048	4·0106	4·0040
2483	4·2739	4·2821	—	—	4·2780

The Dispersion Formula.

According to theory the magnetic rotation δ of a diamagnetic substance can be represented by means of the formula

$$\delta = \frac{1}{n} \Sigma_r \frac{A_r' \lambda^2}{(\lambda^2 - \lambda_r^2)^2},$$

where n is the refractive index, and the A_r''s and λ_r's are constants. Bruhat and Guinier have shown that a single term in the summation is insufficient to represent their results. The next simplest formula may be written

$$\delta = \frac{1}{n}\left[\frac{A'}{\lambda^2} + \frac{B'\lambda^2}{(\lambda^2 - \lambda_0^2)^2}\right],$$

where A′ and B′ are constants. If, for convenience, we

denote after Bruhat and Guinier, the ratio δ/δ_{4357} by m, we have

$$m=\frac{1}{n}\left[\frac{A}{\lambda^2}+\frac{B\lambda^2}{(\lambda^2-\lambda_0^2)^2}\right]. \quad . \quad . \quad . \quad . \quad . \quad (1)$$

It is usual when attempting to find the constants of a formula of the above type to take three observations of m, and with these to write down three equations which give, on elimination of A and B, an equation for λ_0. It appears to us that it is better to use all the observations to determine λ_0. This can be done without much calculation and with some control, as follows :—

Writing $1/\lambda^2=\zeta$, $\lambda_0^2=C$, and $mn\lambda^2=M$, equation (1) becomes

$$M=A+\frac{B}{(1-C\zeta)^2},$$

whence

$$\frac{dM}{d\zeta}=\frac{2BC}{(1-C\zeta)^3},$$

or

$$\left(\frac{d\zeta}{dM}\right)^{1/3}=\frac{1}{(2BC)^{1/3}}-\frac{C}{(2BC)^{1/3}}\zeta; \quad . \quad . \quad . \quad (2)$$

so that, if equation (1) is true, $\left(\frac{d\zeta}{dM}\right)^{1/3}$ when plotted against ζ should give a straight line.

As the curvature of a (M, ζ) graph is very weak, we can for any two consecutive observations, say (M_1, ζ_1) and (M_2, ζ_2), take $d\zeta/dM$ for the mean point $\zeta=(\zeta_1+\zeta_2)/2$ to be $(\zeta_2-\zeta_1)/(M_2-M_1)$. Thus, denoting the difference operation by Δ, equation (2) can be replaced by

$$\left(\frac{\Delta\zeta}{\Delta M}\right)^{1/3}=\frac{1}{(2BC)^{1/3}}-\frac{C}{(2BC)^{1/3}}\bar{\zeta}.$$

Fig. 5 shows the calculated values of $(\Delta\zeta/\Delta M)^{1/3}$ plotted against ζ. As they lie very nearly on a straight line it shows that our results can be represented by equation (1). To avoid prejudice in drawing the best line to fit the observations we have deduced the equation of the straight line to Cauchy's method. From the constants of this line B and $\lambda_0(=C^{1/2})$ can be determined.

The values of A for each observation can now be found from equation (1). These values should be constant, and

for the purpose of calculation we have used the mean value of A. We find in this way

$$mn\lambda^2 = \cdot 06979 + \frac{\cdot 15291}{[1-(\cdot 1311/\lambda)^2]^2} \quad . \quad . \quad . \quad (3)$$

The values of m calculated by means of this formula are given in Table III., column (ii.). The ratio $10^3\ (m_{\text{obs.}} - m_{\text{calc.}})/m_{\text{obs.}}$ given in column (iii.) show that in only one case does this exceed one part in a thousand, so that the dispersion of our mean values can be represented by formula (3) almost to this accuracy.

TABLE III.

λ in Å.	(i.) $m_{\text{obs.}}$	(ii.) $m_{\text{calc.}}$	(iii.) $10^3 \frac{m_{\text{obs.}} - m_{\text{calc.}}}{m_{\text{obs.}}}$	(iv.) $10^3 \frac{m_{\text{obs.}} - m'_{\text{calc.}}}{m_{\text{obs.}}}$	(v.) Verdet constants (min. per cm. gauss).
5893	—	—	—	—	·01308
5780	·5384	·5380	+0·8	+0·2	·01364
5461	·6090	·6079	+1·8	+1·3	·01543
4357	1·0000	1·0006	−0·6	−1·3	·02534
4046·5	1·1858	1·1852	+0·5	−0·3	·03004
3652	1·5111	1·5096	+1·0	+0·3	·03828
3341·5	1·8787	1·8779	+0·4	−0·2	·04760
3132	2·2152	2·2142	+0·5	0	·05612
2803·5	2·9825	2·9853	−0·9	−1·7	·07557
2653	3·4907	3·4941	−1·0	−1·5	·08844
2536	4·0040	4·0070	−0·7·5	+0·6	·10145
2483	4·2780	4·2790	−0·2	+1·5	·10839

We have not been able to observe the rotation for the Na line ·5893 μ, as we were not able to construct a sufficiently steady sodium source. We have therefore calculated from formula (3) the m value for the wave-length ·5893 μ, which we find to be ·5162. Taking the Verdet constant of water at 22° C. to be ·01308 minutes per cm.-gauss (calculated from Rodger and Watson's formula *), the equation for the Verdet constants ρ becomes

$$\rho n\lambda^2 = \cdot 001768 + \frac{\cdot 0038723}{[1-(\cdot 1311/\lambda)^2]^2} \quad . \quad . \quad . \quad (4)$$

* Rodger and Watson, Phil. Trans. A, clxxxvi. p. 621 (1895).

The Verdet constants calculated from the observed m values are given in column (v.) of Table III.

Ingersoll * has measured the Verdet constants of water for a number of wave-lengths in the near infra-red, which we record in Table IV. We give in the last column of this table the values of the Verdet constants for these wave-lengths calculated from equation (4). The agreement is satisfactory in view of the accuracy stated by Ingersoll for his measurements in this difficult region.

TABLE IV.

λ in μ.	Ingersoll.	Calculated.
0·6	·0126	·01259
0·8	·0070	·00689
1·0	·0044	·00436
1·25	·0029	·00277

Comparison of Results.

Bruhat and Guinier †, and later Bruhat ‡, have compared the m values of previous investigators §. In order to complete the review of the subject we give the constants of the dispersion formulæ representing the earlier results.

Roberts and (presumably) Miescher do not give dispersion formulæ, while Landau's formula is not in the form of equation (1). We have therefore calculated by the above procedure the dispersion constants of these authors' results. Their values of $(\Delta\lambda^{-2}/\Delta M)^{1/3}$ are plotted against $1/\lambda^2$ in figs. 1 and 2. The straight lines fitting these observations have been deduced by Cauchy's method. The deviations of the points from the straight line give some idea of the precision attained.

We have indicated in fig. 2 the lines derived from the formulæ given by Richardson and by Stephens and Evans.

* L. R. Ingersoll, J. O. S. A. vi. p. 663 (1922).

† *Loc. cit.*

‡ G. Bruhat, *Journ. de Phys.* v. p. 152 (1934).

§ S. Landau, *Phys. Zeits.* ix. p. 417 (1908). S. S. Richardson, Phil. Mag. xxxi. p. 232 (1916). D. J. Stephens and E. J. Evans, Phil. Mag. iii. p. 546 (1927). R. W. Roberts, Phil. Mag. ix. p. 361 (1930). E. Miescher, *Helv. Phys. Acta.* iv. p. 398 (1931) (this paper is not accessible to us, and we have therefore taken the results quoted by Bruhat).

As these authors have determined their rotations in a different way from the others, we have not analyzed their results. Finally, we give in Table V. the dispersion constants of all the investigations known to us. All the values of A and B have been calculated by assuming Rodger and Watson's value for the Verdet constant. Figs. 1–6 and Table V. show at a glance the divergent dispersions of the magnetic rotation of water given by the photographic investigations. The precision of the photo-electric observations of Bruhat and Guinier, and to a slighter extent that of our own photographic observations, are at once evident from figs. 5 and 6.

TABLE V.

	λ_0 in μ.	A.	B.
Landau.....	·1532	·003047	·002444
Richardson	·1375	·002411	·003266
Stephens & Evans ..	·1192	—	·005554
Roberts	·1196	·000296	·005262
Miescher	·1413	·002675	·002985
Present authors	·1311	·001768	·003872
Bruhat & Guinier ..	·1296	·001701	·003947

The closeness of the lines representing the work of Stephens and Evans and of Roberts is striking. The λ_0 values of these observers are ·1192 μ and ·1196 μ respectively.

As mentioned by Bruhat and Guinier the m values of these observers are rather too large in the ultra-violet. They attribute these large values to the errors which can be produced when a double monochromator is not used. We do not think, however, that this is the main reason for the large m values ; for our results, which have been obtained without the use of a double monochromator, give almost the same dispersion as that obtained by Bruhat and Guinier. Furthermore, the addition of a monochromator to our optical system for series IV. did not substantially affect our results. The errors arising from the lack of monochromatism are therefore small.

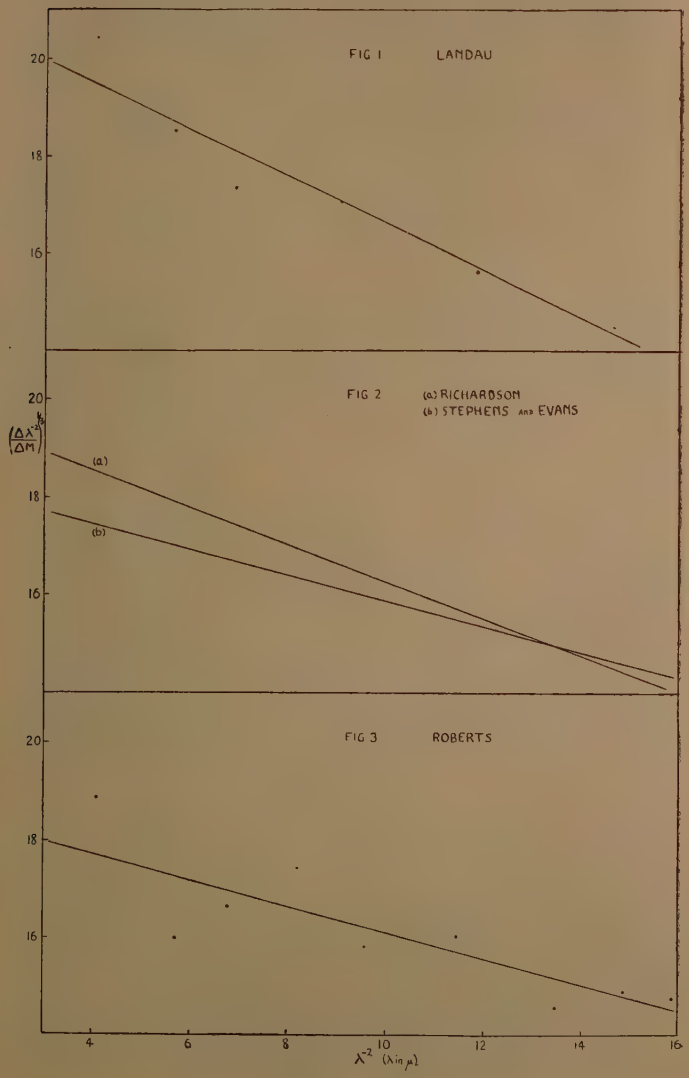
FIG 1 LANDAU
20
18
16
FIG 2 (a) RICHARDSON
(b) STEPHENS AND EVANS
$\left(\frac{\Delta\chi^2}{\Delta M}\right)_{\lambda}$
(a)
(b)
20
18
16
FIG 3 ROBERTS
20
18
16
4
6
8
10
12
14
16
χ^{-2} (λ in μ)

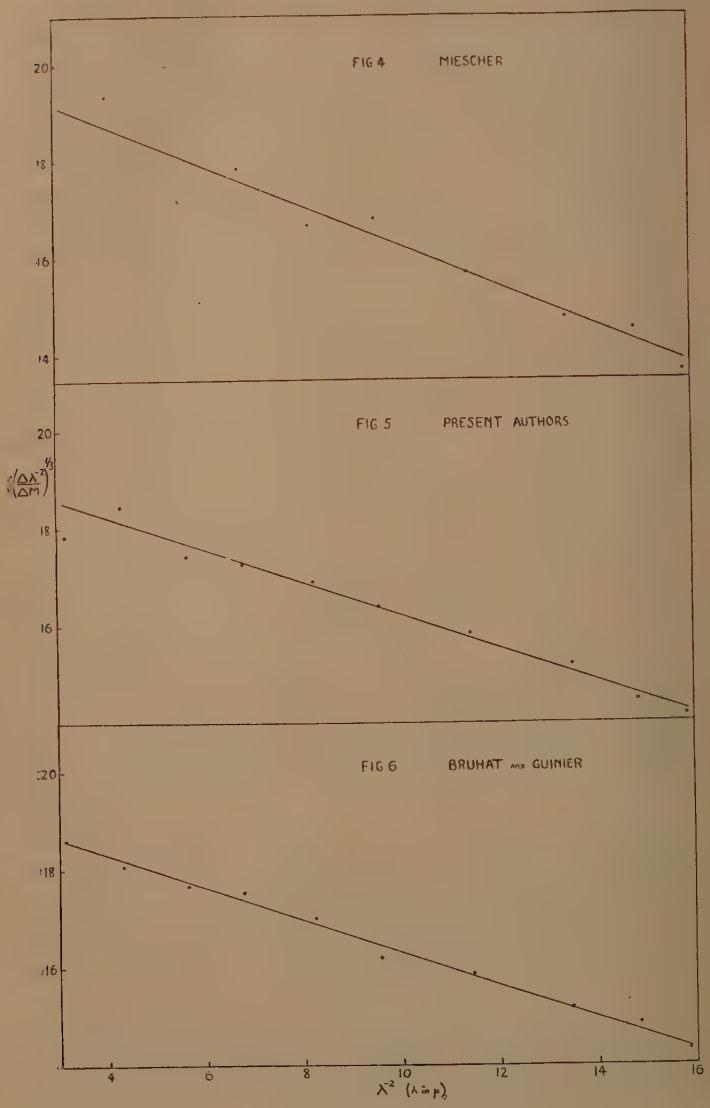
FIG 4 MIESCHER
20
18
16
14
FIG 5 PRESENT AUTHORS
20
18
16
FIG 6 BRUHAT AND GUINIER
20
18
16
4
6
8
10
12
14
16

We believe the reason for the high values obtained by Stephens and Evans and Roberts is due to their using a defective polarizing system (a modified Jellett polarizer giving a non-normal field). The same criticism applies to Landau's work, as his analyzer was a Jellett-Cornu prism.

The rather steep line (fig. 1) representing Landau's results suggests the presence of another source of error, which we believe to be his over-correction for the effect of the light multiply reflected in the cell. We think it better to avoid this correction when using short cells with an electromagnet, by making the cell faces slightly inclined.

It may be thought that the slight differences in the dispersion constants determined by Bruhat and Guinier and by us result from the different methods adopted in calculating λ_0. We give in Table III. col. (iv.) the values of $10^3(m_{\text{obs}}-m'_{\text{calc.}})/m_{\text{obs.}}$ when m' is calculated by means of the formula

$$m'n\lambda^2 = \cdot 06481 + \frac{\cdot 15780}{[1-(\cdot 1296/\lambda)^2]^2},$$

which was obtained by assuming $\lambda_0 = \cdot 1296\,\mu$.

It will be seen that this formula does not fit our results quite as well as formula (3). Further, as the constants A and B obtained by assuming $\lambda_0 = \cdot 1296\ \mu$ differ from those of Bruhat and Guinier, it follows that the two dispersions are distinctly different.

Although according to Flatow * the wave-length λ_0 increases with temperature the difference between $\cdot 1311\,\mu$ and $\cdot 1296\,\mu$ is too great to be attributed to a difference in temperature of only 6 degrees Centigrade.

Summary.

We have determined the magnetic rotation of water for eleven lines in the mercury spectrum from $\cdot 5780\,\mu$ to $\cdot 2483\,\mu$ by means of the photographic method of Bruhat and Pauthenier. Assuming Rodger and Watson's value for the Verdet constant of water at 22° C. to be $\cdot 01308'$ per cm.-gauss, the dispersion of the Verdet constant (ρ) is given to a precision of almost one part in a thousand by the formula

$$\rho = \frac{1}{n\lambda^2}\left\{\cdot 001768 + \frac{\cdot 0038723}{[1-(\cdot 1311/\lambda)^2]^2}\right\}.$$

* E. Flatow, *Ann. der Phys.* xii. p. 85 (1903).

This formula shows satisfactory agreement with Ingersoll's measurements in the infra-red.

The constants of the formula differ slightly from those obtained by Bruhat and Guinier with their photo-electric polarimeter.

The dispersion formulæ for a number of earlier investigators have been summarized.

We owe our best thanks to Prof. L. R. Wilberforce for the facilities and apparatus placed at our disposal; to Mr. L. A. Wallace, M.Sc., for his collaboration with us in taking the first two series of observations; and to Mr. R. Dutton for the great care he has taken in the construction of the microphotometer.

The George Holt Physics Laboratory,
The University, Liverpool.
June 21st, 1935.

X. *Numerical and Mechanical Methods in Double Fourier Synthesis.* *By* J. Monteath Robertson, *M.A., D.Sc.* *

[Plate I.]

THIS paper gives a brief description of computational methods employed by the writer in the preparation of electron density maps of various organic molecules [1] by Fourier synthesis from the X-ray data. In the Bragg double series [2] the density of scattering matter or electron density, ρ, in any centro-symmetrical projection of a crystal structure is given by

$$\rho(x, y) = \frac{1}{A} \sum_{-\infty}^{+\infty} \sum_{-\infty}^{+\infty} F(hk0) \cos 2\pi (hx/a + ky/b). \quad . \quad (1)$$

A is the area of the projection, a and b are the lengths of two crystal axes, h and k, x and y being the corresponding indices and coordinates. (The projection is here taken along the third crystal axis, c.) $F(hk0)$ is the structure factor of the reflexion $(hk0)$, and is a quantity whose magnitude can be determined from experimental measurements of intensity. But the sign of F, whether positive or negative, represents the phase

* Communicated by Sir W. H. Bragg, O.M., K.B.E., M.A., F.R.S.

constant of the reflexion, and this can only be determined from preliminary trial and error analysis. The method is thus essentially one of successive approximation. From some preliminary analysis a number of the phase constants are determined with reasonable certainty. The application of the Fourier synthesis then leads to a refinement of the atomic coordinates which enables the phase constants to be checked, and perhaps some weaker additional terms included.

Now the evaluation of the series (1) represents a considerable amount of numerical work for complex structures. For example, in the projections to which reference is given [1] the total number of terms of the type (1) involved for all the points computed amounts to approximately a quarter of a million, and, in addition, several of the projections have been repeated after initial refinement and correction of the phase constants. Thus any method of systematizing and shortening the work is of importance.

Possible Mechanical Methods.

Various mechanical methods for dealing with the double Fourier synthesis are possible. One has already been described by the writer [3]. Another might be found in some adaptation of the weighing method for harmonic analysis, which has been described by J. Harvey [4]. Such methods are in general likely to meet with two main objections:

(*a*) Any machine with a sufficient number of components to be generally useful for complicated crystal structures would be extremely cumbersome and expensive. As many as 200 components might be necessary.

(*b*) The accuracy obtainable with a many-component machine would usually not be high.

There is, however, another principle which might lead to much more promising mechanical devices for dealing with the double Fourier synthesis. Instead of the multi-component machine, indicating the sum of the whole series at one point after another on the surface of the projection, imagine a machine of only *one* component which will very quickly describe a single term of the series over the entire projection. This

is not difficult because each term is merely a sinusoidal ripple of a certain amplitude and phase. We must now be able to reset our one component machine quickly, so that it can describe one term after another of the series, and at suitable points on the projection surface have recorders which will add up the amplitudes received from the machine. An arrangement of this kind would not be open to objection (*a*) above, and with regard to (*b*) there would seem to be a better chance of obtaining a high accuracy.

Some very rough models embodying this principle have been made by the writer. The most simple consisted of a bar carried across the surface on wheels while describing a sinusoidal ripple. The recorders could then be in the form of cyclometers operated by plungers making contact with the bar. Another device, dispensing with the need for sinusoidal motion altogether, consisted of a set of recorders in the form of planimeter wheels in contact with a plane surface which could be translated by an amount depending on the amplitude of the term. The angular setting of the planimeter wheels relative to the direction of motion of the surface then gives the necessary sine or cosine factor. There is, however, an inevitable error due to slip in all planimeter machines [5], and the accuracy obtainable with a device of this kind would be difficult to assess.

Perhaps the most practical mechanical method would be to employ an ordinary one-dimensional Fourier synthesizer, such as the Kelvin tide predictor or a similar type, with about 15 or 20 components, and use this in conjunction with some numerical work and the expanded form of the series described by Beevers and Lipson [6] and further dealt with below.

It is obvious that the design of a really good machine employing any of the above principles would be a long and difficult research, and necessarily expensive. For these reasons the writer has always employed numerical methods, and, in fact, when the work is arranged systematically with the simple mechanical sorting devices described below the time involved in the Fourier synthesis is quite short—almost negligible in comparison with the time spent in making the experimental observations and in approaching the structure by trial. The time factor is important, because, if the method is

sufficiently fast, it means that the Fourier method can be employed frequently on the same structure if necessary as a method of successive approximation.

Numerical Method with Mechanical Sorting Device.

We make use of the expanded form of the series which has been described by Beevers and Lipson [6]. Reference should be made to their paper. The expression for the density becomes

$$\rho(x, y) = \Sigma\left[\Sigma F(hk0) \cos 2\pi \frac{ky}{b}\right] \cos 2\pi \frac{hx}{a} - \Sigma\left[\Sigma F(hk0) \sin 2\pi \frac{ky}{b}\right] \sin 2\pi \frac{hx}{a}.$$

The summations in the brackets may be effected first, and these totals then become the new coefficients for the final summation, which may be written

$$\Sigma A \cos 2\pi \frac{hx}{a} - \Sigma B \sin 2\pi \frac{hx}{a}.$$

The method greatly reduces the number of terms in the final summations, but introduces sine factors as well as cosine factors and increases the number of different coefficients, A and B, which have to be considered. It obviously becomes worth while to prepare a set of sine and cosine factors of all the numbers likely to be employed, and have these arranged in an accessible form, with some kind of sorting device which will enable us to select quickly the sets of numbers which it is desired to add in the summations.

The simple arrangement described below has been used by the writer during the past five years (with various modifications and improvements from time to time), and has proved very rapid, while making numerical mistakes practically impossible.

For the purpose of computation it is convenient to subdivide the crystal axis into 60 parts, and express the coordinate as a definite fraction of the axial length.

Let $x = \frac{na}{60}$; then the terms to be added become

$$A \cos hn\ 6^\circ \quad \text{and} \quad B \sin hn\ 6^\circ.$$

We now consider only integral values of n, *i. e.*, sines or cosines of multiples of 6°.

A table has been prepared giving the quantity $A \cos hn\ 6°$ to three decimal places for all values of A from 1 to 1000 and for n from 1 to 15 *. Coefficients from 1 to 1000 were calculated to provide for computations to at least three significant figures. For most ordinary crystal work, however, it would probably be sufficient to have coefficients from 1 to 200 or 300 only.

These figures, to the nearest whole number, were typed out on strips of thin Bristol board, one strip for each coefficient, as shown in fig. 1 for A=1000.

Reading from the left-hand end we have 1000 cos 0°, 1000 cos 6°, 1000 cos 12°, etc., and from the right-hand end 1000 sin 6°, 1000 sin 12°, etc. Thus the same strip serves for sines and cosines, because we have taken the precaution of subdividing the axis into a number of parts (60) which makes the interval (6°) a factor of 90°.

Fig. 1.

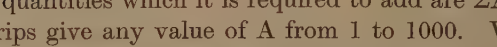

Strip for A=1000.

The quantities which it is required to add are $\Sigma A \begin{matrix}\cos\\ \sin\end{matrix} hn$. The strips give any value of A from 1 to 1000. Various values of the index h are provided on a series of scales described below. We select a strip giving A, attach it to a slide running on the appropriate scale for h, and the various values of n are obtained by moving the slide along the scale, when the required result, $A \begin{matrix}\cos\\ \sin\end{matrix} hn\ 6°$, appears in a fixed column, ready to be added to other similar results above and below.

The arrangement is shown diagramatically in fig. 2. The cardboard strip of figures can be attached to the slide CE in either of two positions, between C and D or between D and E, depending on whether the coefficient A is positive or negative. Scales are shown below the slide for $h=1$ up to $h=7$ for sines, and also in the lower part of the diagram for cosines. The numbers on the scales are the integral values of n from 0 to 15. Divisions

* We do not reproduce this table, as its computation can be performed very quickly with an ordinary adding machine.

Fig. 2.

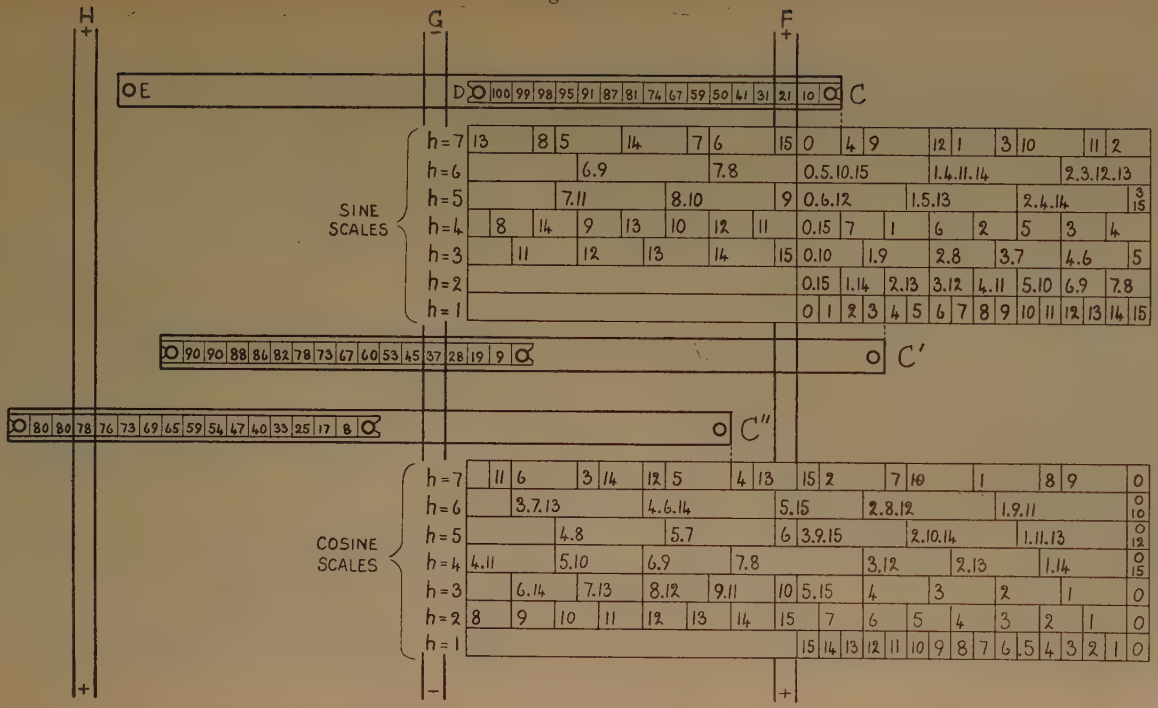

Scales and slides.

on the scales are marked by vertical lines, with the value or values of n to the right. As h may be a factor of 60 there are sometimes only a few divisions on the scale, *e. g.*, for $h=6$. Different numbers applying to the same scale division are then separated by a dot. There is actually a slide like CE running *over* each of the scales (compare Pl. I. fig. A), but here we only show specimen slides at C, C′, and C″. These three slides may be considered to run over the sine scales $h=7$ and $h=1$, and over the cosine scale $h=7$. There are fixed columns at F, G, and H in which the products $A^{\cos}_{\sin}\ hn\ 6°$ appear, F and H collecting the positive numbers and G the negative.

For example, the upper strip, on C, is set in the positive position (between C and D) and represents a coefficient of $A=+100$. The slide is set, on the scale beneath, at the division $n=4$. The number appearing in the column F is thus $A \sin hn\ 6° = +100 \sin (7\times 4\times 6°) = +21$. The strip on C′ is set in the negative position, and represents a coefficient of -90. It is also at the division $n=4$, on the scale $h=1$, and the result, which now appears in the negative column G, gives

$$A \sin hn\ 6° = -90 \sin (1\times 4\times 6°) = -37.$$

Similarly, the strip on C″, operating on the cosine scale $h=7$ at the division $n=4$, gives

$$A \cos hn\ 6° = -80 \cos (7\times 4\times 6°) = +78.$$

The design of the scales will be clear from the fourteen examples given in fig. 2, and there will be no difficulty in extending them for indices higher than 7. Each scale contains thirty-one divisions. For cosines we begin numbering from 0 on the extreme right in steps of h divisions to the centre, then jump to the extreme left, number to the centre and back to the left; then jump to the centre and number back to the starting-point on the extreme right, when the cycle repeats. For sines we begin numbering from 0 at the centre in steps of h divisions to the right and back to the centre; jump to the extreme left, number to the centre and back to the left again; then jump back to the original starting-point at the centre.

We have only marked the values of n from 0 to 15 on the scales. This represents 90°, or a quarter of the

primitive translation of the crystal. Further values of n up to 60, giving the full translation, could easily be added to the scales if desired, but this is unnecessary if advantage is taken of the following system of subtotals in carrying out the computations. We arrange the scales and slides in four groups :

T_1=cosines with h even,

T_2=cosines with h odd,

T_3=sines with h even,

T_4=sines with h odd.

These four groups may be summed separately, giving the subtotals T_1, T_2, T_3, T_4. The final sum required is the difference of the sine and cosine totals

$$\Sigma A \cos hn\ 6^\circ - \Sigma B \sin hn\ 6^\circ.$$

To derive the sum for points between $n=15$ and $n=60$ from computed values between $n=0$ and $n=15$ we make use of the relations

$\cos (30-n)h\ 6^\circ = \cos nh\ 6^\circ$ when h is even . . . (T_1),

$\cos (30-n)h\ 6^\circ = -\cos nh\ 6^\circ$ when h is odd . . $(-T_2)$,

$\cos (60-n)h\ 6^\circ = \cos nh\ 6^\circ$ for all values of h . (T_1+T_2),

$\sin (30-n)h\ 6^\circ = -\sin nh\ 6^\circ$ when h is even . $(-T_3)$,

$\sin (30-n)h\ 6^\circ = \sin nh\ 6^\circ$ when h is odd . . . . (T_4),

$\sin (60-n)h\ 6^\circ = -\sin nh\ 6^\circ$ for all values of h $(-T_1-T_4)$.

Hence the sum at the point $(30-n)$ is obtained by combining the subtotals for the point n as follows :—

$$(T_1-T_2)-(-T_3+T_4),$$

and all the other sums can be obtained similarly.

Thus, finally,

Sum at n $=T_1+T_2-T_3-T_4$.

Sum at $(30-n)=T_1-T_2+T_3-T_4$.

Sum at $(30+n)=T_1-T_2-T_3+T_4$.

(or $60-(30-n)$)

Sum at $(60-n)=T_1+T_2+T_3+T_4$.

Constructional Details.

The apparatus at present in use is shown in Pl. I. fig. A. It is of very simple construction. The slides which carry the cardboard strips of coefficients are made of oak strips, $26'' \times \frac{1}{2}'' \times \frac{1}{8}''$, such as can be obtained from fretwork accessory stores at 2*d.* each. Three drawing-pins on each of these slides retain the cardboard strip with its V ends in either of two positions (compare also fig. 2). The slides are mounted on a plain board measuring $43\frac{1}{2}'' \times 26''$. (An ordinary drawing-board of about this size serves very well.) On the right of the board is a sheet of cardboard with the scales drawn on it. These scales give all values of h up to 22 and are arranged in four groups for convenience in obtaining the subtotals, as explained above. But the scales and slides can be very quickly interchanged and rearranged in any other desired manner. The three columns are narrow gaps in a cover of thin sheet metal which is hinged at the top of the board, and can be quickly swung up out of the way (Pl. I. fig. B). At the top of this cover, near the hinges, three covered lamps are mounted for convenient illumination of the columns.

The strips of coefficients (compare fig. 1) are prepared with a standard typewriter on thin (two-sheet) Bristol board. The spacing between the individual figures is then the standard $1/10''$, and between the separate numbers $\frac{1}{2}''$. The overall length of each strip is $8\frac{1}{2}''$, containing fifteen numbers with a $\frac{1}{2}''$ gap at either end, in which $\frac{1}{4}''$ V's are cut, which slip under the drawing-pins, the slight springiness of the Bristol board holding the strip accurately in position. The standard $\frac{1}{2}''$ distance between the numbers on the strips determines all the other dimensions. Thus the scales have $\frac{1}{2}''$ divisions and are $15\frac{1}{2}''$ long, and the distance between the columns is $8''$.

The strips of coefficients are filed in a book, as shown in Pl. I. fig. A, with ten to a page. The coefficients run from 1 to 1000, and each strip is in duplicate. A less comprehensive set, however, would be sufficient for many purposes.

For accurate work it is very desirable to use an adding and listing machine of the type shown in Pl. I. fig. A below the board. The machine adds and prints the numbers and totals. The printed list is compared with the

numbers in the columns after each operation, and in this way an almost infallible check is obtained on the numerical work. Thus, if we assume a rather inefficient operator who makes one mistake for every 100 numbers, and a similar inefficiency in comparing the printed list with the original, then the chance of an undetected numerical error is only one for every 10,000 numbers. Much faster types of adding machine could be used, but at this stage of the work accuracy is more important than speed.

The above arrangement of board and scales has been described in some detail because it is very easy to construct and has been found most efficient, particularly for very long syntheses. The length of a synthesis may be measured by the product of the number of different coefficients and the number of different points computed on the asymmetric portion of the projection. This would be the number of terms to be added if no advantage were taken of any shortening device. A synthesis of 50,000 terms, by this measure, can be carried out by one operator without assistance in about three days, working throughout to three significant figures, and with sufficient care to make the chance of one numerical mistake in the final figures very small. On the other hand, if one were to work as fast as possible and dispense with checking the printed slips, and omit the smaller coefficients in the final summations, the work could probably be accomplished within a day. Still further speeding up might be attained if the slides were operated by a set of ratchets or cams to save the time spent in setting each one to its scale division by hand. Such refinements, however, appear at present to be rather unnecessary, as the time required to prepare a really accurate contour map from the summation totals, by making sections and cross-sections of the results, and accurately plotting the points through which the contour lines pass, is actually greater than the time required for the numerical work.

If one crystal axis is short, say less than about 8 Å., a subdivision into thirty parts may be sufficient. Then we need employ only the even values of n. If the crystal axes are both about 10 Å. a division of each into sixty parts is rather unnecessary; then it is convenient to divide one into sixty parts, and for the other sum one line at even values of n, the next at odd values

of n, and so on; the result being a staggered array of totals which is equivalent to dividing the diagonal (about 14 Å.) into sixty parts. In the case of an exceptionally long crystal axis of about 20 Å., or where great accuracy is required, it might be necessary to employ half-values of n, *i. e.*, an interval of 3°. Half-values of n could be marked on the scales. Integral values of n could be summed first, with the existing strips of coefficients. For the half-values we would require new strips, giving the cosines at 3°, 9°, 15°, etc. *for the odd values of h only.*

Various other sorting devices based on similar principles can be devised. A type with only one column instead of three is shown in Pl. I. fig. C. Here the strips of figures are longer, and positive and negative numbers are written out in complete cycles. This board deals with the series in the form $\Sigma\Sigma A \cos(hx+ky)$ without expansion. The scales are also of slightly different design, and are seen on the left. There are a number of small boards, each carrying a set of strips running on scales, and each small board itself moves on another scale fixed relative to the large board. One set of scales gives hx and the other ky, the combined movement displacing the strip by $(hx+ky)$. The figure in the column is then the cosine of this quantity. All the scales can be quickly dismantled and are interchangeable, and various small boards of different size can be used. One strip of figures is used for each term in the series, and when all the strips of figures are set up on the board they do not require to be changed throughout the projection. The method is quite efficient, especially for small projections; but when there are more than about fifty terms in the series the other method which we have described in detail is faster.

The single column method seems worth mentioning, however, because it might be adapted to deal with the case of a non-centrosymmetrical projection, in which the phase-angle constants to be attached to each term can have any value. A negative coefficient in a centrosymmetrical projection is equivalent to displacing the strip of figures by 180°, or half a complete cycle. In a non-centrosymmetrical projection the strips could be displaced by any desired angle depending on the phase constant of the term, but only in steps of 6° or other

interval adopted for the summation. The strips require to be written out in complete cycles to avoid discontinuities.

Summary.

Computational methods for the summation of double Fourier series are described particularly applicable to complicated crystal analysis. After a review of possible mechanical synthesizers the method favoured is a numerical one, assisted by a simple mechanical sorting device for the terms. Sine or cosine factors in steps of 6° of all the natural numbers from 1 to 1000 are written out on strips of cardboard. The sorting device then selects the required numbers and presents them in columns ready for addition. The method is fast, accurate to three figures, and the number of strips is a minimum, because each can be used either for a sine or a cosine factor, or for a positive or negative coefficient. An alternative device on the same principle is described. These arrangements have been used in computations involving over 250,000 terms.

References.

(1) J. M. Robertson, Proc. Roy. Soc. A, cxl. p. 79; cxlii. pp. 659, 674 (1933); cl. pp. 106, 348 (1935); 'Nature,' cxxxvi. p. 755 (1935); I. E. Knaggs, Proc. Roy. Soc. A, cl. p. 576 (1935).
(2) W. L. Bragg, Proc. Roy. Soc. A, cxxiii. p. 537 (1929).
(3) J. M. Robertson, Phil. Mag. xiii. p. 413 (1932).
(4) J. Harvey, Proc. Phys. Soc. xlii. p. 245 (1930).
(5) Maxwell, Trans. Royal Scottish Soc. Arts, iv. pt. 4 (1855); Collected Papers, i. p. 230.
(6) C. A. Beevers and H. Lipson, Phil. Mag. xvii. p. 855 (1934).

Davy Faraday Laboratory,
Royal Institution, London, W. 1.
21st October. 1935.

XI. *The Influence of the Radiation Field from an Electrical Storm on the Ionization Density of the Ionosphere.*

By R. H. Healey, *M.Sc., Demonstrator in Physics, University of Sydney* *.

1. *Introduction.*

THERE is a considerable amount of evidence that thunderstorms in the lower atmosphere are associated with increases in the ionization of the ionosphere.

* Communicated by Prof. V. A. Bailey, M.A., D.Phil.

Various explanations of this connexion have been given by C. T. R. Wilson *, Bailey and Martyn †, and others. On account of the importance of this effect it is proposed to use the methods of Bailey and Martyn to examine more closely the influence of a highly damped electric wave on the ionosphere, since these authors give only an approximate solution.

2. *Average Work done, over a Mean Free Path, by a damped alternating Electric Force acting on an Electron in a Magnetic Field.*

We select a right-handed system of axes such that the x-axis is parallel to the electric force E, and the magnetic force H lies in the xz-plane.

Let

$\mathrm{E}=Ae^{-kt}\sin pt$ (e.m.u.).

τ=free time, *i.e.*, the interval of time between two given successive collisions of an electron.

δ/p=the time at which the first collision occurs.

e=the charge on an electron.

ρ=e/m, the specific charge of an electron in e.m.u. $=1{\cdot}77\times10^{7}$.

H_p=the component of H perpendicular to E.

$\omega=\mathrm{H}_p\rho=\mathrm{H}_p$ e/m.

$\mathrm{U}=\dot{x}$.

$\mathrm{V}=\dot{y}$.

ν=number of collisions per second made by an electron.

In the interval $t=\delta/p$ to $t=\tau+\delta/p$ the equations of motion of an electron are

$$\dot{\mathrm{U}}=\rho\mathrm{E}+\omega\mathrm{V}, \quad . \quad . \quad . \quad . \quad . \quad . \quad (1)$$

$$\dot{\mathrm{V}}=-\omega\mathrm{U}. \quad . \quad . \quad . \quad . \quad . \quad . \quad . \quad (2)$$

Therefore

$$\ddot{\mathrm{U}}+\omega^2\mathrm{U}=-\rho\mathrm{A}(p^2+k^2)^{\frac{1}{2}}e^{-kt}\sin\overline{pt-\alpha_1}, \quad . \quad . \quad (3)$$

where

$$\alpha_1=\tan^{-1}(p/k).$$

* C. T. R. Wilson, Proc. Phys. Soc. xxxvii. 32D (1925).

† V. A. Bailey and D. F. Martyn, Phil. Mag. xviii, p. 369 (Aug. 1934).

Thus the complete solution of the system (1) and (2) is

$$\left.\begin{aligned} U &= Be^{-kt}\cos pt+\alpha + b\cos\omega t + c\sin\omega t, \\ V &= -Ce^{-kt}\sin pt+\beta - b\sin\omega t + c\cos\omega t, \end{aligned}\right\} \quad . \quad (4)$$

where

$$B=\frac{\rho A(p^2+k^2)^{\frac{1}{2}}}{\sqrt{4p^2k^2+(\omega^2-p^2+k^2)^2}} \qquad C=\frac{\rho A\omega}{\sqrt{4p^2k^2+(\omega^2-p^2+k^2)^2}}$$

$$\alpha=\alpha_2-\alpha_1 \qquad \alpha_2=\tan^{-1}\left\{\frac{\omega^2-p^2+k^2}{2pk}\right\}$$

$$\beta=\beta_2-\alpha_1 \qquad \beta_2=\tan^{-1}\left(\frac{\omega^2-p^2+3k^2}{\omega^2-3p^2+k^2}\right)\times p/k.$$

The initial velocities U_0, V_0 occur at time $t=\delta/p$, and so

$$\left.\begin{aligned} U_0-Be^{-k\delta/p}\cos\delta+\alpha &= b\cos\delta\omega/p + c\sin\delta\omega/p, \\ V_0+Ce^{-k\delta/p}\sin\delta+\beta &= -b\sin\delta\omega/p + c\cos\delta\omega/p. \end{aligned}\right\} \quad (5)$$

The work done on the electron in the free time τ is, therefore,

$$w_\tau=\int_{\delta/p}^{\tau+\delta/p} EeU\,dt=\phi(\tau)-\phi(0), \text{ say}, \quad . \quad . \quad (6)$$

where

$$\phi(\tau)=\int^{\tau+\delta/p} eAe^{-kt}\sin pt(Be^{-kt}\cos pt+\alpha+b\cos\omega t + c\sin\omega t)\,dt$$

$$=Ae\psi(\tau)+Ae\chi(\tau), \text{ say} \quad . \quad . \quad . \quad . \quad . \quad . \quad . \quad . \quad (7)$$

where, provided $\omega \gg k$,

$$\begin{aligned} \psi(\tau)=(p^2-\omega^2)^{-1}e^{-k(\tau+\delta/p)}[&p\cos p\tau+\delta \\ &\times\{-(U_0-Be^{-k\delta/p}\cos\delta+\alpha)\cos\omega\tau \\ &-(V_0+Ce^{-k\delta/p}\sin\delta+\beta)\sin\omega\tau\} + \omega\sin p\tau+\delta \\ &\times\{(V_0+Ce^{-k\delta/p}\sin\delta+\beta)\cos\omega\tau \\ &-(U_0-Be^{-k\delta/p}\cos\delta+\alpha)\sin\omega\tau\}], \quad . \quad . \quad . \quad (8) \end{aligned}$$

and

$$\chi(\tau)=B\int^{\tau+\delta/p} e^{-2kt}\sin pt\cos pt+\alpha\,dt$$

$$=\frac{B}{4}\left[\frac{\sin\alpha}{k}-\frac{\sin 2p(\tau+\delta/p)+\alpha_2}{(p^2+k^2)^{\frac{1}{2}}}\right]e^{-2k(\tau+\delta/p)}. \quad (9)$$

The time δ/p of the beginning of a free path may occur with equal probability at any part of the period of oscillation of the electric force E. The average value of w_τ between the times θ_1/p and θ_2/p is, therefore,

$$w_\tau = \frac{1}{\theta_2-\theta_1}\int_{\theta_1}^{\theta_2} w_\tau\, d\delta$$
$$= \frac{Ae}{\theta_2-\theta_1}\left[\left\{\int_{\theta_1}^{\theta_2}\psi(\tau)\,d\delta\right\}_{\tau=0}^{\tau=\tau} + \left\{\int_{\theta_1}^{\theta_2}\chi(\tau)\,d\delta\right\}_{\tau=0}^{\tau=\tau}\right]. \quad . \quad . \quad . \quad (10)$$

But from (8) we have

$$\int_{\theta_1}^{\theta_2}\psi(\tau)\,d\delta = (p^2-\omega^2)^{-1}e^{-k\tau}$$
$$\times\{p/4k[\mathrm{B}(p\cos p\tau\cos\omega\tau+\omega\sin p\tau\sin\omega\tau)\mathrm{I}_1$$
$$-\mathrm{B}(p\sin p\tau\cos\omega\tau-\omega\cos p\tau\sin\omega\tau)\mathrm{I}_2$$
$$+\mathrm{C}(p\sin p\tau\sin\omega\tau+\omega\cos p\tau\cos\omega\tau)\mathrm{I}_3$$
$$-\mathrm{C}(p\cos p\tau\sin\omega\tau-\omega\sin p\tau\cos\omega\tau)\mathrm{I}_4]$$
$$+\mathrm{U}_0 f(p,\omega,\ldots)+\mathrm{V}_0\mathrm{F}(p,\omega,\ldots)\}, \quad . \quad (11)$$

where

$$\mathrm{I}_1 = \frac{4k}{p}\int_{\theta_1}^{\theta_2} e^{-2k\delta/p}\cos\overline{\delta+\alpha}\cos\delta\,d\delta$$
$$= \left(\cos\alpha+\frac{\cos\overline{2\theta_1+\alpha_2}}{(1+p^2/k^2)^{\frac{1}{2}}}\right)e^{-2k\theta_1/p}$$
$$-\left(\cos\alpha+\frac{\cos\overline{2\theta_2+\alpha_2}}{(1+p^2/k^2)^{\frac{1}{2}}}\right)e^{-2k\theta_2/p}$$

$$\mathrm{I}_2 = \frac{4k}{p}\int_{\theta_1}^{\theta_2} e^{-2k\delta/p}\cos\overline{\delta+\alpha}\sin\delta\,d\delta$$
$$= \left(\frac{\sin\overline{2\theta_1+\alpha_2}}{(1+p^2/k^2)^{\frac{1}{2}}}-\sin\alpha\right)e^{-2k\theta_1/p}$$
$$-\left(\frac{\sin\overline{2\theta_2+\alpha_2}}{(1+p^2/k^2)^{\frac{1}{2}}}-\sin\alpha\right)e^{-2k\theta_2/p}$$

$$\mathrm{I}_3 = \frac{4k}{p}\int_{\theta_1}^{\theta_2} e^{-2k\delta/p}\sin\overline{\delta+\beta}\sin\delta$$
$$= \left(\cos\beta-\frac{\cos\overline{2\theta_1+\beta_2}}{(1+p^2/k^2)^{\frac{1}{2}}}\right)e^{-2k\theta_1/p}$$
$$-\left(\cos\beta-\frac{\cos\overline{2\theta_2+\beta_2}}{(1+p^2/k^2)^{\frac{1}{2}}}\right)e^{-2k\theta_2/p}$$

$$I_4=\frac{4k}{p}\int_{\theta_1}^{\theta_2}e^{-2k\delta/p}\sin\delta+\beta\cos\delta\,d\delta$$
$$=\left(\sin\beta+\frac{\sin 2\overline{\theta_1+\beta_2}}{(1+p^2/k^2)^{\frac{1}{2}}}\right)e^{-2k\theta_1/p}$$
$$-\left(\sin\beta+\frac{\sin 2\overline{\theta_2+\beta_2}}{(1+p^2/k^2)^{\frac{1}{2}}}\right)e^{-2k\theta_2/p},$$
$$\ldots\quad(12)$$

and $f(p,\ \omega,\ \ldots)$ and $F(p,\ \omega,\ \ldots)$ are known expressions. Also from equation (9) we have

$$\int_{\theta_1}^{\theta_2}\chi(\tau)\,d\delta=Bp\sin\alpha(e^{-2k\theta_1/p}-e^{-2k\theta_2/p})e^{-2k\tau}/8k^2$$
$$-Bp\{\sin\overline{2p(\tau+\theta_1/p)+\alpha_3}\,e^{-2k\theta_1/p}$$
$$-\sin\overline{2p(\tau+\theta_2/p)+\alpha_3}\,e^{-2k\theta_2/p}\}e^{-2k\tau}/8(p^2+k^2)$$
$$=G(\tau),\text{ say,}$$

where $\alpha_3=\alpha_1+\alpha_2$;

and so
$$\left\{\int_{\theta_1}^{\theta_2}\chi(\tau)\,d\delta\right\}_{\tau=0}^{\tau=\tau}=G(\tau)-G(0).\quad\ldots\quad(13)$$

Substituting from (11) and (13) in (10), and also averaging over all values of U_0 and V_0, we have

$$\bar{w}_\tau=\frac{Aep}{(p^2-\omega^2)(\theta_2-\theta_1)4k}$$
$$\times[e^{-k\tau}\{B(p\cos p\tau\cos\omega\tau+\omega\sin p\tau\sin\omega\tau)I_1$$
$$-B(p\sin p\tau\cos\omega\tau-\omega\cos p\tau\sin\omega\tau)I_2$$
$$+C(p\sin p\tau\sin\omega\tau+\omega\cos p\tau\cos\omega\tau)I_3$$
$$-C(p\cos p\tau\sin\omega\tau-\omega\sin p\tau\cos\omega\tau)I_4\}$$
$$-\{BpI_1+C\omega I_3\}]+\frac{Ae}{\theta_2-\theta_1}\{G(\tau)-G(0)\},\quad\ldots\quad(14)$$

since $\overline{U}_0=0$, and $\overline{V}_0=0$.

Since the number of free paths which have free times lying between τ and $\tau+d\tau$ is the fraction $e^{-\nu\tau}d(\nu\tau)$ of all the free paths, the average work w done over a mean free path between the times θ_1/p and θ_2/p is

$$\bar{w}=\nu\int_0^\infty\bar{w}_\tau e^{-\nu\tau}d\tau$$
$$=\{(p^2-\omega^2)^{-1}Aep/8k(\theta_2-\theta_1)\}$$
$$\times\{BI_1J_1-BI_2J_2+CI_3J_3-CI_4J_4\}$$
$$-\{AeBp/4k\nu(\theta_2-\theta_1)\}\times G,\quad\ldots\quad(15)$$

where

$$J_1=\frac{\omega\nu^2-p(p-\omega)^2}{\nu^2+(p-\omega)^2}-\frac{\omega\nu^2+p(p+\omega)^2}{\nu^2+(p+\omega)^2},$$

$$J_2=\frac{(p^2-\omega^2)\nu}{\nu^2+(p-\omega)^2}+\frac{(p^2-\omega^2)\nu}{\nu^2+(p+\omega)^2},$$

$$J_3=\frac{p\nu^2-\omega(p-\omega)^2}{\nu^2+(p-\omega)^2}-\frac{p\nu^2+\omega(p+\omega)^2}{\nu^2+(p+\omega)^2},$$

$$J_4=\frac{-(p^2-\omega^2)\nu}{\nu^2+(p-\omega)^2}+\frac{(p^2-\omega^2)\nu}{\nu^2+(p+\omega)^2},$$

and

$$G=\sin\alpha(e^{-2k\theta_1/p}-e^{-2k\theta_2/p})$$
$$-(\sin\overline{2\theta_1+\alpha_3}.e^{-2k\theta_2/p}-\sin\overline{2\theta_2+\alpha_3}.e^{-2k\theta_2/p})/(1+p^2/k^2).$$

As a check of equation (15) it may be noted that when $k\to 0$ (15) leads to equation (10) in the paper of Bailey and Martyn *.

The observed values of p and k are of the order of 500π and 250π † respectively, and we have assumed $\omega>10^5$. We may therefore neglect p in comparison with ω.

If we multiply the work $\overline{w}$ by a factor of 0.815 to make an approximate allowance for the distribution of velocities of the electrons about the mean, and set

$$\theta_1=2\pi n+\phi_1 \quad \text{and} \quad \theta_2=2\pi n+\phi_2,$$

where n is the number of complete cycles which have elapsed from the beginning of the flash to the commencement of the cycle in which lie the moments θ_1/p and θ_2/p, then on using (12) and setting T for the period the relation (15) becomes

$$w=0{\cdot}815\,\rho^2A^2mpe^{-2k\pi T}/4k(\phi_2-\phi_1)$$
$$\times\left[\frac{1}{\nu^2+\omega^2}\{(1-(1+p^2/k^2)^{-\frac{1}{2}}\cos\overline{2\phi_1+\alpha_1})e^{-2k\phi_1/p}\right.$$
$$-(1-(1+p^2/k^2)^{-\frac{1}{2}}\cos\overline{2\phi_2+\alpha_1})e^{-2k\phi_2/p}\}$$
$$-\frac{(p^2+k^2)^{\frac{1}{2}}}{\omega^2\nu}\left\{\left(\sin\alpha-\frac{\sin\overline{2\phi_1+\alpha_3}}{1+p^2/k^2}\right)e^{-2k\phi_1/p}\right.$$
$$\left.\left.-\left(\sin\alpha-\frac{\sin\overline{2\phi_2+\alpha_3}}{1+p^2/k^2}\right)e^{-2k\phi_2/p}\right\}\right]. \quad . \quad . \quad (16)$$

* Bailey and Martyn, *loc. cit.*
† L. B. Turner, 'Wireless.'

As a first approximation we average over a quarter of a period, and remembering $\alpha_3=\alpha_1+\alpha_2\doteqdot\pi/2+\alpha_1$ and $\alpha=\alpha_2-\alpha_1\doteqdot\pi/2-\alpha_1$ we obtain from (16)

$$w_1\doteqdot\frac{0{\cdot}815\,\rho^2Z^2mpe^{-2knT}}{\pi k(p^2+k^2)}\,[\{p^2(1-e^{-k\pi/p})-2k^2e^{-k\pi/p}\}/(\nu^2+\omega^2)$$
$$-(p^2+k^2)^{3/2}\sin\alpha\{1-(1+p^2/k^2)^{-\frac{1}{2}}$$
$$-1-(1+p^2/k^2)^{-\frac{1}{2}}\,e^{-k\pi/p}\}/\omega^2\nu]\,;$$

$$w_2\doteqdot\frac{0{\cdot}815\,\rho^2Z^2mpe^{-2kT(n+\frac{1}{4})}}{\pi k(p^2+k^2)}\,[\{p^2(1-e^{-k\pi/p})+2k^2\}/(\nu^2+\omega^2)$$
$$-(p^2+k^2)^{3/2}\sin\alpha\{1+(1+p^2/k^2)^{-\frac{1}{2}}$$
$$-1-(1+p^2/k^2)^{-\frac{1}{2}}\,e^{-k\pi/p}\}/\omega^2\nu]\,;$$

$$w_3=e^{-kT}w_1\,;$$
$$w_4=e^{-kT}w_2\,; \quad . \quad . \quad . \quad . \quad . \quad . \quad . \quad . \quad . \quad . \quad . \quad . \quad (17)$$

where the subscripts 1, 2, 3, and 4 of w refer to the first, second, third, and fourth quarter periods respectively in the $(n+1)$th cycle.

Now taking $p=2k=500\pi$, (17) becomes

$$w_1\doteqdot\rho^2Z^2me^{-2knT}\{0{\cdot}29/(\nu^2+\omega^2)-220/\omega^2\nu\}\,;$$
$$w_2\doteqdot\rho^2Z^2me^{-2knT}\{0{\cdot}087/(\nu^2+\omega^2)-84/\omega^2\nu\}\,;$$
$$w_3=0{\cdot}041w_1\,;$$
$$w_4=0{\cdot}041w_2. \quad . \quad . \quad . \quad . \quad . \quad . \quad . \quad . \quad . \quad (17a)$$

3. *Quantitative Results.*

Let

u=mean velocity of agitation of an electron.

L=mean free path of an electron in the gas at 1 mm. pressure.

P=pressure of the gas in mm. of Hg.

α=Townsend's ionization coefficient.

g=proportion of its own energy lost by an electron at a collision.

W=the drift velocity of an electron.

The equation (11) of Bailey and Martyn *, which expresses the conservation of energy, may be written in the form

$$\dot{u}=C(w-\tfrac{1}{2}gmu^2), \quad . \quad . \quad . \quad . \quad . \quad (18)$$

* Bailey and Martyn, *loc. cit.*

where C is approximately constant and equal to $3 \times 10^{-2}/m$. Also the rate of generation of fresh electrons per second, by collisions of a single electron, is

$$\gamma = \alpha W = P(\alpha/P)W,$$

where α/P and W correspond to a given value of u. Thus

$$dN = N\gamma\, dt,$$

and so

$$N \doteq N_0 e^{\Sigma\gamma\delta t}, \quad \ldots\ldots\ldots \quad (19)$$

where N_0 and N are the initial and final electron ionization densities respectively.

The quantities g, ν, W, and α/P occurring in equations (18) and (19) are functions of u, which are obtained from the results of Townsend and Tizard *, who give u, L, W,

TABLE I.

X/P	0	2	6·4	10	30	50
$u \times 10^{-7}$ cm./sec.	1·06	5·4	7·3	7·8	9·5	11·6
$L \times 10^2$ cm.	3·3	3·28	2·92	2·82	2·73	2·78
$\nu \times 10^{-5}$	3·0	14·3	21·7	24·0	30·2	36·5
$g \times 10^2$	0	0·26	0·63	1·13	3·4	5·5
$W \times 10^{-6}$cm./sec.	...	1·8	3·6	5·2	12·4	17·3
α/P	...	$<3\times10^{-5}$	$<3\times10^{-5}$	$<3\times10^{-5}$	9×10^{-4}	0·055

Data for X/P = 0 taken from Bailey and Martyn.

and G in terms of X/P, and the results of Sanders †, who gives α/P in terms of X/P; in calculating ν we take the pressure $P = 8{\cdot}7 \times 10^{-4}$ mm. ‡. The values of these quantities used in the subsequent calculations are given in Table I.

Let us now assume a value for the maximum velocity $u_{max.}$ attained by the electrons, say $11{\cdot}6 \times 10^7$ cm./sec., and estimate the resultant increase in ionization and the values of Z necessary to produce this result.

In Table II. are given the approximate values of u at a few instants after u attains its maximum value, calculated from (18) for the value of $\omega = 2{\cdot}5 \times 10^5$, together with the

* Townsend and Tizard, Proc. Roy. Soc. A, lxxxviii. p. 336 (1913).
† Sanders, Phys. Rev. xli, no. 5, Sept. 1932, p. 667.
‡ Bailey and Martyn, *loc. cit.*

corresponding values of γ obtained from the data in Table I.

The values of u shown in Table II. are obtained as follows :—

TABLE II.

Time (millisecs.). ...	0	1	2	3	4
$u\times10^{-7}$(cm./sec.) ...	11·6	9·5	7·8	7·3	5·4
γ	830	9·7	$<0{\cdot}13$	...	...

Since $220/\omega^2\nu$ is small compared with $0{\cdot}29/(\nu^2+\omega^2)$ for the assumed value of $\omega=2{\cdot}5\times10^5$, (17 *a*) may be written in the form

$$(\overline{w}_r)_s \doteqdot 0{\cdot}29\,\rho^2Z^2me^{-2kT\left(s+\frac{r-1}{4}\right)}\Big/(\nu_{s,r}^2+\omega^2),$$

where $(\overline{w}_r)_s$ is the average value of w during the rth quarter of the $(s+1)$th cycle.

If we suppose that u attains its maximum value $u_{max.}$ immediately after Rth quarter of the (S+1)th cycle, then

$$(\overline{w}_R)_S \doteqdot 0{\cdot}29\,\rho^2Z^2me^{-2kT\left(S+\frac{R-1}{4}\right)}\Big/(\nu_{S,R}^2+\omega^2).$$

Hence

$$(\overline{w}_r)_s \doteqdot (\overline{w}_R)_S\,e^{2kT\left(S-s+\frac{R-r}{4}\right)}\left(\frac{\nu_{S,R}^3+\omega^2}{\nu_{s,r}^2+\omega^2}\right).$$

The average value $\overline{y}$ of $\{\overline{w}-(\overline{w}_R)_S\}$ between the times when $u=u_0$ and $u=u_{max.}$ is such that

$$\overline{y}=\frac{(\overline{w}_R)_S}{(4S+R)}\sum_{r,s}\left(e^{2kT\left(S-s+\frac{R-r}{4}\right)}\cdot\frac{\nu_{S,R}^2+\omega^2}{\nu_{s,r}^2+\omega^2}-1\right)$$

$$>\frac{(\overline{w}_R)_S}{(4S+R)}\{kT(4S+R-1)/2\},\quad\ldots\ldots\quad(20)$$

where the last expression $(kT(4S+R-1)/2)$ is the first term in the series indicated by the summation sign.

But in the interval of time $(4S+R)T/4$, u changes from $1{\cdot}06\times10^7$ to $11{\cdot}6\times10^7$, and so

$$\left.\begin{aligned}&\dot{u}\times(4S+R)T/4=10^8,\\ i.e.,\quad&\dot{u}=4\times10^{11}/(4S+R).\end{aligned}\right\}\quad\ldots\ldots\quad(21)$$

Also from (18), when $u=u_{max.}$

$$(\overline{w}_R)_S=\tfrac{1}{2}gmu_{max.}^2=3{\cdot}7\times10^{14}\,m\text{ ergs},$$

and from Table I. it may readily be verified that $\frac{1}{2}gmu^2<\frac{1}{2}gmu^2_{\max.}$ for values of $u<u_{\max.}$, *i.e.*, $\frac{1}{2}gmu^2<(\overline{w}_R)_S$. Hence from (18)

$$\left.\begin{aligned} &\dot{u}>C(\overline{w}-(\overline{w}_R)_S),\\ \textit{i.e.,}\quad &\dot{u}>C\bar{y}. \end{aligned}\right\} \quad . \quad . \quad . \quad . \quad (22)$$

Substitution from (21) in (22) gives

$$\bar{y}<\frac{4\times10^{13}m}{3(4S+R)} \quad . \quad . \quad . \quad . \quad . \quad (23)$$

From the inequalities (20) and (23) it follows that

$$(4S+R-1)<\frac{2(4S+R)\bar{y}}{kT(\overline{w}_R)_S}<\frac{2\times4\times10^{13}m}{3kT(\overline{w}_R)_S},$$

$$\textit{i.e.,}\qquad 4S+R-1<\frac{8\times10^{13}\times4}{3\times\pi\times3{\cdot}7\times10^{14}}<1.$$

Since also S is a positive integer (including zero) it follows that S=0. Hence R−1<1, *i.e.*, R<2. Since by definition R is an integer ≥1, it follows that R=1. Hence u attains its maximum value $u_{\max.}$ during the second quarter of the first cycle.

At the end of the second quarter of the first cycle (where $\delta t=10^{-3}$ sec.) by (18)

$$\dot{u}_2=3\times10^{-2}(\overline{w}_2-\tfrac{1}{2}gmu_2^2)/m.$$

The average value of $\dot{u}$ during the time δt is $\dot{u}_2/2$, and so

$$(\dot{u}_2/2)\times10^{-3}=\delta u,$$

$$\textit{i. e.,}\qquad <10^8.$$

Thus

$$\dot{u}_2<5\times10^{10},$$

and so

$$(\overline{w}_2-\tfrac{1}{2}gmu_2^2)<1{\cdot}5\times10m^{12}.$$

Since $\overline{w}_2$ is approximately $1{\cdot}5\times10^{14}m$, it follows that u_2 is given closely by the equation

$$\overline{w}_2=\tfrac{1}{2}gmu_2^2,$$

which is the equation for the steady state corresponding to $\overline{w}_2$. Similarly it may be shown that we can determine u_3, u_4, and u_5 from the equations $w_3=\frac{1}{2}gmu_3^2$ etc. To carry the approximation further, the simplest method consists in solving (18) by trial and error. In determining u_2, u_4, and u_5 the curves w_2, $\overline{w}_3$, $\overline{w}_4$, and $\overline{w}_5$ are plotted against u on the same diagram as $\frac{1}{2}gmu^2$, and the

points where this latter curve cut the other four curves give the appropriate values of u.

A similar calculation has been carried out with the cycle divided into eight parts. The results are substantially the same within a few per cent. as those given above where the cycle is divided into four parts.

The values of γ from the last row in Table II. are substituted in equation (19) in order to determine the resultant increase in ionization.

Thus

$$N=N_0 \exp (830+9{\cdot}7\ldots)10^{-3}$$
$$\doteqdot N_0 e^{8{\cdot}34} \doteqdot 2{\cdot}3\, N_0.$$

The value of Z corresponding to $u_{max}=11{\cdot}6\times10^7$ is obtained at once from the equation

$$\rho^2Z^2[0{\cdot}29/(\nu^2+\omega^2)-220/\omega^2\nu]=\tfrac{1}{2}gu^2_{max.}=3{\cdot}7\times10^{14},$$

where $\nu=3{\cdot}65\times10^6$. It follows that fields ranging from 8·7 to 20·5 volts/metre according as ω ranges from 10^5 to 10^7 would be required to bring about a duplication of the ionization density.

These fields considerably exceed the observed fields which are of the order 0·6 volts/metre *, and so we conclude that the increase of ionization is in general below the limits of observation.

Alternatively if we take Z=0·6 volts/metre it is found that $u_{max.}\leqslant6{\cdot}9\times10^7$ cm./sec. Since $u=6{\cdot}9\times10^7$ corresponds to X/P=5 and thus $\alpha/P<3\times10^{-5}$ and $W=3\times10^6$, it follows that

$$\Sigma\gamma\delta t<4\times10^{-4},$$

and so by (19)
$$N=N_0(1+\epsilon),$$

where
$$\epsilon<4\times10^{-4}.$$

Hence even with a series of flashes lasting over a few seconds the increase in ionization would be inappreciable.

4. *Conclusions.*

The calculations in (2) and (3) show that the intensity of the radiation fields of lightning flashes are too small to account for the observed increases in the ionization density of the ionosphere.

Bailey and Martyn *, in their approximate treatment of this effect, arrive at a different conclusion, but this is

* Bailey and Martyn, *loc. cit.*

due to a numerical error in their calculation; they conclude that values of Z from 400 to 15,500 mv./m., according as ω ranges from 0 to 10^7, are necessary to cause a notable increase in ionization density, whereas their corrected calculation leads to values of Z from 5,000 to 15,500 mv./m.

In conclusion, I wish to thank Professor V. A. Bailey, who suggested this problem, for his advice and helpful criticism while the work was being done.

5. *Summary.*

The methods developed by Bailey and Martyn in their consideration of the influence of electric waves on the ionosphere have been applied to the situation where a highly damped electric wave, lasting a few milliseconds acts on the ionosphere. Use is made of the results of Townsend and Tizard and of Sanders on the motions of electrons in air to show that the increase in ionization density of the ionosphere due to the radiation field of a lightning flash alone is inappreciable.

Note by Prof. V. A. Bailey.

While reading through section (9) of the paper by Dr. Martyn and myself on "The Influence of Electric Waves on the Ionosphere" Mr. Healey discovered that we had substituted the number 3×10^5 for ν in our formula for Z, in place of the more appropriate value $3{\cdot}8 \times 10^6$, which corresponds to the velocity 12×10^7.

When this mistake is corrected we find, in agreement with Mr. Healey's conclusion, that the observed fields of radiation from electric storms are not strong enough to increase appreciably the ionization in the neighbouring parts of the ionosphere. (None of our conclusions on the interaction of radio waves are affected by this correction.)

Nevertheless the possibility still exists that the field of radiation from an electric storm when added to an approximately constant electric field supposed always present in some part of the ionosphere, may be able to increase the ionization by a notable factor.

Mr. Healey and I hope to publish in the future an investigation of this and related points.

XII. *Notices respecting New Books.*

The Measurement of Inductance, Capacitance, and Frequency. By A. Campbell and E. C. Childs. (Macmillan & Co., Ltd. Price 30*s*.)

IN their preface the authors state that the earlier part of this book is based on articles written for Glazebrook's 'Dictionary of Physics.' It therefore takes somewhat the form of a handbook of the art, within the range of the subjects of the title, and on these grounds is a valuable work filling a long-felt want. The first few chapters treat naturally of sources of alternating voltage (incidentally the authors object to the "misleading term electromotive force") and with measuring and detecting instruments, the vibration galvanometer receiving special treatment. There follow chapters dealing directly with measurement, including the testing of current and potential transformers—a most welcome addition.

The following more critical review of certain chapters may suggest matter for amplification in any later edition.

Chapter V. deals with resistances for use in inductance measurements. The authors say in introduction "In nearly all methods of measuring inductance standard resistances .... form an essential part of the apparatus." In most cases it is desirable that such resistances should be as free as possible from self inductance and self capacitance. In view of this fact, which will be endorsed by all workers on alternating current bridges, it is a pity that this chapter is almost the shortest in the book and that more space is not devoted to the difficult but important art of determining these residual effects in resistance units. Chapters VI., VII., and IX. deal with the calculation and construction of secondary standard inductance coils, and the formulæ for calculation are particularly welcome. In a future edition it may be hoped that there will be more information on the construction of primary standards, again particularly with reference to the elimination or predetermination of "impurities." Chapters XV., XVI., and XVII. give similar information for the construction of capacity units.

Chapter X. is headed "Electrical Networks and Bridges," but only occupies five pages. It should perhaps have included more on the theory of the four-arm impedance bridge, in order that the experimenter may see how to work out the equilibrium of balance of any bridge he may himself design. This criticism, however, must be qualified by the statement that a very large number of bridge circuits are given, and that therefore there is very little need for the experimenter to try new circuits. The student may in fact find it difficult to weigh the merits of the various methods of measurement available,

This book will be a very desirable and even necessary addition to every measurement laboratory, all the more so since the authors have included very complete references to the original sources of information.

X-Rays in Theory and Experiment. By A. H. Compton and S. K. Allison. [Pp. 828+xiv.] (Macmillan & Co., Ltd. Price 31*s.* 6*d.*)

This is the second edition of Professor Compton's well-known 'X-Rays and Electrons.' It preserves many features of the original book, but includes so much new matter that a new title is justified. Large sections have been added on the application of the theory of dispersion to X-rays and on the diffraction of X-rays by perfect crystals. The older work on X-ray scattering is brought up to date by the inclusion of a very useful account of scattering by liquids and gases and of diffuse scattering by crystals. The fact that the title now refers solely to X-rays and omits electrons is significant, for electron scattering and diffraction are not mentioned.

For the ordinary physics student the book is far too comprehensive and detailed to be of very much use except as a reference book, but for the research worker and for anyone who wishes to study the subject in detail it is a magnificent summary of practically all the important work in this field. The book is well printed and bound, and, although it contains over eight hundred pages, the use of thinner and more flexible paper than in the first edition makes it easy and convenient to handle. The name and subject indices are good and ample; references are made in the text to original papers. There is an agreeable absence of that nationalistic spirit which tends to mar some present-day books; so far as the reviewer knows the contributions made by workers in different countries have been adequately represented.

In a series of appendices useful data are given on atomic structure factors, X-ray wave-lengths, critical absorption wave-lengths, and absorption coefficients. The latter are mainly the absorption measurements of S. J. M. Allen. In practice these are not always very convenient, and an additional table would have been very useful giving the mass absorption coefficients for all the elements for frequently used wave-lengths or for a series of closely spaced wave-lengths calculated by Jöhnson's method. This, however, is a minor criticism. Taken as a whole the book is a valuable addition to the literature on X-rays, and can be thoroughly recommended.

[*The Editors do not hold themselves responsible for the views expressed by their correspondents.*]

Fig. A.

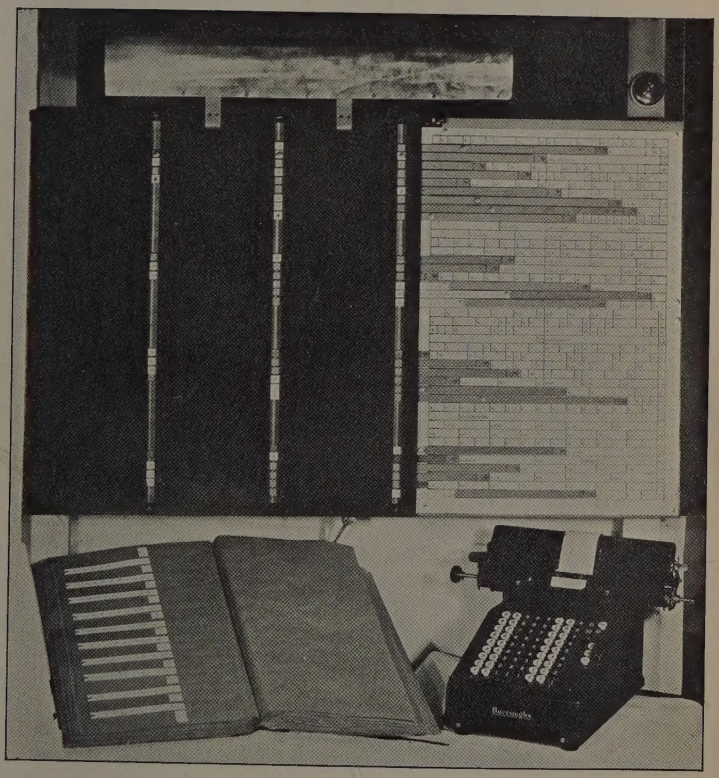

Three-column sorting board for double Fourier synthesis.

FIG. B.

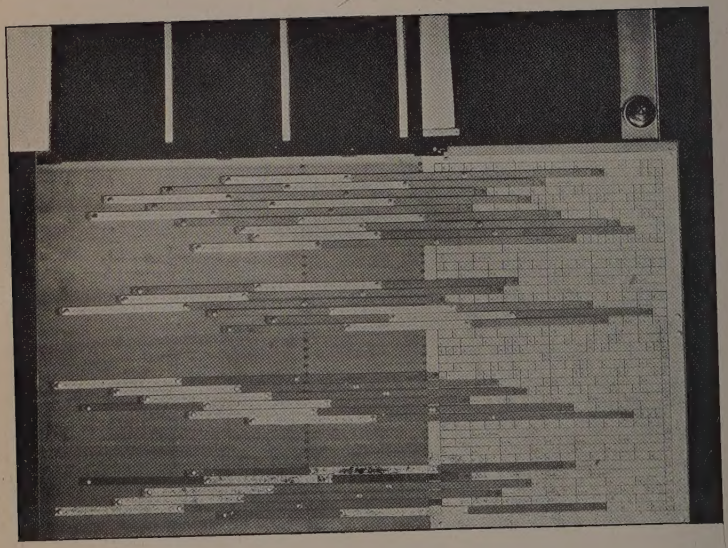

Board showing slides and scales, cover open.